



THE HONG KONG
INSTITUTION OF ENGINEERS
香港工程師學會

An Explanatory Handbook to the Code of Practice for Foundations 2017



Structural Division
The Hong Kong Institution of Engineers

An Explanatory Handbook to the Code of Practice for Foundations 2017

June 2019

**Prepared by a Working Committee of
Structural Division**

The Hong Kong Institution of Engineers

Published by

Structural Division

The Hong Kong Institution of Engineers

Published by the Structural Division of the Hong Kong Institution of Engineers

All information contained in this document is subject to copyright owned by The Hong Kong Institution of Engineers, Structural Division. All rights reserved.

The content of this document is an expression of opinion only. In the preparation of this document, the Structural Division has endeavoured to make the document as accurate and current as possible. It is provided “as is” without any guarantee or warranty of any kind, either expressed or implied.

Guidance and recommendations given in this document should always be reviewed by those using this document in the light of the facts of their particular case. Individuals who use this document in any way assume all risk and accept total responsibility for its use. The Structural Division, its members and the working group who produced this document disclaim liability for damages of any kind which may result from its use.

First published 2015

Revised 2019

Foreword

With an aim to facilitate understanding of the rationale and application of the code of practices published by the Buildings Department of Hong Kong, the Structural Division of the Hong Kong Institution of Engineers has published the “Explanatory Handbook to the Code of Practice for Foundations 2004” for the Foundation Code promulgated in 2004. While the Foundation Code has been updated and published in 2017, the Structural Division has taken the initiatives to revise the Handbook accordingly which is now named “An Explanatory Handbook to the Code of Practice for Foundations 2017”.

The updated handbook adopts similar formats and approaches as the 2004 version. Apart from adding new materials to explain the new topics, a thorough review of the existing topics has also been carried out and with updating as necessary.

We trust that the content of this handbook would help practitioners in design and construction of foundation works for compliance with the current Foundation Code.

With the above, it gives me enormous pleasure to recommend you to read this Handbook. I would also like to congratulate the Working Committee, chaired by Ir Lam King-kong for their dedicated efforts and professionalism which make this handbook a great success.

Ir Prof Ben Young
Chairman
Structural Division, HKIE
October 2019

Acknowledgement

This Explanatory Handbook for the Code of Practice for Foundations 2017 as the revised version to the previous 2004 version of the Foundation Code aims to echo with the revisions in the Code. It incorporates the views and comments of experienced researchers and practicing engineers. It has been compiled by a Working Committee appointed by the Structural Division of the Hong Kong Institution of Engineers. The Working Committee Members are as follows-

Chairman : Ir Lam King-kong

Members : Ir Cheung Ping-yip, Sammy
Ir Lau Chi-kin
Ir Sze Wang-cho, James
Ir Tse Wai-keung, Ben

(in alphabetical order)

Secretary : Ir Law Chi-wai

The Chairman of the Working Committee would like to express his deep gratitude to each Committee Member and those who contributed during the course of the compilation work over the past years, including the Structural Division Committee Members of the Hong Kong Institution of Engineers. Without their remarkable contributions and unreserved efforts, this Explanatory Handbook would not have been successfully finalized and published.

Contents

	Page No.
H1 General	1
H1.1 Scope	1
H1.2 Glossary	1
H1.3 Abbreviation	5
H1.4 Symbols	5
H2 General Design Requirements	6
H2.1 General	6
H2.1.1 Basic Requirements	6
H2.1.2 Compatibility of Design and Construction	6
H2.1.3 Classification of Soils and Rocks	7
H2.2 Allowable Bearing Pressure, Bond or Friction of Ground	7
H2.2.1 Rational Design Method	7
H2.2.2 Presumed Values	8
H2.2.3 In Situ Testing Method	9
H2.2.4 Bearing Capacity Equation Method	9
H2.2.5 Other Methods	10
H2.3 Foundation Settlement and Rotation	10
H2.3.1 Estimation of Settlement	10
H2.3.2 Acceptable Settlement and Rotation	12
H2.4 Structures on Reclaimed Land	13
H2.4.1 General Design Rules	13
H2.4.2 Alternative Approach	14
H2.4.3 Long-term Monitoring and/or Maintenance	14
H2.4.4 Reclaimed Land with Consolidation Substantially Completed.	14
H2.5 Structural Requirements	14
H2.5.1 General	14
H2.5.2 Design Loads	14
H2.5.3 Underground Water	15
H2.5.4 Resistance to Sliding, Uplift and Overturning	15
H2.5.5 Materials and Stresses	17
H2.6 Corrosion Protection of Foundations	21
H2.6.1 General	21
H2.6.2 Concrete Foundations	21
H2.6.3 Steel Piles	23
H2.6.4 Marine Foundations	25
H2.7 Foundation Plans	26
H2.8 Foundation Design in Scheduled Areas	26
H2.9 Foundation Design in Designated Area	27
H2.10 Foundation Design in Sloping Ground	27

H3	Site Investigation	28
H3.1	General	28
H3.2	Documentary Studies	28
H3.3	Site Survey	29
H3.4	Ground Investigation	30
H3.4.1	General	30
H3.4.2	Supervision for Ground Investigation Works	31
H3.4.3	Preparation of Ground Investigation Reports	31
H3.4.4	Soil and Rock Sampling	32
H3.4.5	Number and Disposition of Boreholes/Trial Pits	32
H3.4.6	Depth of Ground Investigation	32
H3.4.7	Groundwater	33
H3.5	Ground Investigation in Scheduled Areas	34
H3.6	Ground Investigation within Designated Area	36
H4	Shallow Foundations	37
H4.1	General Requirements	37
H4.2	Allowable Bearing Pressure and Settlement	37
H4.2.1	Shallow Foundations on Categories 1(a), 1(b), 1(c), 1(d) or 2 Rock	37
H4.2.2	Shallow Foundations on Soil	37
H4.3	Structural Requirements	40
H4.4	Common Types of Shallow Foundations	42
H4.4.1	Pad Footings	42
H4.4.2	Strip Footings	43
H4.4.3	Raft Foundations	43
H5	Pile Foundations	44
H5.1	General	44
H5.1.1	Recognized Types of Pile Foundations	44
H5.1.2	Group Effect	44
H5.1.3	Minimum Pile Spacing	46
H5.1.4	Horizontal Restraints to Piles and Pile Caps	46
H5.1.5	Piles Providing Resistance against Sliding	46
H5.1.6	Piles Providing Resistance against Uplift, Overturning and Buoyancy	46
H5.1.7	Pile Group Settlement	47
H5.2	Negative Skin Friction	47
H5.2.1	Design Requirement	47
H5.2.2	Conventional Approach	48
H5.2.3	Alternative Approach	49
H5.3	Pile Capacity of Piles	49
H5.3.1	Structural Strength	49
H5.3.2	Ground Resistance for Piles in Compression	50
H5.3.3	Ground Resistance for Piles Subjected to Uplift Forces	58
H5.3.4	Ground Resistance for Piles Subjected to Lateral Load	60

H5.4	Common Pile Types	62
H5.4.1	Steel H-Piles/Steel Tubular Piles	63
H5.4.2	Socketed Steel H-Piles	65
H5.4.3	Precast Reinforced Concrete Piles	66
H5.4.4	Precast Prestressed Spun Concrete Piles	66
H5.4.5	Driven Cast-in-Place Concrete Piles	68
H5.4.6	Small Diameter Bored Piles	69
H5.4.7	Large Diameter Bored Piles	71
H5.4.8	Mini-Piles	74
H5.4.9	Barrettes	77
H5.4.10	Hand-Dug Caissons	81
H5.4.11	Steel H-Piles Driven to Bedrock	81
H5.4.12	Steel H Shear Piles	82
H5.5	Pile Caps	82
H6	Other Foundation Types/Elements	84
H6.1	Basements and Hollow Boxes	84
H6.2	Diaphragm Walls	86
H6.3	Retaining Walls	89
H6.4	Ground Anchors	89
H6.5	Re-use of Existing Foundations	90
H7	Construction Practice and Site Safety for Foundation Works	91
H7.1	General	91
H7.1.1	General Requirements	91
H7.1.2	Quality Supervision for Foundation Works	91
H7.1.3	Construction Materials	91
H7.1.4	Excavation	92
H7.2	Effect of Foundation Works on Adjacent Structures and Land	94
H7.2.1	Assessment of the Effects of Foundation Works	94
H7.2.2	Shoring and Underpinning	95
H7.2.3	Monitoring Plan	96
H7.2.4	Ground Settlement	96
H7.2.5	Dewatering	97
H7.2.6	Vibration	97
H7.2.7	Public Relations Plan for Piling Works	98
H7.2.8	Blasting	98
H7.3	Foundation Records and Reports	98
H7.4	Pile Construction	99
H7.4.1	Driving Test and Trial Piles	99
H7.4.2	Test Boring	99
H7.4.3	Pre-Drilling	99
H7.4.4	Post Construction Proof Drilling	99
H7.4.5	Proof Tests	99
H7.4.6	Further on Site Tests	99
H7.5	Construction Tolerances	100

H7.6	Ground Treatment	100
H7.7	Control of Nuisance	100
H7.8	Foundation Works in Scheduled Areas	102
H8	Testing of Foundation and Ground	103
H8.1	General	103
H8.2	Plate Load Test	103
H8.3	Standard Penetration Test	104
H8.4	Compression Loading Test	104
H8.5	Core-Drilling Test	108
H8.6	Sonic Logging	109
H8.7	Sonic Echo Test	112
H8.8	Vibration Test	112
H8.9	Dynamic Load Test for Driven Piles	112
H8.10	Tension Loading Test	112
H8.11	Lateral Load Test	114
H8.12	Ultrasonic Echo Sounder Test	114

Appendices

	Page No.
Appendix HA	Practical Examples of Inspection of Rock Samples A-1
Appendix HB	A Worked Example on Determination of Ultimate Bearing Capacity of an Inclined Rectangular Footing B-1
Appendix HC	Determination of Settlement and Support Stiffness of Footings on an Elastic Subgrade C-1
Appendix HD	Design of General Flexural Reinforcement in a R.C. Plate Bending Structure D-1
Appendix HE	A Worked Example on Determination of the Group Reduction Factor (Geotechnical Capacity) of a Pile Group in Cohesionless Soil E-1
Appendix HF	Worked Examples for Determination of Ultimate Lateral Shear Resistances of Piles F-1
Appendix HG	Checking of Piles against Uplift, Overturning and Buoyancy of a Hypothetical Pile Group G-1
Appendix HH	Equivalent Raft Method H-1
Appendix HI	Buckling of Slender Piles – Embedded, Partially Exposed or Sleeved in Soil..... I-1
Appendix HJ	Principle and Derivation of the Hiley Formula J-1
Appendix HK	Discussion on Limits of “Final Set” and Criteria for Formulation of the “Final Set” Table K-1
Appendix HL	More Details and Examples in Wave Equation, the Case Method and CAPWAP for Analysis of Pile Capacities L-1
Appendix HM	Closed Form Solution for the Bearing Capacity Factor N_q in accordance with Berezantsev M-1
Appendix HN	Worked Examples for Determination of Ultimate Uplift Resistance of Piles N-1

Appendix HO	Determination of Horizontal Displacement of Pile Cap under Lateral Loads in accordance with the Elastic Continuum Theory	O-1
Appendix HP	Lateral Restraint on a Pile by the Winkler's Spring Assumptions – Cohesionless Soil	P-1
Appendix HQ	Lateral Resistance of a Piled Foundation – Distribution of Lateral Loads among the Piles and the Pile Cap	Q-1
Appendix HR	Assessment of Effects on Adjacent Structures due to Loads from a New Structure by the Continuum Theory based on Mindlin's Equations	R-1
Appendix HS	Seepage Analysis of Excavation in a Homogeneous, Isotropic Soil Medium	S-1
Appendix HT	Trench Stability Calculation of Bentonite Slurry Excavation	T-1
Appendix HU	Photographic Demonstration of Construction Procedures of Some Common Types of Foundations	U-1
Appendix HV	Estimation of Interactions of Piles in Close Proximity under Vertical Loads by Randolph's Approach	V-1
		Page No.
References		Ref-1

List of Tables

		Page No.
Table H5.1	Values of n_h for Cohesionless Soils	61
Table H5.2	Data of Common Precast Prestressed Spun Concrete Pile	67
Table H5.3	Determination of Geotechnical Capacity of a Small Diameter Bored Pile	70
Table HG-1	Example of Checking of Piles against Uplift, Overturning and Buoyancy of a Hypothetical Pile Group	G-1
Table HH-1	Summary for Calculation for Worked Example HH-1	H-3
Table HH-2	Calculation for Worked Example HH-2 by the Approach in Appendix HC	H-3
Table HI-1	Restraint Conditions on Lateral Load Analysis on Pile by the Finite Difference Method	I-3
Table HI-2(a)	Table showing Variation of “Equivalent Length Factor” with L/T ratio and Pile Exposed Length Factor for End-bearing Piles with Bottom Free	I-4
Table HI-2(b)	Table showing Variation of “Equivalent Length Factor” with L/T ratio and Pile Exposed Length Factor for End-bearing Piles with Bottom Pinned	I-5
Table HI-2(c)	Table showing Variation of “Equivalent Length Factor” with L/T ratio and Pile Exposed Length Factor for End-bearing Piles with Bottom Fixed	I-5
Table HI-2(d)	Table showing Variation of “Equivalent Length Factor” with L/T ratio and Pile Sleeved Length Factor for End-bearing Piles with Bottom Free	I-6
Table HI-2(e)	Table showing Variation of “Equivalent Length Factor” with L/T ratio and Pile Exposed Length Factor for End-bearing Piles with Bottom Pinned	I-6
Table HI-2(f)	Table showing Variation of “Equivalent Length Factor” with L/T ratio and Pile Exposed Length Factor for End-Bearing Piles with Bottom Fixed	I-7
Table HK-1	Final Set Values per 10 Blows with No Restriction on the S values	K-3
Table HK-2	Final Set Values per 10 blows (i) with limits between 25mm and 100mm per 10 Blows; (ii) and $(c_p+c_q)/L \leq 1.15$ where c_p+c_q is in mm and L is in m	K-3
Table HK-3	Final Set Values per 10 blows (i) with limits between 25mm and 100mm per 10 Blows; (ii) $(c_p+c_q)/L \leq 1.15$ where c_p+c_q is in mm; and L is in m; and (iii) S capped at 50mm	K-4
Table HL-1	Estimation of Ultimate Static Resistance of a Hypothetical Pile by the Case Method	L-9
Table HN-1	Computation of Ultimate Uplift Resistance of a Driven Pile (Effective Stress Method)	N-6
Table HN-2	Computation of Ultimate Uplift Resistance of a Driven Pile (SPTN Values)	N-7
Table HO-1(a)	Coefficient of Translation Soil Poisson’s Ratio $\mu = 0.3$	O-7

Table HO-1(b)	Coefficient of Translation Soil Poisson's Ratio $\mu = 0.35$	O-7
Table HO-1(c)	Coefficient of Translation Soil Poisson's Ratio $\mu = 0.4$	O-8
Table HO-1(d)	Coefficient of Translation Soil Poisson's Ratio $\mu = 0.45$	O-8
Table HO-1(e)	Coefficient of Translation Soil Poisson's Ratio $\mu = 0.5$	O-8
Table HO-2(a)	Coefficient of Rotation Soil Poisson's Ratio $\mu = 0.3$	O-9
Table HO-2(b)	Coefficient of Rotation Soil Poisson's Ratio $\mu = 0.35$	O-9
Table HO-2(c)	Coefficient of Rotation Soil Poisson's Ratio $\mu = 0.4$	O-9
Table HO-2(d)	Coefficient of Rotation Soil Poisson's Ratio $\mu = 0.45$	O-10
Table HO-2(e)	Coefficient of Rotation Soil Poisson's Ratio $\mu = 0.5$	O-10
Table HP-1	Restraint Conditions on Lateral Load Analysis on Pile by the Finite Difference Method	P-1
Table HP-2	Use of Coefficients for Determination of Displacements, Rotations, Shears and Moments in Piles by the Finite Difference Method	P-2
Table HP-3(a)	Deflection and Moment Coefficients for Pile with Free Head and Tip Unrestrained from both Lateral Movement and Rotation due to Horizontal Shear at Cut-off Level	P-4
Table HP-3(b)	Deflection and Moment Coefficients for Pile with Head Restrained from Rotation and Tip Unrestrained from both Lateral Movement and Rotation due to Horizontal Shear at Cut-off Level	P-4
Table HP-3(c)	Deflection and Moment Coefficients for Pile with Free Head and Tip Restrained from Lateral Movement but Free to Rotate due to Horizontal Shear at Cut-off Level	P-4
Table HP-3(d)	Deflection and Moment Coefficients for Pile with Head Restrained from Rotation and Tip Restrained from Lateral Movement but Free to Rotate due to Horizontal Shear at Cut-off Level	P-5
Table HP-3(e)	Deflection and Moment Coefficients for Pile with Head Pinned and Tip Restrained from both Lateral Movement and Rotation due to Horizontal Shear at Cut-off Level	P-5
Table HP-3(f)	Deflection and Moment Coefficients for Pile with Head Restrained from Rotation and Tip Restrained from both Lateral Movement and Rotation due to Horizontal Shear at Cut-off Level	P-5
Table HP-4(a)	Rotation Coefficients for Pile Tip Unrestrained from both Lateral Movement and Rotation due to Moment at Pile Head	P-6
Table HP-4(b)	Rotation Coefficients for Pile Tip Restrained from Lateral Movement but Free to Rotation due to Moment at Pile Head	P-6
Table HP-4(c)	Rotation Coefficients for Pile Tip Restrained from both Lateral Movement and Rotation due to Moment at Pile Head	P-6
Table HP-5(a)	Shear Coefficients for Pile Tip Unrestrained from both Lateral Movement and Rotation due to Moment at Pile Head	P-7
Table HP-5(b)	Shear Coefficients for Pile Tip Restrained from Lateral Movement but Free to Rotation due to Moment at Pile Head	P-7
Table HP-5(c)	Shear Coefficients for Pile Tip Restrained from both Lateral Movement and Rotation due to Moment at Pile Head	P-7
Table HP-6	Comparison of Results between Worked Examples HP-1 and HP-2	P-10
Table HQ-1	Lateral Stiffness of the Piled Foundation of Worked Example HQ-1	Q-4

Table HQ-2	Summary of Stiffness of the Piled Foundation of Worked Example HQ-1	Q-4
Table HQ-3	Summary of External Lateral Load of Worked Example HQ-1	Q-5
Table HQ-4(a)	Summary of Pile and Pile Cap Reactions to Wind in X-direction ...	Q-5
Table HQ-4(b)	Summary of Pile and Pile Cap Reactions to Wind in Y-direction ...	Q-6
Table HS-1	Summary of Heads/Pressures of Worked Example HS-1	S-3
Table HS-2	Summary of Heads/Pressures of Worked Example HS-2	S-6
Table HT-1	Summary of Stresses in Worked Example HT-1	T-3

List of Figures

		Page No.
Figure H1.1	General Configuration of Bell-Out of Bored Pile	2
Figure H1.2	Typical Final Set Graph	3
Figure H1.3	Modes of Failure for Ultimate Bearing Capacity	5
Figure H2.1	Measures to mitigate the Migration of Soil into any Voids that may be formed underneath the Suspended Structure	13
Figure H2.2	Worked Example H2.1 for Checking Stability	16
Figure H2.3	Typical Socketed H-Pile with Cross Bars as Shear Connectors	19
Figure H2.4	Chemical Process of Corrosion	23
Figure H2.5	Splash and Tidal Zone in a Marine Foundation	24
Figure H2.6	Examples of Cathodic Protection to Piles in Marine Foundations ..	25
Figure H3.1	Vertical Stress Bulb beneath a Square Footing or a Circular Footing (or Pile)	33
Figure H4.1	Ground Pressure Distribution beneath Footing under Different Assumptions	38
Figure H4.2	Explanation of Ground Bearing Pressure under the Continuum Theory	39
Figure H4.3	Demonstration of the Determination of Design Forces on Sections of Footing	40
Figure H4.4	Plans showing Pad Footings, Strip Footings and Raft Footings	42
Figure H5.1	Illustration of Pile Group Effect on Pile Settlement	44
Figure H5.2	Load Displacement Path for Set and Temporary Compression of Soil	52
Figure H5.3	Splicing Details for H-pile (for Lengthening of Pile)	64
Figure H5.4	Details for Pile Head	64
Figure H5.5	Acceptable Details for Pile Toe – Strengthened for Hard Driving on or close to Bedrock	65
Figure H5.6	Details of a 14"×14" Precast Reinforced Concrete Pile	66
Figure H5.7	Details of Pile Shaft of a Precast Prestressed Spun Concrete Pile ...	68
Figure H5.8	Typical Pile Head Details of a Precast Prestressed Spun Concrete Pile.....	68
Figure H5.9	Pile Shoe Details of a Precast Prestressed Spun Concrete Pile	68
Figure H5.10	Pile Head Details of a Driven Cast in Place Pile	69
Figure H5.11	Details of a Small Diameter CFA Pile	71
Figure H5.12	Details of a Typical Large Diameter Bored Pile	73
Figure H5.13	Shear Plane for Checking Bond Stress between Steel Bars and Grout for 4T50 and 5T50 Mini-pile	75

Figure H5.14	Structural Configuration of Raking Mini-pile Resulting in Pure Axial Loads in the Pile	75
Figure H5.15	Details of a 4T50 Mini-pile	77
Figure H5.16	Construction of Typical Barrette	80
Figure H5.17	Details of a Hand-dug Caisson	81
Figure H5.18	Additional Bars to Trim Wide Spacing of Main Bars to Avoid Conflict with H-piles in Pile Cap as per clause 5.5 of the Code	83
Figure H6.1	Differential Settlements of Linking Services or Structures to Basement	85
Figure H6.2	Increase of Water Flow Path by Cut-off by Impermeable Wall	86
Figure H6.3	Illustration of the “Locked-in” Stresses Formulation in a Top-down One Storey Basement Construction and the Method of Analysis	88
Figure H6.4	Illustration of Mobilization of Soil Mass against Uplift for Foundation Elements in Close Proximity	89
Figure H7.1	Photographic Illustration of Excavation	93
Figure H7.2	Common Preventive Measures in Foundation Construction	94
Figure H7.3	Double Raking Shore to Enhance Stability of Building	95
Figure H7.4	Photographic Illustrations of Monitoring of Ground and Structure Movement and Ground Water Level	96
Figure H7.5	Dewatering in Excavation to Lower Ground Water Table	97
Figure H7.6	Noise Nuisance Reduction Measures	101
Figure H7.7	Exhaust Purifier for Diesel Power of Reverse Circulation Drill	102
Figure H7.8	Spraying of Water for Dust Suppression	102
Figure H8.1	Set-up of Loading Test on Top Level of Pile	106
Figure H8.2	A typical Load Settlement Curve in a Pile Load Test	108
Figure H8.3	Twin Tube and Single Tube Set-up of Sonic Logging Test	110
Figure H8.4	Example Demonstrating Sonic Coring Test Revealing Anomaly	112
Figure H8.5	Photograph showing Arrangement of a Tension Pile Test (Raking Pile)	113
Figure H8.6	Tension Pile Test using Ground as Reaction	113
Figure H8.7	Example of “Traces” Revealed by Ultrasonic Echo Sounder Test ...	114
Figure HA-1	Representation of a Corestone-bearing Rock Mass (Malone, 1990)	A-1
Figure HB-1	Worked Example of Determination of Ultimate Bearing Capacity of Footing	B-1
Figure HB-2	Failure Mode under a Strip Footing	B-2
Figure HB-3	Demonstration of Interpolation of Ultimate Bearing Capacity	B-4
Figure HC-1(a)	Variation of Depth Factor with L/B Ratios for Soil of Poisson’s Ratio = 0.3	C-2
Figure HC-1(b)	Variation of Depth Factor with L/B Ratios for Soil of Poisson’s Ratio = 0.35	C-2
Figure HC-1(c)	Variation of Depth Factor with L/B Ratios for Soil of Poisson’s Ratio = 0.4	C-3
Figure HC-1(d)	Variation of Depth Factor with L/B Ratios for Soil of Poisson’s Ratio = 0.45	C-3
Figure HC-1(e)	Variation of Depth Factor with L/B Ratios for Soil of Poisson’s Ratio = 0.5	C-3

Figure HC-2	Illustration of Symbols used in the Equations for Estimating Corner Settlements of Rectangular Footing	C-4
Figure HC-3	Calculation of Settlement of a Point X under a Point of a Footing Exerting a Uniformly Distributed Load on an Elastic Subgrade	C-4
Figure HC-4	Settlement Contours for a Rectangular Footing Exerting Uniformly Distributed Load on an Elastic Subgrade	C-5
Figure HC-5(a)	Coefficients for Determination of Average Settlement of Rectangular Footing Resting on Top of an Elastic Half-space of Finite Depth to Hard Stratum, Soil of Poisson's Ratio =0.3	C-6
Figure HC-5(b)	Coefficients for Determination of Average Settlement of Rectangular Footing Resting on Top of an Elastic Half-space of Finite Depth to Hard Stratum, Soil of Poisson's Ratio =0.35	C-6
Figure HC-5(c)	Coefficients for Determination of Average Settlement of Rectangular Footing Resting on Top of an Elastic Half-space of Finite Depth to Hard Stratum, Soil of Poisson's Ratio =0.4	C-7
Figure HC-5(d)	Coefficients for Determination of Average Settlement of Rectangular Footing Resting on Top of an Elastic Half-space of Finite Depth to Hard Stratum, Soil of Poisson's Ratio =0.45	C-7
Figure HC-5(e)	Coefficients for Determination of Average Settlement of Rectangular Footing Resting on Top of an Elastic Half-space of Finite Depth to Hard Stratum, Soil of Poisson's Ratio =0.5	C-8
Figure HC-6	Estimation of Settlement outside Rectangular Plan Footing Carrying u.d.l.	C-9
Figure HC-7	Estimation of Settlement inside Non-rectangular Plan Shaped Footing	C-9
Figure HC-8	Illustration of Calculation of Footing Settlement in 2 Layered Subgrade	C-10
Figure HC-9	Worked Example HC-2	C-10
Figure HD-1	Derivation and Nature of the "Twisting Moment"	D-1
Figure HD-2	General Moments at a Point in a Plate Bending Structure	D-2
Figure HD-3	Bending and Twisting Moment as Represented by the Mohr Circle	D-2
Figure HD-4	Plots of Normal Moments and Strengths by Wood Armer Equation for Worked Example HD-1	D-4
Figure HD-5	Plots of Normal Moments and Strengths by Wood Armer Equation for Worked Example HD-2	D-5
Figure HE-1	Worked Example HE-1 for Pile Group Reduction Factor	E-1
Figure HF-1	Worked Example HF-1 for Determination of Ultimate Lateral Shear Resistances of Piles Pinned at Pile Cap	F-1
Figure HF-2	Worked Example HF-2 for Determination of Ultimate Lateral Shear Resistances of Piles Rigidly Connected at Pile Cap	F-2
Figure HH-1	Extract from Tomlinson (2008) Demonstrating the Principles of the Equivalent Raft Method	H-1
Figure HH-2	Worked Example HH-1	H-2
Figure HI-1	Illustration of the Buckling Phenomenon of Piles in Elastic Soil ...	I-1
Figure HI-2	The Finite Difference Model for the Simulation of a Pile	I-1
Figure HI-3	Illustration of Exposed Length and Sleeved Length Factors	I-4
Figure HI-4	Numerical Example of a 4-T50 Mini-pile	I-8

Figure HJ-1	Energy Transfer Process as Assumed by the Hiley Formula	J-1
Figure HJ-2	Work Done in Quake and Set as Assumed by the Hiley Formula ...	J-3
Figure HL-1	Derivation of Wave Speed in Pile	L-1
Figure HL-2	Derivation of the Basic Wave Equation	L-2
Figure HL-3	Pile Forces and Velocities	L-4
Figure HL-4	Wave Transmission in Pile Shaft	L-5
Figure HL-5	Typical Plot of Measured Forces and Velocities of a Pile by PDA Test	L-9
Figure HL-6	Smith's Idealization of Pile	L-10
Figure HL-7	Typical Graphs showing Good Matching between the Measured Forces and Calculated Forces with Time	L-11
Figure HL-8	Wave Forms of P and $Z \cdot v$ of a Pile undergoing PDA Test and Photograph showing the Defected Portion	L-12
Figure HM-1	Bearing Capacity Factor N_q for Circular Foundations (after Kezdi, 1975)	M-1
Figure HM-2	The Shapes of Failure Modes at the Pile Tips as assumed by (a) Terzaghi and Berezantsev; (b) Meyerhof; (c) Vesic	M-2
Figure HM-3	Bearing Capacity Factors of Berezantsev and Brinch Hansen (after Tomlinson 2008)	M-2
Figure HM-4	Variation of N_q with ϕ at Different L/d ratios to Berezantsev	M-4
Figure HN-1	Geometrical Shapes due to Overlapping of Soil Columns and Rock Cones of Two Adjacent Circular Piles	N-1
Figure HN-2	Worked Example for Checking Uplift of a Large Diameter Bored Pile	N-3
Figure HN-3	Overlapping of Soil Columns and Rock Cones of 4 Large Diameter Bored Pile for Worked Example HN-2	N-4
Figure HN-4	Pile Layout for Worked Example HN-5	N-8
Figure HO-1	Illustration of the Use of (Eqn HO-1)	O-1
Figure HO-2	Coordinate System for Calculation of Lateral Displacement of Pile Cap	O-2
Figure HO-3	Calculation of Horizontal Displacement of a point X on the Front Face of a Uniformly Distributed Load acting on a Vertical Plane within a Semi-infinite Homogenous Elastic medium	O-2
Figure HO-4	Lateral Deflection Contour of a Vertical Plane Exerting u.d.l. in a Semi-infinite Homogenous Elastic Medium	O-3
Figure HO-5	Front face of a Pile Cap divided into a Number of Equal Rectangular Elements	O-4
Figure HP-1	Illustrative Plots of Deflection and Moment Coefficients of Pile under Lateral Load	P-3
Figure HP-2	The Winkler's Spring Model for Piles under Lateral Load	P-9
Figure HP-3	An Example Demonstrating the Differences in Deflection and Bending Moment of a Pile with Free Head with and without $P-\Delta$ Effect	P-11
Figure HP-4	An Example Demonstrating the Differences in Deflection and Bending Moment of a Pile with Fixed Head with and without $P-\Delta$ Effect	P-12
Figure HQ-1	Piling Layout Plan and Details for Worked Example HQ-1	Q-3

Figure HR-1	Illustration of Mindlin's Equations for Determination of Various Components of Stresses due to a Vertical Load in a Semi-infinite Elastic Medium	R-1
Figure HR-2	Worked Example HR-1	R-2
Figure HR-3(a)	Normal Stress Contours in kPa on the Wall of Worked Example HR-1	R-3
Figure HR-3(b)	Shear Stress Contours in kPa on the Wall of Worked Example HR-1	R-3
Figure HS-1	Worked Example HS-1	S-2
Figure HS-2	Hydrostatic Pressures on Wall in Worked Example HS-1	S-4
Figure HS-3	Worked Example HS-2	S-5
Figure HS-4	Hydrostatic Pressures on Wall in Worked Example HS-2	S-6
Figure HS-5	Soil Medium Idealized into a Regular Rectangular Mesh	S-7
Figure HS-6	"Flow net" Analysis of Worked Example HS-2 by the Finite Difference Method	S-8
Figure HS-7	Hydrostatic Pressure Contour of Worked Example HS-2	S-9
Figure HS-8	Finite Difference Mesh after Elimination of Nodes of Negative Water Heads and Final Water Profile	S-10
Figure HT-1	Soil Profile for Worked Example HT-1	T-2
Figure HT-2	Graphical Representation of Variation of Stresses with Depth in Worked Example HT-1	T-4
Figure HV-1	Extract from GEO 1/2006 (Figure 6.26) to Explain Randolph's Approach in Settlement Determination	V-1
Figure HV-2	Extract from GEO 1/2006 (Figure 7.9) to Explain Randolph's Approach in Pile Interaction of Settlement	V-3
Figure HV-3	Worked Example HV-1 for a Tension Loading Test	V-3

List of Photographs in Appendix U

		Page No.
HU.1	Driven Steel H-Piles	
Photo HU-1.1	Welding of Pile Shoes	U-1
Photo HU-1.2	Setting-Out of Pile on Ground	U-1
Photo HU-1.3	Installation of Pile in Correct Position	U-1
Photo HU-1.4	Checking Verticality	U-1
Photo HU-1.5	Pitching of Pile (by Hydraulic Hammer)	U-1
Photo HU-1.6	Connection of Pile by Welding	U-1
Photo HU-1.7	Test of Weld	U-1
Photo HU-1.8	Pitching to the Required Depth	U-1
Photo HU-1.9	Installing Transducers on Pile for the PDA Test	U-1
Photo HU-1.10	Pile Driving Analyzer Test Data Displaced on Screen	U-2
Photo HU-1.11	Final Set Measurement	U-2
Photo HU-1.12	Close-up of Final Set Measurement	U-2
Photo HU-1.13	Static Loading Test – Set-up with Kentledge	U-2
Photo HU-1.14	Static Loading Test – Close-up of Load Cell on Top of Pile	U-2

HU.2 Large Diameter Bored Pile

Photo HU2.1	Setting-Out of Pile on Ground	U-2
Photo HU2.2	Set up the Hydraulic Oscillator with Crawler Crane and Drive the Temporary Steel Casing into the Ground	U-2
Photo HU2.3	Excavation using Hammer Grab inside Temporary Steel Casing ...	U-3
Photo HU2.4	Extending the Temporary Steel Casing by Bolting or Welding Connection	U-3
Photo HU2.5	Excavation of rock or similar hard material using Reverse Circulation Drilling Rig for Formation of the Rock Socket.....	U-3
Photo HU2.6	Formation of Bellout by Hydraulic Bellout Bit using Reverse Circulation Drilling Rig	U-4
Photo HU2.7	Installation of Permanent Liner (usually in Zone of Weak Soil) inside the Temporary Casing to Avoid “Necking”	U-4
Photo HU2.8	Installation of Steel Reinforcement Cage inside the Bored Pile Shaft using Crawler Crane	U-4
Photo HU2.9	Cleaning of Pile Base using Airlifting Method by Compressed Air	U-5
Photo HU2.10	Placing Tremie Concrete with Gradual Extraction of the Temporary Steel Casing Concurrently	U-5
Photo HU2.11	Rotary Drilling Rig for Concrete Core Test	U-5
Photo HU2.12	Sonic Logging Test	U-5
Photo HU2.13	Sample of Concrete / Rock Interface	U-5

HU.3 Socketed Steel H-Pile

Photo HU3.1	Drilling with the first Temporary Casing	U-5
Photo HU3.2	Checking Alignment	U-5
Photo HU3.3	Drilling Works by ODEX Method	U-5
Photo HU3.4	ODEX Drilling Bit	U-6
Photo HU3.5	Prefabrication of Steel H-pile for Socket Length Portion	U-6
Photo HU3.6	Double Shelter for Noise and Dust Reduction during Piling	U-6
Photo HU3.7	Casing Joint Preparation	U-6
Photo HU3.8	Splicing of Temporary Casing	U-6
Photo HU3.9	Splicing of Steel H-pile	U-6
Photo HU3.10	Obtaining Rock Sample after Completion of Drilling Operation ...	U-6
Photo HU3.11	Preparation Works for Grouting Work	U-6
Photo HU3.12	Air-lifting before Grouting Work	U-6
Photo HU3.13	Cement Grouting Work for the Socketed H-Pile	U-7
Photo HU3.14	Extracting Temporary Steel Casing by Vibrating Hammer	U-7
Photo HU3.15	Extracting Temporary Steel Casing by Hydraulic Jack under Adverse Condition	U-7
Photo HU3.16	Grouting Testing Work.....	U-7

HU.4 Mini-pile

Photo HU.4.1	Drilling Rig for Mini-pile on Working Platform	U-7
Photo HU.4.2	Drilling Work in Progress (Vertical Mini-pile)	U-7

Photo HU.4.3	Drilling Work in Progress (Raking Mini-pile)	U-8
Photo HU.4.4	Checking Alignment of Mini-pile	U-8
Photo HU.4.5	Splicing of Steel Casing	U-8
Photo HU.4.6	Collecting Rock Sample at Founding Level	U-8
Photo HU.4.7	Air Lifting at Completion of Drilling	U-8
Photo HU.4.8	Prefabrication of Steel Bars	U-8
Photo HU.4.9	Installation of Steel Bars	U-8
Photo HU.4.10	Completion of Pile by Cement Grouting	U-8

HU.5**PIP Pile**

Photo HU5.1	Setting Out of Pile	U-9
Photo HU5.2	Auger Drilling Rod	U-9
Photo HU5.3	Drilling Work in Progress	U-9
Photo HU5.4	Extension of Auger Drilling Rod	U-9
Photo HU5.5	Drilling Completed to the Required Depth of Pile	U-9
Photo HU5.6	Grouting Work of Pile	U-9
Photo HU5.7	Flow Cone Test for Grout	U-9
Photo HU5.8	Initial Setting Time Test for Grout	U-9
Photo HU5.9	Grouting Cube Compression Test	U-9
Photo HU5.10	Completion of Grouting Work	U-10
Photo HU5.11	Prefabricated Steel Cage	U-10
Photo HU5.12	Installation of Steel Cage into the Pile Shaft	U-10
Photo HU5.13	Surveying of the Top Level of Steel Bar	U-10
Photo HU5.14	Stabilizing the Steel Cage (in Grout) by U-bolts	U-10
Photo HU5.15	Inspection of Grout at Top Level of Pile before Backfill	U-10

HU.6**Barrette Construction**

Photo HU6.1	Shallow Trench formed and surrounded by Guide Walls and filled by Bentonite Slurry	U-10
Photo HU6.2	Silos on Site for Re-circulation of Bentonite Slurry	U-10
Photo HU6.3	The Hydromill Machine for Trench Excavation	U-10
Photo HU6.4	Cutter at the bottom of The Hydromill Machine	U-11
Photo HU6.5	Excavation by Hydromill within Guide Walls	U-11
Photo HU6.6	Scrapers used to Clean Trench sides by Removing Excess Filter Cake	U-11
Photo HU6.7	Reinforcement Cage Pre-fabricated on Site	U-11
Photo HU6.8	Lifting Reinforcement Cage	U-11
Photo HU6.9	Lowering Reinforcement Cage into Excavation Trench	U-11
Photo HU6.10	Tremie Concreting for Barrette	U-11
Photo HU6.11	Finished Barrette after Concreting / Grouting	U-11

HU.7**Hollow Box Footing**

Photo HU7.1	Open Excavation for Raft Footing Construction	U-12
Photo HU7.2	Blinding the Bottom Level of the Raft Footing	U-12
Photo HU7.3	Reinforcement Fixing for the Bottom Slab	U-12

Photo HU7.4	Concreting for the Bottom Slab	U-12
Photo HU7.5	Reinforcement Fixing for the Walls	U-12
Photo HU7.6	Concreting for the Walls	U-12
Photo HU7.7	Formwork Erection and Reinforcement Fixing for the Top Slab	U-13
Photo HU7.8	Concreting for the Top Slabs	U-13

H1 GENERAL

As similar to the Handbook to Code of Practice for Foundations 2004, this Handbook explains and elaborates the Code of Practice for Foundations 2017 on a clause by clause basis, with the clause numbers prefixed by the letter “H” for ease of identification and distinction. Figures, tables and equations in the Handbook are also prefixed by “H” for the same purpose.

H1.1 SCOPE

The “Code of Practice for Foundations” is referred to as “the Code” hereafter in this Handbook.

The Code covers mainly analysis, design, site investigation, construction and testing of foundations. Relevance to local practice is emphasised.

The Code contains deemed-to-satisfy requirements (satisfying the Hong Kong Building (Construction) Regulations). However, justifications based on the principles of mechanics are also permitted, including rational design methods for determination of the ultimate capacity of subgrades.

Cross references to other technical documents and codes including the current Codes of Practice for the Structural Use of Concrete and Steel for design are also included. The Code permits both ultimate limit state and permissible stress methods in the design of structural elements. However, avoidance of over-stressing a foundation element beyond its yield strength under the application of the required test load needs also to be considered in design which constitutes a limiting minimum design strength constraint.

Analysis and design approaches together with a number of worked examples have been included in this Handbook to illustrate the use of recognized approaches in solving specific engineering problems. But it must be stressed that these do not represent the only acceptable approaches. Others based on sound laws of mechanics with justified design parameters are also acceptable.

H1.2 GLOSSARY

Elaborations / clarifications of some of the terms defined by the Code in this section are stated as follows :

Allowable load and Allowable bearing pressure

The allowable load refers to the working load being applied to the foundation and the subgrade which is usually the “characteristic load” (normally defined as the load with a 5% chance of being exceeded). The allowable bearing pressure is often taken as the “ultimate bearing capacity” divided by a factor of safety which is checked against the allowable load in design.

Bell-out

The function of the bell-out of a bored pile is to increase the end-bearing capacity of the pile due to the enlarged base area so that the structural capacity of the concrete can be more fully utilized. The general configuration of a bell-out is as shown in Figure H1.1 in relation to the rockhead and founding levels, with the limitation of the bell-out diameter to 1.65 times the shaft diameter of the pile (Re clause 5.4.7) which can be taken as that formed above bedrock as shown in the figure. The limitation of the bell-out size is to avoid ineffective spreading of the load from the bored pile shaft to the rock bearing stratum. Furthermore, in addition to the bearing on rock under the use of bell-out, the Code also allows inclusion of bond / frictional resistance derived from rock for a height not greater than the lesser of 3m and the rock socket diameter as part of the pile's load carrying capacity as provided in clause 5.4.7. However, the socket length can be doubled (the lesser of 6m and twice the rock socket diameter) if no bell-out is used.

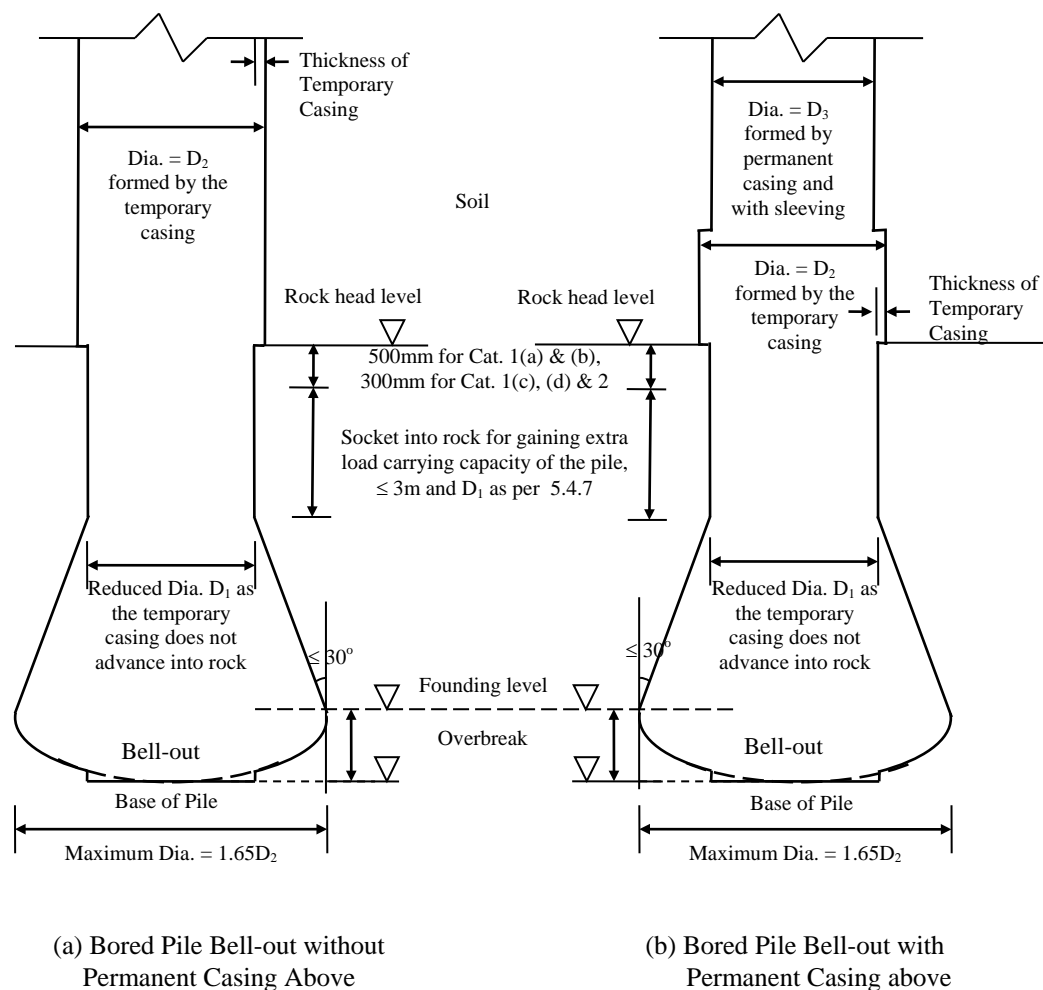


Figure H1.1 – General Configuration of Bell-Out of Bored Pile

Final set

The final set (denoted by the symbol s) is defined in the Code as the penetration per blow of the driving hammer which is the same as that GEO Publication 1/2006. As distinguished from the elastic displacement of the pile and the soil (usually denoted by $C_p + C_q$), which is recoverable after the strike by the hammer, the set is the permanent settlement of the pile which is non-recoverable.

The local practice generally is to calculate the final set as the average set value of the last 10 pile driving blows in accordance with the following typical final set graph contained in Figure H1.2.

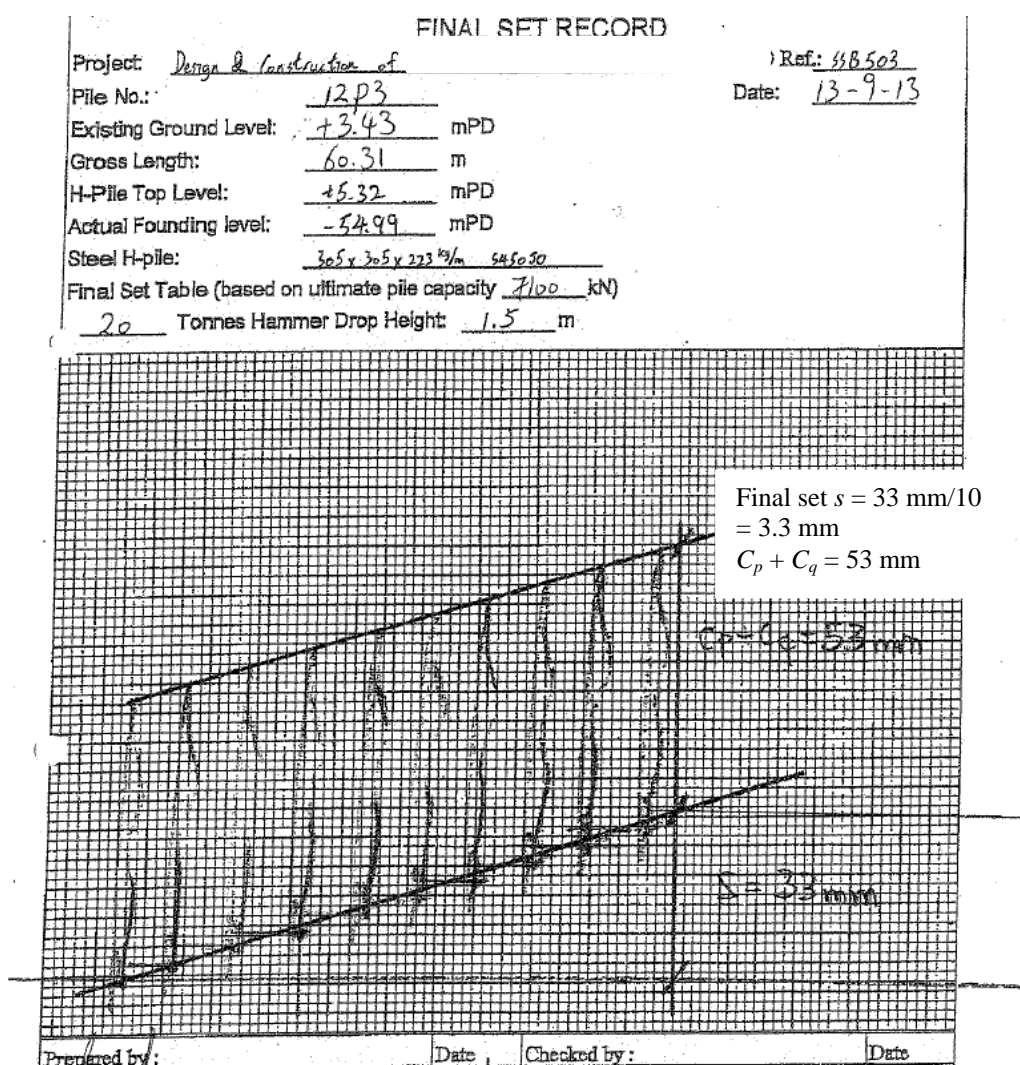


Figure H1.2 – Typical Final Set Graph

Rock Socket

Rock should be of the required design grade or better.

Test Driving of Pile

Test driving of a pile is often carried out prior to commencement of the main piling work and is required even for recognized types of piles, normal installation method and normal ground geology. Apart from verification of design assumptions, integrity and constructability can also be verified with respect to the installation method, ground geology and founding level by the test driving. The term should include installation of both percussive and non-percussive piles such as driven piles, socketed piles and mini-piles. Loading test is normally not required.

Test pile

A test pile refers to a completed working pile chosen among others to undergo testing (usually a loading test) for verification of its load-carrying capacity and/or displacement characteristics. The success or failure of the test will lead to acceptance, rejection or a requirement for further tests of the bulk of the remaining working piles represented by the test pile.

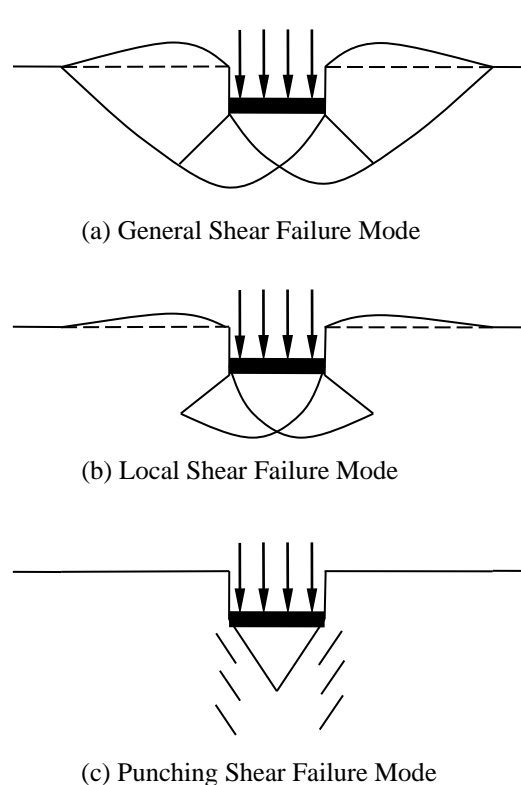
Trial pile

A trial pile is often required for (i) a new pile type; (ii) an unconventional design method, or verification of a set of design parameters, and/or a new installation method; (iii) a pile type and/or installation method where there is inadequate local experience; and/or (iv) a site with complex geology, and/or (v) steel H-piles driven to bedrock with design net length shorter than 10m and for any other special reasons. Installation and test of the trial pile is often carried out prior to commencement of the main piling work. Loading test, if feasible, will normally be required.

Ultimate Bearing Capacity

The definition in the Code includes both full mobilization of the resistance of the bearing stratum and substantial deformation. However, the latter is not well defined or quantified. BS8004:2015 which names by another term “ultimate unit base resistance” has referred to BSEN1997-1-2004 for defining the term “resistance” as “capacity of a structure to withstand actions without failure, e.g. resistance of the ground.” Conventionally ultimate bearing capacity is defined as failure (shear failure according to Craig (2004)) of the subgrade which involves splitting or tearing away of the subgrade structures generally in the modes illustrated in Figure H1.3 with reference to a strip footing.

The deformation at ultimate bearing failure is very large and is normally not quantified as a criterion for defining ultimate bearing capacity. The control of deformation, however, is taken as a separate criterion for foundation design as in clause 2.1.1 in which a foundation has to be designed so that it (i) possesses a factor of safety of 2 or 3 over the ultimate bearing failure; and (ii) has a limiting deformation (quantified) under the working load condition. It should also be noted that the equation given in clause 2.2.4 based on soil mechanics principle, is only suitable for failure mode (a) in Figure H1.3.



- (a) General Shear Failure Mode is the mode in which a continuous failure surface occurs as illustrated in the diagram. Ultimately a state of plastic equilibrium is fully developed throughout the soil above the failure surfaces. Upheaving of ground will occur. This mode occurs in soil of low compressibility, i.e. dense or stiff soils;
- (b) Local Shear Failure Mode is the mode in which there is significant compression of the soil underneath the foundation but only partial development of the state of plastic equilibrium. Failure surfaces do not reach the ground and only slight upheaving is found. The failure is associated with large displacement which is not well defined;
- (c) Punching Shear Failure Mode occurs when shearing failure occurs in the vertical direction along the edges of the foundation, causing large displacements. This mode of failure occurs also in soil of low compressibility.

In Hong Kong, generally footings on loose sand are not preferred. If founding has to be carried out on loose sand, failure modes (b) or (c) may take place which is/are not preferred.

The bearing capacity equation quoted in H2.2.1 is applicable to Mode (a).

Figure H1.3 – Modes of Failure for Ultimate Bearing Capacity

H1.3 ABBREVIATIONS

In addition to those of the Code, the following abbreviations are added :

GI	Ground Investigation
GIU	Geotechnical Information Unit of the Civil Engineering Library in the Civil Engineering and Development Department
HKB(C)R	Hong Kong Building (Construction) Regulation
SPT N value	Uncorrected Standard Penetration N value before foundation installation

H1.4 SYMBOLS

A number of symbols are listed in this clause of the Code. Nevertheless, the following should be noted :

- (i) L has been defined as the symbol for pile length in mm in this clause. However, the same symbol has been defined as length of core run in Note (11) under Table 2.1.

H2 GENERAL DESIGN REQUIREMENTS

H2.1 GENERAL

H2.1.1 BASIC REQUIREMENTS

The Code describes the basic requirements for foundation design and construction in this sub-clause. The following are highlighted and discussed:

- (i) The checking of adequacy of the founding soil/rock of a foundation is based on the “allowable capacity” (for bearing, bond or friction) of the soil/rock which should be checked against the “working load” (normally the characteristic load without load factors) imposed on it;
- (ii) The “allowable capacity” of the soil/rock can be determined by the lesser of
 - (1) the “ultimate capacity” (defined as the least pressure which will cause shear failure of the soil/rock) divided by an adequate factor of safety against failure; and
 - (2) limited movement and/or deformation.

The determination of the factor of safety for the former is based on a number of factors as stated in the Code. In practice, the factor of safety is in the range of 2 to 3, depending on the uncertainties in the behaviour of the foundation. For example, the allowable bearing capacity of soil can be obtained from the ultimate bearing capacity divided by a factor of safety of 3, though it is often the settlement or differential settlement which is the controlling criterion. Another example for determination of “allowable capacity” in accordance with the settlement criterion is that of a common driven pile which is the least load acting on the pile to cause a pre-determined limiting settlement divided by a factor of safety of 2;

- (iii) The allowable capacity can be increased by 25% when such increase is solely due to wind which induces load of transient nature.

It should be noted that a foundation should be designed for dead, imposed and wind loads where imposed load covers live loads, water uplift and earth load. This is to accord with the Building (Construction) Regulations and the Code of Practice for Dead and Imposed Load 2011.

H2.1.2 COMPATIBILITY OF DESIGN AND CONSTRUCTION

When determining ultimate capacity or estimating settlement of a foundation, it is important to ensure compatibility among the design approach, use of parameters, method of construction, testing, acceptance standards etc.

H2.1.3 CLASSIFICATION OF SOILS AND ROCKS

GEOGUIDE 3 is referred to by the Code for the classification of soils and rocks. As described by the Guide, there are two kinds of rock descriptions to serve specific purposes. The one for engineering usage of ‘rocks’ and ‘soils’ gives an indication of the likely engineering properties of the rock. The geological classification of ‘rocks’ and ‘superficial deposits’ enables interpretation of the geological structure of an area and good correlation between boreholes. In practice, the geological classification does not include the engineering properties of rock but the engineering properties are often closely related to the geological characteristics.

Rock material weathering in Hong Kong rarely produces a homogeneous weathered rock mass where all rock material is weathered to the same degree, or even a simple weathered profile where the degree of weathering decreases progressively with depth. Complex variation of weathering throughout the rock mass is often the rule as seen in the Worked Example HA-1 in Appendix HA which is abstracted from Figure 4 of the GEOGUIDE 3. The presence of discontinuities and the effects of weathering have a great influence on engineering behaviour and should be treated with care.

H2.2 ALLOWABLE BEARING PRESSURE, BOND OR FRICTION OF GROUND

H2.2.1 RATIONAL DESIGN METHOD

Apart from adopting presumed values for the allowable capacity of soils and rocks, the Code allows using a rational design method for calculating the ultimate bearing capacity which, by applying a factor of safety, can be converted to an allowable capacity. A factor of safety of 3 is normally adopted with respect to geotechnical capacity in view of the uncertainties involved. An example of the rational design method is that based on the ultimate bearing capacity equation in the form of $q_u = cN_c + 0.5B\gamma N_\gamma + q_o N_q$ for shallow strip footings as found in common soil mechanics textbooks. A more detailed form of the equation taking account of dimensions and load eccentricities at the footing is given in Vesic (1973) which is also quoted in GEOGUIDE 1 and reproduced in clause 2.2.4 of the Code. It should be noted that the allowable bearing capacity should be checked against the loading pressure calculated based on the effective dimensions of the shallow footings (i.e. B_f' and L_f') instead of the maximum bearing pressure derived from the eccentricity of the loading.

Other factors of safety may be adopted having regard to the nature of the soil or rock, its variability over the site and the reliability of the design method or whether there is some form of proof-testing that has been carried out during pile installation. This applies to the situation when well-established design methods are used. For example, if the Hiley formula is adopted in driven pile design, where the pile will be subject to some form of proof-testing by achieving an acceptable final set value, a lower factor of safety of 2 can commonly be used which is applied to the design working load.

H2.2.2 PRESUMED VALUES

(1) General

The Code has included in H2.2.2 a set of “Presumed Values” for the allowable vertical bearing pressures on horizontal ground in its Table 2.1. These values can be adopted under the conditions stated in paragraphs (1) (a) and (b) of the Code which refers to the sites where site investigations have been carried out and normal structures are to be constructed. It should be noted that the use of the “Presumed Values” does not preclude the requirement for consideration of settlement of the structure which may need to be assessed separately.

(2) Allowable Vertical Bearing Values

The Code refers to Table 2.1 for presumed values of vertical bearing values of soil and rock on the basis of the material description. Some points are discussed as follows :

(i) Category 1(d) Rocks

According to GEOGUIDE 3, a six-fold grade scheme for material decomposition is used to classify the state of decomposition. For engineering design purposes, grade I to III materials generally cannot be broken down by hand and are considered as rocks. Grade IV to VI materials generally can be broken down by hand into their constituents and are considered as soils. Soils of grades IV and V are termed saprolites. They can be distinguished by a simple slaking test because slaking can be readily seen in grade V soil, but not in grade IV, when they are immersed in water.

(ii) Interpretation of Category of Rock Mass against Total Core Recovery

The determination of the “Presumed Values” of rock depends very much on the Total Core Recovery (TCR) and TCR is one of the criteria for the classification of rock as given in Table 2.1 of the Code. It is clarified that recovering rock of a grade lower than the design grade in a core run is acceptable. For example, a Cat 1(c) rock core run can have no more than 15% of material of lower grade than grade III. This is in line with the weathering of the rock mass represented by the Worked Example HA-1 in Appendix HA. In addition, by Notes (5) and (11) following Table 2.1 of the Code, core run (L) should be taken as 1.0m for determination of TCR. And for the determination of TCR of a designated grade of rock, the TCR of 5 consecutive core runs have to achieve the TCR of the grade.

Furthermore, attention should be given to the rock stratum immediately underneath the foundation level which must be rock of the required grade or a better material. However, the weathering of the rock mass may vary in complex fashion and sometimes it is difficult to determine the founding rock from the TCR of a borehole.

(iii) Recommendation on Depth of Pre-design Ground Investigation Boreholes

Note (5) of Table 2.1 requires that the founding stratum should be proved to a depth of at least 5m into the specified category of rock because a rock layer of thickness less than 5m is traditionally treated as corestone. However, in the case of piles with a rock socket, the requirements on pre-drilling should be followed as stipulated in para. 10 of PNAP APP-18. In such cases, the drilling should be sunk into the rock mass for at least 5m below the rock head of the specified grade or the designed length of the rock socket of the nearest pile, whichever is the deeper.

(3) Allowable Lateral Bearing Pressure for Rock

Clause 2.2.2(3) of the Code is self-explanatory.

(4) Allowable Bond or Friction between Rock and Concrete

Table 2.2 of the Code specifies different values of presumed allowable bond or friction between rock and the concrete of piles for the conditions “under compression or transient tension” and “under permanent tension.” It should be understood that transient tension refers to tension in the foundation structure under transient loads such as wind loads whereas permanent tension results from persistent dead loads, soil loads and the like. As an example, a load case of “Dead Load minus Wind Load” resulting in tension should be considered a transient tension. However, tension resulting from flotation should not be considered as transient as the duration of the flotation load can be long, possibly half a day in the case of tidal variation or even longer for severe storm conditions.

(5) Footings of Minor Temporary Structures

The clause allows the use of allowable vertical bearing pressure of 100kPa (if dry) or 50kPa (if submerged) for the design of minor temporary structures which should include fencing, hoarding, lamp pole, covered walkway, disabled ramp, minor single storey buildings – e.g. refuse collection point, pergola.

H2.2.3 IN SITU TESTING METHOD

Examples of insitu testing methods include the “Plate Load Test” and the full scale loading test.

H2.2.4 BEARING CAPACITY EQUATION METHOD

Allowable Vertical Bearing Pressure of Shallow Foundation founded on Soil

The clause first lists an equation for determination of allowable vertical bearing pressure q_a for shallow foundations (depth to bottom not greater than 3 m by Note (1)) as follows :

$$q_a = \frac{q_u - q_o}{F} + q_o$$

where q_u is the ultimate bearing capacity, q_o is the effective overburden pressure at the base of the foundation due to the soil originally exists above the foundation and F is the

factor of safety not less than 3. The applicability of the formula is irrespective to whether there will be soil backfill over the top of the foundation after construction.

The above equation is actually derived from the following relation :

$$\frac{q_u - q_o}{q_a - q_o} = F$$

where $q_u - q_o$ and $q_a - q_o$ refer to the effective ultimate bearing capacity and allowable bearing capacity after reduction of q_o which is often known with high certainty. The ratio of $q_u - q_o$ to $q_a - q_o$ is the required factor of safety F .

The clause lists the general equations for determination of q_u for shallow foundation with limitations based on the work of Vesic (1973, 1975) which have been quoted in GEOGUIDE 1. A worked example is contained in Appendix HB of this Handbook.

Nevertheless, it should be noted that though the use of the bearing capacity equation for foundations on soil can often achieve values significantly higher than the presumed values in Table 2.1, two restraints are imposed :

- (i) q_u is limited to 3000kPa;
- (ii) Plate load tests have to be carried out as per clause 4.2.2(2).

In addition, the Code has provided in Figure 2.4 that the application of the bearing capacity equation to an irregular shaped shallow footing can be taken as that of a rectangular one with dimensions as the largest inscribed rectangle in the irregular shape of the footing. As the bearing capacity increases generally with the plan dimension of the footing, the approach is generally a conservative one for homogeneous soil or for soil strata with strength increasing with depth.

H2.2.5 OTHER METHODS

Clause 2.2.5 of the Code is self-explanatory.

H2.3 FOUNDATION SETTLEMENT AND ROTATION

H2.3.1 ESTIMATION OF SETTLEMENT

(1) General

The Code outlines the general principles in foundation settlement estimation in this clause which should be determined by principles of mechanics based on appropriate soil parameters obtained by proper site investigation and laboratory work. Also settlement comprises immediate settlement and secondary settlement (or creep).

(2) Foundations on Granular Soils

The Code lists the following formula for estimation of immediate settlement of foundations on granular based on the elastic theory

$$S_e = \frac{q_{net} B_f ' F_o}{E_s}$$

where the symbols are defined in the Code.

The formula is a popular one listed in common text books which can used to calculate the settlement of a rectangular loaded area with different values of F_o depending on length breadth ratio of the footing, hard stratum depth to footing breadth ratio, buried depth to footing breadth ratio and Poisson's ratio of the soil. The Code refers the determination of the coefficient F_o to GEO Publication No. 1/2006 (in clause 3.2 of the Publication). Poulos & Davis (1974) and Tomlinson (2008) contain charts and tables for deriving the F_o under different loading configurations and loaded area in resting on elastic medium. A series of charts for quick estimation of mean settlements of rectangular footings covering variations of the afore-mentioned parameters, together with the basic principles, analytical approach and worked examples for single and multi-layered soils are included in Appendix HC for ease of use by the readers.

[A digital copy of the book by Poulos & Davis (1974) is published and with the permission of the authors and can be downloaded in this link:

<http://research.engr.oregonstate.edu/usucger/PandD/PandD.htm>

(3) Foundations on Fine-Grained Soils

In fine grained soils, the immediate settlement depends on the rate of the dissipation of excess pore water pressure caused by the application of the foundation loads. This is usually termed as primary consolidation settlement. Soils continue to deform after the primary consolidation settlement and this process is termed as secondary compression (or creep). Nevertheless, the followings are highlighted for reference by the readers :

- (i) Primary consolidation is the process by which water is expelled from the fine-grained soil leading to decrease in volume and thus settlement under long term loading. As the permeability of the soil is low, the consolidation process will take time, the completion of which may take years. Primary consolidation can be regarded being completed when the excess pore water pressure has dissipated to zero;
- (ii) Secondary consolidation follows that of the primary consolidation which is caused by creep – gradual readjustment of the soil particles to a more stable configuration which leads to further settlement. The time at which secondary consolidation commences is not well defined. A pragmatic approach is to assume that the secondary consolidation settlement commences when 95% of the primary consolidation is reached;
- (iii) The soil is described as over-consolidated, normally consolidated or under-consolidated if it has been under a pre-consolidated stress which is higher, identical or smaller stress in the past as compared with the present

- stress. The past history of stress affects the consolidation settlement under applied stress $\Delta\sigma_v$;
- (iv) The soil parameters including the pre-consolidated stress can be estimated by the oedometer test.

(4) Young's Modulus

In the estimation of settlement, the use of soil and rock parameters based on ground investigation results are crucial. The determining parameter, which is the Young's modulus, E of soil can be determined by appropriate laboratory or in-situ tests such as the plate load test. Nevertheless, the Code suggests the correlation $E = N$ (in MPa) for granular soils in the absence of more accurate if the design allowable bearing capacity is not greater than 250kPa. In addition, there are also recommendations in other references including GEO Publication 1/2006 (2006) Table 6.10 relating E to SPT N values.

(5) Poisson's Ratio

The Code suggests ranges of Poisson's ratios of soils as related to their SPT N values. As high Poisson's ratio implies more significant effects from lateral strains or stresses, smaller soil settlement in the direction of the applied load and higher lateral stress / strain are anticipated in the soil with higher Poisson's ratio.

H2.3.2 ACCEPTABLE SETTLEMENT AND ROTATION

(1) General

Clause 2.3.2(1) of the Code is self-explanatory.

(2) Reference Criteria

Notwithstanding (1), the Code suggests some reference criteria for settlements and rotation at base of footing and under-side of pile cap for buildings or structures not particularly sensitive to movement under conditions listed in the clause. Nevertheless, as the settlement of upper levels of a building structure due to dead load can be adjusted throughout the construction sequence, it should be reasonable to take half of the dead load for estimation of settlement.

Criteria of other recommendations and codes are listed as follows for readers' reference. These include that by Skempton and MacDonald (1956) recommending maximum slopes (between any two points within a single foundation unit or in separate foundation units) to vary from 1 in 500 for steel and concrete frame infilled structures to 1 in 200 where there is no infill or no danger of damage to the cladding. Furthermore, Meyerhof (1956) recommended limiting slopes to 1 in 250 for open frames, 1 in 500 for infilled frames. Burland (1975) gives a comprehensive summary of the recommendations of these past researches. In addition, the Eurocode BSEN1997-1:2004 Annex H states that total settlements up to 50mm are often acceptable for normal structures with isolated foundations and a maximum relative rotation of 1 in 500 is acceptable for many structures in a sagging mode and half of that value for a hogging mode. Furthermore, the

Canadian Foundation Engineering Manual (1992) suggests that the total settlement is not to exceed 80mm for structures on clay and 40mm for structures on sand and the maximum slopes for reinforced concrete frames to vary from 1 in 400 to 1 in 250 and for steel frames to be 1 in 500 (continuous) and 1 in 200 (simply supported), leaving the maximum deflection between supports to be determined by design. So the limits of 1 in 500 for gravity load and 1 in 500 for transient loads are of the same order as the above and generally on the conservative side. But as far as the structural integrity is concerned, differential settlement is often more critical than absolute settlement.

(3) Individual Case

The Code requires checking of the structure against ultimate and serviceability limits if the criteria in (2) cannot be satisfied.

H2.4 STRUCTURES ON NEWLY RECLAIMED LAND

Clause 2.4 of the Code is self-explanatory.

H2.4.1 GENERAL DESIGN RULES

The Code has set a number of design rules in this sub-clause which are generally applicable to structures built on newly reclaimed land. The rules, being more or less identical to those listed in PNAP APP-103, aim at minimizing damage to structures and non-structural components due to settlements and differential settlements.

To avoid the migration of soil into voids underneath a pile cap formed by ground consolidation as discussed in item (f) of the sub-clause, Figure H2.1 illustrates an effective measure for reference which is the construction of a short wall. The figure is reproduced from the figure in Appendix A of PNAP APP-103 with the additional illustration of the short wall.

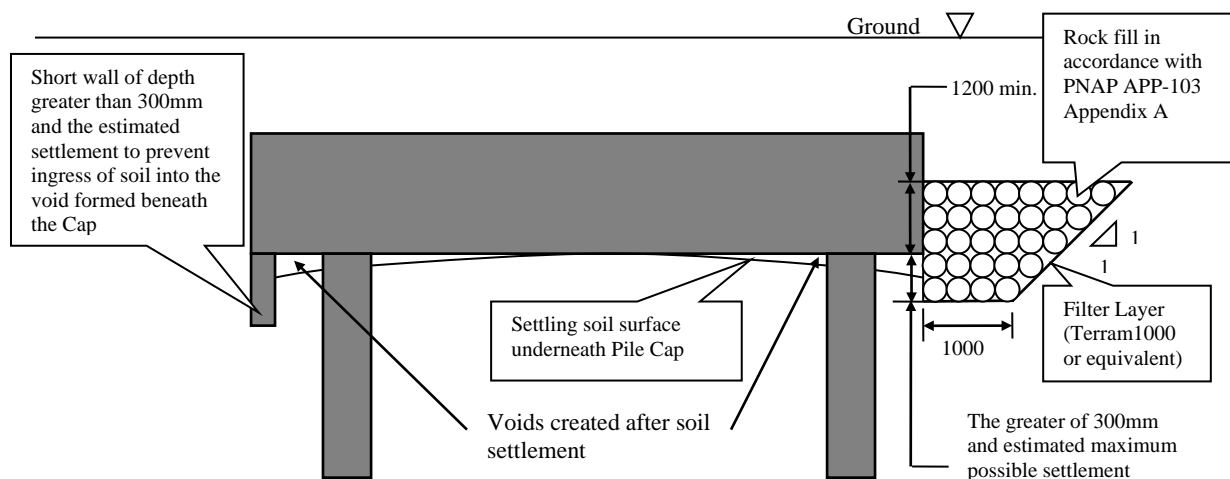


Figure H2.1 – Measures to mitigate the Migration of Soil into any Voids that may be formed underneath the Suspended Structure

Nevertheless, it should be understood that assessment of settlements cannot be totally ignored even if measures in this sub-clause have been implemented.

H2.4.2 ALTERNATIVE APPROACH

In addition to the considerations discussed in this sub-clause when an Alternative Approach is adopted for design of structure on newly reclaimed land, effects due to loads from adjacent features, including structures, should also be considered as necessary as they might create extra stresses and deformations.

H2.4.3 LONG-TERM MONITORING AND/OR MAINTENANCE

The long-term monitoring and/or maintenance requirements may take the form of a “performance review” which may be required in Scheduled Areas, sites of complex geology and for special structures. The usual forms of long-term monitoring include building settlement and tilt and ground-water table monitoring.

H2.4.4 RECLAIMED LAND WITH CONSOLIDATION SUBSTANTIALLY COMPLETED

Theoretically the time of a certain percentage of consolidation completion depends on the coefficient of consolidation c_v and the length of drainage path. The latter can be taken as the thickness of soil layer if the bottom level touches an impermeable layer or halved the thickness of soil layer, if otherwise. Nevertheless, the Code has, as a general guidance, tabulated the number of years for achieving 95% consolidation for different ranges of thickness of clayey deposits. Apart from those design rules being exempted from complying with clause 2.4.1, other design considerations such as negative skin friction can also be ignored.

H2.5 STRUCTURAL REQUIREMENTS

H2.5.1 GENERAL

In addition to the compliance requirement with the Hong Kong Buildings (Construction) Regulations, reference to relevant requirements from other well-established codes of practice such as the British Codes and European standards and the general laws of mechanics can also be made for the structural design of foundations.

H2.5.2 DESIGN LOADS

Apart from the Building (Construction) Regulations Section 17, the Code of Practice for Dead and Imposed Loads 2011 published by the Buildings Department should be referred to for the determination of the design loads. In addition, reference should be made to the circulars issued by the Fire Services Department giving updated loads for fire engines if the structure has to be designed to carry fire engines.

It is a popular local trade practice to design separately the foundation and superstructure of a building. The foundation is designed using a set of assumed loads from the

superstructure prior to detailed analysis of the superstructure. Nevertheless, the Code requires the design to demonstrate that the loads from detailed calculations of the superstructure do not exceed the assumed loads used in the foundation design.

In addition, in the case that a foundation design is controlled by sliding or overturning stability and stability is ensured only by a heavier gravity load from the superstructure, the foundation may need to be re-checked under a gravity load reduced from the original assumed loads.

For a foundation which has to undergo a “static load” test, the maximum test load can be 2 to 3 times the foundation working load which is generally greater than the partial load factors used for ultimate strength design. So this can be regarded as another limit state that has to be taken into account for design.

For the determination of soil loads, active pressure only should be used in checking stability of the whole structure where adequate soil movement is allowed. Full passive pressures should only be included when the designer is confident that they will be mobilized for the duration of loading. It should be noted that the movement to fully mobilize the passive pressure is usually large unless there is a lock-in movement due to the construction sequence of the structure. Generally the structural design of members should be based on at rest soil pressure instead of active soil pressures.

H2.5.3 UNDERGROUND WATER

Clause 2.5.3 of the Code is self-explanatory.

H2.5.4 RESISTANCE TO SLIDING, UPLIFT AND OVERTURNING

The clause is identical to the provisions in the current Building (Construction) Regulations except that the factor applied to the uplift force due to ground water as a de-stabilizing load based on “highest possible groundwater table” is 1.1 instead of 1.5. Summarizing the provisions stated in the clause, (Eqn H2.1) to (Eqn H2.3) can be listed as below as stability check against sliding, uplift and overturning respectively. The structure can be regarded as having achieved the required factor of safety in stability check if the equations are satisfied.

$$\frac{S_{\text{stabilizing}}}{f_u \times S_{\text{sliding (flotation)}} + 1.5 \times S_{\text{sliding (others)}}} \geq 1.0 \quad (\text{Eqn H2.1})$$

$$\frac{F_{\text{stabilizing}}}{f_u \times F_{\text{uplift (flotation)}} + 1.5 \times F_{\text{uplift (others)}}} \geq 1.0 \quad (\text{Eqn H2.2})$$

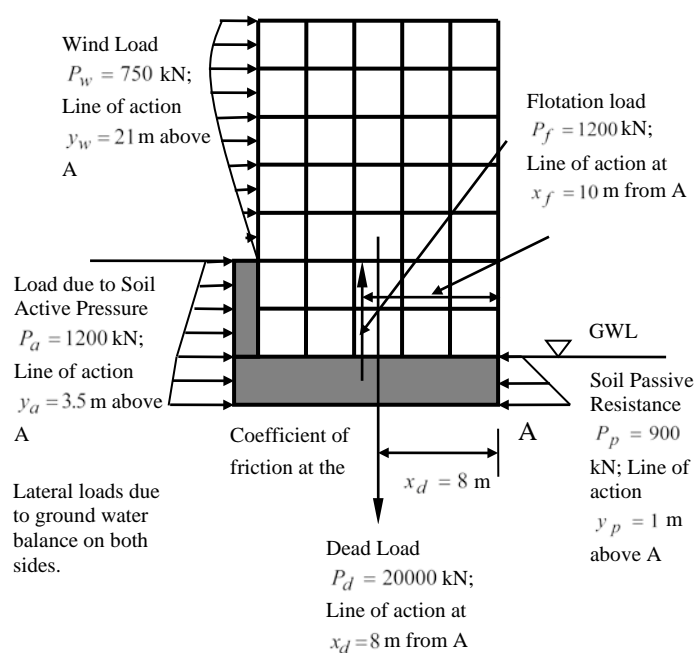
$$\frac{M_{\text{stabilizing}}}{1.5 \times M_{\text{overturning (wind)}} + f_u \times M_{\text{overturning (flotation)}} + 2.0 \times M_{\text{overturning (others)}}} \geq 1.0 \quad (\text{Eqn H2.3})$$

In the above inequalities, the terms S , F and M in the numerators represent stabilizing lateral forces, vertical forces and moments against the wind, soil, water flotation loads causing instability respectively. These stabilizing forces and moments are usually provided by the structure’s own weight and other anchoring forces to the ground, if any.

For the factor f_u , it is 1.5 if the check is based on highest anticipated groundwater table and becomes 1.1 if the check is based on highest possible groundwater table.

Worked Example H2.1 for the structure shown in Figure H2.2 demonstrates the use of the above inequalities. In the example, the case of highest anticipated groundwater table is considered with level as marked on the figure by which lateral hydrostatic load balances out. It should be noted that the most adverse combination of loads should be used in determining the factor of safety including (i) wind and soil loads acting in the same direction; (ii) the live load in the building ignored; (iii) live load acting as surcharge only on the active soil pressure side; and (iv) highest water table on the active pressure side. In addition, the stabilizing force due to the soil passive pressure may have to be ignored if there is probable removal of the soil offering the passive resistance during the life time of the building.

Worked Example H2.1



(i) Check Sliding Stability

Sliding Force

kN

Passive Soil Resistance = 900kN

Friction at the Base of the Building

kN

Factor of Safety against Sliding is

O.K.

(ii) Check Uplift Stability

O.K.

(iii) Check Overturning Stability (about A)

Overturning moment by wind about A is

kNm

Overturning moment by active soil pressure about

A is

kNm

Overturning moment by flotation about A is

kNm

Stabilizing moment by passive soil pressure about

A is

kNm

Stabilizing moment by dead load about A is

kNm

Checking against Overturning is

O.K.

Figure H2.2 – Worked Example H2.1 for Checking Stability

It should also be noted that the clause is for checking global stability of the whole building or structure. It is generally not necessary for buildings with adequate rigidities or ties at the foundation level to check that every foundation element of the building such as individual footings or piles can achieve the same factor of safety. However, if each foundation element can achieve the same factor of safety, stability of the whole structure can be deemed satisfactory. An example is the checking of all piles. If there is no tension in any piles, this obviously implies stability of the whole building or structure against overturning. Checking of pile loads can be carried out according to the following inequality which is extracted from clause 5.1.6 :

$$P_{\min DL} + 0.9P_{\text{anchorage}} \geq 1.5P_{\text{wind}} + f_u P_{\text{floatation}} + 2.0P_{\text{others}} \quad (\text{Eqn H2.3})$$

where $P_{\min DL}$ is the minimum dead load on the pile

$P_{\text{anchorage}}$ is the effective ground anchorage

P_{wind} is the uplift load on the pile due to wind

$P_{\text{floatation}}$ is the uplift load due to flotation

P_{others} is the uplift load due to that other than wind and flotation

f_u is 1.5 if the upthrust is due to the highest anticipated ground water table but can be reduced to 1.1 if the water is due to highest possible groundwater level

H2.5.5 MATERIALS AND STRESSES

(1) General

Traditionally design of foundations in Hong Kong has been based on the working stress method for both the checking of ground bearing and the structural design of individual structural elements. However, in recent years limit state design has been becoming popular for concrete foundation members, though not yet so popular for structural steel members. This clause in the Code reflects this practice by making references to the current Codes of Practice for Structural Use of Concrete and Steel which are based on limit state design.

Nevertheless, the permissible stress design method is still allowed which can be conveniently used in design of mini-piles and steel piles because of the requirement to ensure that the steel bars or sections are not to be stressed beyond their material yield strength during a load test where the test load is twice that of the design working load.

(2) Concrete

The followings are highlighted :

- (i) Limit state design should be adopted generally for structural design of footings, cast-insitu-piles while leaving the bearing stresses on rock or soil to be checked against working loads. However, the design of driven precast concrete pile may still have to follow the permissible stress method as the Code limits the axial compressive stress on the pile under working loads to $0.2f_{cu}$;
- (ii) The Code specifies a 20% reduction in “strength” for concrete where water is likely to be encountered during concreting or when concrete is placed underwater or alike. The requirement is more general than the provision in the Hong Kong Building (Construction) Regulation (HKB(C)R) which instead limits concrete stresses to 80% of the appropriate limitation of “design stress”;

(3) Grout

Clause 2.5.5(3) of the Code is self-explanatory.

(4) Steel

The followings are highlighted :

- (i) Though allowable stresses for structural element design are specified in the clause, the Code allows both the permissible stress method and the use of the Code of Practice for the Structural Use of Steel 2011 which involves ultimate limit state in structural element design. A practitioner can easily work out that the structural design of steel to the limit state, in accordance with the Code of Practice for the Structural Use of Steel 2011, is more economical than the permissible stress method by simply comparing the design working axial stress (stress due to axial load only) of steel, of the order of 30% to 50% of the yield stress to that of the limit state method based on the almost full yield stress, ($0.9p_y$ to $1.0p_y$) even with the application of partial load factors ranging from 1.2 to 1.6. Nevertheless, as there is again the requirement of a loading test with a test load twice the working load, as for a mini-pile and others, the load carrying capacity will be capped at values similar to those applying the permissible stress method;
- (ii) The allowable bond stress between steel and grout (minimum characteristic strength 30MPa at 28 days) for both compression and tension specified in the Code are 400kPa or 320kPa when grouting under water. However, local testing work by Chung (2005) and Wang et. al (2005) showed that the ultimate values for compression are in the range of 300kPa to 600kPa if grouting is done in dry conditions and the grout is unconfined, giving allowable values of 150kPa to 300kPa upon an application of a safety factor of 2 which are significantly less than those specified in the Code. Nevertheless, the ultimate bond strengths are significantly increased when the grout is placed under confined conditions (confinement in the steel tube), up to 850 to 1160kPa with their allowable values (ultimate values divided by 2) in the order of the values specified in the Code. The phenomenon of higher bond strengths where the grout is confined occurs because the confinement increases the lateral stresses and subsequently the bond strengths (largely contributed by friction) which depends on lateral stress;
- (iii) The use of shear connectors can obviously enhance bond stress between the section and the grout. The Code allows the increase in the allowable bond stress to 600kPa (or 480kPa when grouting under water) under the use of shear studs designed in accordance with the Code of Practice for the Structural Use of Steel 2011. The Code also mentions that steel sections or other means as substitute for shear studs may also be used. It has been a practice of the local industry to weld steel cross bars along the flanges of the steel pile for shear connections as illustrated in Worked Example 2.2 which follows;

- (iv) It is therefore advisable to (a) adopt reduced bond strengths between the grout and the steel section above the rock socket; and (b) enhance the bonding in the rock socket by the use of “shear connectors” which can sustain at least 50% of the bond force. Typical arrangements for the use of welded cross bars for enhancement of bond within the socket for a socketed pile are shown in Figure H2.3;

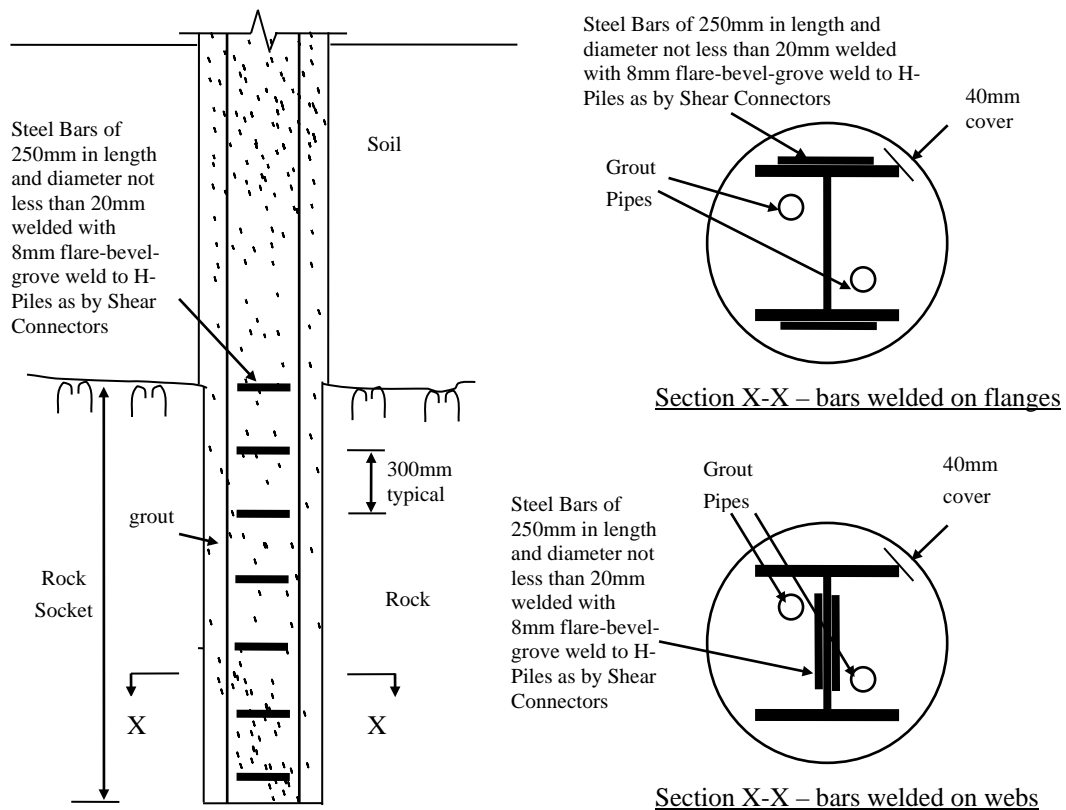


Figure H2.3 – Typical Socketed H-Pile with Cross Bars as Shear Connectors

The following Worked Example H2.2 for a grade S450J0 305×305×223kg/m socketed pile with bond strength enhanced by shear studs is demonstrated as follows :

Worked Example H2.2 :

Pile Section : grade S450J0 305×305×223kg/m

Perimeter of the Pile Section = 1918mm

Maximum Pile Compression Load : 6000kN

Pile Socket Length : 5m

Shear Studs (Class 1) : nominal shank diameter $d = 22 \text{ mm}$;
 nominal height $h = 100 \text{ mm}$

Ultimate Tensile Strength of Stud : $f_u = 450 \text{ MPa}$

Grout Cube Strength : $f_{cu} = 30 \text{ MPa}$

Young's Modulus of Grout : $E_{cm} = 22000 \text{ MPa}$

(The E_{cm} value is quoted from Table 3.2 of the Code of Practice for the Structural Use of Concrete 2013 for concrete of grade C30, as the Code cl. 2.5.5(3) states that the requirements (including the use of the Young's modulus) of concrete applies to that of grout)

Allowable bond stress between steel and grout (concreting under water) = 320kPa without shear studs or other substitutes.

So the total bond force that can be provided by the bare bond between the grout and the pile is $1.918 \times 5 \times 320 = 3068.8 \text{ kN}$

If shear stud is to be used to enhance the bond force, characteristic strength of a shear stud is (in accordance with Eqn (10.20) of the Code of Practice for the Structural Use of Steel 2011)

$$P_k = 0.29d^2\alpha\sqrt{0.8f_{cu}E_{cm}} = 0.29 \times 22^2 \times 1\sqrt{0.8 \times (0.8 \times 30) \times 22000} \times 10^{-3} = 91.22$$

$$\text{kN} \leq 0.8f_u\left(\frac{\pi d^2}{4}\right) = 0.8 \times 450 \times \left(\frac{\pi \times 22^2}{4}\right) \times 10^{-3} = 136.85 \text{ kN (shear resistance of$$

the stud) as $\frac{h}{d} = \frac{100}{22} = 4.55 > 4 \Rightarrow \alpha = 1$ (Note: f_{cu} of grout is discounted by 20% to allow for grouting in water).

As the shear stud is Class 1 material, the partial strength factor $\gamma_{m1} = 1.0$ is used in accordance with Table 4.1 of the Code of Practice for the Structural Use of Steel 2011. So the design strength of the shear stud is $P_k = 91.22 / \gamma_{m1} = 91.22 \text{ kN}$.

Treating the shear stud as if it is in slab under negative moment as per clause 10.3.2.1 of the Code of Practice for the Structural Use of Steel 2011 for conservative design, its design resistance is $P_n = 0.6P_k = 0.6 \times 91.22 = 54.73 \text{ kN}$.

The bond strength of a socketed pile can thus be enhanced by adding an appropriate number of shear studs, bearing in mind that the overall bond strength has to be capped at 480kPa according to the Code which is 50% over the bare bond strength of 320kPa. So the enhancement should be limited to $3068.8 \times 0.5 = 1534.4 \text{ kN}$, requiring $1534.4 / 54.73 = 28$ nos. of shear studs.

Alternatively, T20 cross bars of length $L_b = 250 \text{ mm}$ with spacing $s = 300 \text{ mm}$ along the pile can be used as shear connectors. The shear connection is derived from the bearing resistance of the bars on the grout. By cl. 6.2.2.3(m) of the Code of Practice for Structural Use of Concrete 2013, the ultimate bearing strength is $f_{bu} = 0.6f_{cu} = 0.6 \times 0.8 \times 30 = 14.4 \text{ N/mm}^2$.

The allowable bearing strength is $f_{ba} = 0.5f_{bu} = 0.5 \times 14.4 = 7.2 \text{ N/mm}^2$;

The bearing area of a bar is $A_b = 20 \times 250 = 5000 \text{ mm}^2$;

The allowable resistance per a bar is $f_{ba} \times A_b = 36 \text{ kN}$.

So $1534.4/36 = 42.6$ or 44 nos. of cross bars are required.

During loading test when the applied load is twice the working load, the bond stress should at most be twice the working stress and this load can be safely resisted as the ultimate bond strength is twice that of the allowable working stress.

H2.6 CORROSION PROTECTION OF FOUNDATIONS

H2.6.1 GENERAL

In general, this sub-clause requires that corrosion by the external environment (soil and underground water) will not weaken the foundation to such an extent that structural inadequacy results during the life time of the foundation. For example, the loss in thickness of a steel pile will not render its strength inadequate (by reduction of the cross sectional area) to resist the imposed load during its life time (say 50 years).

H2.6.2 CONCRETE FOUNDATIONS

Concrete is a comparatively durable material. Yet, it is still susceptible to attack by sulphates, chlorides, alkali-aggregate reactions, acids etc. in the presence or absence of reinforcements. This sub-clause requires protections proposed to mitigate these effects to be shown on the foundation plans if these aggressors exist in the ground. The mechanisms of corrosion by such aggressors on concrete are briefly discussed as follows :

- (a) Sulphate attack on concrete, in accordance with Neville (1995), refers to the chemical reactions in hardened concrete in which (i) tricalcium aluminate (C_3A) hydrate in the concrete reacts with a sulphate salt from outside to form calcium sulfoaluminate which will result in a volume expansion of 227%; and (ii) base exchange between calcium hydroxide and the sulphate to form a gypsum with volume expansion of the solid phase up to 124%. As the expansions are within the framework of the hydrated cement paste, gradual disintegration of concrete takes place. However, as remarked in the MTR New Works Design Standards Manual (2008) (NWDSM), Hong Kong soils contain negligible amounts of naturally occurring sulphates and therefore sulphate attack in natural soil is generally insignificant. Nevertheless, if sulphate content is found to be excessive in areas of reclaimed land, marine environments, leaking water mains and/or service reservoirs, preventive measures including use of sulphate resisting cement concrete should be implemented. The sulphate resisting cement has a low content of C_3A . Use of PFA and GGBS as cement replacement, which can alternatively decrease the content of C_3A is also beneficial to sulphate resistance. NWDSM classifies soils with sulphate content below 0.24% and groundwater with sulphate content below 0.4 gm/litre as non-aggressive.

Chloride attack is distinct in that its primary action is the corrosion of the steel reinforcement in the concrete instead of direct corrosion of the concrete. The chloride first breaks through the protective passivity layer formed by the alkaline environment of the concrete around the reinforcement, followed by corrosion of the steel in the presence of water and oxygen. The products of corrosion occupy a

volume several times larger than the original steel which results in cracking and/or disintegration of the concrete. Nevertheless, Neville (2003) indicates that such corrosion will not take place in dry concrete, probably below a relative humidity of 60%, nor in concrete fully immersed in water (where oxygen is very small amount) except when water can entrain air, for example by wave action. As the chloride attack usually arises from ingress of chloride ions from outside the concrete and the primary action is on the steel reinforcement, a dense concrete with adequate cover to the reinforcement is the best protection against chloride attack. NWDSM classifies soils with chloride content below 0.05% and groundwater with chloride content below 200ppm as non-aggressive. Miguel et al. (2010) has developed and quotes formulae for predicting chloride diffusion rates of concrete in tidal zones.

Aggressive chemicals or agents other than sulphates and chlorides may include acidic chemicals. Cement in the concrete, being highly alkaline, is not resistant to attack by strong acids or compounds that may convert to acids. Generally, the attack occurs by way of decomposition of the products of hydration and the formation of new compounds which will either be disruptive or soluble. Consequently, concrete should not be used in locations where this form of attack may occur, unless with adequate protection such as effective coating. In accordance with Neville (1995) concrete will be subject to attack by acid in an acidic environment with a pH value below 6.5. A pH value below 5.5 indicates a severe environment and below 4.5 a very severe environment (the former is consistent with NWDSM whilst the latter is consistent with the classification in Table 4.1 of the Code of Practice for the Structural Use of Concrete 2013).

- (b) Alkali Aggregate Reaction (AAR) is a chemical process in which alkalis, mainly from the cement, combine with certain types of minerals in the aggregate (alkali-reactive aggregates) in the presence of moisture to produce a gel that can absorb water and subsequently expand to cause cracking and disruption of concrete. An effective means of reducing the risk of AAR is to control the alkali content in the cement, and with appropriate use of cement replacement such as PFA in accordance with PNAP APP-74. Appendix A of the PNAP has a full description of control of the AAR, requiring that the “equivalent sodium oxide content” in concrete is not to exceed 3.0kg/m^3 .
- (c) For foundations constructed on a landfill site where there may be various kinds of fills with the probable existence of aggressive materials, investigation of the contents of the materials may have to be taken and appropriate measures implemented.
- (d) Damage by abrasion which refers to damage by abrasive machinery, metal tyred vehicles or water carrying solids is not common in foundations as they are not normally exposed to such abrasive actions except for marine foundations subject to wave attack. However, if abrasive actions do exist, protection which may take the forms of protective barriers or coatings may have to be provided.

From the above discussion, it can be seen that the composition of concrete, its denseness and adequacy of cover to reinforcement in concrete foundations are important to corrosion resistance. The requirements should be more stringent for more severe environments (which may also require additional measures such as cathodic protection as

will be discussed in H2.6.4). Rough guides to minimum concrete grades and concrete covers for reinforced concrete structures in general for various categories of “exposure” are given in the Code of Practice for the Structural Use of Concrete 2013 and other standards. In addition, crack widths sometimes need to be estimated against pre-determined limits to ensure durability.

H2.6.3 STEEL PILES

As for concrete foundations, this sub-clause requires corrosion protection to be provided in the foundation plans for steel piles where items (a) to (e) listed in the sub-clause exist. A discussion of these items is as follows :

- (a) Sulphate, chloride, aggressive chemicals or other similar agents (including oxygen) present in the ground will react chemically with steel (with iron as its major composition) to form other materials which cause corrosion. The corrosion is chemically a reduction oxidation process in which the iron is “oxidized”. In the corrosion process, the presence of water is essential and an acidic environment will accelerate the corrosion process. Figure H2.4 illustrates the chemical process of corrosion by water and oxygen.

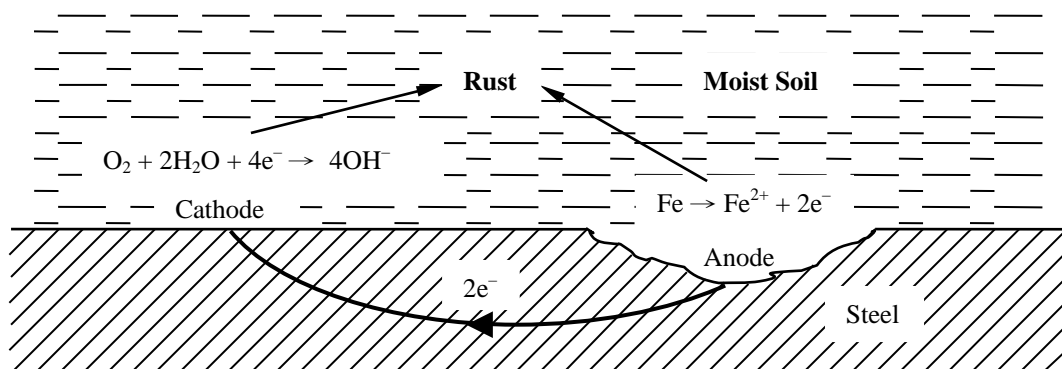


Figure H2.4 – Chemical Process of Corrosion

From the figure it can be readily deduced that if (i) the steel is negatively charged, i.e. the steel becomes a cathode or (ii) electrically connected to a metal of higher reducing power (e.g. zinc) by which formation of iron cation (Fe^{2+}) is not favoured, the corrosion process will be inhibited. Anti-corrosion provisions for steel can therefore be based on these two phenomena.

- (b) The alternate wetting and drying by sea waves in the “splash and tidal zones” of steel piles installed through the sea will accelerate the corrosion rates as illustrated in Figure H2.5 and therefore special treatment in corrosion protection is required for the piles. CEDD (2002) recommends that steel piles have to be fully protected against corrosion (by effective coating and/or cathodic protection described below) above the seabed throughout their design life;

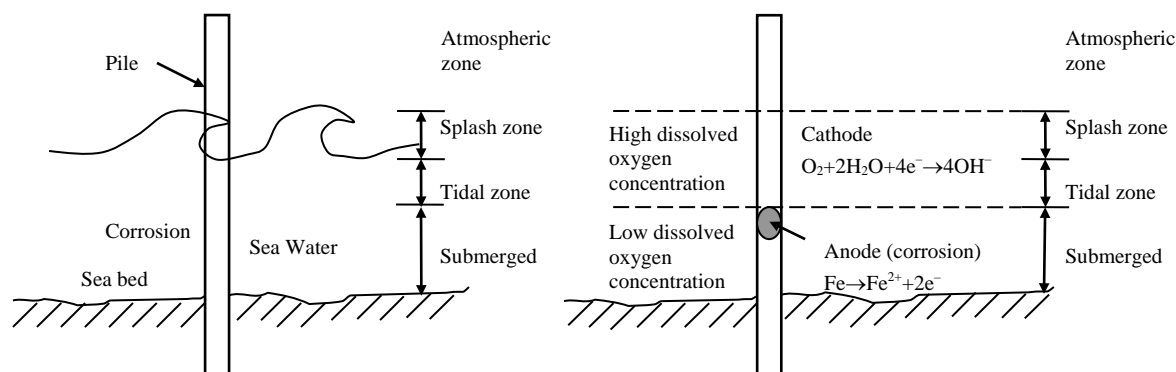


Figure H2.5 – Splash and Tidal Zone in a Marine Foundation

- (c) If the steel pile (with iron as its major composition) is in contact with other metals of lower “reducing power” such as copper (or alternatively described as having lower position in the “electrochemical series” in chemistry), oxidation and therefore corrosion of the steel will be accelerated. It is in fact a common protective measure to protect steel piles by electrically connecting them to a metal rod of higher reducing power (such as zinc as illustrated in Figure H2.6(a)) so that corrosion takes place in that metal instead of the steel pile;
- (d) “Stray direct electric current” through the piles are direct electric currents flowing through the earth from a source not related to the piles affected. When these stray direct currents accumulate on the steel pile, they can induce “electrolytic corrosion” of the iron by which iron is lost to the surrounding soil which acts as an electrolyte. Sources of stray current include existing cathodic protection systems, direct current power trains or trams, arc-welding equipment, direct current transmission systems, and electrical grounding systems. Fortunately, in most cases, these corrosion currents are only measured in thousandths of an ampere and so the effects are normally not significant. One technique to minimize the corrosion effect involves insulating or shielding the pile from the stray current source and another involves draining the collected current by either electrically bonding the pile to the negative side of the stray current source or installing grounding cell(s). The phenomenon and techniques are also applicable to underground pipelines.
- (e) As for concrete foundations, potential damage by abrasion, if any, needs to be considered.

The rate of corrosion of steel in soil is of the order of about 0.02mm/year in undisturbed natural soils to 0.05mm/year in non-compacted and aggressive fills (ashes, slag....) as deduced from BSEN14199:2005 Annex D. The measures protecting against the corrosion processes mentioned in the above include :

- (i) Use of protective paint or coatings (made of polyethylene, epoxy or asphalt);
- (ii) Casting in cement mortar or concrete;

- (iii) Sacrificial steel thickness by which the pile is over-sized so that a certain thickness of steel is reserved for “sacrifice” by corrosion during the lifetime of the pile;
- (iv) Zinc coating, as zinc is a stronger reducing agent than iron and can effect protection by actions as explained in H2.6.3(c); and
- (v) Electro-chemical (cathodic) protection by turning the pile into the cathode of a corrosion cell.

H2.6.4 MARINE FOUNDATIONS

More stringent protective measures for foundations are naturally required in marine conditions. The Code has highlighted some of the measures which are adopted in the “Port Works Design Manual Part 1” by CEDD (2002) for both concrete and steel foundations. Generally the protective measures mentioned in 2.6.2 and 2.6.3 are applicable to marine foundations with higher standards. Further discussion is as follows :

- (i) The intermittent or periodical wetting and drying due to waves and tides accelerate penetration of chlorides from the seawater into the reinforced concrete foundation structure and initiate corrosion of the reinforcement. Therefore, it is important to use a dense concrete mix with comparatively large concrete cover to protect the reinforcements. In addition to the specified minimum concrete cover of 75mm, the Port Works Design Manual also specifies that the cementitious content of the concrete shall be within 380 – 450 kg/m³, of which the dry mass of condensed silica fume shall be within 5 – 10% range by mass of the cementitious content;
- (ii) Steel tubular piles infilled with concrete may be used where the entire thickness of the casing is regarded as sacrificial. That is, the infilled concrete core alone can withstand the imposed load after the casing is entirely eroded in the long term.

Some cathodic protective measures against corrosion are illustrated in Figure H2.6 as discussed by Goran Camitz (2009).

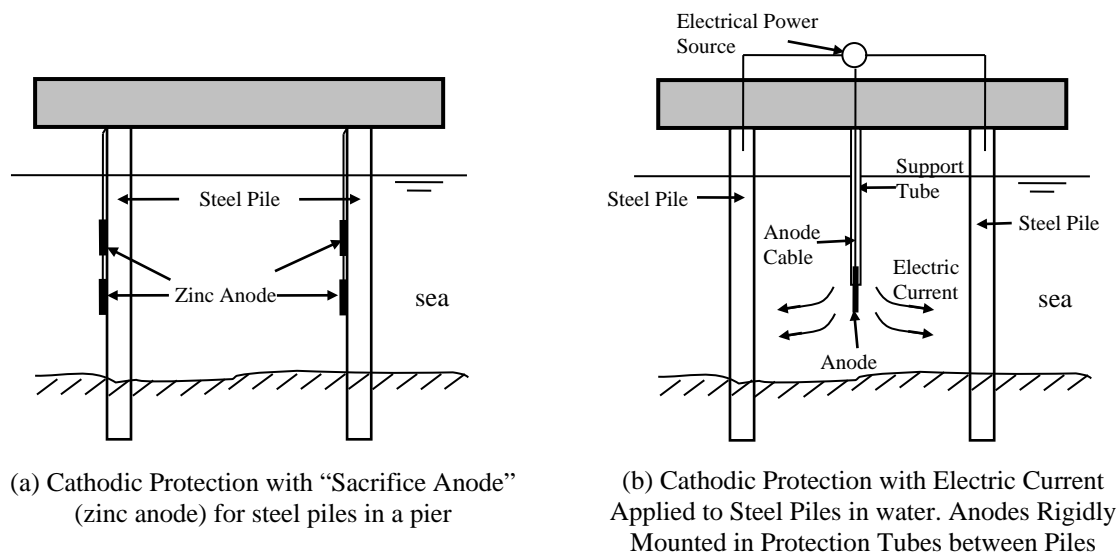


Figure H2.6 – Examples of Cathodic Protection to Piles in Marine Foundations

H2.7 FOUNDATION PLANS

In relation to expected depths and founding levels of the foundation as required in (1)(c) of clause 2.7 of the Code, it is a common practice that bedrock contours for foundations founded on rock and SPT N value contours for driven piles are included in the foundation plan. The SPT N values for plotting contours are subject to different types of driven piles.

H2.8 FOUNDATION DESIGN IN SCHEDULED AREAS

The relevant PNAPs that provide requirements for design in Scheduled Areas include PNAP APP-24 (PNAP 77) for Scheduled Area No. 3, APP-28 (PNAP 83), APP-30 (PNAP 85) for Scheduled Area No. 1, APP-61 (PNAP 161) for Scheduled Areas Nos. 2 and 4, APP-62 (PNAP 165), for Scheduled Area No. 5 ADM-16 (PNAP 225), APP-131 (PNAP 279) for Scheduled Area No. 3. In addition, drawings showing details and extents of the MTR Protection Areas can be inspected in the Buildings Department for Scheduled Area No. 3 or on the website of the MTR given in this link.

[http://www.mtr.com.hk/en/corporate/operations/protection_boundary_map.html]

For Scheduled Area No. 1 (Mid-levels), foundation plans need to be submitted together with the site formation plans (if any) according to Building (Administration) Regulations Section 11A. The foundation design should be such that bulk excavation (e.g. for pile cap construction) should not be lower than the determined bulk excavation limit (DBEL). Information on the tentative bulk excavation limit (TBEL) can be obtained from the Buildings Department upon request in writing. The DBEL will be formally issued upon request when drillhole records for ground investigation and topographic survey covering the required extent outside the site (specified by the BD at the time of issuing the TBEL) have been submitted to the satisfaction of the BD.

For Scheduled Areas Nos. 2 and 4 (with marble formation), the current practices of foundation design are usually based on site characterization using the approach of marble quality designation (MQD). The Code has outlined detailed requirements in 2.8.2 which are consistent with GEO Publication 1/2006 and Chan (1994).

A pile redundancy is provided for the uncertainties which the driven piles can be affected by karst features beneath the pile toe or damaged sustained during driving. The Code provides guidelines on the adoption of the redundancy factors based on the site classification taking into account the karst features underneath the site. Preboring may be used in case the piles have to penetrate overhangs or roofs to install piles at greater depth. In such circumstances, the pile redundancy can be adjusted accordingly that it should correspond to the karst feature (and site classification) underneath the installed piles.

For Scheduled Area No. 3, the MTRCL will impose conditions that may affect the foundation design. In addition to the requirements specified in PNAP APP-24 (PNAP 77), the following restriction should normally apply:

- (i) no foundation work is allowed within 3m from MTR structures;
- (ii) no percussive piling works are permitted within 10m from MTR structure.

H2.9 FOUNDATION DESIGN IN DESIGNATED AREA

The relevant PNAP giving detailed information and layout of the Designated Area of the North Shore Lantau is PNAP APP-134. In accordance with the PNAP, administrative procedures including site supervision of GI work should also follow the Code of Practice for Site Supervision 2009. GI work should also be carried out in stages and with an assessment of whether the building plans should be modified or the buildings relocated for economy of design when complex geology is encountered and deep foundations are involved.

Although the designated area is not different from a non-scheduled area in terms of building control, foundation design should take note of the complex geology of the site when designing site investigation works and selecting the appropriate foundation option for the site.

H2.10 FOUNDATION DESIGN IN SLOPING GROUND

For slope improvement work, it should be noted that the factor of safety has to be upgraded to the current standard in the checking of the slope.

When designing a foundation in sloping ground, due consideration should be given to the effect of vertical and/or lateral loads on the stability of the slope. Reference can be made to GEO Publication 1/2006 for the checking of the bearing capacity for shallow foundation affected by sloping ground and Geotechnical Manual for Slopes by GEO for the checking of slope stability. For the design of pile foundations embedded in slopes which carry lateral load, the slope should be checked for its stability against the imposed lateral load or, as a common practice, the pile should be “sleeved” to avoid imposing lateral load onto the slope.

H3 SITE INVESTIGATION

H3.1 GENERAL

In addition to the various functions of a site investigation report as discussed under this clause of the Code, the site investigation carried out on site for the proposed foundation work should also assist the Engineer to:

- (i) ascertain suitability of the proposed foundation work for the site;
- (ii) choose the most appropriate and/or the most cost effective foundation options for the building work;
- (iii) plan the best method of construction and foresee and mitigate difficulties and delays that may arise during construction;
- (iv) identify the nature of and estimate the volume for waste disposal and surplus materials arising from the foundation work. The site investigation report should support any necessary applications to relevant authorities for disposal arrangement which may require investigation of the impacts on the environment;
- (v) identify suitability of the reuse of excavated fills.

H3.2 DOCUMENTARY STUDIES

Documentary studies are cost and time effective means of compiling available geotechnical information about the Site which can act as the basis for the planning of future ground investigations. In fact, the information revealed by the documentary studies often affects the planning of the permanent work design. The Geotechnical Information Unit (GIU) of the Civil Engineering Library within the Civil Engineering and Development Department possesses a collection of such information across the territory which is most convenient to retrieval and study by practitioners. Reference can be made to PNAP ADM-7 for details of the documentary studies in the GIU concerning the acquisition of such information. A digital platform of the GIU is available for practitioners to examine the ground investigation and laboratory testing reports. It is accessible in this link (www.ginfo.cedd.gov.hk/dgiu). It is important that the documentary studies should be carried out before planning the ground investigation prior to design of foundation work. In addition, the accuracy of the retrieved information should be verified before use.

The documentary studies should aim at compilation of, but not limited to the followings, as far as they are available :

- (i) Previous land use and development;
- (ii) Existing borehole data;
- (iii) Field and laboratory testing reports on soil and rock properties;
- (iv) Information relating to geological profiles;
- (v) Ground water levels monitoring data indicating seasonal fluctuations and storm response;

- (vi) Design and construction records of current and past site formation works such as reclamation, construction of slopes, retaining structures and basements (with highlights on the standards of safety adopted in design);
- (vii) Design and construction records of foundation works such as piling;
- (viii) Past and/or continuing monitoring records and details of special geotechnical works, for example, ground anchor, horizontal drain, building settlements, and slope and retaining wall movements;
- (ix) Tunnels and disused tunnels, including design and construction records of linings and ground support;
- (x) Records of past failures including landslides. Flooding and settlement of ground and structures should also be noted and studied where appropriate.

H3.3 SITE SURVEY

The site survey comprises a topographical survey, geological survey, survey of existing structures, survey of any disused tunnel, nullah or stream course, and a survey of underground services. The following is in addition to items already mentioned and cautioned in the Code under the same headings :

(1) Topographical Survey

A topographical survey is important for the planning and design of the construction work because the topography of the site directly affects the extents of cut and fill work on site which may have significant effects on construction sequence, cost and safety. Topography may also dictate access points and types of construction equipment to be used during construction. For example, on a very steep sloping site, it may be necessary to form elevated flat platforms using steelwork or extensive filling work for the construction of large diameter bored piles. If such platform forming or filling work is costly, the Engineer should carry out feasibility and cost effectiveness studies by taking into account other feasible foundation options such as the socketed H-pile or mini-pile involving the use of lighter machinery.

(2) Geological Survey

This sub-clause describes the purpose of a geological study and lists the key requirements for the geological and ground models in respect of foundations.

(3) Survey of Structures

For the survey of adjacent structures, where required and with permission, sampling tests on structural members of adjacent structures may be carried out to investigate and/or confirm their structural integrity in addition to the assessment of paper records and visual inspection. Agreement from the owners of the adjacent structures must be sought before carrying out the tests. Where tests are to be carried out for old building structures, an assessment of the effects of testing must be made.

For the foundation structures supporting the adjacent structures or buildings, it may not be enough to limit the survey to their structural integrities only as the adequacy

of the bearing strata is also important. If considered necessary, investigation or testing of the bearing strata should also be carried out.

In addition, the effects on these adjacent structures of the proposed temporary and permanent works on site should be carefully studied. These are important items for inclusion in the foundation plan submissions to the Building Authority.

(4) Survey of any Disused Tunnel, Culvert, Nullah or Stream Course

The identification of any disused tunnels, culverts or stream courses is important as they are underground/ground features which directly affect the permanent work design. Damage to these structures and/or hazards may result if they are not properly protected during construction work.

(5) Survey of Underground Services

The survey of underground services aims to locate these services precisely so that damage to them during construction work, leading to suspension of the intended services, can be avoided. In addition, the survey can help to minimize risks originating from underground services such as high voltage power cables, gas pipes and the associated installations. Extreme care must be taken when surveying and/or working in close vicinity to these underground services. Before any trial pits, probes or boreholes are sunk in areas where there may be underground services, hand-excavated inspection pits should be used to establish the presence or otherwise of all such services. Hand-operated power tools to facilitate excavation through hard materials should be used with extreme care in inspection pits.

The conditions of the buried water carrying pipes should be ascertained as far as possible, as bursting of pressurised pipes and leakage of drains are often reported. Relevant departments (e.g. Water Supplies Department, Drainage Services Department and Highways Department) should be approached for obtaining any records of pipe leakage/burst incidents from their services occurred within the past 12 months.

H3.4 GROUND INVESTIGATION

H3.4.1 GENERAL

Ground investigation is that part of a site investigation carried out in the ground. It serves to retrieve information about the ground to aid the proposed foundation work in the following aspects :

- (i) estimation of the depths, adequacy and suitability of the bearing strata for the proposed foundation work;
- (ii) estimation of future settlements;
- (iii) choice of construction methods and necessary precautionary measures for the proper execution of the foundation works and the minimization of damage to

- adjacent structures due to ground movements, vibrations, and groundwater fluctuations;
- (iv) avoidance of conflicts with existing underground utilities and structures;
- (v) determination of the extent of contaminated soils, if present;
- (vi) assessment of the degree of aggressiveness if the site has a known history or potential for significant corrosion and identification of the extent and scope of chemical tests for further confirmation.

Good quality soil samples and continuous rock cores from boreholes should be obtained for both geological logging and laboratory testing purpose. Laboratory tests should be carried out to characterize materials and determine relevant design parameters. These include classification tests to establish the index properties of the ground and strength and compressibility tests to obtain the foundation design parameters based on soil and rock mechanics principles. In addition, in-situ testing (e.g. plate load test, standard penetration test, permeability test) should also be implemented as necessary.

Despite borehole spacing should vary from site to site depending on the complexity of the site geology and the building plan of the proposed development, it may be worthwhile to consider having boreholes at 30m centre to centre for general sites to facilitate the detail design of the proposed foundation works. Additional boreholes shall be sunk in case of abrupt change in ground condition between boreholes is observed. For the sites underlain by complex geology or karst marble, it is recommended to refer to GEO Publication No. 1/2006 for guidelines on the strategy in conducting the ground investigation and spacing of the boreholes.

The Code reminds practitioners of the requirement of the employment of Registered Specialist Contractors (Ground Investigation Field Works) for the ground investigation and laboratory testing work respectively. In addition, the Code stresses the importance of compliance with the Code of Practice for Site Supervision in Ground Investigation Fieldworks.

H3.4.2 SUPERVISION FOR GROUND INVESTIGATION WORKS

The current Code of Practice for site supervision in which ground investigation works is included is the “Code of Practice for Site Supervision 2009” and its corrigenda.

H3.4.3 PREPARATION OF GROUND INVESTIGATION REPORTS

A ground investigation report should comprise the following :

- (i) an introduction stating the purpose, timing, nature and extent of the investigation;
- (ii) a description of the site including the site location, area covered by the investigation, the topography and the structure to be constructed on the site;
- (iii) a description of the geology of the site (including faulting) and the sources from which the geology is extracted;
- (iv) groundwater and its highest and lowest levels and the period of monitoring;
- (v) an account of the field work including the methods of investigation, testing and equipment used. Difficulties encountered should also be described;
- (vi) a summary of the boreholes drilled during the investigation with full reports of the borehole numbers, locations (with Hong Kong Metric Grid Reference), dates of

operation, method of forming boreholes, plant equipment used, ground levels and depths of drilling, descriptions and properties of the soils encountered (except for wash boring where only the bedrock is extracted for investigation); ground water levels;

- (vii) any interpretation/comment based on data obtained by the engineer. Where appropriate, the method of analysis, and cross checking of test results should be also be included.

H3.4.4 SOIL AND ROCK SAMPLING

Clause 3.4.4 of the Code is self-explanatory.

H3.4.5 NUMBER AND DISPOSITION OF BOREHOLES/TRIAL PITS

The Code emphasizes that the number and disposition of boreholes/trial pits should depend on the size, type, performance requirement of the structure, the general conditions of the site and the availability of existing information. Chapter 2.4 of GEO Publication 1/2006 provides the general guideline on the extent of ground investigation works.

Below are requirements stated by the Code under clause 7.4.2 for “pre-drilling” for the following end-bearing pile types, which are applicable generally under all circumstances :

- (i) Large Diameter Bored Pile, Barrettes and the like – one pre-drill hole for each pile;
- (ii) Mini-pile, Socketed H-pile, H-pile driven to bedrock – pre-drilling be carried out such that the tip of each pile will not be more than 5m from a pre-drilled hole.

H3.4.6 DEPTH OF GROUND INVESTIGATION

The Code adopts 5m as the required depth for the definition of “bedrock” and therefore requires drilling into rock for at least 5m for confirmation of bedrock as the end-bearing stratum for foundation units designed for founding on bedrock. However, for complex geology, depth of borehole should be increased.

Apart from the requirements on determination of depth for bedrock investigation, the Code generally requires ground investigation to be carried out to such a depth that stress increase would cause an insignificant strain or displacement. Taking the stresses beneath square and circular footings as examples for determination of the depths where insignificant strains occur, reference can be made to the following “stress bulb” charts as shown in Figure H3.1 which are arrived at by integration of the Boussinesq Equation (for determination of stress in a semi-infinite elastic medium due to a point load at the surface).

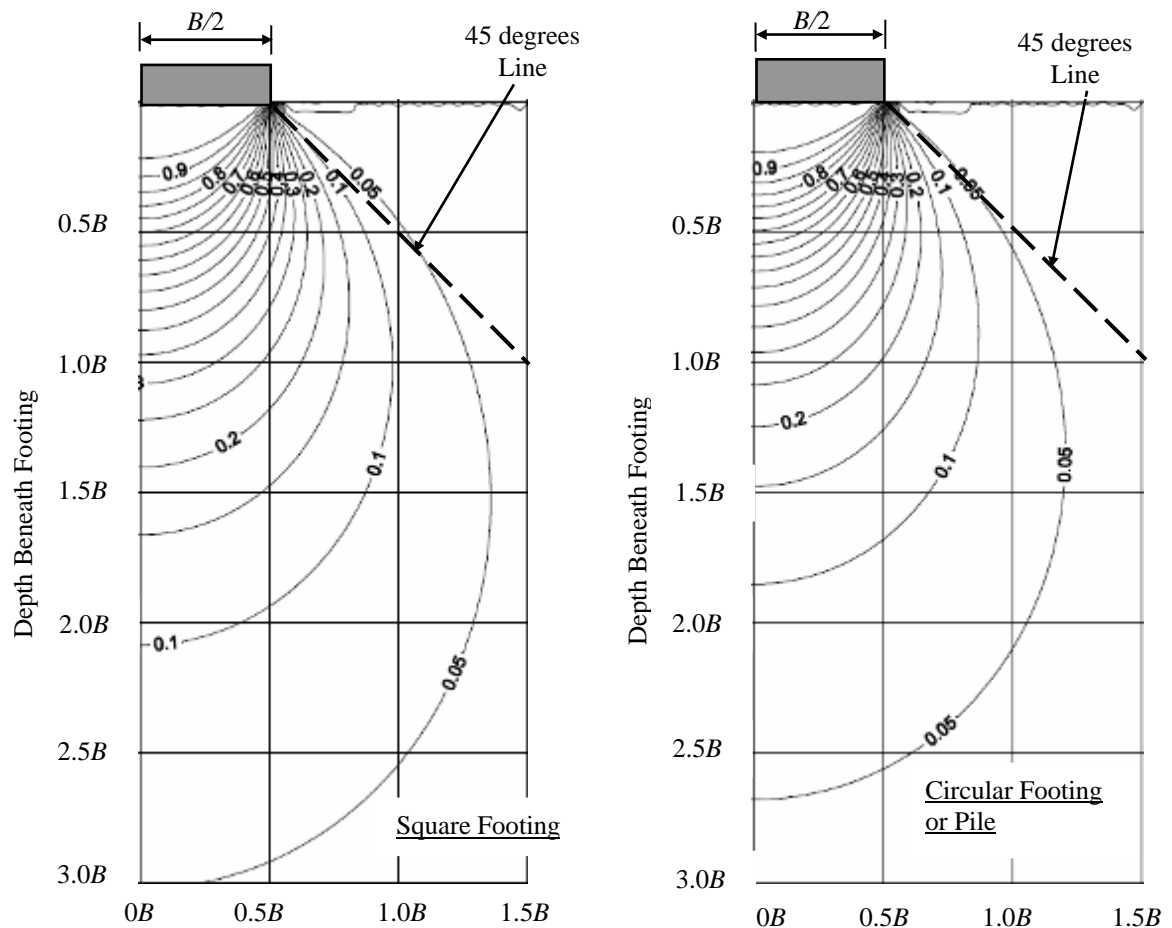


Figure H3.1 – Vertical Stress Bulb beneath a Square Footing and a Circular Footing (or Pile)

From Figure H3.1, at depths greater than $2.1B$ (2.1 times the breadth of the footing) for the square footing and $1.85B$ (1.85 times the diameter of the footing) for the circular footing, the vertical stress is only 10% of the contact pressure at the founding stratum. As such small stresses which imply small strains, further settlements beneath these levels is likely to be insignificant. So the ground investigation can terminate at these levels. Nevertheless, if hard stratum, e.g. rock or stiff clay is encountered above these levels where settlements will be small despite the higher stresses, ground investigation can be terminated at higher levels. It should also be noted that this “stress bulb” approach is applicable to both cohesionless and cohesive soils under the assumption that the soil medium behaves elastically. (The chart for the circular footing can also be used to estimate stresses beneath a circular bored pile.)

Overlapping of stress bulbs will result if footings are in close proximity. By the elastic theory, the stress in an overlapping zone at any point is the sum of the stresses by the individual footings.

H3.4.7 GROUNDWATER

Groundwater level often presents difficulties in the design and construction of foundation work. In permanent work design, a high groundwater level can give rise to flotation

problems where the structure is light. Seasonal fluctuations of groundwater level may induce movements in the permanent structures. During construction when de-watering is required, care should be taken to avoid subsidence of the ground which may affect adjacent structures and utilities. Impermeable cut-off or re-charging of ground water may need to be considered. The groundwater investigation must provide all relevant information needed for geotechnical design and construction which should include the followings as appropriate:

- (i) depth, thickness, extent and permeability of water-bearing strata in the ground and joint systems in the rock mass;
- (ii) the elevation of the groundwater surface or piezometric surface of aquifers and their variation over time and actual groundwater levels including possible extreme levels and their periods of recurrence;
- (iii) the pore water pressure distribution; and
- (iv) the chemical composition of the groundwater.

H3.5 GROUND INVESTIGATION IN SCHEDULED AREAS

Ground investigation works in Scheduled Areas are subject to special control. The relevant PNAPs for ground investigation in Scheduled Areas are:

- (i) ADM-16 (PNAP 225) – Approval and consent is required under the Buildings Ordinance. However, the concurrent processing option is available.
- (ii) APP-28 (PNAP 83) – Requirement for qualified supervision is imposed.
- (iii) APP-30 (PNAP 85) – As Scheduled Area No. 1 is located in the region of sloping ground, a Registered Geotechnical Engineer (RGE) must be appointed under the Buildings Ordinance.
- (iv) APP-61 (PNAP 161) – As the ground conditions in Scheduled Area Nos. 2 and No. 4 are complex, RGE has to be appointed under the Buildings Ordinance.
- (v) APP-24 (PNAP 77) – In Scheduled Area No. 3, railway protection areas have been delineated and shown on relevant plans and a set of building/engineering guidelines produced to safeguard the safety and stability of the railway structures. As a general rule, the boundary of the railway protection areas is about 30m outside the outer surface of the railway structures or the railway fence/wall, or from the nearest rail if there is no railway fence/wall. Proposal for ground investigation works or underground drainage works in or for any existing buildings to be carried out within railway protection areas other than those designated as Schedule Area No. 3 should be forwarded to the MTRCL for comment prior to commencement of the proposed works.
- (vi) APP-62 (PNAP 165) – In Scheduled Area No. 5, all proposals for new building works within 100m from the centerline of the gazetted routes of sewage tunnels shall be subjected to special scrutiny by Government.

For ground investigation works within the Scheduled Areas Nos. 2 and 4, PNAP APP-61 (PNAP 161) describes the geotechnical control measures in respect of building works. By virtue of the Buildings Ordinance, ground investigation in these Areas requires approval and consent of the Building Authority. The AP, RSE and RGE are required to ensure that ground investigation works are carried out to a high standard and are properly supervised. The site supervision requirements and the minimum

qualifications and experience of the supervision personnel and the Competent Person (Logging) for ground investigation field works are given in the Code of Practice for Site Supervision 2009. The cores recovered should be examined and properly logged by the Competent Person (Logging). Pending the substantial completion of the building works, all cores and samples should be retained on site in good conditions for inspection by the staff of the Buildings Department and the Geotechnical Engineering Office.

Technical recommendations on the requirements are also provided by the GEO Technical Guidance Note No. 12 (GEO 2004) and ETWB TC(W) No. 4/2004 (ETWB, 2004).

In addition, for ground investigation within the Designated Area of Northshore Lantau, GEO Technical Guidance Note No. 12 (GEO 2004) outlines the establishment of the Designated Area of Northshore Lantau and the relevant technical recommendations. Related documents are also provided.

The Designated Area is underlain by locally complex geological conditions that require due attention to be given to the potential problems associated with high-rise buildings and other structures involving deep foundations. The complex geological conditions include some, or all, of the following:

- (i) An anomalously deep rockhead, locally in excess of 160m below ground level, in the deeply weathered, mainly intrusive igneous rocks comprising medium-grained granite and dykes of rhyolites;
- (ii) Metasedimentary rocks and their weathering products giving rise to cavities, cavity fill deposits and residual soil;
- (iii) Superficial deposits, typically between 10 and 150m, occupying depressions in the subcrop surface, most of which lie directly above or adjacent to metasedimentary rocks and cavity-fill deposits.

The following additional ground conditions are often contributory to the complex geological conditions and should also be assessed :

- (i) Steep gradients on rockhead; and
- (ii) Faulting.

In site investigations for developments with deep foundations within the Designated Area, some guidelines are recommended for identifying the complex geological conditions:

- (i) During the initial ground investigation phase, emphasis should be directed to developing a representative geological and hydrogeological model rather than just testing.
- (ii) Commonly used ground investigation techniques have limitations in identifying very localized areas of complex geological conditions. Detailed geophysical gravity surveying has proved to be a useful technique for identifying the locations of deeply weathered zones and should be considered as a supplement to and a basis for planning drillholes.
- (iii) Reference can be made to the logging guide by Sewell and Kirk (2002).

H3.6 GROUND INVESTIGATION WITHIN THE DESIGNATED AREA

The Code reminds that ground investigation works within the Designated Area are subject to special administrative procedures in accordance with the Code of Practice for Site Supervision 2009 and ground investigations should be carried out in stages.

H4 SHALLOW FOUNDATIONS

H4.1 GENERAL REQUIREMENTS

The controlling criteria for the design of shallow footing are often settlement and differential settlement that would be experienced by the structure, the magnitude of which are controlled by the serviceability requirements of the structure.

The construction of new footings should avoid conflicts with existing foundations and underground services, as revealed by the ground investigation. Additional stresses and movements induced in the adjacent structures, foundations, services and slopes etc. should also be examined, noting the prescribed values imposed by authorities such as the MTRC, WSD. The analysis can be carried out by (i) using the simple load spread assumption (say 2 (vertical) to 1 (horizontal) in soil and 45° in rock); (ii) the continuum theory by treating the ground as an elastic (or elasto-plastic) medium; or (iii) finite element method analysis. The latter two approaches have to be carried out by computer methods.

H4.2 ALLOWABLE BEARING PRESSURE AND SETTLEMENT

H4.2.1 SHALLOW FOUNDATIONS ON CATEGORIES 1(a), 1(b), 1(c), 1(d) OR 2 ROCK

Clause 4.2.1 of the Code is self-explanatory.

H4.2.2 SHALLOW FOUNDATIONS ON SOIL

(1) Design Procedures

The clause outlines the procedure for design of shallow foundations which mainly aims at establishment of the allowable bearing pressure together with checking of settlements. Plate load test will be required under conditions as stated in clause 4.2.2(2). Nevertheless, the analysis of the working bearing pressures beneath the shallow footing need to be established first.

As a conventional and acceptable practice, the determination of ground bearing pressure due to loads acting on a footing is often based on the assumption of a “Linear Pressure Distribution” and rigid foundation as illustrated in Figure H4.1(a). The adequacy of the plan size of the footing can therefore be ascertained by checking the maximum ground pressure (obtained by the above assumption) against the presumed values of allowable vertical bearing pressure as given in Table 2.1 of the Code, in lieu of the “Rational Design Method” described in clause 2.2.1.

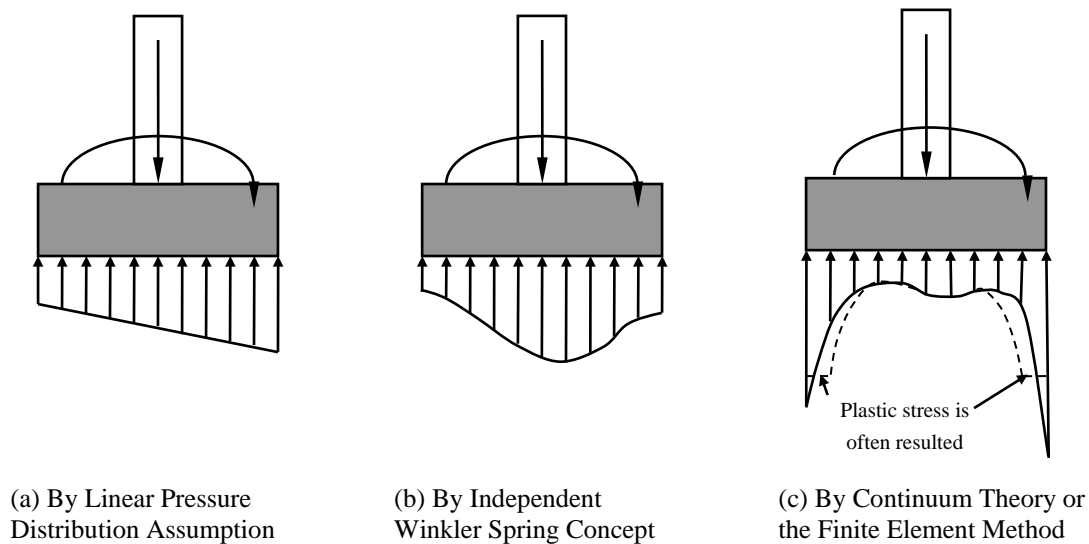


Figure H4.1 – Ground Pressure Distribution beneath Footing under Different Assumptions

However, with the use of structural computer methods, a popular approach involving the use of the “Winkler Spring Concept” is widely used currently. In this method the ground is idealized into a series of isolated spring supports which are independent of each other. Depending on the relative stiffness of the footing structure and the spring stiffness values, local high pressure values exceeding the presumed values may result after analysis (in locations under heavy loads) as shown in Figure H4.1(b) where such a large pressure does not occur using the “Linear Pressure Distribution” method as illustrated in Figure H4.1(a). Nevertheless, the excess ground pressure will be even more significant if the analysis is based on the more accurate “Continuum Theory” approach or the Finite Element Method with the consideration of full subgrade structure interaction as illustrated in Figure H4.1(c).

In comparison, analysis by the Continuum Theory and the Finite Element Method which will result in high ground pressures at the edges and corners of the footing is usually more realistic than the Linear Stress Distribution Method and the Winkler Spring Method as illustrated in Figure H4.2. In fact, for a rigid footing resting on an elastic semi-infinite subgrade, the pressure at the edge of the footing will be at infinity using elastic theory. Reference can be made to the work of Borowicka (1939) for an infinitely long rigid strip and Muki (1961) for a circular rigid disc. But practically the infinite pressure will not exist. The ground will “yield”, resulting in “plastic pressures” as illustrated by the dotted lines in Figure H4.1(c).

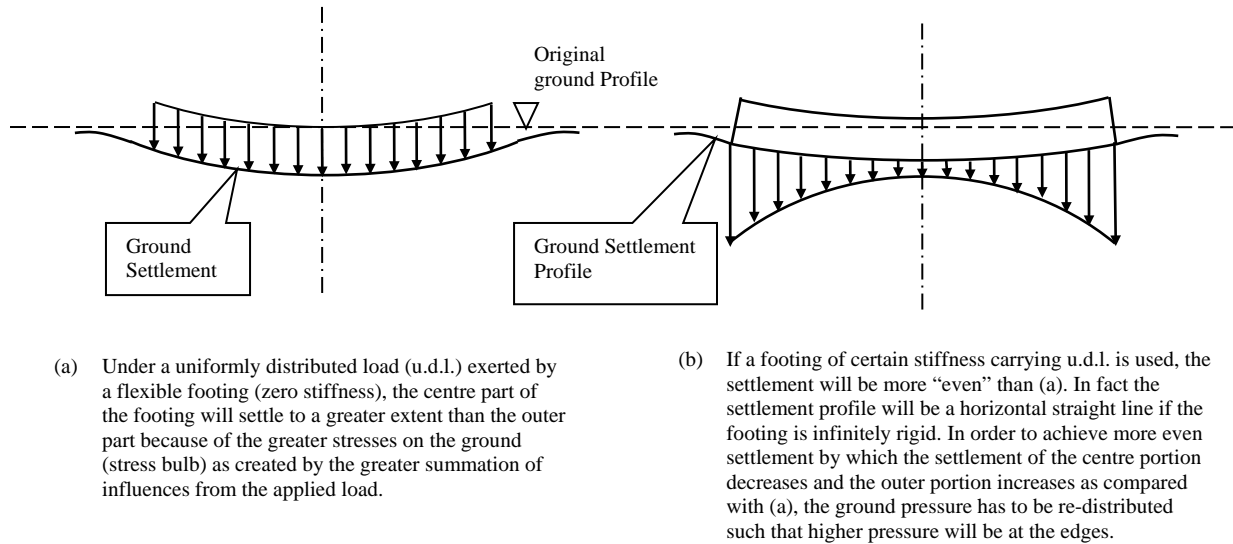


Figure H4.2 – Explanation of Ground Bearing Pressure under the Continuum Theory

The “Linear Pressure Distribution” method is a widely used and accepted method and this method is presumed when the bearing pressures are checked against the presumed values in Table 2.1 of the Code. Nevertheless, as the Code does not preclude more accurate methods of analysis, the Winkler Spring Method or the Continuum Theory are also accepted in the structural design of the footing. Furthermore, it should be noted that both the “Linear Pressure Distribution” method and the “Winkler Spring” method cannot achieve settlement compatibility of the footing structure and the ground. If the designer were to apply the ground reactions arrived by these two methods to the ground for calculation of settlements by the continuum theory, e.g. application of the Boussinesq or Mindlin Equations (or their integrated forms) (Vaziri et al; 1982) or the finite element method, the settlement profiles of the ground and the footing structure will not match and this is thus a draw-back of these approaches. Analytical approaches including the work by Lam et al. (2009), however, have been developed to account for the true subgrade structure interactions through the use of the “Continuum Theory” which can achieve compatibility of settlement of the footing and the subgrade.

In addition, as the Winkler Spring Method and the Continuum Theory may result in very high ground stresses locally, the designer may, with adequate justification and/or by making conservative assumptions, assume certain limits of ground stress (elastic limit) beyond which the stress may remain constant (plastic stage). Reference to other publications for more accurate constitutive laws of rock or soil can be made.

Apart from stresses induced on the ground, settlement is another important controlling design criterion for shallow foundations as required in the flow chart attached at clause 4.2.2 of the Code. Methods for estimating settlement are often based on the elastic theory in cohesionless soil and the consolidation theory in a cohesive soil. Discussions of settlement estimations for cohesionless soil (commonly encountered in Hong Kong) with charts and worked examples are enclosed in Appendix HC.

(2) Testing Requirements

The Code imposes the requirement of carrying out “plate load test” for shallow foundations (founded on soil) described in clause 8.2 when any one of the 3 conditions listed in clause 4.2.2 (2) is satisfied which includes (a) use of presumed values for q_a greater than 300kPa unless $q_a - q_o$ less than 50kPa; (b) use of the bearing capacity equation in clause 2.2.4; (c) use of Young's modulus greater than the $1 \times \text{SPT } N$ values in MPa in settlement determination. The plate load test serves to correlate the settlement of a test plate (300mm to 400mm plan dimension) under the test loads to that of the actual shallow foundation for determination of the Young's Modulus of soil and back-calculation of foundation settlement.

H4.3 STRUCTURAL REQUIREMENTS

The structural design of shallow reinforced concrete footing should be in accordance with the latest version of the Code of Practice for the Structural Use of Concrete 2013.

Generally the structural design of footings should be carried out to resist the “internal forces” determined by structural analysis. In the conventional structural design of footings, the internal forces acting on a cross section are often determined by balancing the applied loads and reactions as demonstrated by Figure H4.3. The analysis and design are effectively based on a “one-dimensional beam model”.

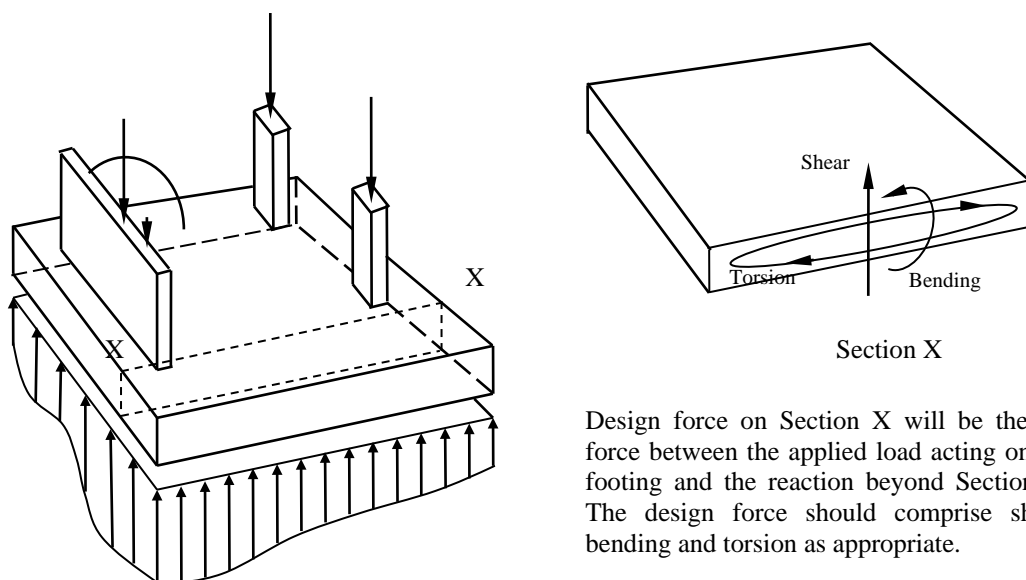


Figure H4.3 – Demonstration of the Determination of Design Forces on Sections of Footing

However, as can be seen readily, the application of the method is quite limited, because (i) the simulation of a plate structure as a beam structure may not be realistic and; (ii) there is difficulty in determining the “effective width” of the cross section beyond which local effects cannot be well captured.

In contrast to the conventional method, the structural analysis of footings in the local industry is now frequently based on the “2-dimensional plate bending model” using finite element analysis. In this approach, the footing is idealized as a 2-dimensional plate bending structure. “Stresses” which comprise the bending moments, twisting moments and shear forces per unit plan width of the footing are the analytical results of the structural design process. The origin and nature of the twisting moment which are not so familiar to some designers are discussed in Appendix HD. Approaches have been developed to arrive at a complete flexural design allowing for the bending moments and twisting moments. The simplest and most popular approach is that based on the Wood-Armer Equations by Wood (1968). The equations have been adopted in the New Zealand Code NSZ 3101 Commentary (2006) and are reproduced in Appendix HD with illustrative worked examples.

Out-of-plane shear stresses (shear forces per unit width) are also obtained for the checking of out-of-plane shear. Under pre-determined global axes in X and Y directions in the mathematical model, shear stresses are denoted along the X and Y directions as V_x and V_y . It can be easily proved (Lam and Law (2009)) that the maximum shear stress for design is $V_{\max} = \sqrt{V_x^2 + V_y^2}$ and the failure plane on a plan view is at an angle of $\tan^{-1}(V_y/V_x)$ to the X axis. Design against out-of-plane shears should be carried out for this value of V_{\max} (in shear force per unit plan width) accordingly.

In addition to the direct approach based on “stress” determined by the Finite Element Method, an approach based on “node force” has been employed in a popular software which is being widely used locally. However, there are shortcomings to the approach which have been discussed by Lam and Law (2009). In short, the “node force” used in the approach is a hypothetical parameter which does not exist in the structure and the design based on this approach fails to take into account some important structural behaviours. A more reasonable approach is to take the average stresses over a design width for the reinforcement design in reinforced concrete, and such an approach is usually a more economical in design which is available in some computer software.

An even more advanced method of analysis is by simulation of the footing structure as an assembly of brick elements (finite elements) by which the mathematical model becomes a 3-dimensional one. The 3-dimensional model is more realistic compared with the 1- and 2-dimensional models as it can capture the strut-and-tie actions that are more likely to take place in a thick footing structure instead of the pure bending coupled with out-of-plane shear in plate bending structures. However, the structural design has to take account of the of the 3-dimensional stress components which comprise 3 components of direct stresses and 3 components of shear stresses. The analysis is obviously much more complicated. Law et al. (2007) has developed a design method which is based on extension of the approach by Clark (1976) for 2-dimensional in-plane problems. A different approach has also been developed by Foster et al. (2003). These methods may be used for sophisticated design for an entire footing structure or local examination of a footing for locations where the structural behaviours are complicated.

The Code also notes that the stability of shallow foundations should comply with clause 2.5.4.

H4.4 COMMON TYPES OF SHALLOW FOUNDATIONS

The Code distinguishes three types of footing foundation, namely the “pad footing”, “strip footing” and “raft footing” in this Section. By common understanding of the profession, the distinction between the three types of footing is roughly based on their plan sizes or plan length to width ratios as roughly shown by Figure H4.4, though no strict limits of plan sizes and length to width ratios have been imposed.

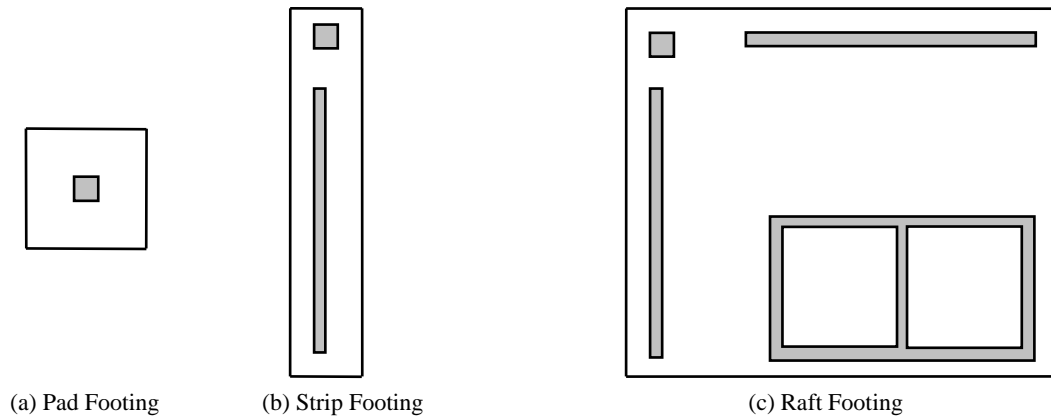


Figure H4.4 – Plans showing Pad Footings, Strip Footings and Raft Footings

Footings in close proximity will likely adversely affect each other in settlement and stress superimposition which may need to be accounted for. Nevertheless, it may be a rule of thumb that the effects of a different footing at a higher level can be ignored if the footing is outside the “2 (vertical) in 1 (horizontal)” (in soil) and 45° (in rock) stress spread from the higher footing, as illustrated in Figure H3.1. Alternatively, simple superimposition of the stresses due to different footings can be carried by the continuum theory under the elastic theory.

H4.4.1 PAD FOOTINGS

A pad footing is one which is relatively small in plan size and usually supports a single column. Pad footing foundations are usually used to support structures with isolated columns where the bearing pressures are within allowable limits of the subgrade. However, the use of isolated pad footings may result in significant differential settlements between the footings due to different stress levels on the subgrade and/or the varying bearing capacities and stiffnesses of the subgrade in different locations. In addition to the differential settlements that will be incurred to the superstructure as cautioned by the Code, the overlapping of “stress bulbs” in the subgrade together with consideration of the cross influences between settlements should also be considered for pad footings in close proximity.

The Code has imposed in clause 2.3.2(2) limit of differential settlement to 1:500 for shallow foundations generally for buildings or structures not particularly sensitive to movement. This limit between adjacent footings supporting a structure is also generally

acceptable for design of reinforced concrete structures of adequate flexibility. However, smaller values may be required for a comparatively stiff superstructure (such as one with shear walls and/or wall beams) and sensitive structures such as water tanks.

H4.4.2 STRIP FOOTINGS

A strip footing is one which is narrow in the transverse direction normally supporting walls. Ties by beams in the direction perpendicular to the length of the strip footing may sometimes be required to enhance stability or to cater for construction errors and the beams should be designed for at least certain eccentric moments.

Depending on the ratio of the structural width of the strip footing to the structural depth and length, the structural behaviour of a strip footing may resemble that of a beam structure rather than a plate structure. Analysis and design as a beam structure may therefore be more appropriate.

H4.4.3 RAFT FOUNDATIONS

A raft footing is relatively large in plan size and usually supports a number of columns and walls. The use of a raft footing is common for structures (i) with closely spaced vertical members; (ii) with a comparatively large loading or if resting on weak subgrade requiring a large bearing area; and (iii) varying intensities of imposed loads across the raft or resting on varying subgrade where differential settlements can be significant. A raft structure enables differential settlements to be more effectively minimized. Nevertheless, the Code has cautioned that raft footings should be designed with adequate strengths to withstand the differential settlements.

In addition, “two way bending” structural behaviour is often more pronounced in raft footings. Therefore design assuming plate bending behaviour would be more appropriate than that according to the beam theory as discussed in H4.3.

Traditionally, it is believed that a stiff structure can achieve an even stress distribution on the subgrade. Although a stiff foundation structure can more effectively spread the loads from the interior columns or walls over large areas, very high local pressures can still result along the edges of the foundation as discussed in H4.2. Nevertheless, “local overstress” of the subgrade (which may turn the subgrade from the elastic stage to the plastic stage) can be tolerated and the concept average bearing pressure should be followed in foundation design.

H5 PILE FOUNDATIONS

H5.1 GENERAL

In addition to the general requirements for a pile foundation as discussed by the Code, it should be noted that “settlement” and “structural capacity” are the usual controlling design criteria for piles, with settlement often proving to be the dominant criterion.

H5.1.1 RECOGNIZED TYPES OF PILE FOUNDATIONS

The Building Authority maintains a list of recognized types of pile foundations for ease of control. The common types of pile such as the driven steel H-pile, prebored H-pile, large diameter bored pile, barrette and mini-pile, for example are included. There are provisions in this Section for the inclusion of new types of pile into the list comprising the submission of technical data, past performance and demonstration of performance which likely include loading tests.

H5.1.2 GROUP EFFECT

The performance of a single pile will be different if load carrying piles are installed in close proximity because of the overlapping of stresses created by the piles in the subgrade. The effect is commonly known as the “Group Effect” and is generally an adverse effect which may reduce the load carrying capacity of any single pile and increase settlement as illustrated in Figure H5.1.

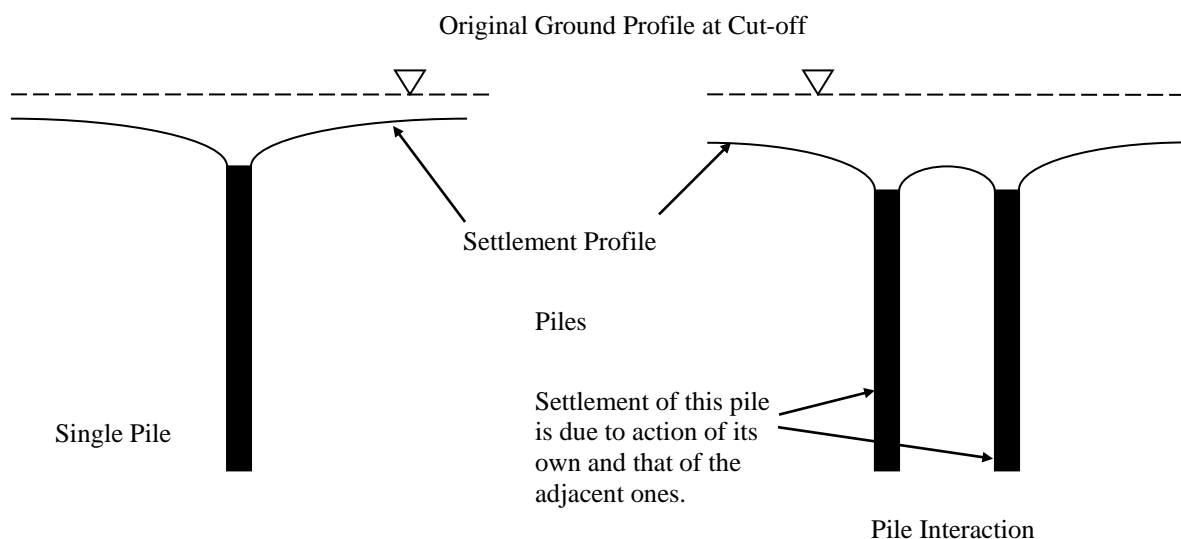


Figure H5.1 – Illustration of Pile Group Effect on Pile Settlement

But there are cases when the effect can become beneficial, e.g. when the subgrade is densified by closely spaced driven piles increasing the load carrying capacity.

Obviously the group effect is more pronounced for friction piles than for end-bearing piles founded on competent stratum. The Code does not require consideration of group

effects for end bearing piles (including piles driven to firm soil of SPT N value ≥ 200) and piles founded on rock of Category 1(c) or better.

The Code has adopted a simple approach whereby a group reduction factor of 0.85 can be applied for piles under prescribed conditions. The factor is applied to the pile capacity of individual piles (for friction piles spaced at less than 3 times the pile perimeter), not the settlement. Theoretically, there are two group reduction factors, one relates to settlement and the other to geotechnical capacity. It is well accepted that a pile group has a larger average settlement than a single pile with the same average load. However, for piles installed in sand the group capacity is usually higher than that arrived by summation of the capacities of all the individual piles. An illustrative example is enclosed in Appendix HE in which a pile group with its piles, pile cap and the soil mass among the piles is idealized as an integrated structure behaving as a sunken footing founded at the average founding level of the piles. By determining the ultimate bearing capacity of the “idealized footing” and with the application of a factor of safety of 3, the allowable total bearing of the pile group can be determined and compared against the summation of the capacities of all the individual piles. A pile group factor exceeding unity can be obtained in this way. As the Code does allow use of factors other than 0.85 (including unity) when justified by recognized engineering principles, the method can be adopted to justify for the use of a pile group factor exceeding 0.85.

Despite this easy-to-use provision in the Code, there are also other theoretical approaches to allow for the interactions between piles and the subgrade and/or the pile cap structure. Relevant works include that of Randolph (1977) and Poulos & Davis (1980). Both Randolph and Poulos & Davis’ work take into account the superposition of stresses and/or settlements of the adjacent piles in determining pile settlements so that the settlement of any pile is actually the summation of the actions of its own and others. The work of Randolph was based on the shear deformation of soil whilst Poulos & Davis (1980) used the integrated forms of Mindlin’s Equation to calculate pile settlements. Randolph developed a software PIGLET (1980), (2004) for analyzing piles (vertical and raking) under rigid caps with employment of his theory. Cheng (2013) extended the approach to cover flexible pile cap cases while keeping Randolph’s theory in assessing pile-soil interactions in the software PLATE. However, these approaches are based on elastic deformation of soil only. More sophisticated geotechnical-structural finite element computer programs have incorporated more advanced soil models including plastic stress-strain behaviour of soils.

Notwithstanding the foregoing discussion in relation to pile-cap-soil interactions, there is a simpler approach by which the cap is simulated by a mathematical model as a flexible structure with piles supports. However, the stiffness of the pile support which actually involves pile soil interaction effects is difficult to simulate and simple assumption of a free standing pile restrained at its tip is often employed. Though the approach seems more advanced than the “rigid cap” approach in which the pile cap is assumed to possess infinite “out-of-plane” stiffness, accuracy is not significantly improved since the pile support stiffness is not properly represented. In fact, the unreasonable phenomenon will result in that a pile driven to greater depth will attract smaller load if the free pile length approach is adopted.

H5.1.3 MINIMUM PILE SPACING

The Code specifies minimum pile spacing for various types of pile so as to (i) minimize the group effects of overstressing the subgrade and/or creating excessive settlement; and (ii) allow for positional and verticality tolerances in pile construction. However, the requirement (i) may be waived for piles founding on competent strata. For example, for a mini-pile or socketed pile where the bearing capacity is derived from rock, the minimum pile spacing requirement could be based on consideration of construction tolerances only.

With full justifications based on recognized engineering principles or tests, proposals for other minimum pile spacing values may be accepted.

H5.1.4 HORIZONTAL RESTRAINTS TO PILES AND PILE CAPS

The Code specifies that for driven piles and small diameter piles, adequate horizontal restraints in at least 2 directions shall be provided for individual piles or pile caps. However, the restraint should only be necessary for potentially “unstable” pile groups, for example a pile group comprising only one or two piles where restraint is effected by tying at the pile cap levels to other pile groups or foundations. A pile group with a large numbers of driven piles or small diameter piles is stable and tying to other foundations is not necessary.

H5.1.5 PILE PROVIDING RESTRAINTS AGAINST SLIDING

The clause simply requires

$$\frac{\text{Ultimate Lateral Resistance by the Ground on the Piled Foundation}}{\text{External Applied Lateral Load}} \geq 1.5$$

The passive resistance of the ground has to be determined by recognized soil mechanics principles. Ultimate lateral resistances to movements of the pile cap and the pile group in soil and rock depend on the passive resistance of the soil and the ultimate lateral bearing capacity of the rock. Reference can be made to clause 5.3.4 and Appendix HF for determination of the ultimate lateral resistance to movement of a pile while that of the pile cap is generally governed by the passive resistance of the soil.

Nevertheless, it should be borne in mind that deflection is another controlling design criterion as in addition to the ultimate resistance.

H5.1.6 PILE PROVIDING RESTRAINTS AGAINST UPLIFT, OVERTURNING AND BUOYANCY

The clause is concerned with checking the stability of the piled foundation against uplift, overturning and buoyancy by achieving the required factors of safety as stated in clause 2.5.4 for the whole structure. In addition, if all piles of the structure satisfy the following two equations, then stability of the whole structure is deemed to have satisfied.

$$(a) \quad D_{\min} + 0.9R_u - 2.0I_a - 1.5U_a \text{ (or } 1.1U_p) - 1.5W_k \geq 0 \text{ (ultimate load condition);}$$

$$(b) \quad D_{\min} + R_a - I_a - U_a - W_k \geq 0 \quad (\text{working load condition});$$

where the symbols are defined by the Code. It can readily be seen that generally equation (a) controls the pile design unless R_u has a very high value comparatively and $R_u > 2R_a$. A demonstration is enclosed in Appendix HG for a hypothetical pile group in which the loads on each pile for various load cases are analyzed.

The clause allows stability check to be carried out “globally” as in Worked Example H2.2 by which the entire structure is treated as an integral unit with the assumption that the structure possesses adequate stiffness and the structural members have adequate strengths to effect global behaviour. Generally, if the structural analysis is carried out for the “integral structure” used for global analysis for stability (with the same load factors for stability check) and the structural design is carried out accordingly, the stiffness and strengths of the members are deemed to satisfy the stability requirements. However, it should be noted that some individual piles may not possess adequate factors of safety against uplift if equation (a) above is not satisfied while global stability is found satisfactory to clause 2.5.4. So, instead, equation (b) above should be checked to ensure all piles do not fail uplift under working load, or otherwise non-linear analysis has to be carried out, by which the piles reaching their maximum values will stay at these values and excess being taken up by others.

H5.1.7 PILE GROUP SETTLEMENT

The equivalent raft method as mentioned by the Code for determination of pile group settlement is a conventional method which applies to pile groups of closely spaced piles. The closely spaced piles with the soil held by the piles can effectively perform as a sunken raft footing. The settlements are then estimated as if the pile group is a sunken footing at the levels equal to two thirds of the pile group in case the piles are end-bearing on soil or at the hard rock stratum if founded on hard rock stratum. The method is fully described by Tomlinson (2008) which also specifies the spread of the foundation loads. Detailed discussions of the method together with a worked example are enclosed in Appendix HH. Nevertheless, it should be noted that there are quite a number of methods complying with recognized engineering principles for the estimation of pile group settlements, apart from the equivalent raft method.

H5.2 NEGATIVE SKIN FRICTION

H5.2.1 DESIGN REQUIREMENT

Negative skin friction (NSF) on a pile originates from the downward drag action due to the settlement of soil that surrounds the pile. The relative movement between the installed piles and the surrounding soils is usually caused by the consolidation settlement of fine-grained soils that take a long time to complete after the pile installation. It is common that the effect of NSF should be considered on sites in newly reclaimed land where consolidation settlement of fine-grained soil strata is still on-going after the completion of the structure. In addition, as the soil strata above the consolidating stratum will also settle, the determination of NSF should include effects due to the consolidating stratum and all soil strata above it.

In considering provision of a double skin permanent liner infilled with inert flexible material to reduce NSF, such a pile may be free-standing for certain height and is not embedded in the soil. The ‘buckling’ problem may lead to reduction of the load carrying capacity of the pile.

Two more general aspects for NSF are discussed as follows:

- (i) NSF depends on the relative displacement between the piles and the surrounding soils. If there is subsequent settlement of the pile against the surrounding soil, the NSF will be reduced or even eliminated;
- (ii) NSF will develop with time as the soil consolidates. When it exists, NSF acts together with the dead load and permanent imposed load (a term used in clause 2.3.3.3 of the Code of Practice for the Structural Use of Concrete 2013) on the pile. Therefore the pile must be structurally designed to resist dead + permanent imposed load + NSF. However, a transitory imposed load creating a transitory pile settlement will help reduce NSF and therefore needs not be taken into account in design unless it is greater than twice the NSF which, apart from entirely nullifying the NSF, adds a load greater than the NSF itself, thus constituting a critical design load, leading to a design load of dead + permanent imposed + transitory imposed load.

The Code outlines two approaches for the determination of NSF in clauses 5.2.2 and 5.2.3.

H5.2.2 CONVENTIONAL APPROACH

The Conventional Approach requires NSF to be included in the checking of structural integrity of the pile and the bearing capacity of the ground. In the equation for assessing NSF on the pile, which is $\int_0^l \tau_s \cdot p \, dl = \int_0^l \beta \sigma' \cdot p \, dl$, where $\tau_s = \beta \sigma'$ is the unit skin friction on the pile shaft in which β is the coefficient directly converting the effective vertical stress σ' to the friction τ_s and p is the perimeter of the pile. Analytically it may be considered that $\beta = K_s \tan \delta$ where K_s and $\tan \delta$ are respectively coefficients for converting the effective vertical stress in the soil to horizontal stress and for converting horizontal stress to a friction (Bowles 1996). The use of this β coefficient constitutes the “Beta approach”. The β values can be back analyzed from pile loading tests to derive the positive skin friction force which assumes the relationship $\tau_s = K_s \sigma' \tan \delta$ as described in more details in 5.3.2 (1)(b). It should be noted that the method of pile construction would influence the horizontal stress. The derivation of K_s may be correlated to the at-rest lateral coefficient of the soil, K_0 . GEO Publication 1/2006 gives some guidance on the use of K_s for displacement and replacement piles. Table 6.3 of the Publication summarizes the range of β values interpreted from pile loading tests conducted in saprolites in Hong Kong. From the table it can be seen that the β values can vary a lot for different installation method and types of piles. The clause in the Code recommends the use of a typical value of 0.25 in saprolites, sand or marine deposit in

design, in the absence of more accurate assessment. However, economy of the pile design in term of NSF consideration may be achieved by deriving the β values using recognized engineering principles and/or verified by tests.

The length of the pile, for determination of NSF is taken conservatively to the depth of the consolidation stratum, though strictly speaking NSF ends at the “neutral point” which is at a higher level. However, the determination of the neutral point is generally difficult.

The group effect should also be considered in the determination of negative skin friction.

H5.2.3 ALTERNATIVE APPROACH

In the alternative approach, NSF does not need to be considered when checking the ground bearing capacity (geotechnical capacity) of the pile, but the NSF does need to be fully considered in the checking of the structural capacity. This is based on the consideration of the limit state that where the ground supporting the pile has reached the ultimate condition, the pile under this limit state would be settled leading to a reversal of relative movement between the pile and the surrounding soils. Therefore all NSF in the pile is eliminated and needs not be considered in the following equation / condition :

Ultimate ground bearing capacity of pile \geq ultimate loads excluding NSF

Assuming the allowable ground-bearing capacity of the pile has a safety factor of not less than 2 and the load factors for ultimate loads are not greater than 2, the above equation / condition may be simplified to :

Allowable ground bearing capacity of pile \geq working loads excluding NSF.

In addition, the Code requires that checking of the settlement behaviour of the pile under total loads including NSF should be satisfactory.

The Code allows the test load for a pile designed by the alternative approach be $2P_c + \text{NSF}$ instead of the normal requirement of twice of the total allowable load which should be $2(P_c + \text{NSF})$ where P_c is the allowable bearing load for the pile and NSF is determined in accordance with clause 5.2.2. This is because (i) the NSF so determined is an ultimate load as discussed above which should be divided by 2 for conversion to allowable load; (ii) the excessive settlement of the pile during a loading test can effectively eliminate the NSF.

More detailed discussion on NSF can be found in Fellenius (1989) and other references.

H5.3 LOAD CAPACITY OF PILES

Clause 5.3 of the Code is self-explanatory.

H5.3.1 STRUCTURAL STRENGTH

Structural strength design can be based on the appropriate limitation of stresses as

specified. Furthermore, the Code reminds that the buckling capacity of piles should be checked to allow for embedment in soft strata. Slender piles with considerable lengths which are sleeved or exposed should also be checked for buckling. A discussion of the buckling phenomenon in piles based on Law (2013) together with design tables is given in Appendix HI.

H5.3.2 GROUND RESISTANCE FOR PILES IN COMPRESSION

(1) Driven piles

The ultimate bearing capacity of a driven pile can be determined from (a) dynamic formula; (b) a static formula; and (c) a loading test.

(a) Dynamic Formula

The Code has listed the Hiley formula as a dynamic formula and values / ranges of parameters for the production of final set tables. The Handbook, as in addition to the Hiley Formula, also includes discussions on various popular techniques including wave equations, PDA, Case Equation, CAPWAP in the determination of pile load capacity and pile integrity.

(I) Hiley Formula (1925)

The Hiley Formula listed in the clause which is also the commonest dynamic formula used locally is reproduced as follows

$$P_u = \frac{E_h W_h h}{s + 0.5(c_c + c_p + c_q)} \left\{ \frac{W_h + e^2(W_p + W_r)}{W_h + (W_p + W_r)} \right\} \quad (\text{Eqn H5.1})$$

where the definition of the symbols are listed in the clause.

If a follower is used, its weight should be added to W_p . The underlying principle and derivation of the formula is based on the energy and momentum conservation principles as detailed in Appendix HJ. There are many uncertainties, however, with this method discussed as follows :

(i) The Hammer Efficiency E_h

The loss in potential energy of the hammer represented as $W_h h$, does not convert entirely into kinetic energy of the hammer before impact. The cables and/or guide rails within the hammer absorb some of the energy so that only $E_h W_h h$ remains. The E_h (hammer efficiency) of the hammer is entirely a characteristic of the hammer and recommendations, which are only approximations, are given in reference books (Poulos & Davis (1980)) for different types of hammer varying from 0.7 to 0.9. The Code has adopted the value of 0.7 for drop hammer, unless verified otherwise by test. New techniques such as the PDA test which can measure the velocity U_h of the hammer just before impact enable the user to back-calculate the factor using

$E_h = 0.5(W/g)U_h^2/W_h h = U_h^2/2gh$. But it is tedious to calibrate E_h by the technique as E_h is not independent of drop height as is often assumed.

(ii) Momentum during Impact

The formula assumes “rigid body collision” between the hammer and the pile in setting up the momentum transfer equation (Re (Eqn HJ-2) in Appendix HJ) as part of the derivation of the Hiley Formula. This assumes that every part of the pile is affected and moves with the same velocity after impact. This is obviously not valid as the pile is compressible and the error is significant for a long pile in which the pile and the hammer may separate (momentum transfer completed) before the impact “wave” can travel to the tip of the pile. As such, only a certain length of the pile (termed the “affected length”) is affected during impact. The factor $\frac{W_h + e^2(W_p + W_r)}{W_h + (W_p + W_r)}$ representing the percentage of energy remaining after impact, as derived in (Eqn HJ-8) of Appendix HJ, is an under-estimation of the factor and consequently lead to under-estimation of the pile capacity.

(iii) Energy in Temporary Compression of Cushion and Pile

The terms representing the energy used in a temporary compression of the cushion and the pile represented respectively by $0.5P_u c_c$ and $0.5P_u c_p$ are taken as static in the derivation. As the actions are actually dynamic, the energy loss is under-estimated in the temporary compressions. In addition, a constant value of c_c in the range of 4 mm to 6 mm is often assumed in actual trade practice, regardless of the variation of other parameters, which again induces further errors. A current practice utilizes a video camera to measure the actual value of c_c .

(iv) Energy in Temporary Compression of the Soil

The formula assumes elasto-plastic behaviour of the soil and that the load on the soil increases slowly from zero to the maximum at P_u where the soil reaches its elastic limit at c_q , beyond which the soil continues to slip (deform) at the constant load P_u until S which is the permanent toe movement of the Pile or the “Final Set” measured in pile driving. The energy transfer assumed by the Hiley Formula is represented by the area below the load displacement line in Figure H5.2(a). But in fact, the problem is not a static one as, in addition to the static force, a “damping” force in the soil is also mobilized when the pile moves relatively to the soil at a certain speed so that the actual “load path” diagram should be represented by Figure H5.2(b). As this soil damping force consumes some energy which dissipates to the soil around when pile driving has finished, the pile will exhibit static behaviour only, and the load carrying capacity of the soil is overestimated by the formula.

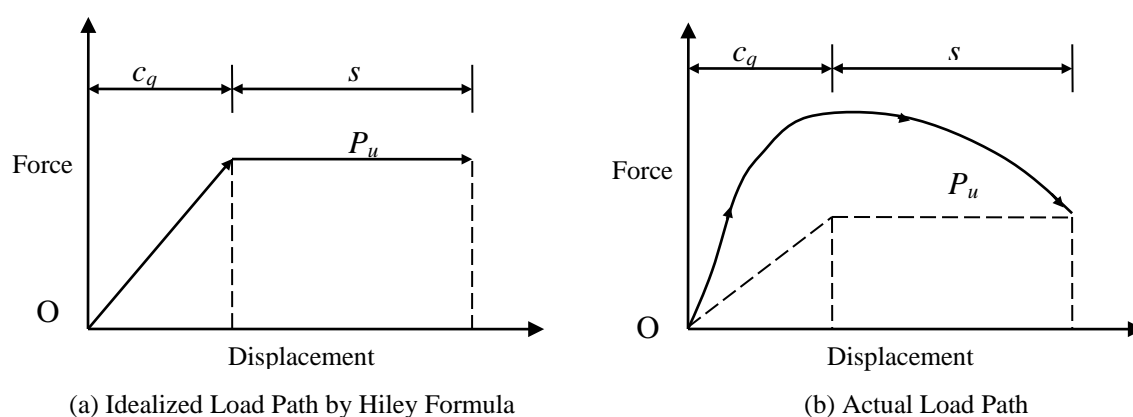


Figure H5.2 – Load Displacement Path for Set and Temporary Compression of Soil

Two major sources of error are identified in relation to the foregoing discussion but there are means to minimize them:

(1) “Affected Length” of the Pile

In relation to the phenomenon that only a portion of pile length (affected length) can be mobilized during driving as “body movement” when the pile length is long, GEO Publication No. 1/2006 has commented that “According to dynamic stress wave theory, it is not rational to take into account the full weight of the pile in the Hiley Formula where the pile length exceeds about 30m, depending on the velocity of wave propagation through the pile.” This is also evidenced by the phenomenon that when $W_h h$ of a given hammer exceeds a certain threshold value, $c_p + c_q$ become insensitive to an increase of drop height h , indicating that a maximum c_p exists (as c_q is comparatively very small, of the order of 2.5mm), and that the maximum “affected length” has been reached. There are suggestions in the estimation of W_p using only a portion of the length (affected length) of the pile in the dynamic formula. Cornfield (1961) advised that, “Wave equation suggests that for steel bearing piles of normal weights the effect of variation in pile length may be insignificant in which the lengths are over about 50ft (around 15m).” Triantafyllidis (2000), based on the principles of wave mechanics, derived a method for estimating the “affected length of the pile”. However, the method is not commonly used and there appears to be no simple approach that can fairly accurately determine the affected length of the pile.

(2) Energy injected to the Pile

Another major source of error is the determination of the energy transferred to the pile after impact. The error can be eliminated however if the energy at the top level of the pile after impact can be measured. The measurement can be made using techniques such as the Pile Driving Analyzer (PDA) test. So if the energy can be measured and expressed as a fraction of the loss in potential

energy of the hammer $W_h h$ as $XW_h h$ where X is the energy transfer ratio, the following relation can be established as :

$$E_{\max} = XW_h h = P_u s + 0.5P_u(c_p + c_q) \Rightarrow P_u = \frac{XW_h h}{s + 0.5(c_p + c_q)} \quad (\text{Eqn H5.2})$$

with X allowing for the effects of hammer efficiency and energy loss due to impact. But these factors are related to the characteristics of the hammers and the site geology and therefore need to be established on site through energy measurements and back-calculations. The factors would have different values even on the same site for different hammers, different pile lengths, soil geology etc.

Summing up, it is generally accepted that Hiley's Formula under-estimates the pile capacity (determined by static loading test as required by the Code) or requires more than adequately stringent "Set" to achieve the required pile capacity, especially for long piles. Past practice is to limit the final "Set" values to certain ranges including "not less than 25mm per 10 blows unless rock has been reached", resulting in very narrow range for the Set values available. In recent years there is a modification that "Set" between more than 50mm but not greater than 100mm per 10 blows can also be accepted though capped at 50mm per 10 blows in the calculation of P_u . In addition, the calculated final "Set" should be discarded if the corresponding $(c_p + c_q)/L > 1.15$ where c_p , c_q are in mm and L in m for the purpose of limiting the driving stress in the pile. The practice is formally incorporated in the clause. A discussion of the evolution and demonstration of the use of these limits are given in Appendix HK.

(II) Wave Equations

The realization that pile driving cannot be accurately analyzed by rigid-body mechanics has led to the development of an analysis that utilizes the wave theory on an elastic body. This analysis takes into account the fact that stress waves (created in the pile by impact of the driving hammer) of varying magnitudes move down the length of the pile at the speed of sound. The pile is not stressed equally and simultaneously along its length, as assumed in the conventional dynamic formulae. In addition, the wave equation analysis also considers individually the effects of various factors in the driving process such as pile and hammer characteristics, cushion stiffness, soil damping effects by inserting appropriate parameters. The ultimate static load capacity of the pile offered by the soil can be estimated more correctly.

The basic wave equation for pile driving follows a partial differential equation. The equation is a one dimensional (geometrically) solution describing the displacement of any point of the pile at co-ordinate x and at time t which reads :

$$\frac{\partial^2 u}{\partial t^2} = c^2 \frac{\partial^2 u}{\partial x^2} + S(x, t) \quad (\text{Eqn H5.3})$$

where

- u is the displacement of a point in the pile from its original position;
- x is the co-ordinate of a point on the pile, often taken as distance from the pile top;
- t is time;
- c is the wave speed in the pile which is equal to $\sqrt{E/\rho}$ where E and ρ are the Young's Modulus and the density of the material making up the pile respectively; and
- $S(x, t)$ is the term representing the soil resistance force at x and t comprising both the static and dynamic components

Derivation of the differential equation can be found in Appendix HL and text books including Poulos & Davis (1980) and Bowles (1996). By solving the equation the displacement at any point of the pile and at any time can be obtained provided that $S(x, t)$ and other boundary conditions of the differential equation such as initial displacements, velocities etc. are known. However, it is often the other way round in that by measuring the displacements (sets) and velocities etc. and making assumptions on parameters such as the form of distribution of resistance, soil spring values, quake (elastic limit of the soil), damping constants of soil etc., the soil resistance which represents the load capacity of the pile is calculated instead. Smith (1962) suggested an approach to solve the equation in which the pile is idealized into a series of masses connected by elastic springs and “dashpots” as illustrated in Figure HL-6 in Appendix HL. Each of the masses meets soil resistances, both static (dependent on displacement of soil) and dynamic (dependent on the velocity of the mass when the pile is struck by the hammer) components. A pile capacity versus final set values can be obtained. The analysis is tedious and the iterative computation usually requires a computer programme to derive the solution.

(III) Pile Driving Analyzer (PDA)

Use of the Pile Driving Analyzer (PDA) is a technique by which the pile dynamic behaviours during driving including pile forces and accelerations are measured by such electronic devices as transducers and accelerometers installed at the top of the pile. By applying wave theory analysis to these measured quantities, the load carrying capacity, soil parameters, energy transfer, pile driving stresses and integrity of the pile can be estimated. Among these methods, the Case method and CAPWAP are relatively common and are described in details in Appendix HL.

Generally the following quantities can be measured in PDA tests :

- (i) Maximum energy delivered to the pile by the ram (EMX). As discussed, this energy can be used to calibrate the hammer efficiency and the impact factor used in the Hiley Formula. The quantity can be found for a single hammer blow and an averaged value over 10 blows can also be calculated;
- (ii) Maximum impact force (FMX) which is usually the first maximum force as shown in Figure HL-7 in Appendix HL. This force can be used to calculate the static capacity of the pile by the Case Method commonly used in the industry as described below and in Appendix HL;
- (iii) Forces and velocities (particle velocities) at the top of the pile are normally

taken at 1024 (2^{10}) “time measurement points” (or multiples). (The use of the 1024 time measurement points is for facilitation of the working of “Fast Fourier Transform”.) Thus if the total time taken for measurement is 102.4ms (millisecond), the readings are taken at 0.1ms intervals;

The following quantities can then be calculated based on the measured quantities:

- (i) The maximum compressive stress (CSX), which is simply the measured maximum force in the pile divided by the cross sectional area of the pile;
- (ii) The ultimate static capacity of the pile (RMX) which can be calculated by the Case Method under various assumed J_c values (soil damping constants) as demonstrated in HL.3.2 in Appendix HL;
- (iii) The pile integrity factor (BTA) which is arrived at by examination of the wave forms. More detailed discussion is given in Appendix HL;
- (iv) The compressive stress at the bottom of the pile (CSB);
- (v) Total skin friction (SFT).

(IV) Case Method

The Case Method (Rausche et al., 1985) is a closed-form solution based on the assumptions of a uniform pile cross-section, linear elastic pile behaviour; and others as stated in Appendix HL Section HL.3. For a pile with impedance $Z_p = EA/c$ where E , A and c are the Young’s Modulus of the pile material, cross sectional area of the pile and wave propagation velocity of the stress-wave in the pile respectively, the ultimate static capacity is approximately given by

$$R = \frac{(1 - J_c)}{2} (F_1 + Z_p v_1) + \frac{(1 + J_c)}{2} (F_2 - Z_p v_2) \quad (\text{Eqn H5.4})$$

where R is the ultimate static capacity of the pile;
 F_1 is the pile head force measured at time t_{c1} ;
 F_2 is the pile head force measured at time t_{c2} ;
 v_1 is the pile head velocity measured at time t_{c1} ;
 v_2 is the pile head velocity measured at time t_{c2} ;
 t_{c1} is the time when the pile head force F_1 is recorded;
 $t_{c2} = t_{c1} + 2L/c$;
 L is the length of pile measured from pile head instruments to pile toe;
 c is the propagation of velocity of stress-wave in pile and can be calculated by $c = \sqrt{E/\rho}$ where E and ρ are the Young’s Modulus and density of the piling material respectively;
 J_c is the “Lumped Case damping factor” which defines the dynamic component of the pile at the pile toe. Its value depends on the type of soil at the pile toe and the dimensions of the pile.

With the appropriately chosen J_c value, R is determined as the maximum value that can be arrived at among various measured sets of F_1 , F_2 , v_1 , v_2 . A detailed description of the Case Method with illustration of its use by a numerical example

is given in Appendix HL. It should be noted that Case method is more accurate when the end bearing resistance is the dominating component, as the damping factor is lumped at the pile toe only.

(V) CAPWAP (Case Pile Wave Analysis Program) or Similar

CAPWAP is a computer program developed by the Case Institute of Technology in the late 1960s. It originated from the Smith (1960) model by combining the PDA data in the form of a force and velocity development against time (wave traces) with the Wave Equation Analysis of Pile (WEAP) program (Rausche et al. 1972, Rausche et al. 1988) and computes R iteratively by signal matching.

With this technique, the velocities and forces are first measured by the PDA method at the top of the pile during the strike by the hammer. The pile head forces (or pile head velocities) are then input into the Wave Equation as ‘input excitation’ to carry out analysis under a set of initially assumed soil parameters including quake, damping constant, ultimate friction distribution along pile shaft etc. Normally, the back-calculated pile head velocities (or pile head forces) would be different from the measured ones. The soil parameters are then adjusted and the Wave Equation reanalyzed until a reasonably good matching between the calculated and measured values is obtained. Then, there is a good reason to assume that the correct soil parameters have been ascertained and the ultimate static capacity of the pile can be calculated. However, it should be noted that the answers may not be unique, i.e. different sets of soil parameters can all result in good matching with the measured quantities.

Thus CAPWAP analysis is actually an extension of Wave Equation Analysis with the following improvements :

- (i) The hammer input excitation is measured by electronic devices. The energy at the top of the pile can also be estimated. It thus eliminates the use of the assumed values of hammer efficiency and the elastic compression C_c ;
- (ii) In the Wave Equation Analysis, the only measurable quantity to be checked against the calculated pile load capacity is the “set”. However, the CAPWAP enables pile load capacity to be arrived at by achieving a match between the calculated and measured pile head velocities and forces. Thus CAPWAP should be able to give more accurate answers.

The matching mechanism of the CAPWAP method is illustrated in Appendix HL. In actual CAPWAP operation, an automatic matching approach is used where the matching is carried out by the optimization algorithm built in the program. However, as good matching by the algorithm can still be achieved by unreasonable soil parameters and load capacity of the pile, the results should be carefully assessed by experienced HOKLAS accredited laboratories and where necessary exercise manual signal matching with soil parameters within reasonable ranges.

(VI) Using CAPWAP to Calibrate the Final Set Table

As CAPWAP can give a fairly accurate pile load capacity, the CAPWAP capacity can be used to calibrate the parameters, including the hammer efficiency E_h and the coefficient of restitution e used in the Hiley Formula by back-substitution. The calibrated formula can then be used to determine the final set table. The calibrated parameters may not carry any physical meanings by which they were derived. They may be considered simply as coefficients to fit into the Hiley Formula which may only be used in the particular site and hammer with certain fall heights.

(b) Static Formula

The static formula for determination of the geotechnical load capacity of pile is based on soil mechanics principles from which shaft friction and end-bearing of the pile in the soil are determined and the sum gives the total capacity of the pile. Generally the unit shaft friction and end-bearing are determined by the following expressions which is based on soil mechanics theory.

$$\text{Unit shaft friction} \quad \tau = c + K_s' \sigma' \tan \delta' \quad (\text{Eqn H5.5a})$$

$$\text{Or} \quad \tau = c + \beta \sigma' \quad (\text{Eqn H5.5b})$$

$$\text{End-bearing} \quad q_b = cN_c + \sigma' N_q + 0.5\gamma B N_\gamma \quad (\text{Eqn H5.6})$$

$$\text{Total shaft friction is} \quad P_s = \int_0^L \tau \cdot p \, dl \quad (\text{Eqn H5.7})$$

$$\text{Total end bearing is} \quad P_b = q_b A_b \quad (\text{Eqn H5.8})$$

$$\text{Total pile capacity is} \quad P = P_s + P_b \quad (\text{Eqn H5.9})$$

For the above equations, the symbols are defined as follows :

- τ is the unit skin friction;
- q_b is the unit end-bearing;
- σ' is the effective vertical earth pressure;
- K_s' is the coefficient of horizontal pressure;
- δ' is the angle of friction between the soil and the pile shaft;
- β is the shaft friction coefficient converting effective vertical earth pressure to unit shaft friction;
- N_c , N_q and N_γ are the bearing capacity factors for cohesion, end bearing and overburden pressures;
- γ is the unit weight of the soil;
- B is the lateral dimension of the pile;
- p is the perimeter length of the pile;
- A_b is the base area of the pile;
- L is the pile length.

Formulae and charts to determine the parameters can be found in various publications including Poulos & Davis (1980) and GEO Publication 1/2006 which are often based on soil parameters such as ϕ , c and SPT N values of the soil. However, it should be noted that the correlations with these parameters are largely

based on limited field data. Accurate assessments are often difficult, but the assessments tend to be on the conservative side.

As for the end bearing capacity in accordance with (Eqn H5.6), the component $\sigma' N_q$ is often the pre-dominant one. There are different theoretical approaches for the determination of N_q by Berezantsev, Vesic, Hansen etc. However, according to Poulos (1980), Vesic (1967) had pointed out that Berezantsev et al. (1961) appeared to fit the available test data best. GEO Publication 1/2006 has included the design chart in Poulos (1980) based on Berezantsev's work. Nevertheless, a more precise chart showing relations with pile length to diameter ratio is found in Tomlinson (2008) which is extracted in Appendix HM together with some discussions on Berezantsev's approach and the mathematical expressions.

In addition, loading test on instrumented pile can be carried out to determine the soil parameters. Strain gauges are installed along their shafts so that the strains and consequently stresses along the pile shaft can be measured and finally skin frictions and the end-bearing of the pile can be determined. The measured values can then be applied to other piles in the same site for pre-determination of their bearing capacities.

(c) Loading Test of the Pile on Site

Compliance criteria for a pile loading test are often in terms of limitation of settlements and/or residual settlements. The test is often specified for verification of pile loading capacity. The testing procedures involved for common types of piles are clearly stipulated in the Code.

(2) Non-Driven piles

Determination of the bearing capacity of piles socketed into rock by the Code is comparatively straightforward when compared with driven piles as the capacity is usually based on the geometry of the pile and the allowable bearing pressures and/or bond strengths of different categories of rock. The Code explicitly allows the combined use of end-bearing and shaft resistance in the determination of the total bearing capacity of large diameter bored piles in accordance with clause 5.4.7 of the Code. However, for all other piles, the combined use of end-bearing and shaft resistance is restricted unless it can be justified that settlements under working load conditions are acceptable and adequate to mobilize the required shaft resistance and end bearing simultaneously. This is because mobilization of the required shaft friction and end-bearing may require movements of the subgrade of different orders which might not be compatible along the pile shaft and the pile base, taking into account the shortening of the pile under the applied load. In addition, the minimum socket length in rock specified in Note (3) under Table 2.1 of the Code could be ignored in pile bearing calculation for large diameter bored piles and other piles socketed in rock.

H5.3.3 GROUND RESISTANCE FOR PILES SUBJECTED TO UPLIFT FORCES

(1) General

The clause defines allowable and ultimate anchorage resistance (R_a and R_u) of a pile against uplift as respectively the allowable and ultimate uplift resistance of pile shaft plus “effective self-weight” of the pile. The anchorage resistance refers to the frictional resistance of soil on the pile shaft with methods of determination stipulated in sub-clause (3). Nevertheless, the Code further states that anchorage resistance is limited by the effect weight of soil mass/cone weight the pile mobilized as a check against “pull out failure” of the pile with the weight of rock cone and soil column effectively carried by it. It should, however, be noted that the Code lists the limitation by a mathematical inequality for R_u only as

$$R_u - W_p' \leq W_1' + W_2'$$

While there is no similar inequality listed for R_a , similar check for R_a is therefore not necessary. In fact, it should be very adequate to take the effective weight as an upper limit in checking for stability as the load factors for the de-stabilizing forces are all taken into account in cl. 5.1.6.

(2) Piles with Rock Socket

The clause reminds that friction and bond resistance of the pile shaft with rock should be based on simple figures in Table 2.2 of the Code and also that the ultimate bond stress is related to the allowable value by a factor of safety of 2.

Detailed criteria are laid down in the clause for determination of the extent of the rock / soil cone / column the pile can mobilize as weight against uplift. The criteria are based on conservative consideration with the maximum half angle of the inverted rock cone limited to 30° which is for heavily jointed or shattered rock. In addition, the weight of the soil mass is also limited to that directly over the rock cone while neglecting friction between the outer face of the soil column and the surrounding soil as shown in Figure 5.1(a) of the Code which also illustrates that soil weight beyond boundary to be ignored. In addition, as a conservative approach, the bell-out (if any) is considered not effective by the Code in mobilizing the cone and cylinder shaped mass of soil and rock above the base of the pile. As the determination of the volume of rock and soil is complicated in case the soil columns and rock cones of adjacent piles overlap as shown in Figure 5.1(b), some useful algebraic expressions are given in Appendix HN, together with worked examples. Although the worked examples are for large diameter bored piles, the same approach can be applied to rock socketed piles.

Unlike friction piles in sub-clauses (3)(a)(ii) and (iii) which require uplift resistance due to permanent tension to be half of that of transient tension, the uplift resistance for piles with rock socket determined in this sub-clause applies equally to transient and permanent tension.

(3) Piles in Granular Soil

This clause is for determination of uplift resistance of piles from shaft friction only in granular soil. Three methods are outlined for driven steel H-piles. The first method is based on a nominal uniform allowable shaft friction of 10kPa, with the

ultimate value doubled. The second method is based on effective stress theory which correlates the shaft friction to the horizontal stress acting normally to the circumference of the pile which in turn depends on the effective vertical stress. The third method is based on empirical correlation of shaft friction to SPT N values of soil. For the second and third method, limiting values are imposed unless verified by trial piles and the values determined are for transient tension with that due to permanent tension being halved. So for the application of the equations in clause 5.1.6 which contain single value for R_u and R_a , they may have to be modified as follows

$$(a) \quad \frac{2.0I_a + 1.5U_a \text{ (or } 1.1U_p) - D_{\min}}{R_{u-\text{permanent}}} + \frac{1.5W_k}{R_{u-\text{transient}}} \leq 0.9$$

$$(b) \quad \frac{I_a + U_a - D_{\min}}{R_{a-\text{permanent}}} + \frac{W_k}{R_{a-\text{transient}}} \leq 1$$

In fact, the two relations listed above are equivalent to adoption of the original formulae in the Code with the transient wind loads to be checked against the transient resistance, i.e. $R_{u-\text{transient}}$ and $R_{a-\text{transient}}$.

The Code has not specified specific design requirements for other pile types. It would be acceptable so long recognized engineering principles are complied with.

Assessment of the effective weight of the soil cone/soil column for pile groups in granular soil also involves complicated geometry. A worked example demonstrating compliance with the design requirements is included in Appendix HN.

H5.3.4 GROUND RESISTANCE FOR PILES SUBJECTED TO LATERAL LOAD

Horizontal restraint can be provided by the piles or the pile cap alone or the combined action of both. Estimation of the restraint of a pile cap can be based on the elastic continuum theory where the pile cap is embedded in a semi-infinite elastic medium. Mindlin's Equations or their integrated forms (Vaziri et al. 1982) can be used to determine restraints on pile cap. More in-depth discussions based on Law & Cheng (2014) are given in Appendix HO in which tabulated values are given for determination of the lateral restraint by a more rigorous approach taking compatibility of the pile cap and the soil movement into account. Nevertheless, caution should be taken in design if there is probable removal of the embedding soil to the pile cap.

The Code requires checking of the load carrying capacity of the pile and capacity of the lateral soil resistance, as an addition to deflection when considering group effects. Lateral deflection of pile is discussed first in this section.

As for the pile cap case above, the lateral deflection of a pile can also be based on the elastic continuum method (summarized by Poulos & Davis 1980) or the finite element method. Randolph (1981) has fitted the results of finite element analysis into algebraic expressions and proposed formulae which are reproduced in GEO Publication 1/2006.

However, a simpler method based on Terzaghi's "subgrade reactions" method (1955) which is in turn a Winkler's spring approach is commonly used in the local industry and this approach is adopted for granular soil in the Code where the "Constant of Horizontal Subgrade Reaction" are listed in its Table 5.1. Under the "subgrade reactions" method, the soil restraint is idealized as a series of elastic springs (independent of each other) on the pile shaft. Design charts based on the approach are found in Tomlinson (1994), DM-7 (1971) and GEO Publication 1/2006. Detailed discussion of the method with tabulated coefficients for quick determination of deflection and bending moments in the piles are given in Appendix HP with illustrative worked examples. Unlike the charts given by Tomlinson (1994), DM-7 (1971) and GEO Publication 1/2006 which are confined to piles with pile heads at ground level, the tabulated coefficients cover piles with cut-off levels below ground, which is more general in use.

In accordance with Terzaghi (1955), the "coefficient of horizontal subgrade reaction" which is the pressure on the soil required to produce unit displacement is, for a given type of soil, directly proportional to depth and inversely proportional to the width (or diameter) of the pile. The relationship is given by equation (Eqn HP-1) in Appendix HP with the proportionality constant known as the "constant of horizontal subgrade reaction" (symbol n_h) as termed by Terzaghi (1955). Terzaghi (1955) further recommended typical values of n_h for "loose", "medium" and "dense" soils which are extracted in Table H5.1 after conversion into metric unit. To substantiate the effect due to denseness of the soil, GEO Publication 1/2006 has added the SPT N values which are also appended in Table H5.1 as follows and basically identical to Table 5.1 of the Code.

	Loose (SPT N value = 4 – 10)	Medium (SPT N value = 11 – 30)	Dense (SPT N value = 31 – 50)
n_h for dry or moist sand	2200 kN/m ² /m	6600 kN/m ² /m	17600 kN/m ² /m
n_h for submerged sand	1300 kN/m ² /m	4400 kN/m ² /m	10700 kN/m ² /m

Table H5.1 – Values of n_h for Cohesionless Soils

From (Eqn HP-1) in Appendix HP, it follows that the final restraint exerted by the soil on the pile is independent on the width (or diameter) of the pile which appears not very reasonable. Poulos & Davis (1980) actually proposed that k_h in (Eqn HP-1) (the coefficient of horizontal subgrade reaction of the soil defined as the pressure required to move the soil by unit length) should be proportional to $(z/B)^n$ where n is slightly greater than 1 for sandy soil and $n=0$ for clayey soil. Since n is close to unity, k_h can be approximately taken as independent of pile diameter. In addition, Siu (1992) alternatively proposed to modify k_h by applying the factor $(B/B_0)^{0.25}$ where B is the diameter of the pile in metre and $B_0 = 1$ m for a circular pile.

According to GEO Publication 1/2006, the n_h values quoted in Table 5.1 of the Code are valid for stresses up to half of the ultimate bearing capacity of the soil with allowance made for long term movement.

To account for the group effect, reductions on the n_h value as functions of pile spacing in the direction of loading have been proposed in the Canadian Foundation Engineering Manual (1978) which is reproduced in Table 5.2 of the Code. Nevertheless, if interpolation of values is assumed, the relation can be fitted to a linear equation as

$$\text{Reduction Factor} = \text{Ratio of pile spacing to pile diameter} \times 0.15 - 0.2 \quad (\text{Eqn H5.10})$$

Both the Canadian Foundation Engineering Manual and the Code have no clear indication on the reduction factor when the ratio of pile spacing to pile diameter is less than 3 but the pile spacing still satisfies the minimum requirements in cl. 5.1.3 of the Code. Nevertheless, it should be reasonable to adopt a value as extrapolation from the values of Table 5.2 which is the simple application of (Eqn H5.10).

In Appendix HP, the analysis of a pile under lateral load is illustrated with results in deflections and internal forces of the pile. For structural design, partial load factors should be applied as appropriate.

For checking the lateral load capacity of a pile which is governed either by the ultimate soil strength or the structural strength of the pile, approaches by Broms (1964a & 1964b) and Poulos & Davis (1980) may be followed respectively for floating piles and socketed piles. The ultimate loads so arrived at should be divided by a factor of safety of 3 for checking against the characteristic lateral load. Illustrations of the checking of the ultimate lateral resistance of a floating pile assuming pinned and fixed connections to the pile cap is demonstrated in Appendix HF with numerical worked examples.

As a control to excessive pile deflection, the Code requires P- Δ effects to be addressed when estimated pile deflection exceeds 25mm by elastic analysis. Both deflections and internal forces in the pile will be increased when P- Δ effect is included in design consideration. Some detailed discussion is outlined in Appendix HP, with reference to Appendix HI.

The Code further warrants that piles and pile caps should not be used together to resist lateral forces unless a distribution of forces between piles and pile caps can be demonstrated. The distribution can be calculated assuming compatibility of displacement of the piles and pile cap with the pre-determined lateral stiffness of the piles and the pile cap. A recommended approach with a numerical example is given in Appendix HQ. Analysis can also be carried out by computer with appropriate lateral stiffness inputs of the piles and pile cap.

H5.4 COMMON PILE TYPES

The clause outlines particular requirements for some specific types of pile commonly used in Hong Kong. The following serves to highlight the characteristics of each type of pile and elaborates the requirements further with illustrations by figures and practical examples.

The points in common relating to the design of all types of piles under this clause are listed as follows :

- (i) The load carrying capacities of the piles can be increased by 25% due to wind load under the permissible stress method as per clause 2.5.5(1) of the Code;
- (ii) Pile group reduction factors should be applied where appropriate in accordance with clause 5.1.2 of the Code;

H5.4.1 STEEL H-PILES/STEEL TUBULAR PILES

The following considerations apply to this type of pile :

- (i) Loading Capacity of the Pile;

Allowable working loading capacity (axial load) of the pile is limited by clause 2.5.5(4) of the Code as follows :

$$P = 0.3 \times f_y \times A_p \quad (\text{Installed by Driving}) \quad (\text{Eqn H5.11})$$

$$P = 0.5 \times f_y \times A_p \quad (\text{Installed by Preboring or Jacking}) \quad (\text{Eqn H5.12})$$

where f_y is the yield strength of the steel and A_p is the cross sectional area of the pile. The lower factor of 0.3 for a pile installed by driving is to reduce the bearing capacity of the driven pile so as to minimize the use of the heavy hammer and high drop height to avoid high stresses during pile driving.

The minimum steel yield stresses should be determined from the “design strength” of steelwork in accordance with Table 3.2 of the Code of Practice for the Structural Use of Steel 2011 or BSEN10025. The yield stresses depend on the grades and thicknesses of the steel pile sections. A thicker section has a smaller yield strength because of the greater locked-in stresses created during the cooling of the hot-rolled section.

Nevertheless, the Code also allows the use of limit state design in the structural design of piles in accordance with the Code of Practice for Structural Use of Steel 2011. So the designer may use limit state design for pile sections under axial load and bending, while limiting axial load to comply with (Eqn H5.11) and (Eqn 5.12).

The geotechnical capacity of the driven pile can also be ascertained by a dynamic formula. For driven steel H pile or small diameter tubular piles, the pile would generally be founded on soil of a specified SPT N values, e.g. not lower than 200. However, driven piles founded on soil of SPT N values < 200 are also acceptable if their capacities can be justified by other rational means.

- (ii) The clause also requires “splicing”, “pile head” and “pile tip” details to be included in the foundation plan. Typical details are illustrated in Figures H5.3 to H5.5. In addition, the clause lists the requirements for weld testing in relation to the control of workmanship including certification of welder tests, welding procedure specification and the welding procedure test. Sample rates of not less than 10% of the total number of welded joints by non-destructive testing are also specified for destructive testing.

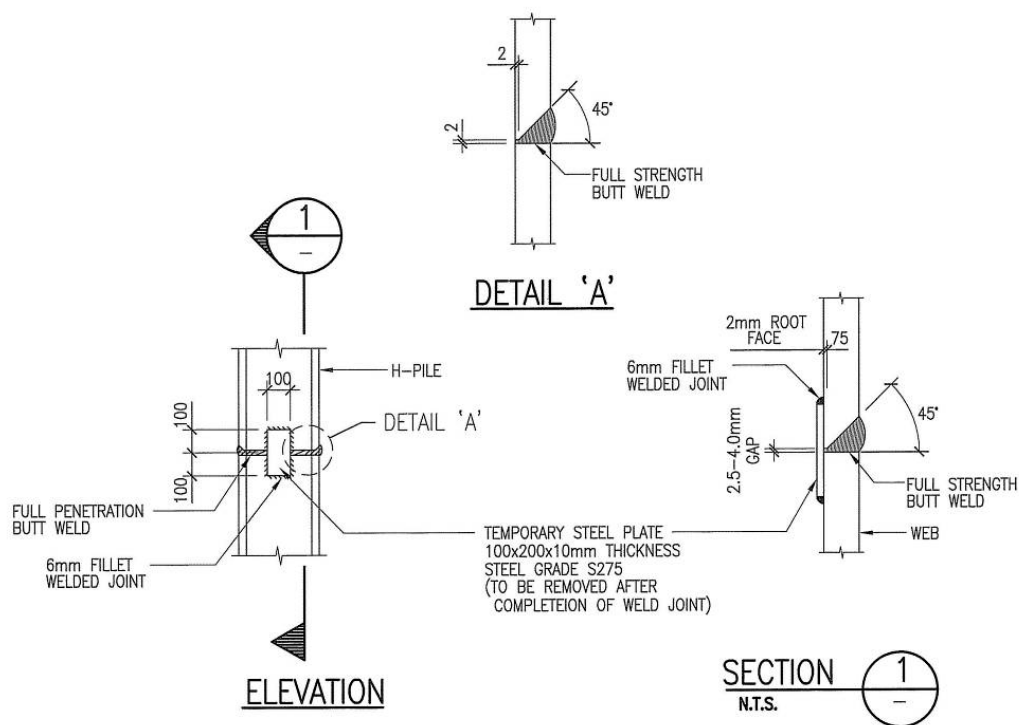


Figure H5.3 – Splicing Details for H-pile (for Lengthening of Pile)

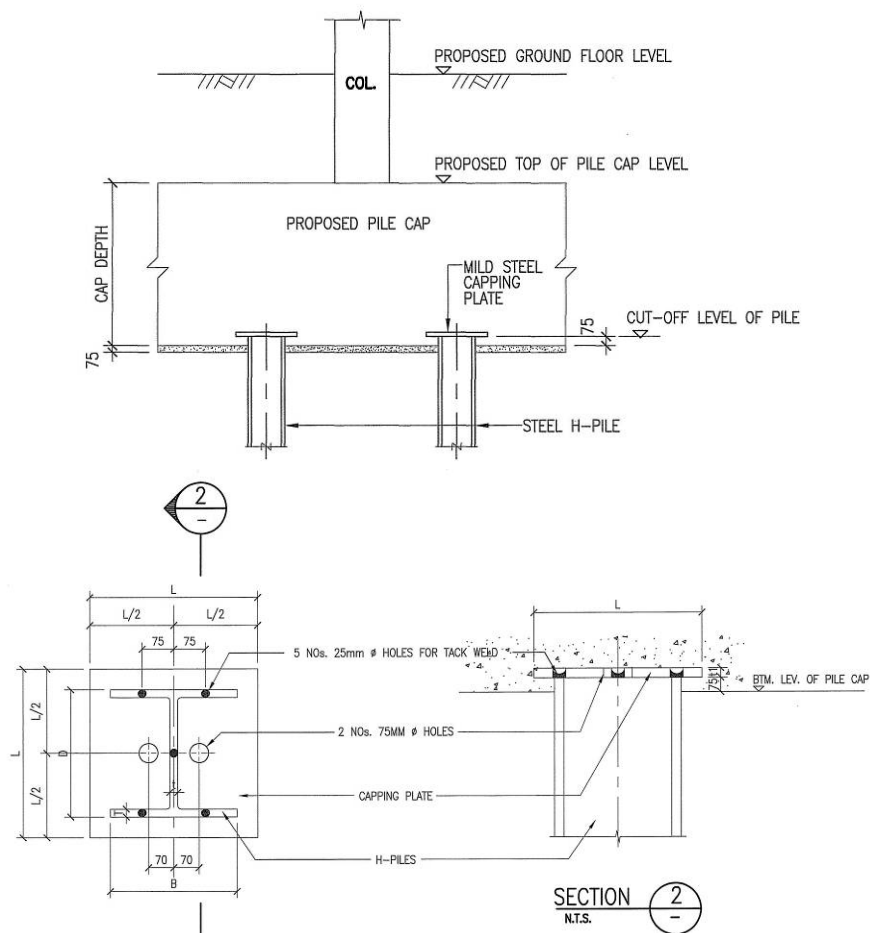


Figure H5.4 – Details for Pile Head

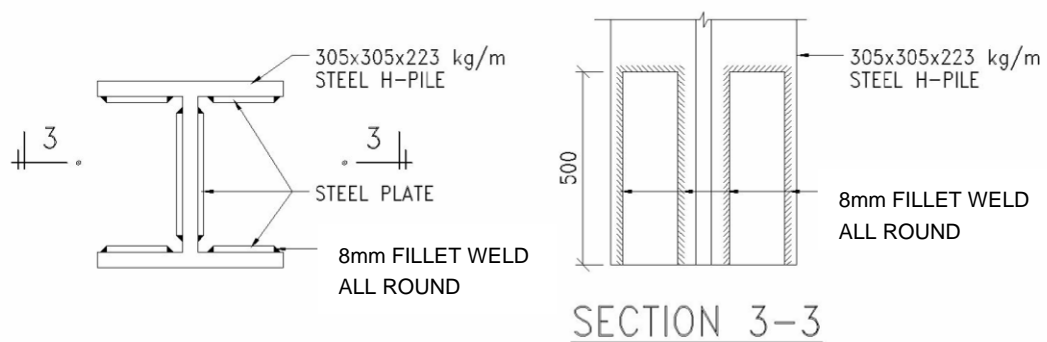


Figure H5.5 – Acceptable Details for Pile Toe – Strengthened for Hard Driving on or close to Bedrock

H5.4.2 SOCKETED STEEL H-PILES

As the pile is installed after pre-boring, its design axial load capacity is given by (Eqn H5.12) in accordance with clause 2.5.5(4) of the Code. Reference to Table 3.4 of the Code of Practice for the Structural Use of Steel 2011 or BSEN10025 for the design strength of steel should also be made.

The following Worked Example H5.1 illustrates the determination of the required bond lengths between (i) the steel section and the grout; and (ii) the grout and the rock.

Worked Example H5.1 :

Steel Section is S450J0 305×305×223 H-Section of cross sectional area 284cm²

Diameter of the bore hole in the rock = 550mm

Perimeter of the Steel Section = 1918mm;

Rock encountered : Category 1(c) rock, 700 kPa as the presumed allowable friction between rock and concrete or grout taken from Table 2.2; and 480kPa as the bond strength between the grout and steel given the use of shear connectors in accordance with clause 2.5.5(4) of the Code

Design of Load Carrying Capacity of the Pile (excluding casing and grout)

(i) Due to structural strength of the Steel Section :

$$P = 0.5 \times 430 \times 28400 \times 10^{-3} = 6106 \text{ kN}$$

(ii) To withstand the maximum load capacity of 6106kN, the minimum socket grouted length in rock should be $6106 / (0.55\pi \times 700) = 5.048 \text{ m}$;

(iii) Again to withstand the same maximum load, the minimum bond length between the grout and the steel section is $6106 / (1.918 \times 480) = 6.632 \text{ m}$ which should be measured within the rock socket where effective confinement to the grout can be provided by rock for achievement of the 480kPa bond strength.

So, to maximize the load carrying capacity of the pile as per its structural provisions and taking the required bond length into account, the minimum bond length required in Category 1(c) rock (as derived in the foregoing) is 6.632m.

Shorter bond lengths can be used if the pile is not designed for its maximum load carrying capacity.

Details of the splicing of piles and the pile head for socketed steel H-piles are similar to those for Steel H-piles/Steel Tubular Piles as discussed in H5.4.1, Figures H5.3 to H5.5. Typical elevation of the socketed portion of a socketed pile is shown in Figure H2.3.

The Code requires rock sockets of sufficient strengths (and depths) to resist the ultimate shears and moments acting at the pile tip. The ultimate lateral strength of the rock can be assumed to be one third of the vertical allowable bearing pressure provided that there are no unfavourable joint sets or a steeply inclined rock surface in accordance with clause 2.2.2(3) of the Code. Reference can be made to Figures 51 to 53 of GEOGUIDE 1 for determination of the required depths of the socket.

H5.4.3 PRECAST REINFORCED CONCRETE PILES

The precast reinforced concrete pile is a large displacement pile driven into the ground where the geotechnical capacity is usually determined by a dynamic formula. Due to the relatively low load carrying capacity of the pile (governed by its small structural size and materials) and its limited penetration power through underground obstructions, the pile is usually used to support low or medium rise buildings on ground without significant amount of boulders or corestones. In addition, the pile should not be subjected to hard driving which can easily lead to damage of the pile head and pile toe.

Currently the pile is not commonly used in the local industry. A typical pile of square 14 inch (355.6mm) and concrete mix grade 20 (allowable concrete stress = 5MPa) possesses a maximum structural load carrying capacity of the order of $355.6^2 \times 5 \times 10^{-3} = 632 \text{ kN}$.

The capacity may be further limited by the geotechnical capacity as determined by its final set value in accordance with a dynamic formula. A typical detail of the 14 inch square pile is shown in Figure H5.6.

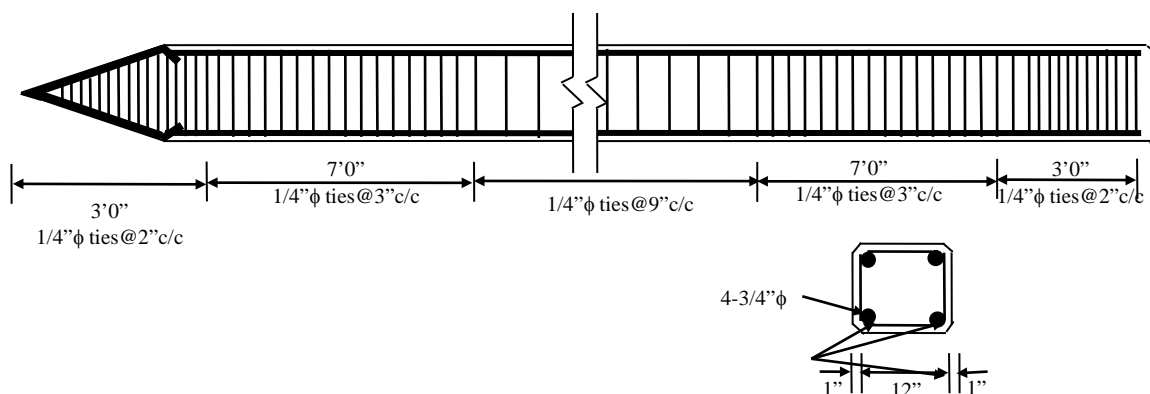


Figure H5.6 – Details of a 14''x14'' Precast Reinforced Concrete Pile

H5.4.4 PRECAST PRESTRESSED SPUN CONCRETE PILES

The precast prestressed spun concrete pile is manufactured using high grade concrete (cube strength up to 78MPa) with prestressed tendons embedded in the pile. Spinning of the pile shaft is involved during manufacture of the pile. The prestressing force in the tendons serves to resist the transient tensions which may be induced during pile driving, though it takes up some of the compressive load carrying capacity of the pile.

Like precast reinforced concrete piles, the pile is a large displacement pile and both share similar construction problems such as a low resistance to hard driving to penetrate underground obstructions. Reports of structural damage were not uncommon when the piles were hard driven to decomposed rock strata of high SPT N values with significant boulder contents. (as often pre-determined in design). The advantage of this type of pile is that they are normally terminated at soil strata with SPT N values greater than 120, which would usually be founded at a shallower depth when compared with small diameter displacement piles, such as driven steel H pile. However, the driving sequence has to be planned carefully to minimize the difficulty in driving the piles in over-densified soil due to driving of the already installed piles and pile rising, e.g. pile driving in the outward directions. Re-driving of pile (after suffering from pile rising) may also be needed. So the pile has to be constructed with great care.

The load carrying capacities of the common types of precast prestressed concrete piles are listed in Table H5.3. It should be noted that the maximum compressive load capacity of the pile is obtained by multiplying the cross sectional area of the pile by one quarter of the cube strength of concrete after deduction of the strength taken up by the pre-stressing tendons. A sample calculation is done for the second item in Table H5.2 as $0.25 \times (78.48 - 5.33) \times 125664 \times 10^{-3} = 2298 \approx 2300 \text{ kN}$

where the concrete cube strength and the ultimate stress induced in the concrete by the prestressing tendons are 78.48MPa and 5.33MPa respectively.

Outside Diameter (D) (mm)	Inside Diameter (mm)	Wall Thickness (T) (mm)	Cross Sectional Area (cm ²)	Effective Prestress (MPa)	Allowable Bearing Capacity of Pile (kN)	Tensile Strength of Pile (kN)		Allowable Shearing Strength (kN)	Allowable Cracking Bending Moment (kNm)
						Allowable	Ultimate		
400	206	97	923	5.10	1,690	471	969	227	73.55
500	300	100	1257	5.33	2,300	669	1347	304	137.29
500	250	125	1473	5.03	2,700	741	1536	361	147.10
600	390	105	1633	4.95	3,000	809	1690	382	215.75
600	340	130	1920	5.24	3,500	1005	2041	466	245.17

Table H5.2 – Data of Common Precast Prestressed Spun Concrete Pile

Precast prestressed spun concrete piles should not be designed to resist bending and/or tension. Also, a follower is not recommended for use with this piling system.

Figure H5.7 to Figure H5.9 show typical details of this type of Pile. For driving the pile into stiff soil, there are two common types of pile shoes, one being conical type, the other being cross type. The cross type pile shoe with cross stiffeners is shown in Figure H5.9.

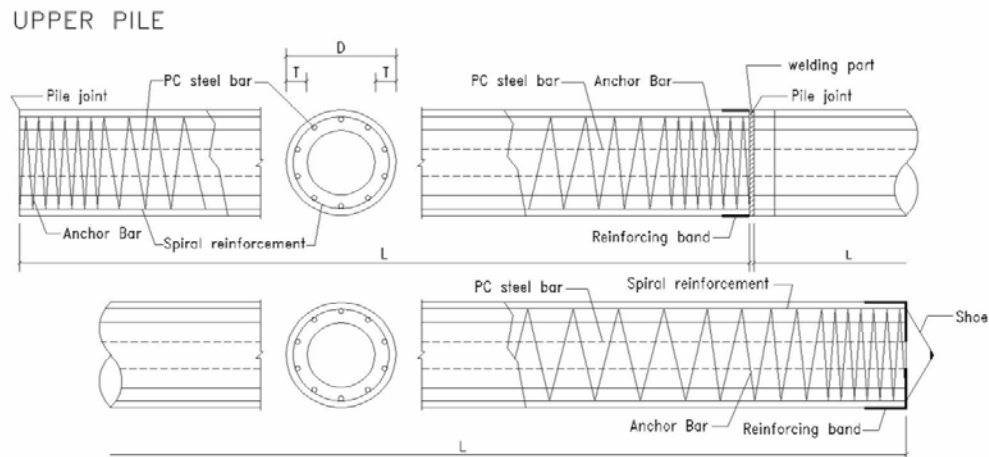


Figure H5.7 – Details of Pile Shaft of a Precast Prestressed Spun Concrete Pile

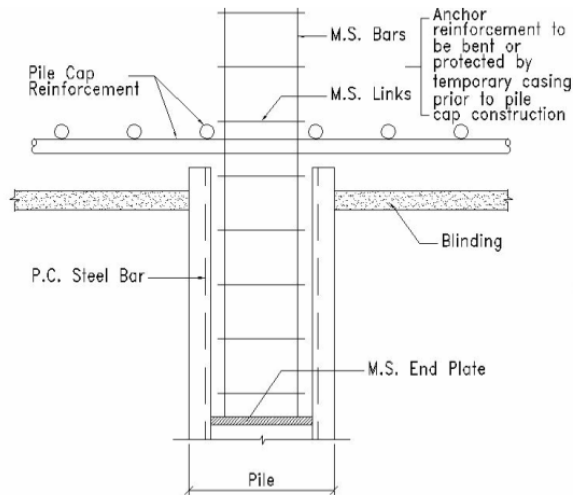


Figure H5.8 – Typical Pile Head Details of a Precast Prestressed Spun Concrete Pile

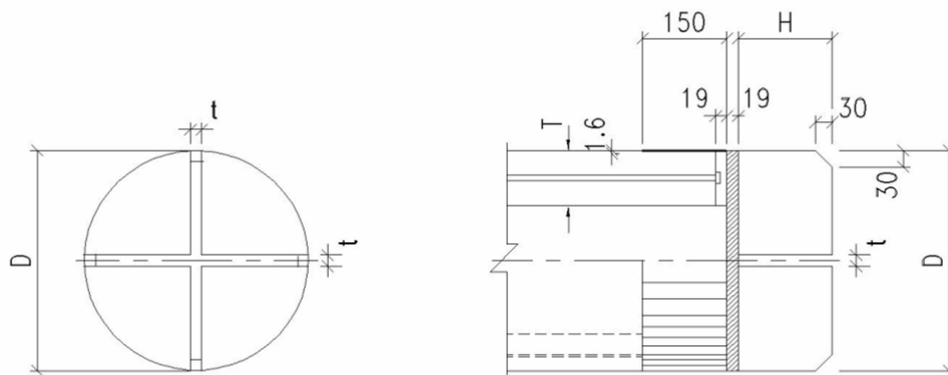


Figure H5.9 – Pile Shoe Details for a Precast Prestressed Spun Concrete Pile

H5.4.5 DRIVEN CAST-IN-PLACE CONCRETE PILES

The pile is constructed by driving a steel tube capped at the bottom into the ground until a satisfactory “set” has been achieved in accordance with a dynamic formula or for a length

determined by a static formula for the load carrying capacity which is usually pre-determined by the structural provisions. Concrete is then poured into the tube with reinforcing steel and the steel tube extracted (with the bottom cap detached) before the concrete hardens.

The Code limits the size of the pile to 750mm. Popular sizes used in the 1980s were 610mm diameter and 635mm diameter with grade 25 concrete (permissible stress = 6.25MPa). The capacities are therefore

$$0.25 \times 610^2 \pi \times 6.25 \times 10^{-3} = 1827 \text{ kN and } 0.25 \times 635^2 \pi \times 6.25 \times 10^{-3} = 1979 \text{ kN.}$$

Figure H5.10 shows the pile details.

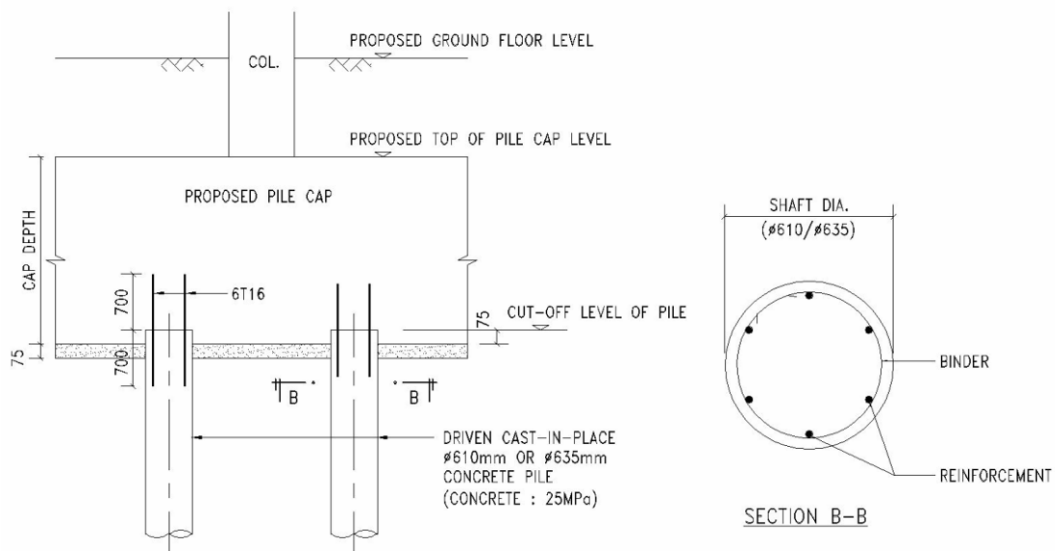


Figure H5.10 – Pile Head Details of a Driven Cast-in-Place Pile

As vibrations may adversely affect the integrity of newly poured concrete, the Code does not allow driving of new piles which are less than 5 diameters away within 24 hours.

H5.4.6 SMALL DIAMETER BORED PILES

(1) General

The Code defines a small diameter bored pile as a bored pile with diameter not exceeding 750mm which may be formed by boring a casing into the ground and subsequently filling the hole with concrete or grout. As the pile derives its bearing largely from skin friction, pressure grouting or pressurized concrete are favoured.

Basically, the total allowable bearing capacity of the pile is derived from skin friction and end-bearing which are often related to the SPT N values.

Trial piles are generally necessary for this type of pile as the bearing capacities and the integrity of the pile are affected by so many uncertainties related to the site geology and construction method. Even with adequate trial piles to justify the

friction factor μ (used to correlate unit skin friction to SPT N values), the factor is recommended to be capped at 0.7 generally.

(2) Continuous Flight Auger Pile (CFA Pile)

The CFA pile is a small diameter bored pile formed by augering into the ground and then subsequently filling the hole with cement sand grout (by pumping) and a reinforcement cage. Under pressurized grouting, a higher friction factor μ can be allowed for this type of small diameter bored pile. The Code allows the factor to be 1.0 which can be increased to 1.6 with trial pile tests. A sample design calculation of a CFA pile with pressurized cement sand grout is presented below as Worked Example H5.2. The design data for the pile and calculations are as follows :

Worked Example H5.2

Pile Diameter = 610mm;

Shaft resistance taken as $0.61 \times \pi \times \mu \times N_{av}$ kN per metre depth with the use of trial pile where N_{av} is the average SPT N value capped at a maximum value of 40;

Concrete strength = 25MPa;

No. of piles under the same pile cap : less than 4 (i.e. no pile group reduction factor is required)

The permissible stress of the concrete is 6.25MPa. But allowing for 20% reduction in strength due to concreting under water, the permissible stress is reduced to 5MPa.

The geotechnical capacity of the pile is determined in accordance with the empirical relations that shaft friction is $1.6N_{av}$ ($\mu = 1.6$) kN/m² and end-bearing is $5N_b$ kN/m² in accordance with the Code with N_{av} capped at 40. The SPT N values of the soil embedding the pile are listed in Table H5.3 by which the total shaft friction and end-bearing are calculated as 1709.60kN.

Depths Below Ground	Soil Description	Layer of depth (m)	SPT N value from G.I. report	Design SPT N value	Shaft Resistance (kN/m ²)	Shaft Resistance (kN)
0m – 6m	Fill or marine deposit	–	–	–	Neglected	–
6m – 21m	Completely Decomposed Granite	1.50	18	18	28.8	82.79
		1.50	25	25	40.0	114.98
		1.50	36	36	57.6	165.57
		1.50	48	40	64.0	183.97
		1.50	57	40	64.0	183.97
		1.50	62	40	64.0	183.97
		1.50	78	40	64.0	183.97
		1.50	91	40	64.0	183.97
		1.50	104	40	64.0	183.97
		1.50	118	40	64.0	183.97
Allowable Friction resistance						1,651.15
Allowable End bearing resistance = $5 \times 40 \times 0.61^2 \pi / 4$						58.45
Total loading capacity of pile						1,709.60

Table H5.3 – Determination of Geotechnical Capacity of a Small Diameter Bored Pile

Capacity of the pile in accordance with its structural provision is

$$P = 0.25 \times 610^2 \pi \times 5 \times 10^{-3} = 1460 \text{ kN (without wind).}$$

As the geotechnical capacity of the pile which is 1709kN is greater than the structural capacity, the structural capacity of 1460kN dictates.

The Code also stresses the monitoring of the grout factor, because of the relatively high uncertainty of the behaviour of the pile, together with precautionary measures.

Details of a small diameter CFA pile are shown in Figure H5.11. It should be noted that the reinforcement cage is normally not required to extend for the full length of the pile as long as structural adequacy of the pile can be demonstrated.

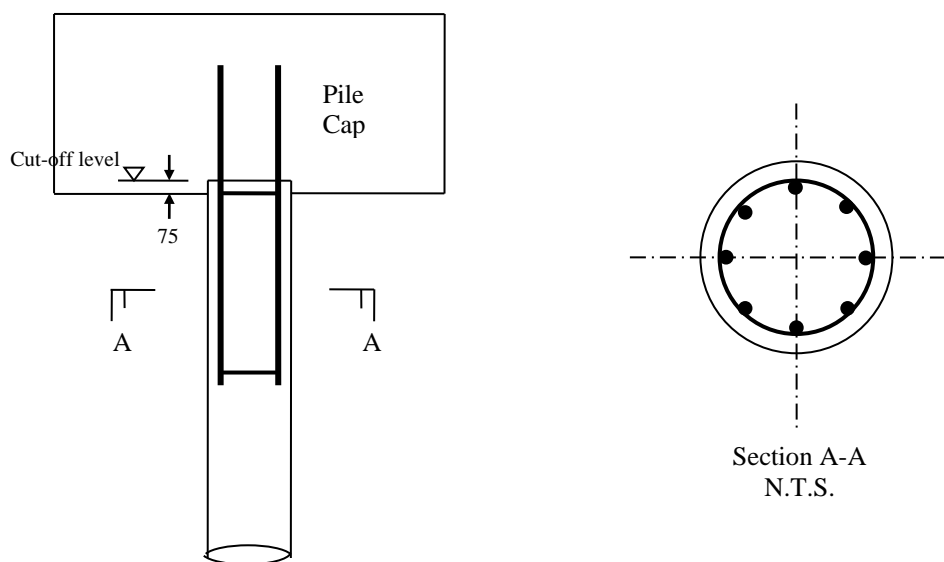


Figure H5.11 – Details of a Small Diameter CFA Pile

H5.4.7 LARGE DIAMETER BORED PILES

A large diameter bored pile is one having a diameter exceeding 750mm.

In Hong Kong, the geotechnical capacity of the large diameter bored pile usually derives from end-bearing with or without inclusion of shaft bond/friction with the rock along its pile shaft. As the concrete grades currently used are usually high, up to grade 45, giving a permissible compressive stress of the order of 11.25MPa which is well in excess of the rock bearing pressure of the order of 3 to 10MPa, bell-outs for enlargement of the end-bearing areas have been extensively used so that the geotechnical capacity can match the structural capacity in the pile shaft. Configuration of the large diameter bored pile with bell-out and the use of the shaft friction is demonstrated in Figure H1.1.

The design principles of large diameter bored pile are summarized as follows :

- (i) The loading capacity of a large diameter bored pile usually derives from the end bearing capacity on rock with or without shaft friction between rock and concrete;
- (ii) If there is a reduction of the cross sectional area in a rock socket, checking of the structural section for the reduced area is required with or without compensating reinforcement as necessary;
- (iii) The presumed values for allowable vertical bearing pressure and shaft resistance are given in Table 2.1 and Table 2.2 of the Code respectively;
- (iv) The maximum bell-out size of large diameter bored pile shall not exceed 1.65 times the shaft diameter and the gradient should not exceed 30° from vertical;
- (v) It should be noted that the nominal socket length of 0.5m or 0.3m as specified in note (3) under Table 2.1 are extra provisions over the limitation on design socket length and should not be counted in the calculation of shaft bond/friction. Normally, the nominal socket length can be well provided by the bell-out, if any;
- (vi) Socket length for bond or frictional resistance of the pile for enhancing bearing capacity of the pile should be limited to the lesser of 1 time the rock diameter and 3m if bell-out is used and the limitation can be relaxed to the lesser of 2 times the rock diameter and 6m if bell-out is not used.
- (vii) The design load capacity of a pile shaft is also governed by the structural section design of the pile, bearing in mind that a reduction of 20% of concrete or grout strength should be adopted if concreting or grouting under water;
- (viii) In steep bedrock profile, two adjacent large diameter bored piles shall be founded at levels differing by not more than the clear distance between them unless stability of the rock can be checked by recognized engineering principle. As the internal friction angle of bedrock is often taken as 40° , it is suggested that an elevation less than 40° can be taken as not being a steep bedrock profile, in which case the requirement can be exempted. In addition, the checking of overstresses as part of rock slope stability check can be based on the continuum theory by which reference can be made to Figure H3.1. For example, a 2m diameter pile with a bearing stress of 4500kN/m^2 , at a clear distance of 2m from and a level 2m above another pile will create a maximum additional stress of $0.08 \times 4500 = 360\text{ kN/m}^2$ at the perimeter of the other pile (0.12 is estimated from Figure H3.1). It can also be seen from Figure H3.1 that additional stress on a pile due to another pile at a higher level will be less than 5% of the bearing stress of the higher pile if their clear distance is more than one diameter apart as marked up by the 45 degrees lines.

A sample design of the load carrying capacity of a large diameter bored pile under Worked Example H5.3 is demonstrated as follows :

Worked Example H5.3 :

- (a) Shaft diameter = 3m in soil;
- (b) Bell-out diameter (at its maximum) = $1.65 \times 3.0 = 4.95\text{ m}$;
- (c) Category 1(c) rock is encountered at its base giving 5000kPa allowable end-bearing pressure and 700kPa shaft resistance under compression (Re Tables 2.1 and 2.2 of the Code.)

End-bearing capacity of the pile without bell-out is $0.25 \times 3^2 \times \pi \times 5000 = 35343\text{ kN}$

End-bearing capacity of the pile with bell-out is $0.25 \times 4.95^2 \times \pi \times 5000 = 96221\text{ kN}$

Effective socket length used without bell-out is $3 \times 2 = 6$ not greater than 6 m
 Shaft Resistance is therefore $3 \times \pi \times 6 \times 700 = 39584 \text{ kN}$

Effective socket length used with bell-out is $3 \times 1 = 3$ not greater than 3 m
 Shaft Resistance is therefore $3 \times \pi \times 3 \times 700 = 19792 \text{ kN}$

The total geotechnical capacity of the pile without bell-out but with socket length of 6m is $35343 + 39584 = 79427 \text{ kN}$

The total geotechnical capacity of the pile with bell-out but with 3m socket length is $96221 + 19792 = 116013 \text{ kN}$

So the use of bell-out (though with less allowable shaft friction) is more efficient in enhancing geotechnical capacity of the pile.

Typical details of a large diameter bored pile are shown in Figure H5.12.

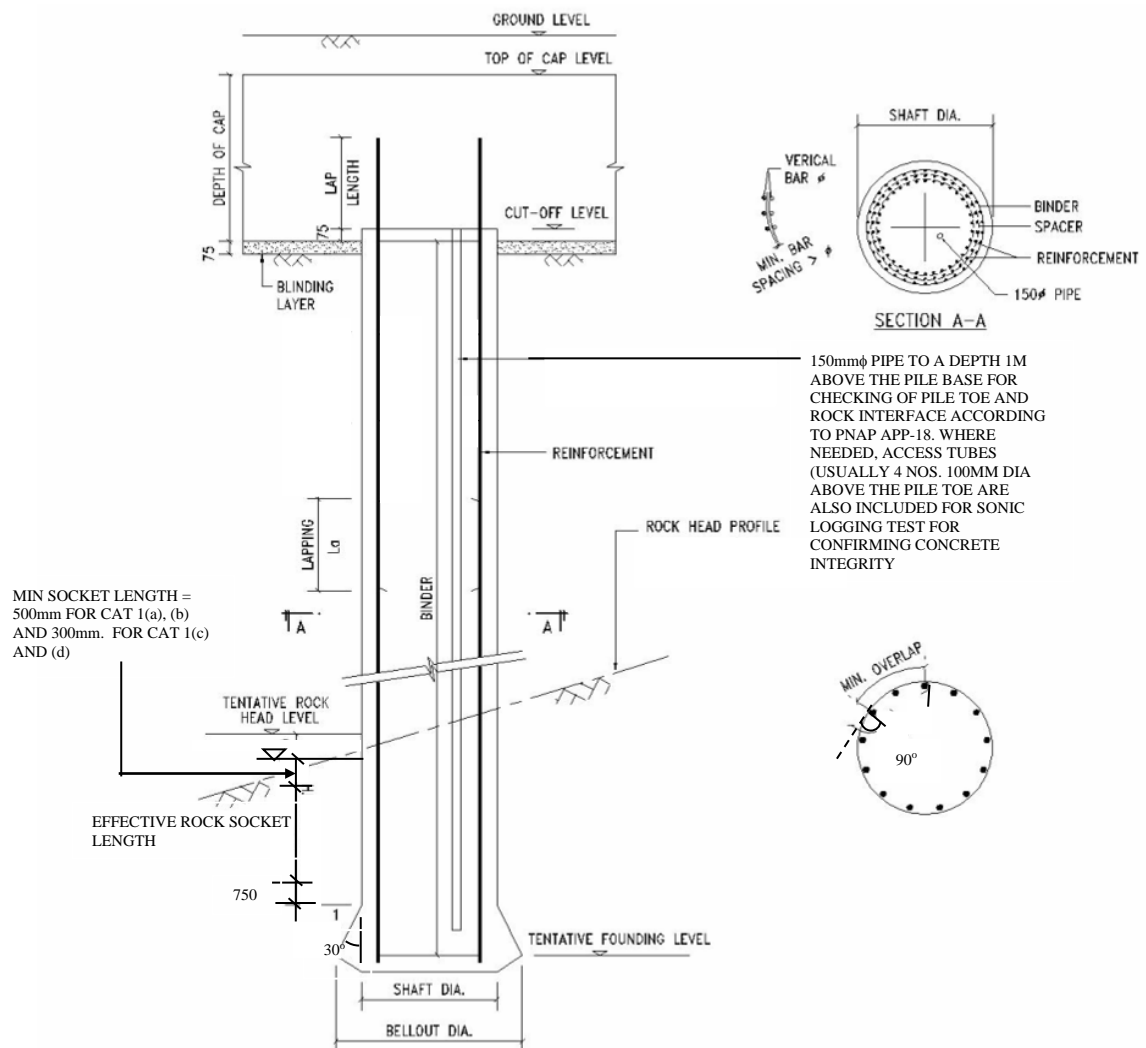


Figure H5.12 – Details of a Typical Large Diameter Bored Pile

H5.4.8 MINI-PILES

A mini-pile usually comprises 4 to 5 nos. of 50mm diameter steel reinforcing bars in a steel casing which is installed into a drill hole in the ground filled by cement grout in the trade practice. The pile derives its geotechnical capacity from bonding of the reinforcing bars with the rock through cement grout at level beneath the steel casing. The rock socket should be formed in Category 1(c) rock or better in accordance with Table 2.1 of the Code. The Code limits the number of bars to 5 and the outer diameter of casing to 450mm. The allowable working load on a mini-pile solely derives from the strength of reinforcing bars which is based on an allowable strength of $0.475f_y$. The use of the factor $0.475 < 0.5$ is to avoid exceedance of the yield strength of the pile during loading test with test load often twice the maximum working load.

The structural capacity of a mini-pile is comparatively low due to its relatively small size. However, as the machinery required for the construction is small and construction is fast, the pile is suitable for construction of buildings in sites where access is difficult. Though the overall load carrying capacity of a mini-pile foundation is not small if the piles are installed to minimum pile spacing (the smaller of 750mm and twice the outer diameter according to clause 5.1.3 of the Code), they may not be suitable for high-rise building as the pile cannot resist lateral load unless “raked”. Where mini-piles are to be adopted for high-rise building, some raking mini-piles are required to resist the lateral loads acting on the building structure.

The Code includes detailed descriptions of the design principles and construction considerations for this type of pile under this clause. The design principles of a mini-pile are briefly summarized as follows :

- (i) With $f_y = 500\text{MPa}$, the load carrying capacity of a normal 4T50 mini-pile is only $4 \times 25^2 \pi \times 0.475 \times 500 / 1000 = 1865\text{ kN}$ and that with 5T50 is 2332kN accordingly which are both less than the limit of 2350kN imposed by the Code;
- (ii) The presumed allowable bond or friction between rock and concrete is given in Table 2.2 of the Code;
- (iii) The perimeter of the shear plane for checking bond stress between the steel bars and grout are shown and determined in Figure H5.13 according to the clause 5.4.8(2)(e) of the Code :

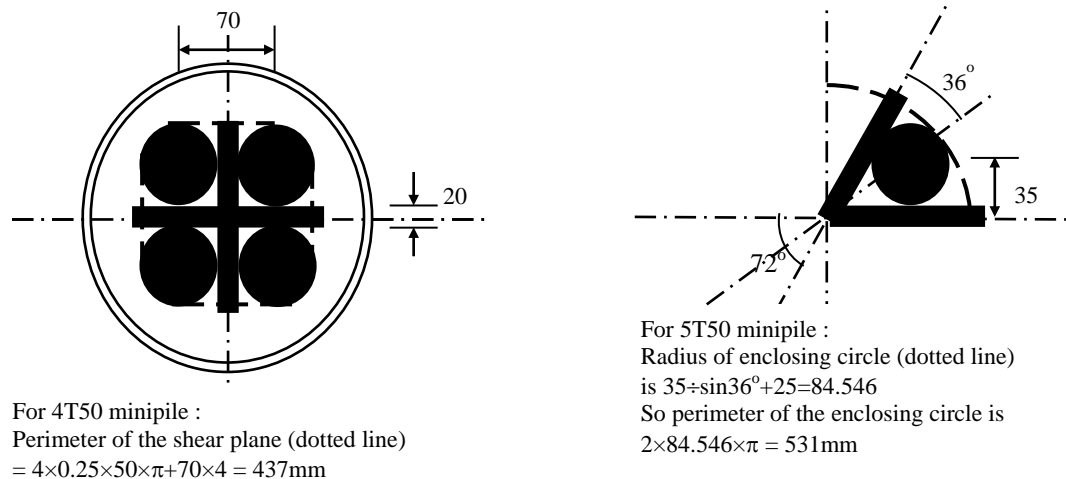


Figure H5.13 – Shear Plane for Checking Bond Stress between Steel Bars and Grout for 4T50 and 5T50 Mini-pile

- (iv) The allowable bond strength between steel bars and grout is limited to 0.8MPa which is small as compared with the ultimate bond strength as stated in clause 8.4.4 of the Code of Practice for Structural Use of Concrete 2013. Taking the 4T50 mini-pile where the perimeter is 437mm, the bond length required to achieve the design capacity of 1865kN is $1865 / (0.437 \times 800) = 5.33\text{m}$ which is the minimum length of a 4T50 mini-pile to develop the full capacity;
- (v) The allowable buckling capacity of the mini-pile may be checked with consideration of lateral restraints from the grout, permanent steel casing and the surrounding soil. A worked example is enclosed in Appendix HI;
- (vi) Only raking mini-pile can be used to resist lateral load in view of the small bending strengths of the pile. Figure H5.14 shows a structural configuration involving a raking pile that can achieve equilibrium in resisting the applied lateral load and result in no bending moments on the piles.

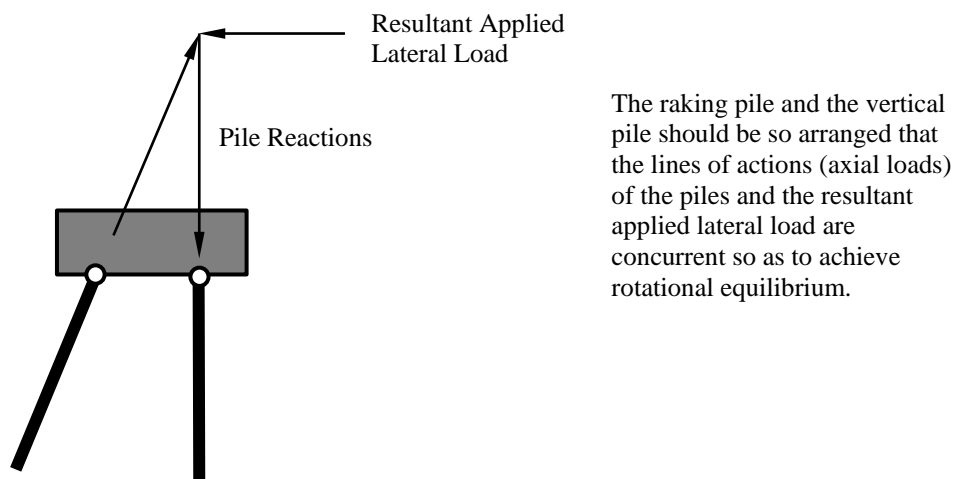


Figure H5.14 – Structural Configuration of Raking Mini-pile Resulting in Pure Axial Loads in the Piles

A sample design of the load carrying capacity of a mini-pile under Worked Example H5.4 in accordance with Figure H5.15 is demonstrated as follows :

Worked Example H5.4 :

Casing to the Mini-pile is Grade S275 263/273 CHS

Steel Casing External Diameter = 273mm;

Steel Casing Thickness = 5mm

Rock hole Diameter = 235mm;

4T50 Grade 500 High Yield Deformed Steel Bar;

Design grout strength = 30 MPa;

Rock encountered : Category 1(c) rock, 700 kPa (presumed allowable friction between rock and concrete or grout) is taken from Table 2.2;

Design of Load Carrying Capacity of the Pile (excluding casing and grout)

- (i) Due to structural strength of the reinforcing bars
$$P = 4 \times 0.25 \times 50^2 \times \pi \times 0.475 \times 500 = 1865 \text{ kN}$$
- (ii) To withstand the maximum load capacity of 1865kN, the minimum socket grouted length should be $1865 / (\pi \times 0.235 \times 700) = 3.61 \text{ m}$.

So, to maximize the load carrying capacity of the pile as per its structural provisions and taking the required bond length with grout into account, the minimum bond length required in Category 1(c) rock (as derived in the foregoing) is $5.33\text{m} > 3.61\text{m}$.

In view of the relatively small slenderness of the mini-pile, the Code reminds checking the allowable buckling capacity. Reference may be made to Appendix HI.

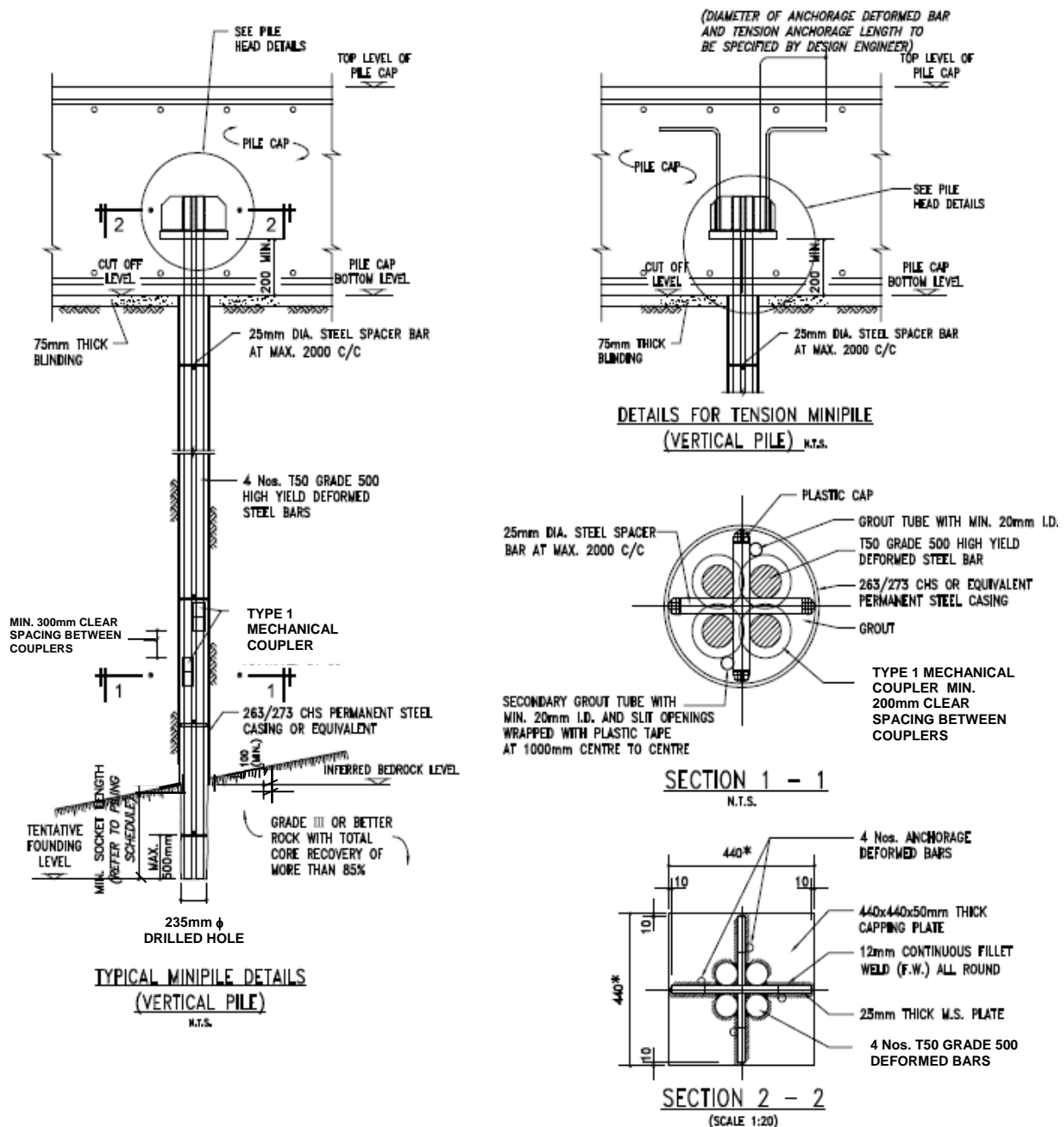


Figure H5.15 – Details of a 4T50 Mini-pile

H5.4.9 BARRETTES

Barrettes or barrette piles are constructed by machine excavation under a slurry filled trench down to the founding level. A reinforcement cage (and other structural elements as necessary, such as stanchions) is then inserted, followed by concreting of the excavated trench by tremie method. Barrettes are usually of rectangular plan section.

More detailed descriptions of this type of foundation are as follows. The descriptions also apply to diaphragm walls, which are essentially a succession of contiguous barrettes and as such can also be used as foundations resisting vertical loads.

(i) General Considerations :

(a) Effect of slurry :

While excavating the trench under bentonite slurry, the water from the slurry tends to filter out into the surrounding soil, driven by the necessary pressure head difference between the slurry and the outside groundwater. In this process, the bentonite clay particles are retained at the soil interface and form what is called a “cake”, plugging the soil pores and rendering the interface impermeable. The cake is generally a few millimetres thick and the performance depends essentially on the permeability of the surrounding soil (water from slurry has to flow out), and the permeability of the bentonite cake itself which in turn depends on the mud quality.

(b) Barrettes founded on rock

Barrettes are normally designed to be founded by end bearing on rock, following the same criteria as for bored piles. Where there is a socket, rock socket friction can also contribute to the bearing capacity.

(c) Barrettes founded in soil

Barrette can also be designed to be founded in soil by deriving bearing from soil friction and end-bearing in locations where bedrock is deep. As the ratio of perimeter over sectional area for a barrette is generally greater than that of large diameter bored pile, more cost effective design can therefore be achieved by using barrettes as friction piles.

The friction capacity of barrettes in soil may also be enhanced using shaft grouting, which consists of grouting the interface between the concrete and the soil, so as to compact the soil and increase the lateral stress acting on the barrette. The foundations of the International Commerce Centre in Hong Kong are a major example of such design.

However, it should be noted that instrumented trial piles are often required before construction of the working piles in order to verify the design assumptions, particularly on the mobilised pile shaft.

(ii) Design principles :

(a) End-bearing in rock :

End-bearing criteria in rock for barrettes and diaphragm walls should generally follow the same criteria as those for bored piles.

(b) Socket friction in rock

Where there is a socket, rock socket friction also contributes to the load carrying capacity, in addition to the end-bearing capacity. Rock socket friction shall follow the requirements of Table 2.2 of the Code in relation to “Presumed Allowable Bond or Friction between Rock and Concrete for Piles”.

(c) Friction & end-bearing in soil :

(1) Friction in Soils :

Minimum nominal friction : When full scale load tests are carried out, it is sometimes attempted to eliminate friction over the top section of the barrettes in order to concentrate the load in the soil stratum to be tested (e.g. CDG). This is usually done by means of creating an artificial interface using “Volclay” panels or similar arrangement. Monitoring results always show that even with such an artificial interface, the mobilized ultimate friction is always in the order of 25 to 30 kPa. Therefore it is concluded that an allowable nominal friction of 10 kPa can be adopted.

Estimation of friction capacity : Friction capacity in soils will depend on the type of soil and on whether shaft grouting is used. For the case of barrettes without shaft grouting, reference shall be made to GEO Publication 1/2006, paragraph 6.4.5.3 and case histories of tests given in Table A1 of its Appendix A.

(2) End-bearing in soils :

An end-bearing component in soil can be considered together with shaft friction in soil. Full scale load tests on “friction + end-bearing” barrettes, when carried to failure, have demonstrated ultimate end-bearing resistance values of 10N or more in C/HDG.

(iii) Construction Requirements

The slurry used for excavation may be based on bentonite, polymers or compatible combinations thereof.

The slurry in the excavated trench should be of sufficient hydraulic head to maintain the stability of the trench, including any surcharge from adjacent structures and construction loads.

Rigid reinforced concrete guide walls are usually provided to maintain alignment and verticality of the excavation as well as for supporting the weight of the structural elements (e.g. reinforcement cage, stanchions) hanging in the trench prior to pouring the concrete.

As for bored piles, the type of concrete used for barrettes and diaphragm walls shall have suitable workability characteristics. Suitable concrete characteristics are provided in BSEN 1538:2010+A1:2015 “Execution of special geotechnical works : Diaphragm Walls”.

Construction of a typical barrette is shown in Figure H5.16.

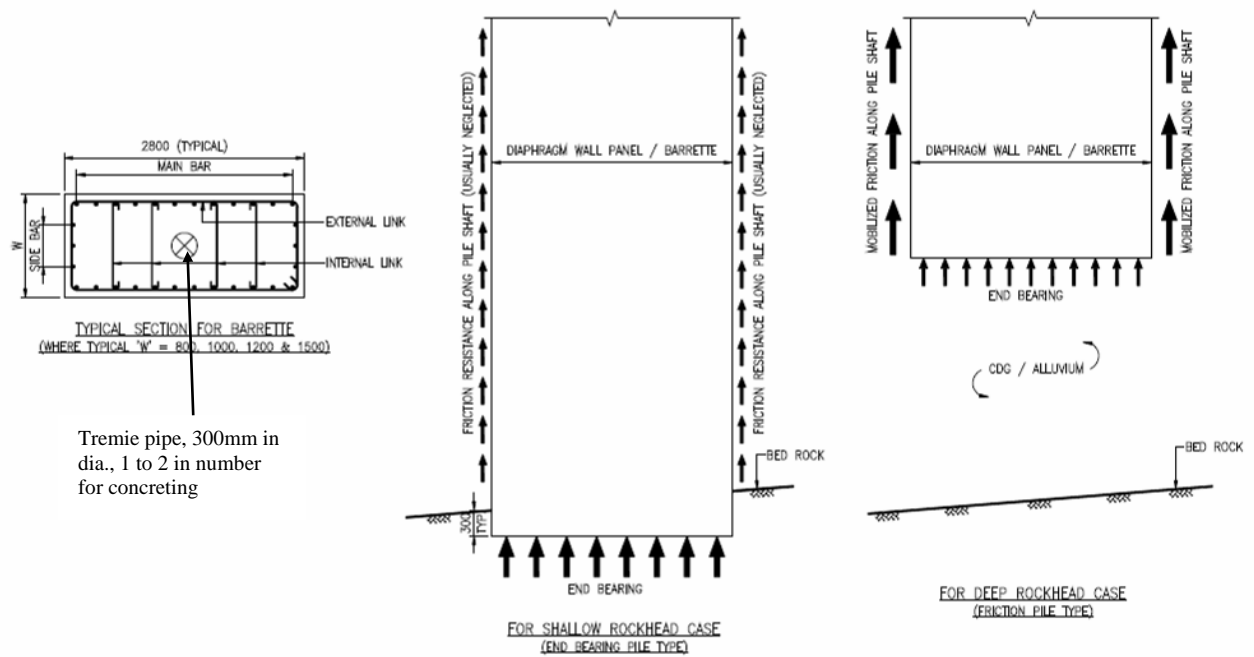


Figure H5.16 – Construction of Typical Barrette

H5.4.10 HAND-DUG CAISSON

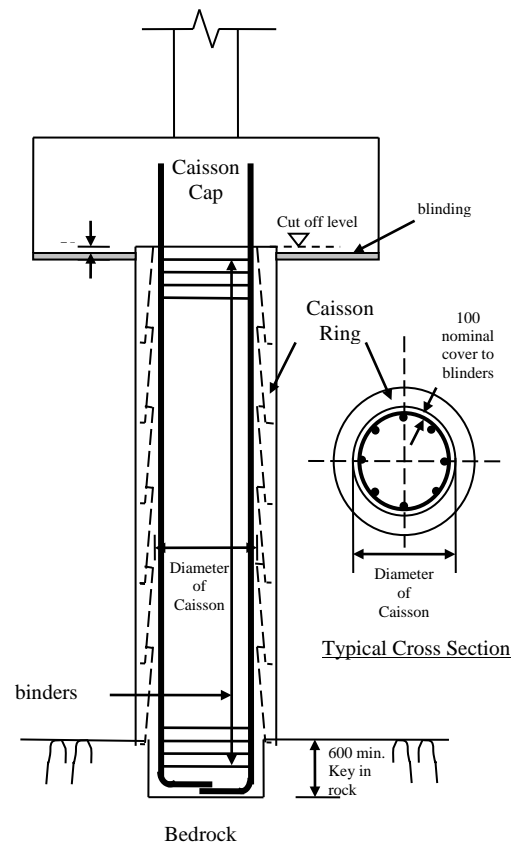


Figure H5.17 –Details of a Hand-dug Caisson

H5.4.11 STEEL H-PILE DRIVEN TO BEDROCK

A steel H-pile driven to bedrock is used in locations where the bedrock is shallow and the soil above bedrock does not have sufficient strength to take the set so that the pile is driven to bedrock for founding. The pile is described as being “driven to refusal” with set value less than 10mm per 10 blows. The bedrock to be founded on should not be inferior to category 1(d) in accordance with Table 2.1 of the Code.

The Code also requires special considerations when the bedrock is steeper than 25° from the horizontal to avoid “slipping” of the pile at the bedrock under hard driving. In addition, even if the slope of the bedrock is less than 25° to the horizontal, the Code cautions that drop heights of the hammer should be reduced when driving is close to the bedrock so as to secure better anchorage of the pile into the bedrock.

The details of the pile are similar to those of steel H-piles discussed in 5.4.1. The Code has cautioned users to check against (i) buckling, construction tolerances and stability due to the relatively thin layer of embedment soil; (ii) the necessity of a strengthened pile base (hard driving when reaching bedrock where the superimposition of the upward and downward stress waves can magnify the stress on the pile toe as discussed in Appendix

HL); and (iii) additional testing requirements including driving a sufficient number of trial piles to demonstrate “buildability” of the pile prior to installation of the working piles.

When piles are short, the Code reminds the users of stability problem. Design of a “fixed head” is recommended especially when the embedding soil is weak. For piles shorter than 10m, trial piles may be required.

The Code also requires the peak driving stress at final set be not less than 75% of the yield stress of the pile when undergoing dynamic load test. The dynamic test may be limited to piles of lengths shorter than 30 m. There is also room for decrease of the peak driving stress to 65% of the yield stress of the pile which should be able to ensure adequacy in the test.

5.4.12 STEEL H SHEAR PILES

Steel H shear piles are effective in enhancing lateral shear capacity of a pile foundation as each provides full lateral shear capacity of a pile with no structural capacity exhausted by axial load. As they are not required to be installed to strong bearing strata and to undergo final set or loading test, the construction time of them are relatively short.

To maximize lateral shear capacity, the pile heads of the steel H shear piles have to be fixed to the pile cap with adequate lengths of anchorage into the pile cap. As the piles will protrude above the lowest layer of reinforcing bars of the pile cap, some construction difficulties will be imposed.

5.5 PILE CAPS

Except for statically determinate cases, the Code requires the analysis of pile load distribution through pile cap be generally carried out by flexible cap analysis incorporating stiffnesses of the pile cap and the piles. In addition, it also stresses on the interaction effects between the piles. While it is easy to incorporate stiffness of a pile cap in the mathematical model, the axial stiffness of a pile is often difficult as strictly speaking the soil restraint along the pile shaft and the settlement of the pile tip in soil which directly affect the axial stiffness are difficult to determine. The interactions between the piles through the soil medium are even more difficult to determine. Methods by Poulos & Davis (1970) and Randolph (1980) involving complicated mathematical expressions, tables or charts for limited cases may be employed but they are not popularly used in the trade practice at present.

The Code reiterates that mini-piles possess limited bending stiffness and only raking mini-piles should be designed to resist lateral load in analysis. So unless raking piles are used, lateral restraints can only be provided by pile cap.

Reinforcement and detailing of pile caps are similar to raft footings as discussed in H4.3 and Appendix HD. Nevertheless, detailing is more complicated in case steel H-piles protrude into the pile cap for fixity against rotation which may interfere with the bottom steel bars. As it is not advisable to use wide spacing of steel bars which may result in excessive cracking affecting durability, the Code requires additional reinforcing bars

when the spacing of the continuous steel bars is increased to 400mm to cope with the commonly used steel pile such as 305×305×223 piles having lateral dimensions in the order of 330mm. Figure H5.18 demonstrates the arrangement.

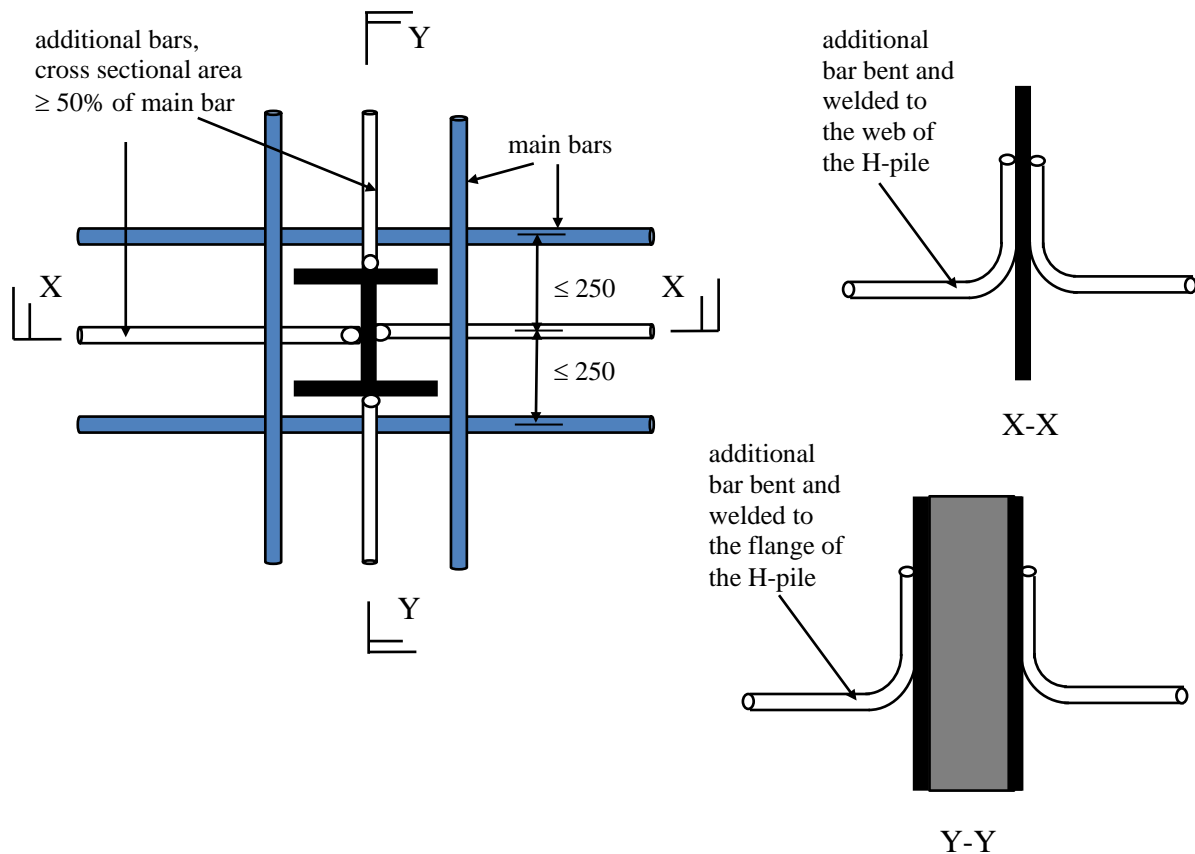


Figure H5.18 – Additional Bars to Trim Wide Spacing of Main Bars to Avoid Conflict with H-piles in Pile Cap as per clause 5.5 of the Code

H6 OTHER FOUNDATION TYPES/ELEMENTS

H6.1 BASEMENTS AND HOLLOW BOXES

A basement or hollow box serving as a foundation is effectively a “floating footing” with an empty space in the foundation that serves to reduce dead weight and “net bearing pressures” on ground by displacing a large volume of soil mass. The Code allows the vertical resistance of ground for the foundation to comprise end bearing at the bottom of the slabs and bases of side walls plus side friction or bond resistance on the external surfaces of the side walls. To assess the allowable bearing pressure of the basement or hollow box, the “net” bearing pressure design concept as discussed in H2.2.4 is applicable by which the allowable bearing pressures are given in Table 2.1 of the Code. As for the bond on the external surfaces of the walls, reference can be made to Table 2.2 of the Code whilst frictional resistance can be derived from the positive skin friction using the same principle as for piles as discussed in H5.3.2(1)(b). It should also be borne in mind that settlement is another controlling criterion as discussed in clause 2.3.2 of the Code.

Similarly, the horizontal resistance of the ground can also be mobilized from bond or side resistance at the side walls and the base, together with the passive resistance of soil. Worked Example H2.1 under H2.5.4 demonstrates mobilization of the horizontal resistance of the ground so that the basement or hollow box structures can achieve acceptable factors of safety against sliding and overturning.

The Code cautions that when more than one component (e.g. base friction plus side friction) is utilized as ground resistance for the basement or hollow box structure, it has to be demonstrated that they can be mobilized simultaneously. Compatibility of movements should be demonstrated.

The Code also requires that unacceptable disturbance (movement and stress) to the ground or adjacent structures and services should not be caused by the foundation structure. Assessment of such disturbance has to be carried out in the design stage, when additional stresses and movements induced should be estimated and where required, measures implemented to keep the disturbances within tolerable limits. Some of the tolerable limits are pre-determined by authorities such as the MTRC, WSD and some are statutory ones. Sometimes monitoring during and/or after construction has to be carried out to ensure that the limits are not exceeded. Assessment of the disturbance in the design stage involves determination of additional stress and movements induced on other structures through the soil medium. For simple configurations, the assessment can be based on charts and/or formulae provided by publications including Poulos & Davis (1973) which are in accordance with the continuum theory. More sophisticated analysis can be carried out by numerical modeling based on either the finite element or continuum method. Nevertheless, a worked example using the continuum theory based on Mindlin’s Equations to estimate the stresses induced on a nearby structure due to a newly constructed structure founded on hollow box foundation is given in Appendix HR.

There is a requirement in the Code that the concrete used should not be inferior to grade C35 and be sufficiently water-tight. This is to avoid the trapping of water inside the box

structure which may upset the pre-determined load balance in design stage. If water-tightness cannot be fully guaranteed, a water pumping system (automatic if required) should be installed.

Stability against buoyancy is important, especially when the dead weight of the structure is less than the water upthrust at the permanent finished stage or during construction. Reference to H2.5.4 and Worked Example H2.1 of this Handbook can be made for the checking of stability against buoyancy. Use of ground anchors may be required to withstand the buoyancy uplift. More details are discussed in H6.4. However, it should be noted that permanent prestressed anchors designed to resist permanent upthrust may not be acceptable to the Buildings Department. This is because the use of permanent prestressed ground anchors in a project would impose a long-term monitoring commitment on the maintenance parties which usually involves appreciable recurrent cost and, should deficiencies be revealed, remedial works may be difficult and expensive. Past experience shows that compliance with such commitment by owners is not practically viable.

The Code remarks that the design of the permanent structure should take into account the stresses that may have developed during the various stages of the construction sequence. An example is the design of the base slab of a basement which has to cater for different distributions of soil and water upthrust at different stages of construction and where the load distribution at the final stage is not the most critical at all locations.

Care has to be taken if there are services or structures (such as tunnels) that have to be connected to a basement structure and the basement is resting on soil where the increase in settlement as construction proceeds is significant. This is because these services or structures connected to other foundations may be subject to different settlements at their other ends, thus creating differential settlements that may be intolerable. Flexible connections may have to be used. Another practice is to defer the connection work to until completion of the superstructure so that the settlement of the basement structure is almost completed (at least due to dead load). Figure H6.1 illustrates the phenomenon.

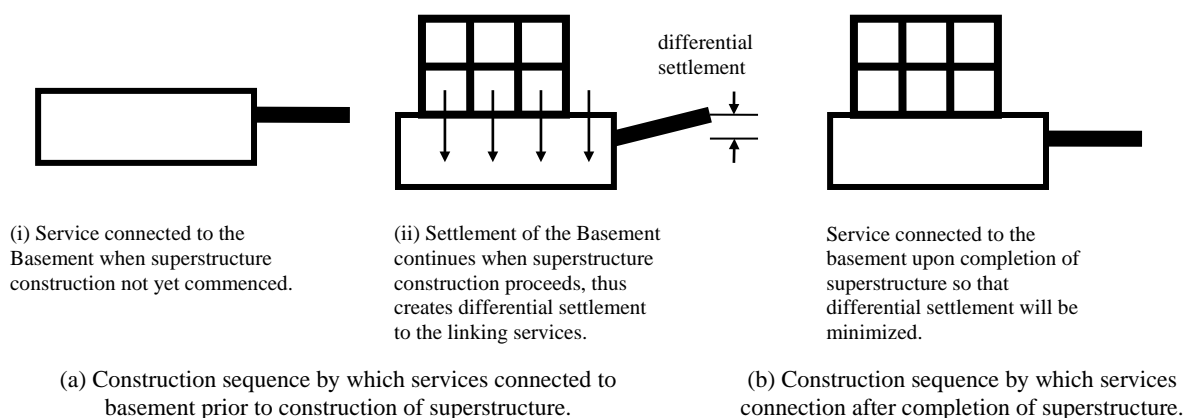


Figure H6.1 – Differential Settlements of Linking Services or Structures to Basement

H6.2 DIAPHRAGM WALLS

The construction of a diaphragm wall is similar to that of a barrette as described in H5.4.9 of this Handbook, though the latter is usually formed by panels with length varying from 2.8m to 7m. In contrast with the barrette, which is usually a vertical load resisting member, a diaphragm wall can also be a flexural member resisting lateral soil pressures. The Code requires the wall thickness to be in excess of 600mm, below which construction is impractical.

The obvious advantage in constructing a diaphragm wall is that temporary works such as sheetpiling can be eliminated as the permanent wall structure can also act as a soil retaining structure during excavation. As the wall structure is very strong compared with steel sheetpiling, shoring work can be minimized and is more suitable in case of deep excavation. In some cases, diaphragm walls are used for the “top down construction method” of basement by which diaphragm walls are first formed, followed by excavation from the ground level downwards and successive construction of the floor slab structures. It is relatively speedy for constructing the basement and superstructure simultaneously provided that good site planning is implemented.

The Code required analysis of diaphragm walls to include the following :

1. Seepage analysis for water cut-off

The diaphragm wall, being an impermeable structure, can serve the water cut-off purpose during excavation work by lengthening the water flow path as shown in Figure H6.2.

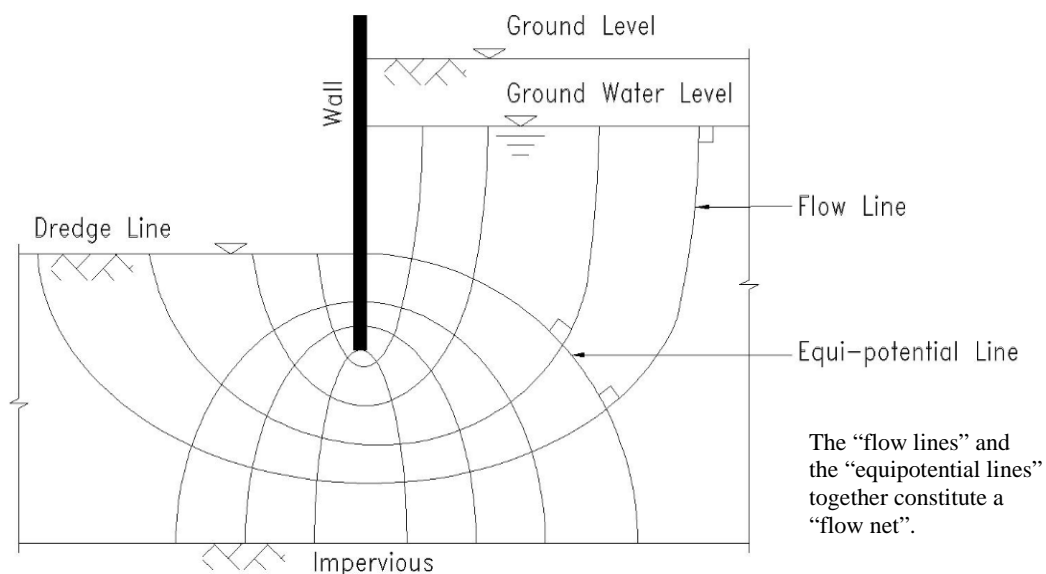


Figure H6.2 – Increase of Water Flow Path by Cut-off by Impermeable Wall

In Figure H6.2, the flow lines indicate the direction of the flow of water and the equipotential lines are contours along which the “total head” (elevation head plus static pore water pressure) is constant. The deeper the key-in of the impermeable wall, the longer is the flow path and therefore the smaller the rate of water flow into

the excavation. Analysis for a 2-dimensional flow field can be based on the fundamental equations listed in Appendix HS. Approximate determination of the hydrostatic pressures on the wall and water seepage rates can be carried out by the “flow net” analysis described in most of the text books in soil mechanics. Nevertheless, analytical solutions of the basic equations are available for some simple configurations and their uses are demonstrated as worked examples in Appendix HS. For more complicated cases, use of the computer analysis software will be necessary.

2. Lateral stability analysis including toe stability

The checking of lateral stability of an excavation involves the determination of earth pressures and hydrostatic pressures. Determination of the earth pressures (active and passive) can be based on GEOGUIDE 1 and that of pore water pressures can be based on “flownet” analysis described in (a). In the absence of rigorous analysis of soil pressure taking deformation of wall into account, “at rest” soil pressure should be used instead of active pressure. If the wall is keyed into rock, the ultimate lateral resistance of the key can be determined by assuming the ultimate lateral strength of the rock to be one third of the vertical allowable bearing pressure, and with reference to Figures 51 to 53 of GEOGUIDE 1.

In addition, commercial softwares based on the finite element method or Winkler’s spring method are available for lateral load analysis.

3. Bending moments, shear forces and deflections due to lateral loads for the proposed construction sequence

The bending moments, shear forces and deflections due to lateral loads for the proposed construction sequence are the results of excavation analysis. The structural strengths of the wall structure should be able to resist the forces induced in them, together with tolerable deflections. The deflections induced in the surrounding ground and structures should also be studied if found significant.

The proposed construction sequence should also be taken into account if found to have significant effects on stresses (locked-in stresses) in the structures and deflections. The phenomenon of “locked-in” stress in a diaphragm wall under “top down construction” sequence is illustrated in Figure H6.3 as a simplified case with only two layers of strutting. In the analysis, apart from the possible changing of soil load profiles as highlighted in the figure, compatibility of displacements of the soil profiles, the wall and the strutting may also need to be ensured. The same phenomenon can in fact apply to other similar excavations such as those supported by sheetpile walls in which successive strutting supports are installed as excavation proceeds downwards from ground level. Commercial software are available to analyze multi-layer strut excavations with full account taken of the construction sequence.

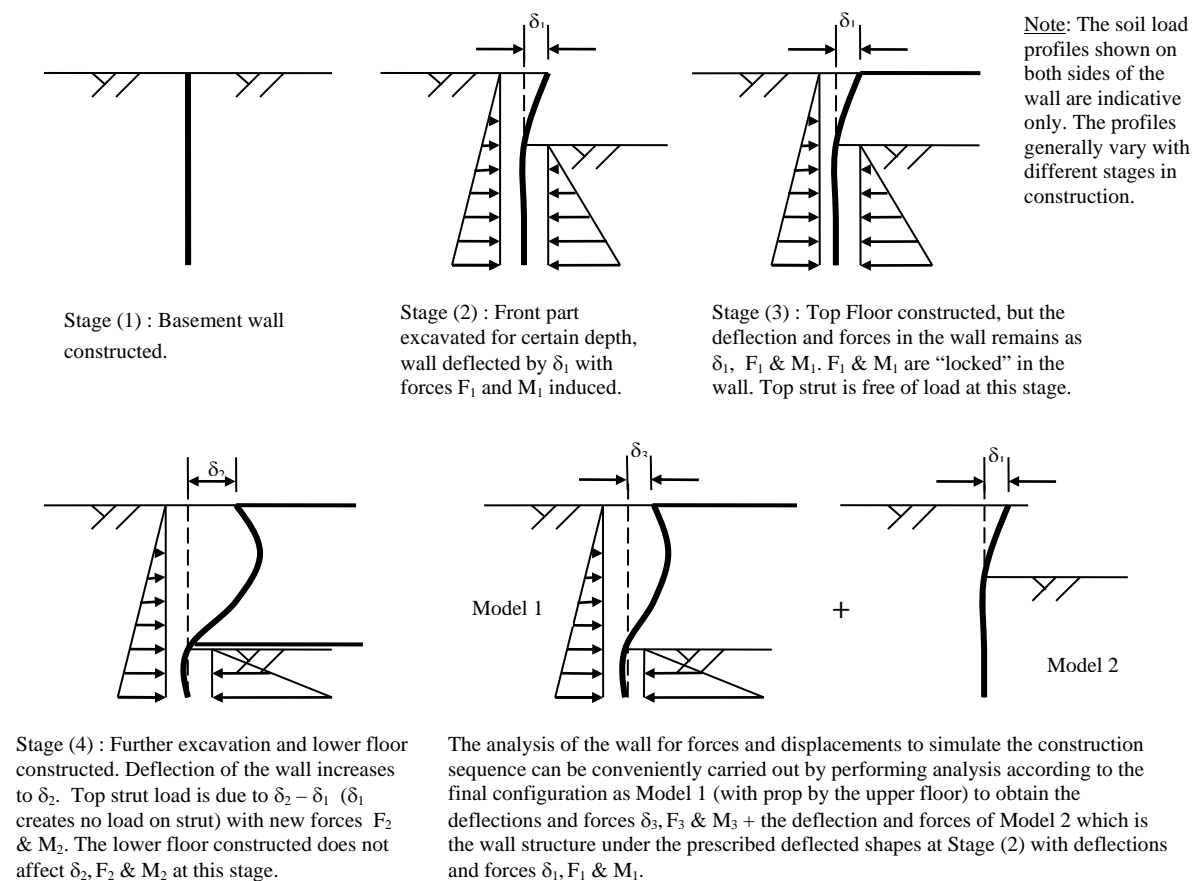


Figure H6.3 – Illustration of the “Locked-in” Stresses Formulation in a Top-down One Storey Basement Construction and the Method of Analysis

4. Bearing capacity for vertical loads

If the bearing capacity is derived from end-bearing, the determination of allowable bearing capacity should be similar to that of an end-bearing pile. However, if the axial capacity is derived from skin friction, it can normally be derived by multiplying the peripheral area by the ultimate friction which is often related to the SPT N values of the soil in the order of 0.8N to 1.4N (N is capped to 200) in kPa in accordance with GEO Publication 1/2006. Additional capping to an absolute value of 200 kPa is also recommended. Shaft friction can however, be enhanced by “shaft grouting” by which cement grout is injected from the surfaces (which may include the bottom level) of the wall into the surrounding soil. Compatibility of settlement may have to be studied if both end-bearing and skin friction are designed to be mobilized simultaneously.

5. Slurry trench stability during excavation

To maintain stability in the slurry trench excavation, the bentonite slurry should be maintained at a certain depth above the groundwater level outside the trench excavation such that the slurry pressures exceed the pressure exerted by the soil and ground water with a certain factor of safety. Reference can be made to Hajinal I. et

al.'s "Construction of Diaphragm Walls" (1984) and others. A worked example is enclosed in Appendix HT.

6. Assessment of settlement induced on adjacent structures, services and ground during construction.

The assessment is particularly important if the diaphragm wall is founded on soil and derives its bearing capacity from skin friction at shallow soil depths. The Finite Element Method and the Continuum Method as described in H6.1 are applicable for such an assessment, with the proper use of soil parameters.

H6.3 RETAINING WALLS

Clause 6.3 of the Code is self-explanatory.

H6.4 GROUND ANCHORS

Where ground anchors are needed to resist the buoyancy force acting on the structure, they are normally formed in rock whereby steel tendon/bars are grouted in drilled holes in the rock. The uplift resistance of the ground anchor depends on (i) strength of the anchor bars; (ii) bond strength of the grout with the steel bars; (iii) bond strength of the grout with rock; and (iv) weight of the rock mass and the overlying soil that will be mobilized by the anchor. Demonstration of item (iv) is shown in Figure H5.3. The effects of adjacent anchors should also be considered with due regard to the overlapping of mobilized rock and soil masses. An illustration is shown in Figure H6.4.

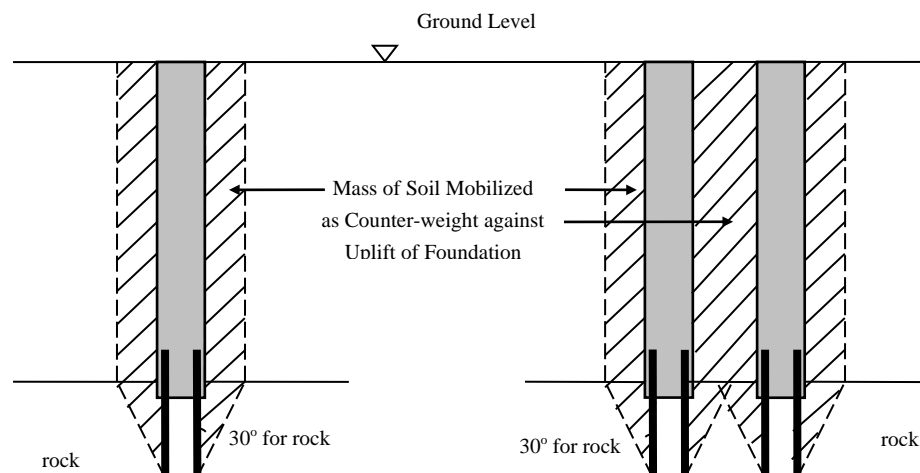


Figure H6.4 – Illustration of Mobilization of Soil Mass against Uplift for Foundation Elements in Close Proximity

Reference can be made to Table 2.2 of the Code for the bond strength of grout with rock. The cement grout should comply with the requirements of GEOSPEC 1 of CEDD (1989) by which the grout should consist of OPC and water only. Sand and PFA should not be used in general. As for the bond strength of steel bars with grout, reference can be made to reliable test data.

For pre-stressed anchors, design and construction shall comply with GEOSPEC 1 of CEDD (1989). Monitoring should also be carried out as necessary.

H6.5 RE-USE OF EXISTING FOUNDATIONS

Re-use of existing foundations should be encouraged as far as possible, as a measure of environmental protection. However, the integrity of the existing foundations and their suitability for re-use should be carefully studied. The Code contains a detailed discussion of the requirements including comprehensive testing schemes concerning the re-use of existing foundations under this clause.

H7 CONSTRUCTION PRACTICE AND SITE SAFETY FOR FOUNDATION WORKS

This Chapter of the Code relates to construction practice and site safety for foundation works. To facilitate understanding of the topics, photographs showing the construction sequence for common types of foundations are enclosed in Appendix HU.

H7.1 GENERAL

In addition to the requirements as stipulated in the Code under this sub-clause, a review of actual site conditions should be conducted to ascertain the adequacy of the design and suitability of the construction method prior to execution of the foundation construction work.

H7.1.1 GENERAL REQUIREMENTS

The list of Registered Specialist Contractors (Foundation Work) can be found in the website of the Buildings Department.

H7.1.2 QUALITY SUPERVISION FOR FOUNDATION WORKS

Adequate resources from the AP, RSE, RGE and RSC Streams must also be ensured so that the quality supervision for foundation works can be carried out.

H7.1.3 CONSTRUCTION MATERIALS

Whilst the Code concentrates on the testing of materials in this sub-clause, discussion in relation to construction practice and safety is also outlined.

(1) Concrete and Grout

In addition to the requirement to comply with CS1 as stipulated in the Code, reference to the Hong Kong Building (Construction) Regulation (HKB(C)R) and Code of Practice for the Structural Use of Concrete 2013 should also be made for the determination of the sizes of test cubes, sampling frequencies and compliance criteria in relation to concrete cube tests. The followings are highlighted for users' attention:

- (i) Whilst the HKB(C)R (2012) requires the standard size of test cubes to be 150mm, an alternative standard size of 100mm is also allowed in the Code of Practice for the Structural Use of Concrete 2013. The use of the smaller size test cubes serves to reduce the crushing loads exerted by the testing machines which might otherwise be too high to test concrete of grade exceeding 60. The alternative size is to meet the increasing demand for the use of high strength concrete which has been gaining popularity in recent years;
- (ii) PFA and GGBS should preferably be used in large volume concrete pour for pile caps and raft footings so as to reduce the heat of hydration. In case of very massive structures, say over 3m thickness, additional precautionary

- measures including the use of icy water in the concrete mix, planned sequential concrete pours, temperature monitoring etc. should be considered;
- (iii) Corrosion protection of the concrete is a concern in adverse sub-soil conditions. More detailed discussion can be found in H2.6.

(2) Reinforcement

Testing reinforcement requirements should be in accordance with CS2 as stated in the Code. In addition, reference should also be made to the Code of Practice for the Structural Use of Concrete 2013 for fixing and bending of reinforcement bars.

When heavy reinforcement cages have to be inter-connected and lifted such as in the case of large diameter bored pile construction, care must be taken to ensure that the connection of the reinforcement cages (usually connected by U-bolts) is secure and the lifting machine has adequate capacity to perform safely.

(3) Steel piles

Structural steel has been classified into Classes 1, 2, 3, 1H and UH in accordance with the Code of Practice for the Structural Use of Steel 2011 with respect to the quality assurance systems implemented and compliance with reference material standards. Frequencies of testing for the different classes are different. For Class 1, being the highest standard, submission of mill sheets will be adequate to prove its acceptability. No additional tests upon delivery to the construction site will be required.

In addition to the testing of the material, tests of welds are also important. Testing methods and frequencies are also illustrated in the Code of Practice for the Structural Use of Steel 2011.

In the driving of steel piles, it is an established practice to limit the driving stress to 80 – 90% of the yield stress of the steel pile in order to avoid damage due to “hard driving”. Measurements of the driving stresses are often made by PDA tests.

H7.1.4 EXCAVATION

Excavations, especially deep excavations, often bring safety concerns. The Building Authority requires prior submission and approval of an “Excavation and Lateral Support Plan” (ELS Plan) if the extent and depth of the excavation exceed that stipulated in the PNAP APP-57. For excavations of minor extent, submissions and acknowledgements of “shoring and excavation procedure details” may be sufficient as required by the Building Authority.

As far as excavation is concerned, the following may also act as guidelines for the design and execution of the excavation :

- (i) Adequate data in relation to soil strengths and ground water levels should be acquired and analyzed;
- (ii) Determination of the type of excavation (open cut excavation or shored excavation) and construction method should be based on factors including (1)

- depth of excavation; (2) strength of the soil; (3) ground water level; (4) environmental consideration (e.g. noise and dust); and (5) anticipated effects on the adjacent structures or utilities;
- (iii) In the case of an open cut excavation, the gradients of the slopes should be designed with adequate factors of safety and if necessary, the surface may have to be protected by such measures as covering by tarpaulin sheets or chunam to prevent surface infiltration if considered necessary. Surface drainage channels should also be provided in order to properly direct the surface run-off to a safe discharge point;
 - (iv) In case of a shored excavation, stability and strength of the shoring should be checked against the soil loads appropriately determined. Effects of the construction sequence should be catered for as appropriate;
 - (v) Monitoring (generally against soil movement, water draw-down, vibration) should be considered as necessary with pre-determined warning and stop-work threshold limits. Generally the three “triggering levels” – alert, alarm and action levels as stipulated in PNAP APP18 can be adopted in monitoring. In addition, authorities including MTRC and WSD have imposed well known threshold limits to induced stresses, movements and vibrations on their structures and installations due to nearby construction;
 - (vi) Effects of water draw-down on adjacent structures and utilities should be assessed as it may create excessive settlements. Re-charging may be necessary to restore ground water to acceptable levels during construction;
 - (vii) The necessity of grouting may be considered for stabilization of the soil and enhancement of water cut-off;
 - (viii) Danger due to the upheaving of soil at the bottom of the excavation needs to be assessed;
 - (ix) According to the Construction Sites (Safety) Regulations, excavations deeper than 1.2m need to be shored. The shoring work is especially important in areas of high ground water.

Photographs showing open and shored excavations are in Figures H7.1(a) and (b).



Figure H7.1(a) – Open Excavation



Figure H7.1(b) – Shored Excavation

Figure H7.1 – Photographic Illustration of Excavation

H7.2 EFFECT OF FOUNDATION WORKS ON ADJACENT STRUCTURES AND LAND

H7.2.1 ASSESSMENT OF THE EFFECT OF FOUNDATION WORKS

The following serve to supplement the assessment as required in the Code. They are suggested measures and should be implemented as necessary to suit actual site conditions. Alternative measure can always be suggested instead :

- (a) In the preparation of the detailed report as required under this sub-clause, the engineer should determine the scope and details of the investigation in accordance with his professional judgement which may include (i) review of existing records, (ii) visual inspections, (iii) determination of tests (non-destructive or destructive) that need to be carried out for assessment;
- (b) Where sensitive structures and services are in close proximity, the estimation of the effects including “stresses”, “movements”, “vibrations” on them as a result of the proposed foundation should be carried out as appropriate;
- (c) Where required, examples of preventive measures proposals may include (i) “sleeving” of newly constructed piles or walls along certain portions of their lengths so as to avoid loads to be exerted by these portions onto the soil which may otherwise create instability; (ii) strutting of excavations to prevent excessive lateral movements of existing foundations; (iii) re-charging of surrounding sub-soil by water to minimize settlements due to water draw-down; and (iv) careful control of the construction procedures to avoid over-break and ground loss during pre-boring process. These are illustrated in Figure H7.2. In addition, the monitoring scheme and contingency plans should also be included where necessary.

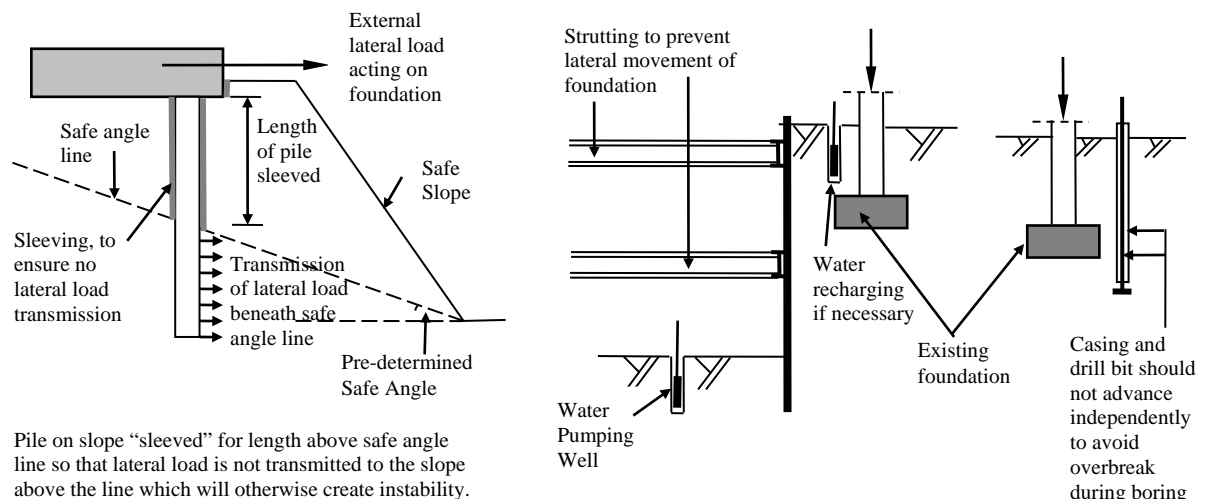


Figure H7.2 – Common Preventive Measures in Foundation Construction

Having completed the detailed report on the structural conditions of all surrounding buildings, land, structures and existing services that are likely to be affected by the proposed foundation works, as well as the estimation of the effect due to the works (such as vibration, ground loss or ground water drawdown), the most appropriate foundation

type and construction sequence should be selected, together with proposals for preventive measures, a monitoring scheme and contingency plans as appropriate.

H7.2.2 SHORING AND UNDERPINNING

Depending on the assessed effect of foundation works, and also the importance of the surrounding buildings, land, structures and existing services, precautionary measures in the form of shoring, underpinning should be included in the foundation proposal as appropriate.

Shoring is a general term in construction to describe the process of supporting a structure to enhance stability or to prevent collapse so that construction can proceed safely. Apart from its use in excavation, shoring in the form of “raking shores” on the superstructure of a building are sometimes carried out to enhance stability as illustrated in Figure H7.3. Raking Shores usually consist of one or more timbers or structural steel members sloping between the face of the structure to be supported and the ground. The most effective support is given if the raker meets the wall at an angle of 60 to 70 degrees. A wall-plate is typically used to increase the bearing area to facilitate stress dispersion.



Figure H7.3 – Double Raking Shore to Enhance Stability of Building

Underpinning is the process of strengthening and stabilizing the foundation of an existing structure by extending it into subsurface strata that is deeper and stronger than the original ground immediately supporting the existing foundation. Underpinning is often applied as remedial work for foundations that have undergone structural or supporting ground failures.

H7.2.3 MONITORING PLAN

The Code gives a comprehensive description of the monitoring plan including the three “Triggering A” levels (“Alert”, “Alarm” and “Action” Levels as stipulated in AP/RSE Practice Notes APP-18) under this sub-clause.

As an example, a parameter for the determination of triggering levels may be the piezometer readings in a construction site involving dewatering in which the “Alert”, “Alarm” and “Action” levels are when the ground water level drops to 1.3mPD, 0.8mPD and 0.3mPD respectively. The responses as listed in Table 7.1 of the Code will be required. Another parameter normally is “settlement measurement”.

Photographs for the various instruments and their installations for monitoring purpose are shown in Figures H7.4(a) to H7.4(e).



Figure H7.4(a) – Settlement Monitoring Marker on Ground



Figure H7.4(b) – Settlement Monitoring Marker on Wall



Figure H7.4(c) – Check Point against Tilting



Figure H7.4(d) – Vibrograph



Figure H7.4(e) – Piezometer (for Checking Ground Water Level)

Figure H7.4 – Photographic Illustrations of Monitoring of Ground and Structure Movement and Ground Water Level

H7.2.4 GROUND SETTLEMENT

Ground settlement is an important indicator to the adverse effects created to nearby buildings by the construction process and should therefore be closely monitored as appropriate. It should be emphasized that different structures and utilities will have different tolerance in accommodating movements of their foundations. Acceptance of estimated ground settlements should be considered on a case-by-case basis. PNAP 137 recommends to define the serviceability limit based on the maximum calculated

movements or the allowable movement of adjacent ground, structures and services. In the absence of these estimation, the typical values given in Table 7.2 may be adopted, provided that no particular sensitive structures and utilities are present.

H7.2.5 DEWATERING

Dewatering using electric submersible pumps to drawdown the groundwater table is very common in keeping the excavation dry for foundation works such as the construction of a raft foundation. Recharging to maintain within design limits the groundwater level outside the excavation may be considered when necessary. The groundwater table during construction is to be properly checked by monitoring stations. Figure H7.5 schematically shows water draw-down by pumping and a photograph of submersible pumps.

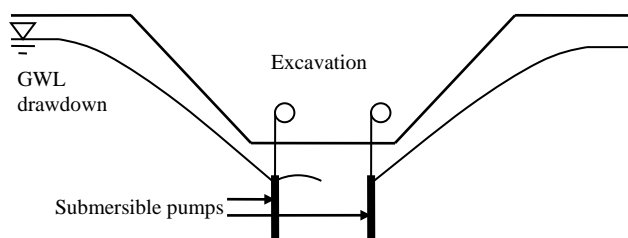


Figure H7.5 – Dewatering in Excavation to Lower Ground Water Table



However, the maximum settlement criteria imposed by various authorities as relevant on their installations should be observed during dewatering e.g. there is a 20mm movement limitation for MTR installations.

H7.2.6 VIBRATION

The classification of vibrations by the Code into “continuous”, “transient” and “intermittent” vibrations is identical to the categorization by BS5228-2:2009 and the limits of ppv are taken from PNAP APP-137.

The Code also cautions that resonance may occur if the frequency of a continuous vibration coincides with the natural frequency of a building structure. However, the vibration is generally a band of ground excitation of many frequencies and the substantial responses of a building may be due to a few of its lowest natural frequencies and careful study has to be carried out to identify the adverse effects. Fortunately, dynamic analysis by computer method is common today. However, care should be taken in assessing stiffness of the building as the non-structural components which are often ignored in structural analysis can contribute substantially to the stiffness and hence lower the natural frequencies.

The formula for estimation of v_{res} is extracted BS5228-2:2009 Table E.1 for percussive piling which is in turn quoted from Hiller and Crabb (2000). The formula takes a similar form to that of Attewell and Farmer (1973). The latter uses horizontal distance from the pile axis as the variable instead of the slope distance used by the former.

H7.2.7 PUBLIC RELATIONS PLAN FOR PILING WORKS

Clause 7.2.7 of the Code is self-explanatory.

H7.2.8 BLASTING

The use of explosives is governed by Dangerous Goods Ordinance Cap. 295 :

- (i) 295A Dangerous Goods (Application and Exemption) Regulations;
- (ii) 295B Dangerous Goods (General) Regulations;
- (iii) 295C Dangerous Goods (Shipping) Regulations;
- (iv) 295D Dangerous Goods (Government explosive depots) Regulations.

Other ordinances include :

- (i) Mining Ordinance (Cap 285);
- (ii) Building Ordinance (Cap 123);
- (iii) Factories and Industrial Undertaking Ordinance (Cap 59);
- (iv) Protected Places (Safety Ordinance) (Cap 260);
- (v) Environmental Impact Assessment Ordinance (Cap 499);
- (vi) Dangerous Goods (General) Regulations Reg. 46 - Permission required for blasting.

Regulatory control on the safety and security on the use of explosives in Hong Kong is under the control of the Commissioner of Mines (Director of Civil Engineering and Development).

When an explosive is detonated, shock waves and vibration are generated. Vibration is measured in terms of peak particle velocity (ppv) in units of mm/sec. A report is generally required for assessing vibrations that would be incurred to the surrounding structures and facilities to ensure that they are within tolerable limits.

H7.3 FOUNDATION RECORDS AND REPORTS

In addition to the records and reports materials as stipulated in the Code, the following should also be included :

- (i) Rockhead contours should be mapped with information obtained from the initial SI report, pre-boring and post construction drilling records;
- (ii) Rockhead contours (for end bearing piles on rock) or contours for soil having SPT N value ≥ 200 for driven steel piles normally, though SPT N value < 200 is sometimes acceptable for other large displacement piles, such as tubular pile, precast prestressed concrete piles, etc.;
- (iii) Sonic Tests on large diameter bored piles;
- (iv) Ultrasonic echo sounder tests on large diameter bored piles;
- (v) Material tests reports including concrete core tests, grout cube tests.

H7.4 PILE CONSTRUCTION

H7.4.1 DRIVING TEST AND TRIAL PILES

If considered necessary, the trial pile may be “instrumented” by which strains, and settlements can be measured for the subsequent derivation of soil resistances along the pile shaft.

In accordance with the Code, test driving is required for driven piles. The current practice also includes test installations for pre-bored piles such as mini-piles and socketed H-piles.

H7.4.2 TEST BORING

Test boring is important for sites where the construction activities may induce excessive settlements and vibrations which are detrimental to nearby structures or utilities.

In addition to item (c) of the test boring proposal requiring the minimum rate of advancement of the drill bit be stated, the maximum rate should also be stated for monitoring.

H7.4.3 PRE-DRILLING

Reference to clause 2.1 of the Code should be made for the definition of “bedrock” in the determination of depth of pre-drilling in rock.

For barrettes which are long on plan (in excess of 5m), it may be worthwhile to consider sinking more than one pre-drilling hole for confirmation of bedrock levels.

H7.4.4 POST CONSTRUCTION PROOF DRILLING

Further investigation may be required if there are substantial differences between the pre-drilling and the post construction proof drilling records. Good quality drilling is required to avoid possible damage to the soundness of the interface. Triple barrel drilling and drilling fluid such as foam, supermud or polymers can be used.

H7.4.5 PROOF TESTS

If the proof tests involve use of instruments, calibrations by accredited laboratories should also be included.

H7.4.6 FURTHER ON SITE TESTS

The tests may include Pile Driving Analyzer Tests (PDA), CAPWAP etc.

H7.5 CONSTRUCTION TOLERANCES

The Code tabulates construction tolerances for foundation elements generally in this clause.

The justification mentioned in Note (2) can comprise re-analysis and / or re-design of the structure with the as-constructed dimensions / layouts.

H7.6 GROUND TREATMENT

Common ground treatment methods include (i) grouting; (ii) dynamic compaction; (iii) vibroflotation; and (iv) stone column construction. While grouting can easily be understood, dynamic compaction is a soil densification process achieved by dropping heavy weights of concrete and steel hammers from heights of 10m to 30m onto a grid pattern. Vibroflotation involves the use of a vibrating probe that can penetrate granular soil to depths of over 30m. The vibrations of the probe cause the grain structure to collapse thereby densifying the soil surrounding the probe. Stone columns are columns of gravel constructed in the ground to improve the bearing pressures. The stone columns can be constructed by the vibroflotation method or by driving steel casings and subsequently filled with gravels which are tamped with a drop hammer as the steel casing is gradually withdrawn.

H7.7 CONTROL OF NUISANCE

(1) Noise

Sources of noise may include but are not limited to the following:

- (i) Percussive / non-percussive piling operation;
- (ii) Excavation of soil / rock using Powered Mechanical Equipment (PME) / manually operated hand tools or equipment;
- (iii) Concreting of raft foundation etc.

Generally noise levels below 75dB(A) are acceptable. In case of percussive piling work where the construction noise levels are very high, limitations to certain period of time for the piling work will generally be imposed.

Measures for reducing noise may involve the use of a noise barrier (Figure H7.6(a)), noise muffler (Figure H7.6(b)) or the use of Quality Powered Mechanical Equipment (QPME) which produce less noise during foundation work.



Figure H7.6(a) – Noise Barrier



Figure H7.6(b) – Noise Muffler Enclosing Hydraulic Hammer during Percussive Piling Work



Figure 7.6 – Noise Nuisance Reduction Measures

(2) Smoke and Fume

Sources of smoke and fumes are usually generated from sources including :

- (i) Combustion of fuel for operating powered mechanical equipment (PME) such as air compressors, generators or construction plant and;
- (ii) Excavation of dusty materials.

Routine maintenance and servicing of the diesel engines of mechanical plant is vital in preventing emission of excessive black smoke and fumes. Figure H7.7 shows the use of an exhaust purifier for a diesel power pack plant, which can help to improve the quality of exhaust gas significantly.

Dust generation can also be reduced by

- (i) covering by tarpaulin sheets;
- (ii) switching off engines when the PME / vehicles are not in use;
- (iii) spraying water over the excavation works;
- (iv) cleaning the wheels of vehicles before leaving site.

Figure H7.8 shows the spraying of water to suppress dust generated by foundation excavation.



Figure H7.7 – Exhaust Purifier for Diesel Power Pack of Reverse Circulation Drill



Figure H7.8 – Spraying of Water for Dust Suppression

(3) Waste water and chemical waste

Disposal of waste water and chemical waste is controlled by the Environmental Protection Department (EPD) as follows:

- (i) A discharge License for disposal of waste water issued by EPD must be obtained prior to discharging waste water into urban drains. Discharged water must be passed through an efficient desilting system (e.g. using a series of desilting tanks) prior to discharging and the discharged water must comply with all the requirements stipulated in the Discharge License.
- (ii) Registration with EPD as a chemical waste producer must be completed and all collection of chemical waste must be handled by chemical waste collectors registered with EPD.

(4) Vibration

Reference may be made to H7.2.5 for its limitation and means of estimating vibrations due to foundation construction.

H7.8 FOUNDATION WORKS IN SCHEDULED AREAS

For foundation works in the Scheduled Areas defined by the Fifth Schedule of Buildings Ordinance, there may be special requirements imposed by the Building Authority. Consequently, sufficient time must be allowed in the planning and designing foundations, as well as in the execution of foundation works in the Scheduled Areas.

H8 TESTING OF FOUNDATION AND GROUND

H8.1 GENERAL

Clause 8.1 of the Code is self-explanatory.

H8.2 PLATE LOAD TEST

The plate load test as described in the Code aims at determination of allowable bearing capacity and estimation of Young's modulus of soil through measurement of the settlement of a square or circular "plate" under pre-determined loading.

The derivation of the formulae listed in the Code for determination of allowable bearing capacity and Young's modulus by plate load tests are as follows :

(A) Allowable bearing capacity on cohesionless soil:

Only N_γ needs be considered as the soil is without cohesion and no adjacent surcharge is applied during the plate load test.

(1) Square Plate : By the formulae listed in Table 2.3 of the Code,
 $\zeta_{\gamma s} = 1 - 0.4 \times 1 = 0.6$

So the ultimate bearing capacity is $q_{ult} = \zeta_{\gamma s} \times 0.5 B \gamma N_\gamma = 0.3 B \gamma N_\gamma$;

Thus $q_{allowable} = q_{ult} \div 3 = 0.1 B \gamma N_\gamma \Rightarrow W_t = 0.1 \gamma B^3 N_\gamma$

(2) Circular Plate : Approximation is made by finding a square of same area of the circle. The side of the square is $\sqrt{\pi/4} B$.

So $W_t = 0.1 \gamma \left(\sqrt{\pi/4} B \right)^2 B N_\gamma = 0.025 \pi \gamma B^3 N_\gamma$.

(B) Young's Modulus

By Poulos (1974), the formulae for calculating settlement S of a square rigid plate and a circular rigid plate with a uniform pressure p , dimension B on soil of Young's modulus E_s , Poisson's ratio ν and as a semi-infinite medium are respectively

$$S = \frac{p \times B (1 - \nu^2)}{1.13 E_s} \text{ and } S = \frac{\pi (1 - \nu^2) p \times 0.5 B}{2 E_s}$$

with W_t as the applied load at which S is measured so that $p = \frac{W_t}{B^2}$ and

$p = \frac{W_t}{0.25 \pi B^2}$ for the square plate and the circular plate respectively and re-arranging the above equations:

$E_s = \frac{W_t(1-\nu^2)}{1.13SB}$ for square plate; and $E_s = \frac{W_t(1-\nu^2)}{SB}$ for circular plate as listed in the Code.

The E_s so determined will be used to verify the design values used in the settlement calculations done in the design stage.

However, there is a criticism that only the top soil (less than half a metre) can be mobilized in the plate load test due to the small plan dimensions of the testing plate whilst the actual footing with much larger plan dimensions can mobilize soil at depths of 1 to 1.5 times the plan dimensions of the footing. The settlement measured can therefore be significantly over-estimated.

Li (2007) discussed the problems of using plate load test as a verification test for proving the bearing capacity of the founding soil. According to the recognized engineering principle, the bearing capacity depends on the dimensions of the shallow footing. The common size of the testing plate ranges between 300mm and 600mm, which is much smaller when compared with the actual dimension of the footing. Failure in the plate load test does not necessarily indicate that the shallow footing will experience a general shearing failure at the same bearing pressure. In many cases, settlement is usually the controlling factor in determining the allowable bearing capacity. In fact, the plate load test is best to determine the soil stiffness, E_s , for confirming the estimated settlement (GEO, 2006). Where there is evidence that weaker soils exist beneath the test level or the soil strength is not increasing with depth, it may be necessary to carry out a series of plate load tests at different levels.

H8.3 STANDARD PENETRATION TEST

The Standard Penetration Test (SPT) is often carried out during ground investigation to assess the ground conditions and to infer the anticipated founding levels for foundations. The procedures for SPT are described in GEOGUIDE 2.

The SPT N values measured give an indication of compactness of the soils. Empirical correlations are available in the literature to relate soil properties, such as soil stiffness and strength parameters, to SPT N values (GEO, 1993; GCO, 1990). It should be cautioned that such correlations may be subject to a high degree of variability and care must be taken in using such correlations, particularly for clayey soils.

H8.4 COMPRESSION LOADING TEST

Test loads used for proof tests of piles are either applied by means of a jack which obtains its reaction from (i) kentledge heavier than the required test load or (ii) tension piles or suitable anchors. For (i), to prevent the applied load from being eccentrically applied to the pile, the centre of gravity of the kentledge should lie on the axis of the test pile. For (ii), the anchor or anchor piles should be at adequate distance from the test pile

so as to minimize effects on settlement of the test pile due to loads in the anchor or anchor piles.

A test pile may be laterally restrained in the loading test if it is also laterally restrained (by the pile cap or tie beams) under the permanent condition. The restraint may be important if the pile is laterally free for a certain height such that buckling or inclination will significantly reduce its bearing capacity.

Procedure and failure criteria for pile load test are discussed in this clause.

- (a) The reason for excluding group effect from determination of test loads is obvious, as normally only single test piles are loaded during the loading test. The Code also states that the test load should be applied at the cut-off level. Nevertheless, if the application of the test load is at a higher level, the allowable maximum settlement as arrived at by (e) (i) below should be modified by the use of a longer value of pile length;
- (b) The test load on a test pile is generally twice its working load ($2W$). However, if the working load is very high so that the imposition of kentledge up to $2W$ is not practical, the test load may be reduced to below $2W$, subject to acceptance by the Buildings Department. Moreover, the maximum allowable settlement for loading test in (e)(i) should be adjusted if the test load is not $2W$. If the test load is xW where $x < 2$, the first term of the formula in (e)(i) for determination of the maximum allowable settlement should accordingly become $\frac{xW}{AE}$. In addition, the terms $\frac{D}{120} + 4$ that follow may also require adjustment;
- (c) The requirement that the load at each incremental stage be held for 10 minutes or longer until the rate of settlement is less than 0.05mm in 10 minutes is to ensure the settlement of the pile is practically completed at the applied load;
- (d) The measuring devices should be calibrated before use. Normally, 4 dial gauges arranged at corners of a square above the pile head are installed to measure the settlement of the pile as shown in Figure H8.1. Average values of the measured settlements should be taken as the settlement of the pile. Care should be taken when there are significant differences in values of the 4 readings which reveal that the pile may have been eccentrically loaded;

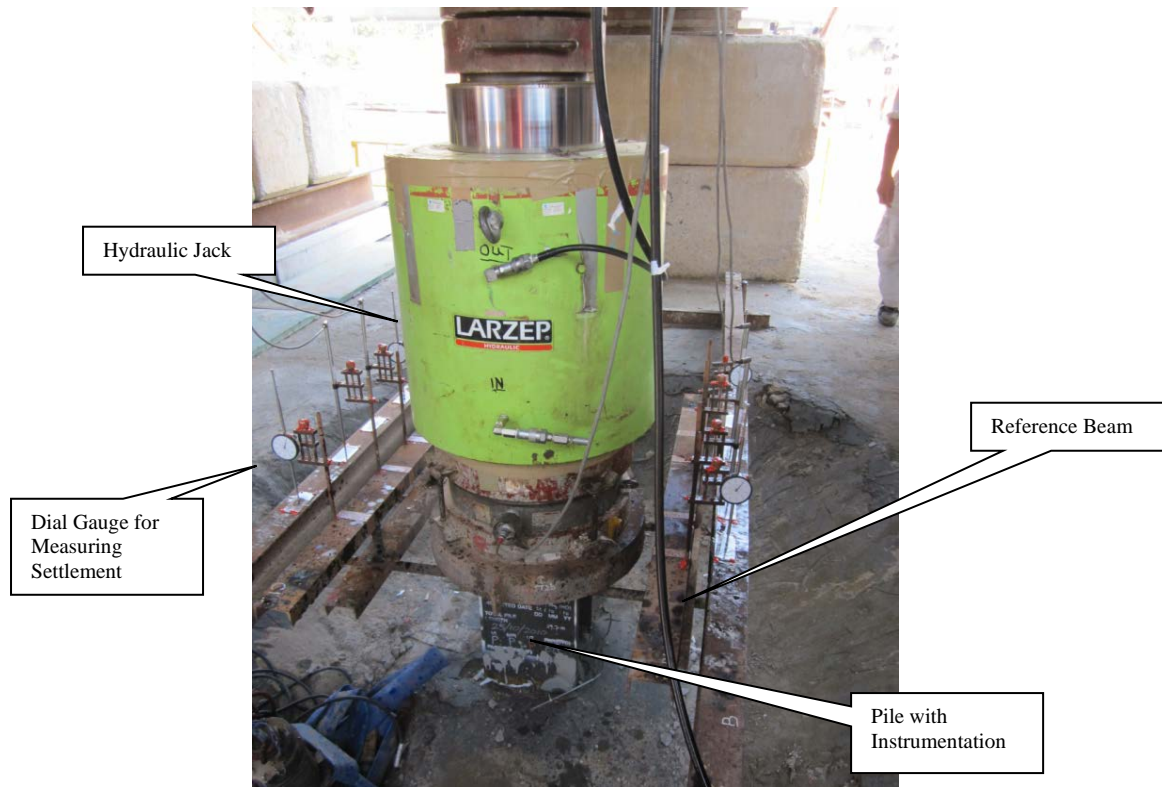


Figure H8.1 – Set-up of Loading Test on Top Level of Pile

- (e) Failure criteria for load test of piles with a least lateral dimension not exceeding 750mm are stipulated in this sub-clause. Load tests for piles exceeding a least dimension of 750mm will probably require test loads of such magnitude that it is impractical to carry out the test. For piles with a diameter or least lateral dimension not exceeding 750mm, the test is deemed to be unsatisfactory if any of the following conditions apply:
- (i) The criterion for maximum settlement at the pile head is stipulated in this sub-clause by the formula $\frac{2WL}{AE} + \frac{D}{120} + 4 \text{ mm}$ in which the symbols are defined in the Code.

This failure criterion is similar to the Davisson (1972) criterion which is one of the most widely used methods in the world. Originally, the Davisson (1972) criterion was intended for quick load test and the settlement due to long term creep is excluded. Nevertheless, it has been developed for end-bearing piles by considering the deformation required to cause yielding of soil at pile toes. This deformation is known as “soil quake” as denoted by Q_t . Based on the loading test results, dynamic measurements and wave equation analysis, Q_t is determined to be 0.10 inch in most soils for a normal pile dimension of 1 foot but increases linearly with pile size. So, when converted to the unit in mm, this term becomes $\frac{D}{120}$ (probably) where D is normally taken as the least dimension of the pile in mm. In a pile load test, ultimate load is presumed to

have reached when the pile head settlement Δ_h is 0.15 inch (= 4 mm) plus Q_i and the sum is below the “elastic deflection index line”. This index line can be calculated by assuming the pile as a fixed-base free-standing column which is $\frac{2WL}{AE}$ at the applied load normally equal to twice the design working load. So, by adding these three terms together, the equation listed in the Code is arrived at;

- (ii) By the Code requirement, the loading test is deemed unsatisfactory if the “residual settlement” exceeds the greater of

$D/120 + 4\text{mm}$; and
25% of the maximum pile head settlement

The criterion $D/120 + 4\text{mm}$ was used only originally, intending to limit the degrees of “yield” or “plastic settlement” that has occurred during pile load testing. 25% of the maximum pile head settlement has been added in recent years to make allowance for the locked in stresses. The requirement is not common in other parts of the world. Past experience indicates that this criterion is more difficult to fulfil than the maximum settlement criterion discussed in (i). As a result, piles often have to be driven to deeper levels in order to fulfil this additional requirement. This may cause problems in pile termination and even pile damage when the piles are long;

- (f) The Code states that grout can be taken into consideration in the calculation of axial stiffness of mini-piles and socketed H-piles while the casing can be included in the determination of axial compression / extension of the pile in the loading test;
- (g) Normally confirmatory tests on large diameter bored piles (diameter > 750mm), barrette piles and hand-dug caissons are performed by concrete coring instead of that by imposition of loads.

A typical load settlement proof test curve due to the imposition of load on a local socketed H-pile is shown in Figure H8.2.

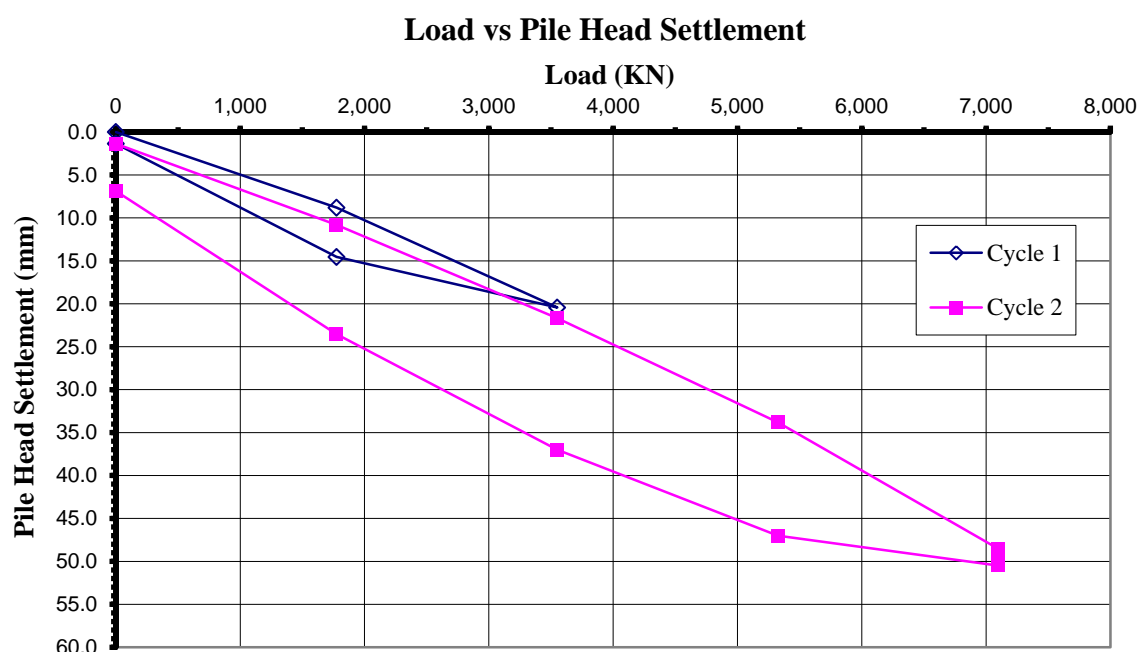


Figure H8.2 – A Typical Load Settlement Curve in a Pile Load Test

H8.5 CORE-DRILLING TEST

Two types of proof core-drilling; namely interface coring and full length coring, are commonly used in large diameter bored piles, barrettes and the like.

Interface coring should be taken through the reservation tube for each of the large diameter bored piles, barrettes and the like to a distance of at least 1m above and below the rock/pile interface. The main purpose is to confirm good contact between the concrete and rock. It can also serve to check the length of pile, quality of the concrete near the pile base and give some indication of the soundness of the founding rock.

Common types of defects at the concrete/rock interface are the presence of sediments, soil inclusions, unbounded aggregates and rock fragments debris. Remedial treatment may be necessary subjected to the review by AP/RSE/RGE (see clause 12 of PNAP APP-18). Typical remedial treatments for bored piles commonly accepted by BD include water jetting and subsequent pressure grouting for sediments and/or segregation at the pile/rock interface not exceeding (i) 50mm for pile lengths less than 30m; and (ii) 100mm for pile length longer than 30m. Verification cores after grouting are normally not necessary. However, sediments and/or segregation in excess of the foregoing will require further investigation of the extent of the defects and the effects on the pile performance. If the defect is localized and the effect on the overall pile performance is not significant, cleaning by high pressure water jetting and pressure grouting shall be used to rectify the defects. However, verification cores are normally required to prove the effectiveness of the treatment. Prescribed methods for remedial treatments of barrettes and the like have not been developed, but reference can be made to those for bored piles.

Local imperfections such as weak seams, more weathered and/or shattered rocks are sometimes present at the bearing stratum below the interface. However, it is sometimes

difficult to distinguish whether the imperfection is above or below the concrete/rock interface, particularly when there is a core loss, because the interface level is traditionally taken as the average of a few levels dipped by a measuring tape. Caution is therefore required to identify the various types of observed occurrences on the interface core logs. If the imperfection at the bearing stratum below the interface is greater than 100mm, further investigation of the extent of imperfection and individual assessment on the capacity of the bearing stratum and the design may be required.

The concrete core taken should not show any sign of honeycombing or segregation of the individual constituent materials. Defects, if identified, should be investigated as to their extent and their effects on pile performance. Destructive compression tests can be carried out to ascertain the concrete strength if required. The compressive strengths of the concrete core can be corrected to equivalent cube strengths which can thus act as a checking or compliance criterion of the permanent concrete work of the pile. If the defect is localized and does not affect overall pile performance, high pressure water jetting and pressure grouting shall be used to rectify the defects, with verification cores to prove the effectiveness of the treatment.

Concrete cores are sometimes included by some practitioners in the calculation of the TCR. On this basis, they argue that the presence of defects at the concrete/rock interface up to 150mm is acceptable due to the achievement of 85% TCR. This is contrary to the Ordinance which requires sound, adequate interface in good contact, and not some irregular materials at the toe due to workmanship. In Hong Kong, rock weathering rarely produces a homogeneous weathered rock mass where all rock material is weathered to the same degree, or even a simple weathered profile where the degree of weathering decreases progressively with depth. The presence of these discontinuities and the effects of weathering have a great influence on engineering behaviour. According to GEOGUIDE 3, TCR is one of the parameters in classifying the engineering properties of a rock mass. Inclusion of a concrete core in the calculation of the TCR is therefore irrational because concrete is an artificial material. Furthermore, this will make TCR become arbitrary as it can vary depending on the start and the end of the drilling in the interface coring. Notwithstanding this, the TCR of founding rock is reported in the drilling log of the interface coring. Caution is required on the interpretation of the capacity of the founding rock since the rock core run is less than 1.0m.

Full coring should be taken throughout the full length of large diameter bored piles, barrettes and the like selected by the BD to a distance of at least half a diameter of the pile base or 600mm whichever is larger into the rock upon which the pile is founded. The main purpose is to confirm the adequacy of the interface between the concrete and rock, quality of the concrete and soundness of the rock for founding. Defects revealed should be treated in similar fashion to those given for the interface coring.

H8.6 SONIC LOGGING

The test should be carried out by a HOKLAS accredited laboratory as per clause 8.1 of the Code. In addition to the provisions in the Code, the followings are discussed :

(i) Introduction

As discussed in the Code, sonic logging is one of the most commonly used types of non-destructive test to examine the integrity and homogeneity of cast-in-place concrete piles, diaphragm walls and barrettes. However, it should be noted that only the existence of, but not the nature of, defects can be identified with this test. Figure H8.3 illustrates the execution of the test.

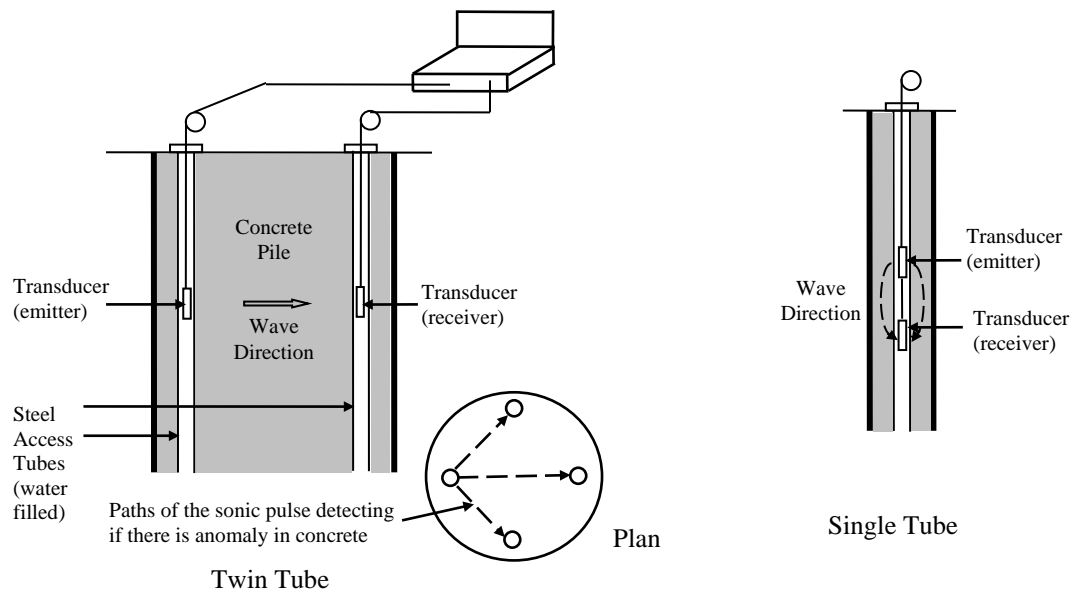


Figure H8.3 – Twin Tube and Single Tube Set-up of Sonic Logging Test

(ii) Equipment

The equipment for sonic logging generally consists of one ultrasonic pulse emission probe, one (or multiple) reception probe(s), a depth encoder and a main unit which is used to record the information collected in the test and for subsequent analysis.

(iii) Access Tube

In order to perform this test, the access tubes are fixed in the desired position before concreting. Although both plastic and metal access tubes can be used, metal access tubes are preferred because of the smaller risk of debonding (i.e. separation between the tube and the concrete). Users should follow manufacturer's instruction in choosing the minimum diameter of the access tube. Sometimes, the access tube can also be used for interface coring to investigate the condition at the bottom of the pile and the interface between the concrete and founding rock/soil. As such, the diameter of the access tube should be large enough to suit the coring process. If the diameter of the tube is double or more than double of the diameter of the probe, a centralizer should be attached to the probe so as to minimize any possible snagging on irregularities in the access tube.

(iv) Principle of Sonic Logging

Although the single tube method is adequate for performing sonic logging, the cross-hole method is preferable as long as the pile (or the concrete element to be tested) is large enough to accommodate two or more access tubes.

During the test, the emitting probe and receiving probe are lowered into the access tube(s) at the same speed as shown in Figure H8.3. Time of propagation (also called first arrival time, FAT) and the attenuation of energy of an ultrasound pulse transmitted from the emitting probe to the receiving probe will be recorded by the equipment. If the concrete is homogeneous, the FAT and attenuation of energy is generally stable. If the time and/or attenuation of energy at certain location is excessively varied, a defect is suspected at that location. The defect can be a soil inclusion, cracks or segregation in concrete.

(v) Test Procedure

- (1) One emitting probe and one receiving probe are lowered down to the bottom of the water-filled parallel tubes;
- (2) The equipment is triggered and the emitting and receiving probes are pulled up simultaneously;
- (3) When the probes are being pulled up, the emitting probe emits sonic signals and the main unit of the equipment will also record the relevant parameters of the signal (i.e. arriving time of the signal, energy, corresponding depth etc.) through the receiving probe and the depth encoder;
- (4) The test result will then be presented graphically. The graph will show the arrival time and energy of signals along the pile.

(vi) Interpretation of Test Results

According to the principle of the test, an excessively long arrival time or severe attenuation of the signal received is an indication of defect. If an anomaly is found at certain levels in one profile, the signals at the corresponding levels of other profiles should be carefully compared. The overall assessment should be made based on the study and comparison of all profiles, taking into account of other factors such as concreting sequence, possibility of air gap around the tube, etc. Because of the limitations of this kind of test, sometimes further investigation such as coring may be required to confirm the existence of a defect. Figure H8.4 shows an “anomaly” to the sonic signal of a pile 14m below ground. Coring of the pile confirmed that there are cracks in the concrete at that location.

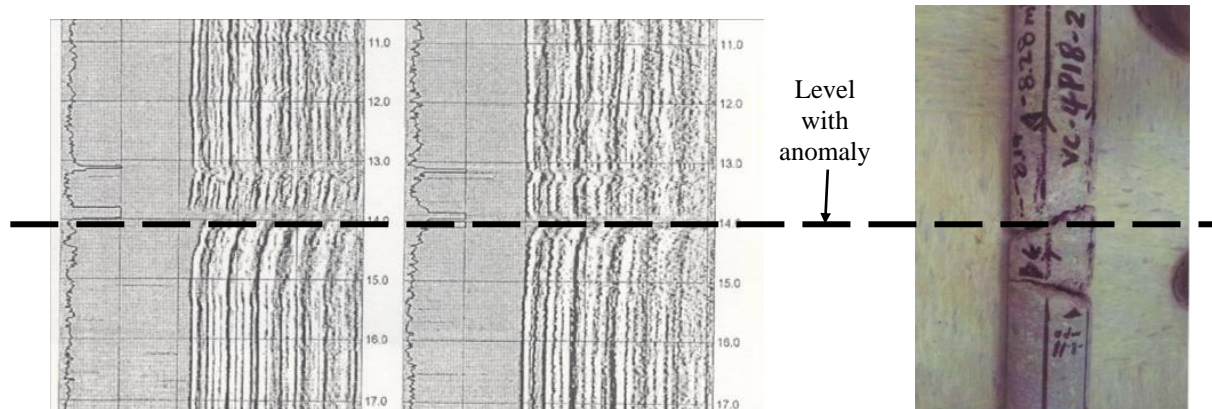


Figure H8.4 – Example Demonstrating Sonic Coring Test Revealing Anomaly

H8.7 SONIC ECHO TESTS

The sonic echo test is also known as the “Pile Integrity Test” (PIT) or “low strain dynamic test”. The name “low strain dynamic” stems from the fact that the strain produced by the hand-held hammer is low. The test is quick and cost effective. Its working principles and limitations are described in the Code. The test should be carried out by a HOKLAS accredited laboratory as per clause 8.1 of the Code.

H8.8 VIBRATION TEST

The test has not been commonly carried out in Hong Kong in recent years.

H8.9 DYNAMIC LOAD TEST FOR DRIVEN PILES

The commonest dynamic load tests comprise the Pile Driving Analyzer (PDA) and the CAPWAP which have been described in detail in H5.3.2 and Appendix HL.

H8.10 TENSION LOADING TEST

The Code requires effects due to pile interaction be made if any reaction piles are closer than the lesser of 3 pile diameter and 2m to the test pile, as in consistency with GEO Publication 1/2006. The interaction may be accounted for by the elastic theory such as Poulos & Davis (1980) or Randolph (1977). They both involve calculation of settlement of soil due to a pile embedded in soil under vertical loads. The method by Randolph is simpler and has been quoted by GEO Publication 1/2006 for pile under compression. While a reaction pile in close proximity to a test pile undergoing tension loading test is under compression, it will then be creating settlement on the test pile which reduces its up-rise during loading. Randolph’s equations are shown in Appendix HV.

A photograph showing a tension test arrangement (for a raking pile) is shown in Figure H8.5.

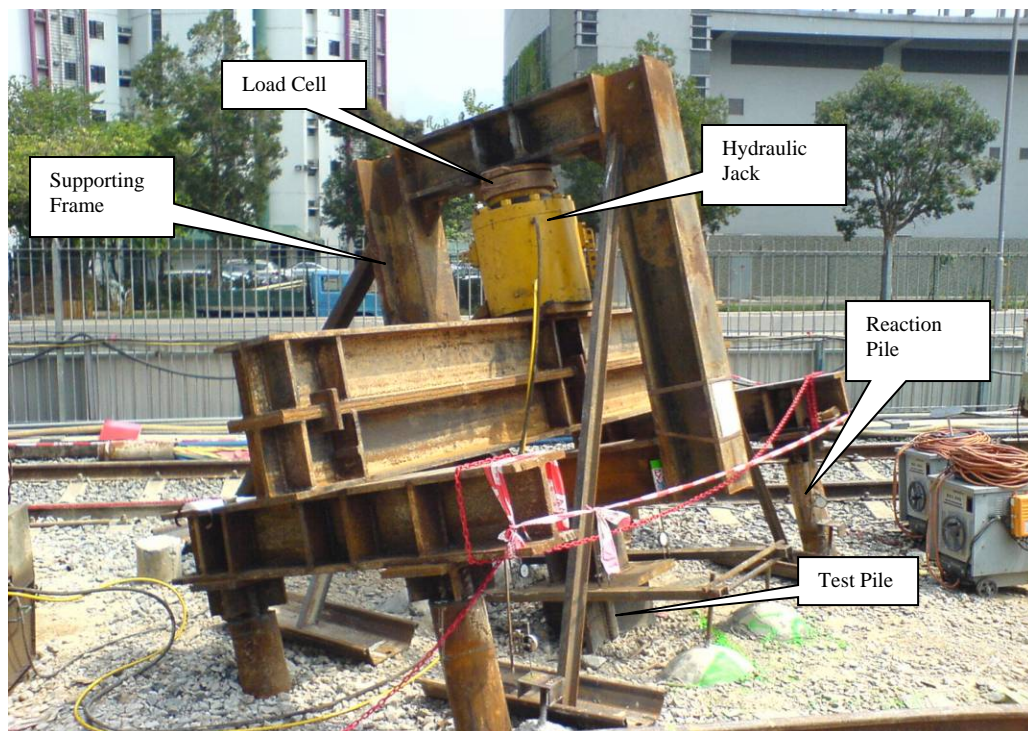


Figure H8.5 – Photograph showing Arrangement of a Tension Pile Test (Raking Pile)

In addition to the provisions / requirements in the Code, the following are added :

- (1) Apart from reaction piles, the ground may be used for reaction purposes to provide the tension load on the pile if it is adequately strong such as sound rock as illustrated in Figure H8.6. Nevertheless, the ground beams or bearers should be spaced at an ample distance from the test pile as otherwise the lateral pressure on the pile induced by the load on the ground will increase the skin friction of the pile;

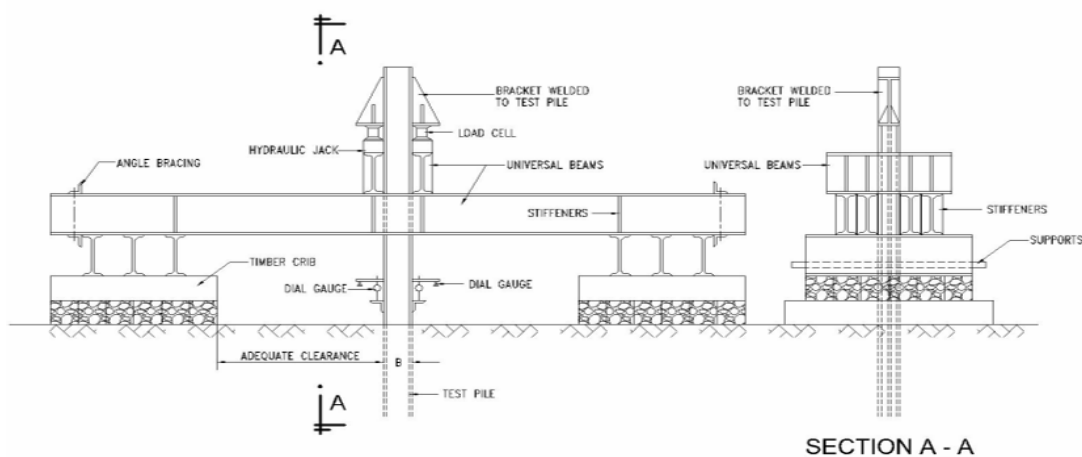


Figure H8.6 – Tension Pile Test using Ground as Reaction

- (2) Effects due to close proximity of the reaction pile should be considered;

- (3) If the tension loads on the pile are intermittent or cyclic in nature, it may be more desirable to adopt repetitive loading sequence on the test pile. Reference can be made to Tomlinson (1994).

H8.11 LATERAL LOAD TEST

In addition to the provisions / requirements in the Code, the following are added :

Lateral load tests on piles may be used to verify soil parameters suitable for a particular analysis or design method. An example is the horizontal subgrade reactions (Terzaghi 1955) based on the Winkler spring theory in which the pile is mathematically modeled as a flexible beam and the soil restraints modeled as lateral springs (Winkler springs). The measured deflection profile can then be used to back-calculate the horizontal subgrade reaction values and these values can be used to predict deflection profiles for other piles together with the forces induced. Reference can be made to H5.3.4.

H8.12 ULTRASONIC ECHO SOUNDER TEST

The descriptions and precautionary measures provided in the Code are comprehensive. An example of the “trace results” of the excavation profile of a large diameter bored pile, including its bell-out is included in Figure H8.7.

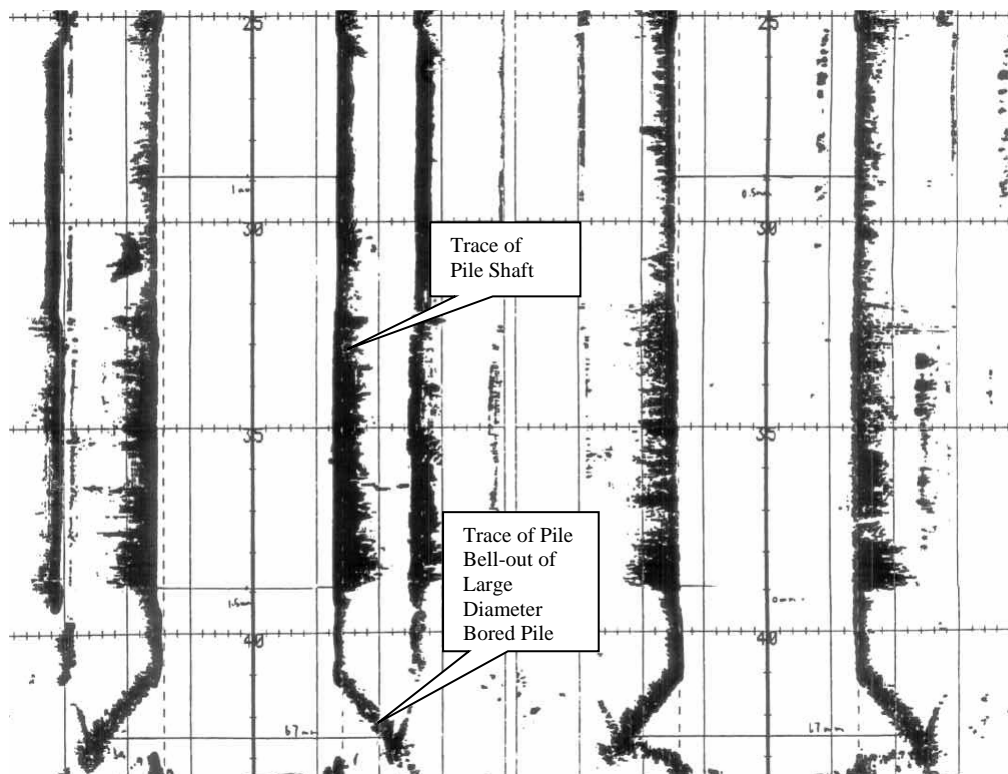


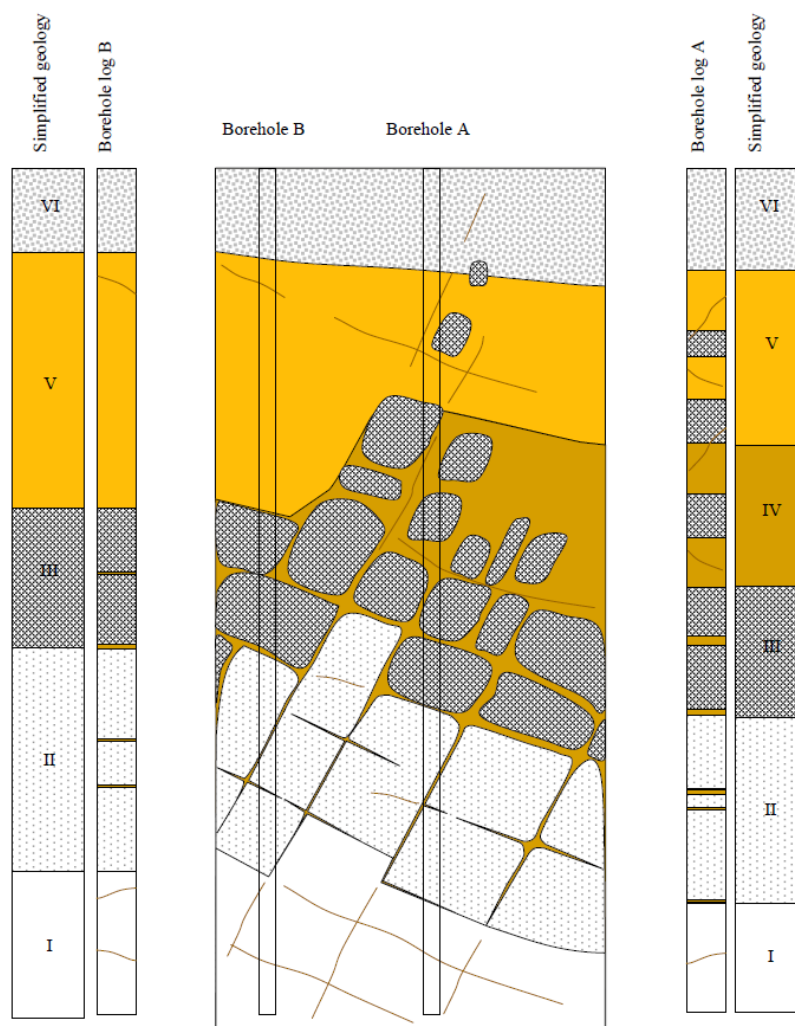
Figure H8.7 – Example of “Traces” Revealed by Ultrasonic Echo Sounder Test

Appendix HA

Practical Examples of Inspection of Rock Samples

Practical Examples in Inspection of Rock Samples

Worked Example HA-1



Note : Refer to Geoguide 3 (GCO, 1988) for classification of rock decomposition Grade I to VI
 Figure HA-1 – Representation of a Corestone-bearing Rock Mass (Malone, 1990)

As described by GEO Publication 1/2006 (2006), the thickness and nature of weathering profiles varying markedly depends on the rock type, topographical location and geological history. Taking an example quoted from GEOGUIDE 3, the corestone-bearing profiles as shown in Figure HA-1 are primarily developed in medium and coarse grained granites and coarse ash tuffs. The incidence of corestones generally increases with depth in a weathering profile, although abrupt lateral variations are also common. The depth and extent of weathering can vary considerably with changes in rock type and discontinuity spacings. Thus, the inherent spatial variability of the soil masses formed from the weathering of rocks insitu and the undulating weathering front are important considerations in the design and construction of foundations.

Appendix HB

A Worked Example on Determination of Ultimate Bearing Capacity of an Inclined Rectangular Footing

A Worked Example on Determination of Ultimate Bearing Capacity of Inclined Footing

Ultimate bearing pressure of a footing of plan dimensions $8\text{ m} \times 6\text{ m}$ under a vertical load of 8000 kN and horizontal load of 1000 kN of eccentricities 0.3 m along its length and 0.4 m along its width from the centre is to be found by the Vesic Equation (1975). The footing is founded at an inclination of 10° to the horizontal and is in close proximity of a 20° slope as shown in Figure HB-1. The soil parameters are also given in Figure HB-1.

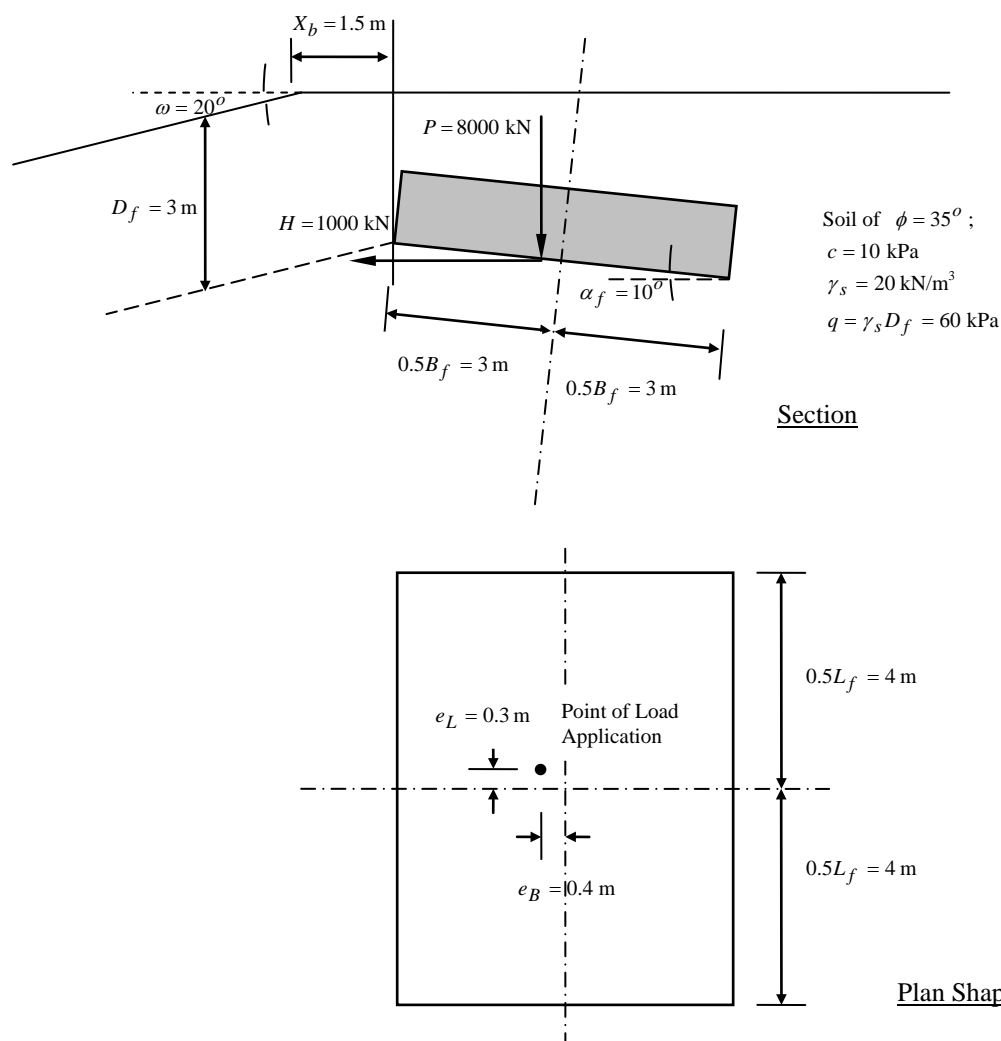


Figure HB-1 – Worked Example of Determination of Ultimate Bearing Capacity of Footing

The ultimate bearing capacity of the footing is determined by the equation

$$q_u = cN_c \zeta_{cs} \zeta_{ci} \zeta_{cr} \zeta_{cg} + 0.5B_{fe} \gamma_s N_\gamma \zeta_{\gamma s} \zeta_{\gamma i} \zeta_{\gamma r} \zeta_{\gamma g} + qN_q \zeta_{qs} \zeta_{qi} \zeta_{qr} \zeta_{qg} \quad (\text{Eqn HB-1})$$

where c is the cohesion of the soil, B_{fe} is the effective width of the footing, γ_s is the unit weight of the soil, q is the surcharge on the area adjacent to the footing and the N factors are the bearing capacity factors.

The original equation in its simplest form is in fact

$$q_u = cN_c + 0.5B\gamma_s N_\gamma + qN_q \quad (\text{Eqn HB-2})$$

for a footing of infinite length without tiling and the footing is resisting vertical load only. The derivation is based on failure mode shown by Figure HB-2.

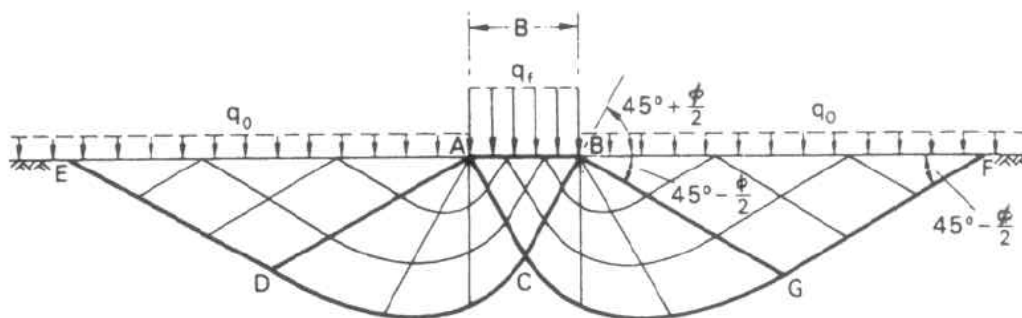


Figure HB-2 – Failure Mode under a Strip Footing

It can be seen that the ultimate bearing capacity by (Eqn B-2) is made up of three components with failures along the assumed failure surface : (i) the first one of which is given by cohesion of the soil; (ii) the second one is due to friction effected by weight of the soil mass; and (iii) the last one is due to friction effected by the adjacent surcharge.

For general use where a footing of finite dimensions which may be tilted and / or adjacent to slope, (Eqn HB-1) is derived based on (Eqn HB-2) with the ζ s as coefficients to account effects for (1) length width ratio of the footing; (2) inclination of resultant loads to the footing; (3) tiling of the footing; and (4) sloping of ground.

For the footing shown in Figure HB-2, the following factors are computed prior to arrival of the final ultimate bearing capacity.

Effective width and Length of the Footing

$$B_{fe} = B_f - 2e_B = 5.2 \text{ m}$$

$$L_{fe} = L_f - 2e_L = 7.4 \text{ m}$$

Bearing Capacity Factors

$$N_q = e^{\pi \tan \phi} \tan^2 \left(\frac{\phi}{2} + 45^\circ \right) = 33.296$$

$$N_c = (N_q - 1) \cot \phi = 46.124$$

$$N_\gamma = 2(N_q + 1) \tan \phi = 48.029$$

Shape Factors

$$\zeta_{cs} = 1 + \frac{B_f}{L_f} \frac{N_q}{N_c} = 1.541$$

$$\zeta_{\gamma s} = 1 - 0.4 \frac{B_f}{L_f} = 0.7$$

$$\zeta_{qs} = 1 + \frac{B_f}{L_f} \tan \phi = 1.525$$

Inclination Factors

$$m_i = (2 + B_{fe} / L_{fe}) / (1 + B_{fe} / L_{fe}) = 1.587$$

$$\zeta_{qi} = \left(1 - \frac{H}{P + B_{fe} L_{fe} c \cot \phi} \right)^{m_i} = 0.821$$

$$\zeta_{ci} = \zeta_{qi} - \frac{1 - \zeta_{qi}}{N_c \tan \phi} = 0.815$$

$$\zeta_{\gamma i} = \left(1 - \frac{H}{P + B_{fe} L_{fe} c \cot \phi} \right)^{m_i + 1} = 0.725$$

Tilt Factors

$$\zeta_{\gamma t} = (1 - \alpha_f \tan \phi)^2 = 0.771$$

$$\zeta_{qt} = \zeta_{\gamma t} = 0.771$$

$$\zeta_{ct} = \zeta_{qt} - \frac{1 - \zeta_{qt}}{N_c \tan \phi} = 0.763$$

Ground Sloping Factors

$$\zeta_{cg} = e^{-2\omega \tan \phi} = 0.613$$

$$\zeta_{qg} = (1 - \tan \omega)^2 = 0.405$$

$$\zeta_{\gamma g} = \zeta_{qg} = 0.405$$

So the ultimate bearing capacity when the footing is at the edge of the slope is

$$q_u = cN_c \zeta_{cs} \zeta_{ci} \zeta_{ct} \zeta_{cg} + 0.5B_{fe} \gamma_s N_{\gamma} \zeta_{\gamma s} \zeta_{\gamma i} \zeta_{\gamma t} \zeta_{\gamma g} + qN_q \zeta_{qs} \zeta_{qi} \zeta_{qt} \zeta_{qg}$$

$$= 271.399 + 394.974 + 779.554 = 1445.926 \text{ kPa} < 3000 \text{ kPa}$$

It can be seen that the surcharge adjacent to the footing gives the greatest contribution in this example.

The ultimate bearing capacity of the same footing without tilting, sloping ground and resists vertical load only is re-calculated. The ultimate bearing pressure increases to $q_u = 5340.727 \text{ kPa}$, (though the Code limits the value to 3000kPa as per Clause 2.2.4). So it can be seen that these factors have significant effects on reduction of ultimate bearing pressure.

When the footing is at ground level which can be assumed for the footing to be located at $4B_{fe} = 20.8 \text{ m}$ from the edge of the slope, the ground sloping factors are all unity, the ultimate capacity becomes

$$q_u = cN_c \zeta_{cs} \zeta_{ci} \zeta_{ct} + 0.5B_{fe} \gamma_s N_{\gamma} \zeta_{\gamma s} \zeta_{\gamma i} \zeta_{\gamma t} + qN_q \zeta_{qs} \zeta_{qi} \zeta_{qt}$$

$$= 442.493 + 976.367 + 1927.042 = 3345.902 \text{ kPa.}$$

By Figure 2.3(c) of the Code, the ultimate bearing capacity of the footing which is at 1.5m from the edge of the slope can be interpolated between the ultimate values at edge = 1445.926kPa and that at $4B_{fe} = 20.8 \text{ m}$ which is 3345.902kPa. The linearly interpolated value is 1582.943kPa as demonstrated in Figure HB-3.

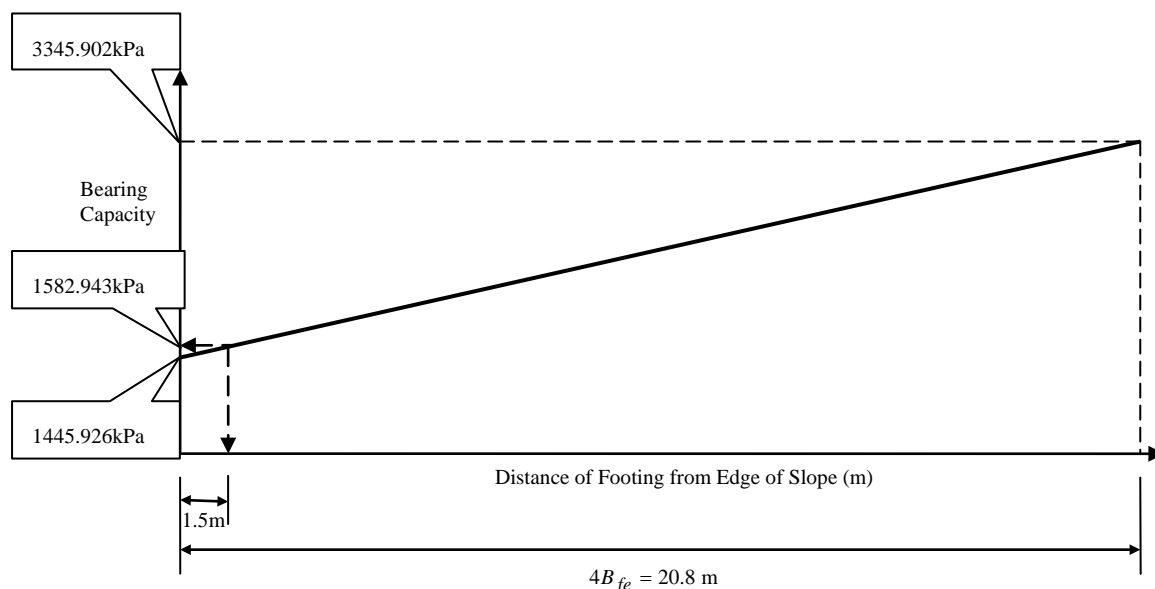


Figure HB-3 – Demonstration of Interpolation of Ultimate Bearing Capacity

So the ultimate bearing capacity of the footing is

$$1445.926 + (3345.902 - 1445.926) \times \frac{1.5}{20.8} = 1582.943 \text{ kPa.}$$

With the overburden pressure $q_0 = \gamma_s D_f = 20 \times 3 = 60 \text{ kPa}$ and by the equation listed in 2.2.4 of the Code, the allowable bearing capacity can be calculated as follows :

$$q_a = \frac{q_u - q_0}{F} + q_0 = \frac{1582.943 - 60}{3} + 60 = 567.648 \text{ kPa.}$$

Comparing with the pressure exerted by the footing which is determined as

$$\frac{P}{B_{fe} L_{fe}} = \frac{8000}{5.2 \times 7.4} = 207.9 \text{ kPa, the pressure is within the allowable bearing capacity.}$$

Appendix HC

Determination of Settlement and Support Stiffness of Footings on an Elastic Subgrade

Determination of Settlement and Support Stiffness of Footings on an Elastic Subgrade

HC.1 Theoretical Background

To estimate the settlement and support stiffness of footings, the basic equation for computation of the corner of a rectangular flexible footing of dimension $B' \times L'$ on the surface of an elastic layer can be used which is computed by the Theory of Elasticity (Timoshenko and Goodier (1951)) quoted as follows :

$$\Delta H = q_0 B' \frac{1-\nu^2}{E_s} \left(I_1 + \frac{1-2\nu}{1-\nu} I_2 \right) I_F \quad (\text{Eqn HC-1})$$

where q_0 is the uniformly distributed pressure applied by the footing;

B' is the lesser plan dimension of the rectangular footing;

L' is the greater plan dimension of the rectangular footing;

H' is the thickness of the elastic subgrade below which is a hard stratum;

E_s is the Young's Modulus of the soil;

ν is the Poisson's ratio of the soil;

I_1 and I_2 are factors given by Steinbrenner (1934) as follows :

$$I_1 = \frac{1}{\pi} \left[M \ln \frac{(1 + \sqrt{M^2 + 1}) \sqrt{M^2 + N^2}}{M(1 + \sqrt{M^2 + N^2 + 1})} + \ln \frac{(M + \sqrt{M^2 + 1}) \sqrt{1 + N^2}}{M + \sqrt{M^2 + N^2 + 1}} \right]$$

$$I_2 = \frac{N}{2\pi} \tan^{-1} \left(\frac{M}{N \sqrt{M^2 + N^2 + 1}} \right)$$

$$\text{with } M = \frac{L'}{B'}; \quad N = \frac{H}{B'}$$

where H is the depth of the elastic half-space.

I_F is the "influence factor" for a footing buried at depth D' below ground.

It is dependent on ν , M and D'/B' ratios which can be calculated by the Fox Equations in Fox (1948). The Fox equation is indicated as follows.

$$I_F = \frac{\sum_{i=1}^5 \beta_i Y_i}{(\beta_1 + \beta_2) Y_1} \quad (\text{Eqn HC-2})$$

$$\text{where } \beta_1 = 3 - 4\nu; \quad \beta_2 = 5 - 12\nu + 8\nu^2; \quad \beta_3 = -4\nu(1 - 2\nu);$$

$$\beta_4 = -1 + 4\nu - 8\nu^2; \quad \beta_5 = -4(1 - 2\nu)^2$$

$$R = 2D';$$

$$R_1 = \sqrt{L'^2 + R^2}; \quad R_2 = \sqrt{B'^2 + R^2};$$

$$R_3 = \sqrt{L'^2 + B'^2 + R^2}; \quad R_4 = \sqrt{L'^2 + B'^2}$$

$$Y_1 = L' \times \ln \left(\frac{R_4 + B'}{L'} \right) + B' \times \ln \left(\frac{R_4 + L'}{B'} \right) - \frac{R_4^3 - L'^3 - B'^3}{3L'B'};$$

$$Y_2 = L' \times \ln \left(\frac{R_3 + B'}{R_1} \right) + B' \times \ln \left(\frac{R_3 + L'}{R_2} \right) - \frac{R_3^3 - R_2^3 - R_1^3 + R^3}{3L'B'};$$

$$Y_3 = \frac{R^2}{L'} \times \ln \left[\frac{(B' + R_2)R_1}{(B' + R_3)R} \right] + \frac{R^2}{B'} \times \ln \left[\frac{(L' + R_1)R_2}{(L' + R_3)R} \right];$$

$$Y_4 = \frac{R^2(R_1 + R_2 - R_3 - R)}{L'B'};$$

$$Y_5 = R \times \tan^{-1} \left(\frac{L'B'}{RR_3} \right)$$

I_F can either be worked out by (Eqn HC-2) or estimated from Figures HC-1(a) to (e). (I_F converges to 1.0 when $D'/B' = 0$)

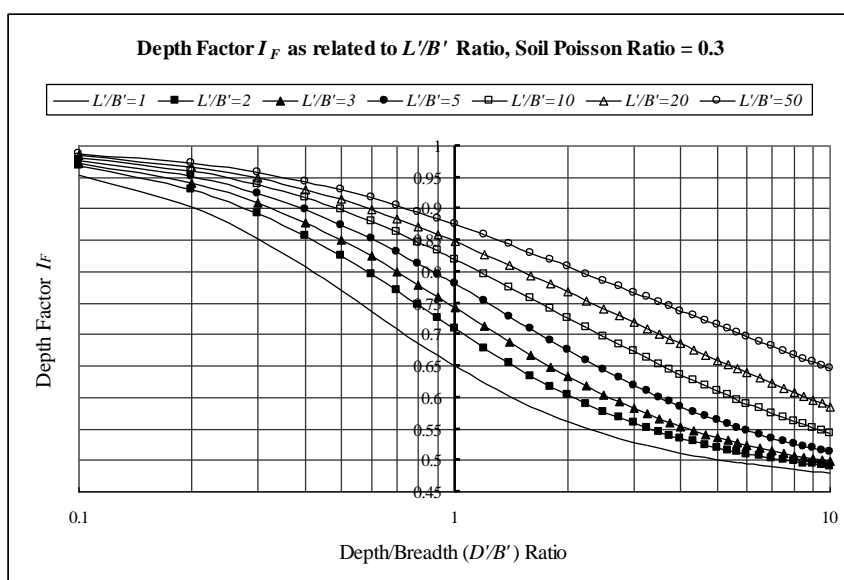


Figure HC-1(a)
– Variation of
Depth Factor
with L/B Ratios
for Soil of
Poisson's Ratio
= 0.3

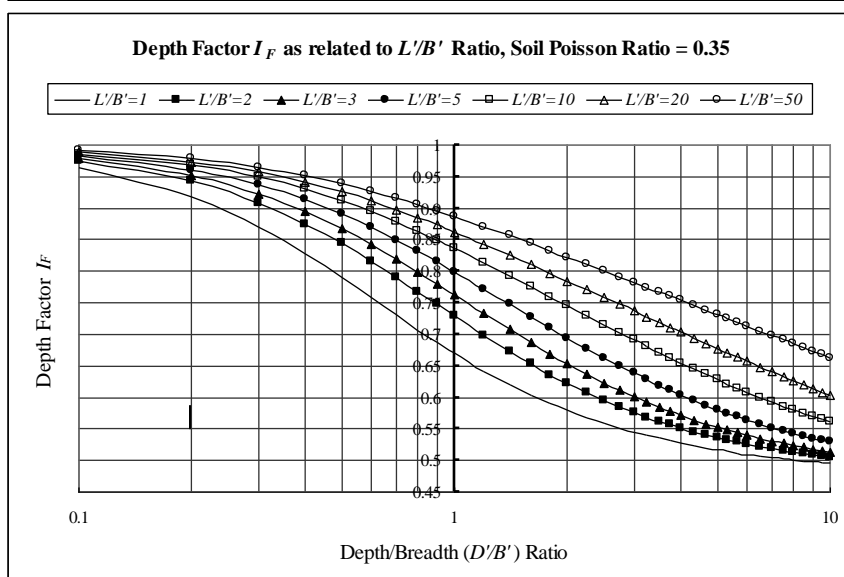


Figure HC-1(b)
– Variation of
Depth Factor
with L/B Ratios
for Soil of
Poisson's Ratio
= 0.35

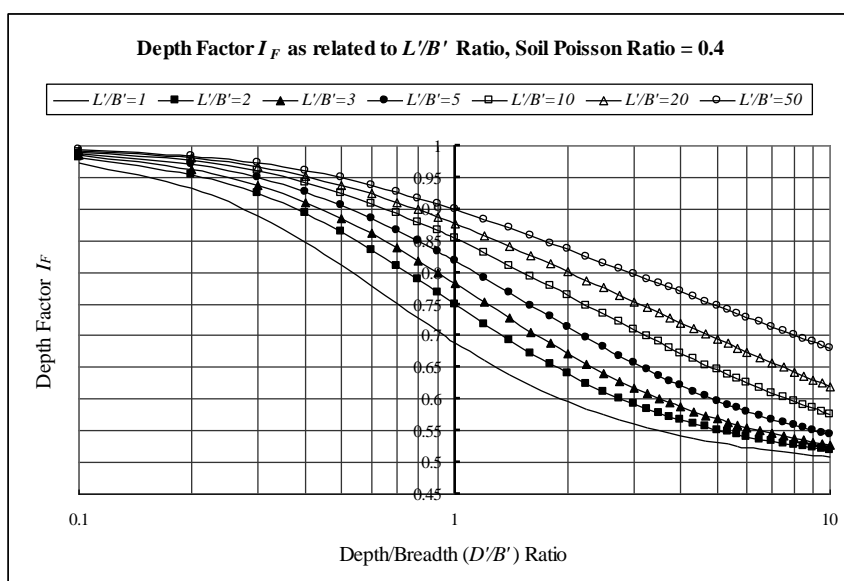


Figure HC-1(c)
– Variation of
Depth Factor
with L/B Ratios
for Soil of
Poisson's Ratio
= 0.4

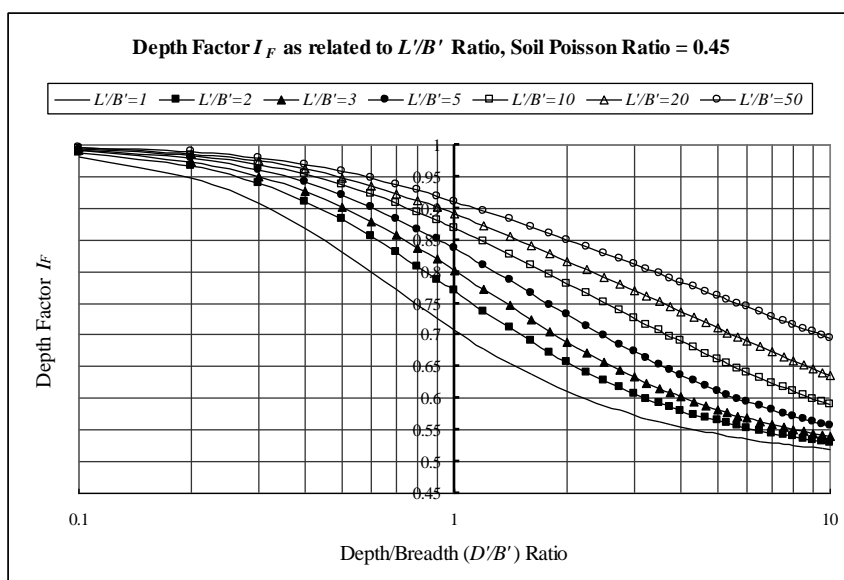


Figure HC-1(d)
– Variation of
Depth Factor
with L/B Ratios
for Soil of
Poisson's Ratio
= 0.45

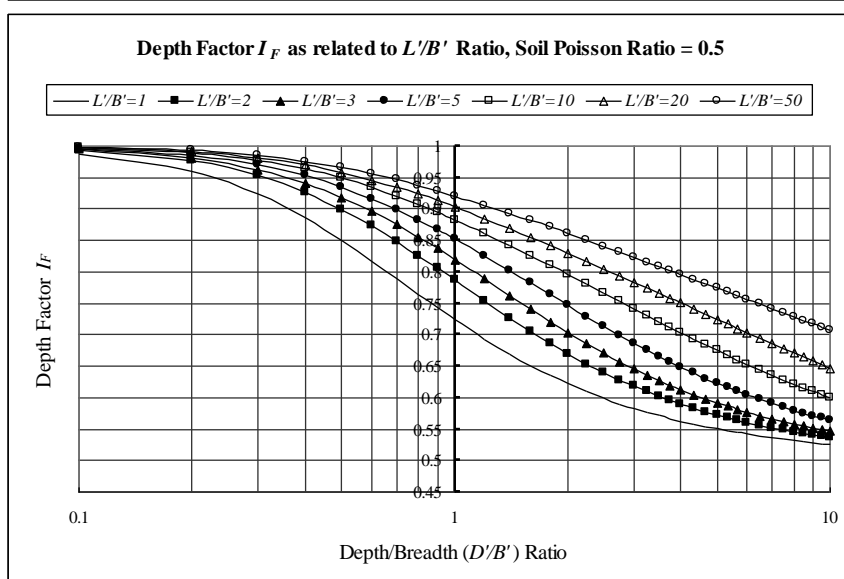


Figure HC-1(e)
– Variation of
Depth Factor
with L/B Ratios
for Soil of
Poisson's ratio
= 0.5

Symbols used in the above equations are illustrated in Figure HC-2.

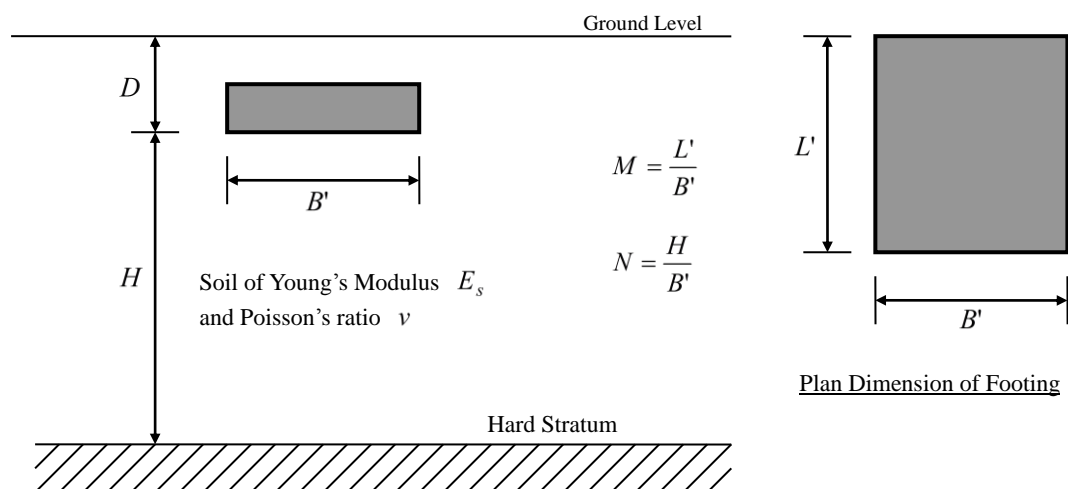


Figure HC-2 – Illustration of Symbols used in the Equations for Estimating Corner Settlements of Rectangular Footing

Settlements at any point beneath the footing can be determined in accordance with the principle illustrated in Figure HC-3.

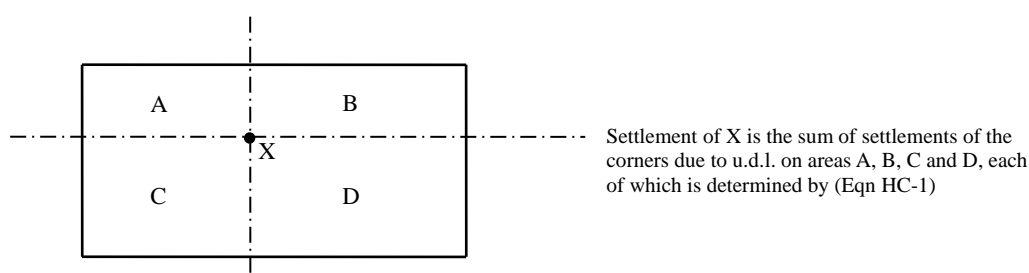


Figure HC-3 – Calculation of Settlement of a point X under a point of a Footing exerting a Uniformly Distributed Load on an Elastic subgrade

It is obvious that settlements at the centre of the footing are greater than those at the corners and the edges if the applied load is a uniformly distributed load.

HC.2 Worked Example HC-1

A footing of plan dimensions 3m by 2m on a subgrade of elastic modulus 15000kPa, Poisson's ratio 0.35, thickness 10m above a hard stratum is exerting a uniformly distributed load of 200kPa on the surface of the subgrade. The settlement is analyzed using (Eqn HC-1) with the procedure described in the last paragraph of HC.1. In the analysis, settlements of 441 nos. of joints (at the interior, edges and corners of the footing) equally spaced in the directions parallel to its length and width are analyzed. The analytical results show that the settlement at the centre portion of the footing is the greatest among all joints as illustrated in Figure HC-4.

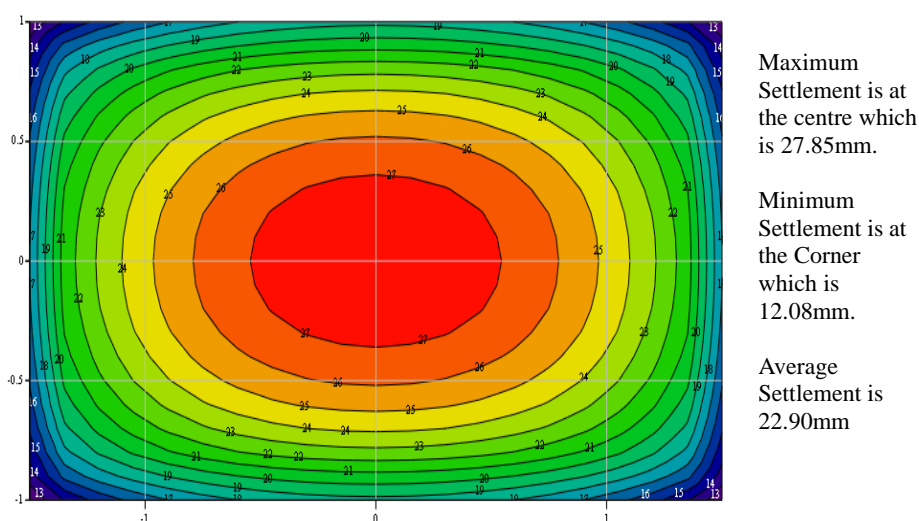


Figure HC-4 – Settlement Contours for a Rectangular Footing exerting Uniformly Distributed Load on an Elastic Subgrade

However, this phenomenon can only be true if the footing is flexible enough to deform with the same settlement contours as the subgrade. If the footing is possessing some stiffness by which the settlements will be less extreme (i.e. the differences in settlements between the centre and the corners and edges are smaller), there will be a redistribution of pressures on the subgrade such that the centre portion will experience smaller pressures than those at the corners and the edges.

HC.3 Design Charts for Rectangular Footing resting on Ground

Charts are drafted for general use in estimating average settlement of rectangular footings under uniformly distributed loads with founding levels on ground. In the exercise, a rectangular footing with its lesser plan dimension equal to unity and the greater plan dimension equal to $M (\geq 1.0)$ is used. In each of the footing, settlements of 441 nos. of nodes spaced at equal intervals in the two directions (including the corner nodes and edge nodes) parallel to the length and breadth of the footing are analyzed in accordance with the approach as described in the foregoing

sections. The coefficient $I = \sum (1 - \nu^2) \left(I_1 + \frac{1 - 2\nu}{1 - \nu} I_2 \right) b'$ (by Eqn HC-1) is

calculated for each node which is in general the sum of the contributions of the 4 rectangles adjoining to the node (see Figure HC-3) and b' is the lesser plan dimension of the adjoining rectangle. Weighted averaging of the I values for the 441 nodes is carried out for the whole footing and the coefficients are plotted against ratio of soil stratum thickness to footing width (the N values in (Eqn HC-1)) in Figures HC-5(a) to HC-5(e) for various values of length breadth ratios (the M values in (Eqn HC-1)) of the footing and Poisson's ratios of soil. According to (Eqn HC-1),

multiplying the coefficients in Figures HC-5(a) to HC-5(e) by $\frac{q_0}{E_s} B'$ will give the

average settlement of the footing. If the footing is a sunken one as shown in Figure HC-2, the settlement should be further multiplied by the factor I_F as calculated by (Eqn HC-2) or estimated from Figure HC-1.

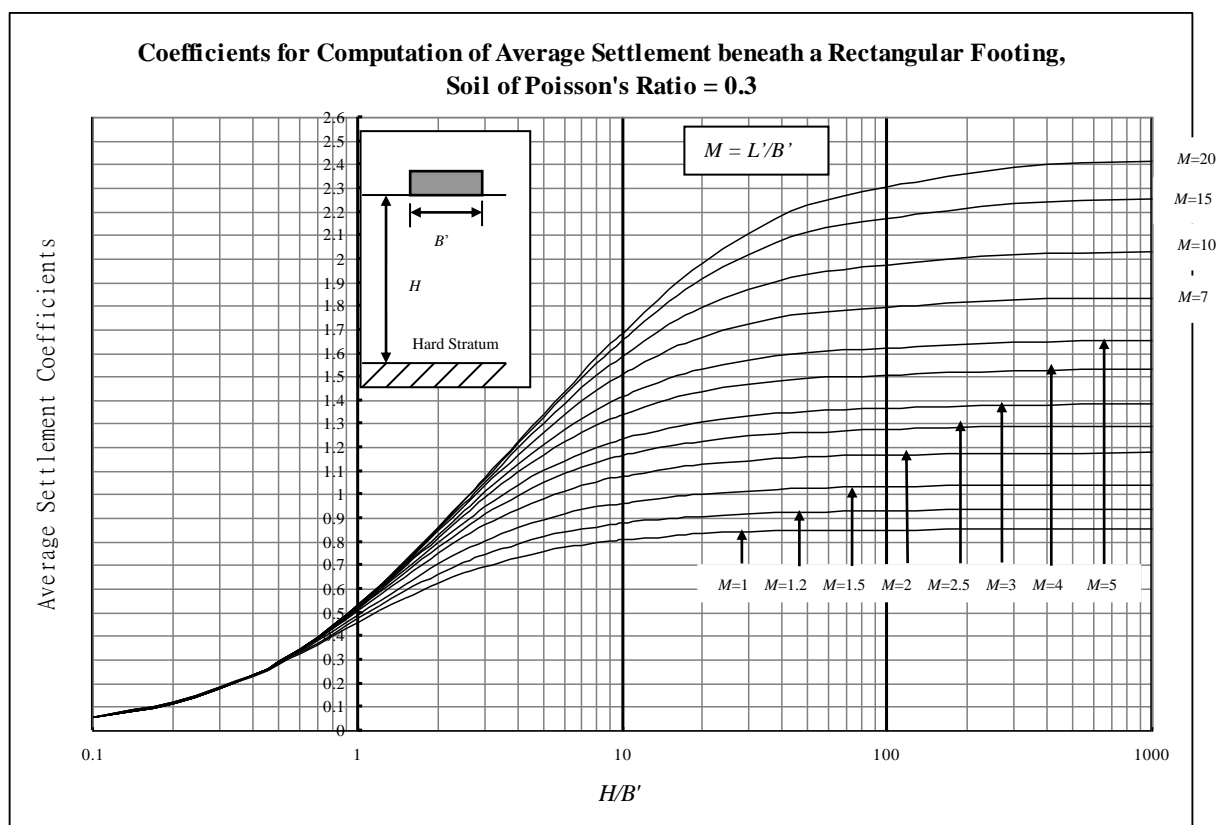


Figure HC-5(a) – Coefficients for Determination of Average Settlement of Rectangular Footing Resting on Top of an Elastic Half-space of Finite Depth to Hard Stratum, Soil of Poisson's ratio = 0.3

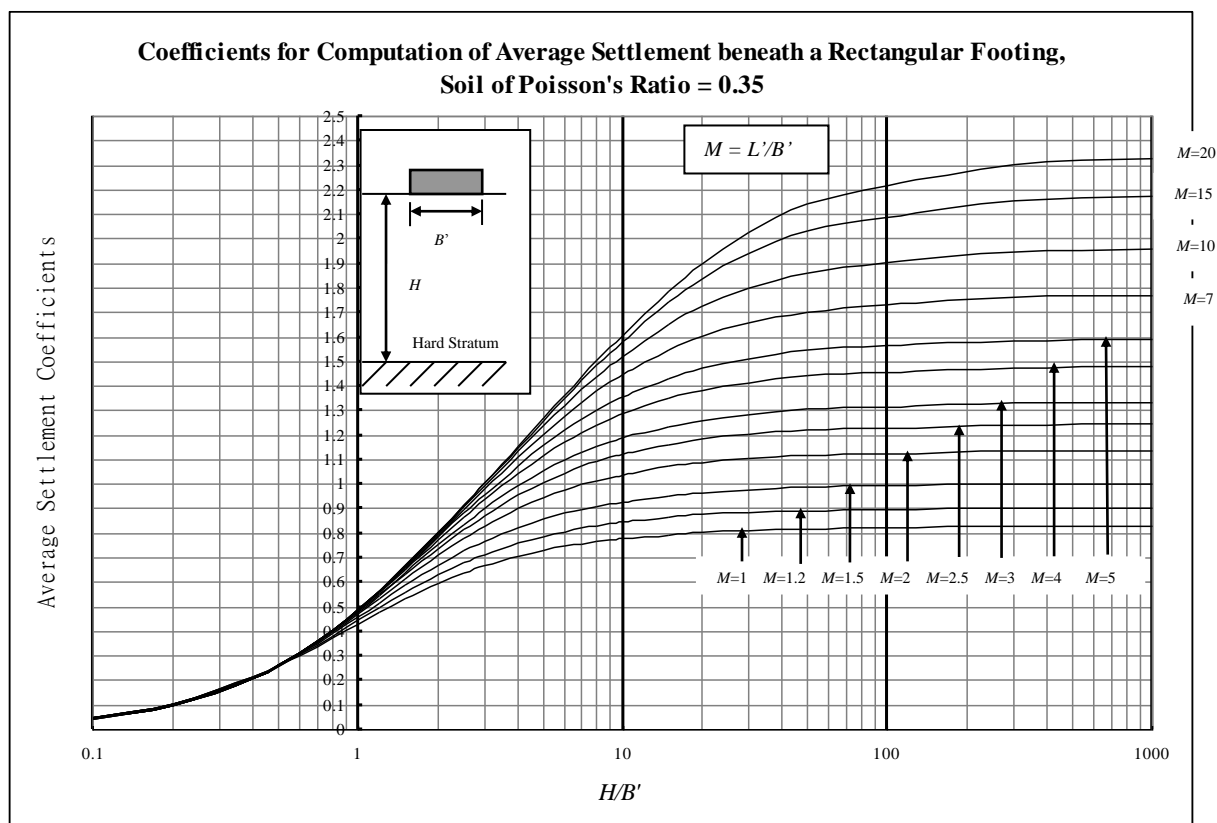


Figure HC-5(b) – Coefficients for Determination of Average Settlement of Rectangular Footing Resting on Top of an Elastic Half-space of Finite Depth to Hard Stratum, Soil of Poisson's ratio = 0.35

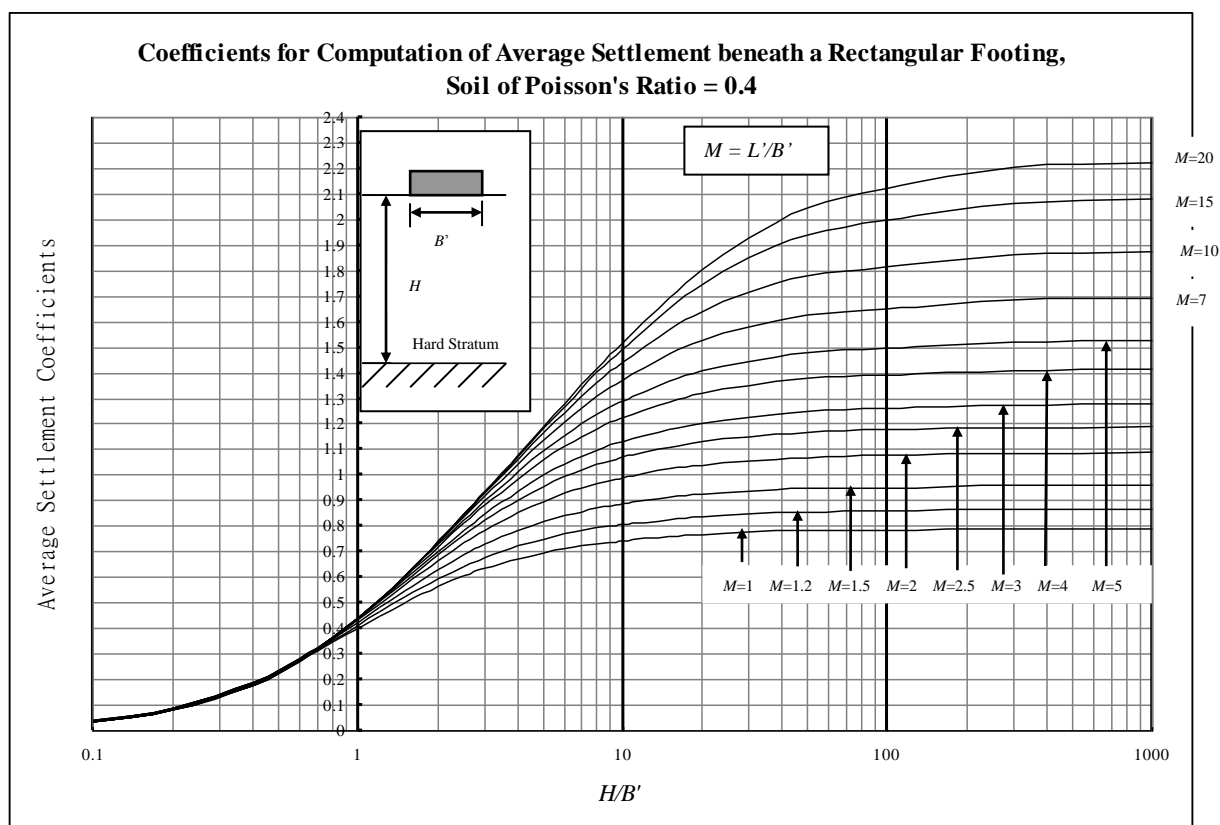


Figure HC-5(c) – Coefficients for Determination of Average Settlement of Rectangular Footing Resting on Top of an Elastic Half-space of Finite Depth to Hard Stratum, Soil of Poisson's ratio = 0.4

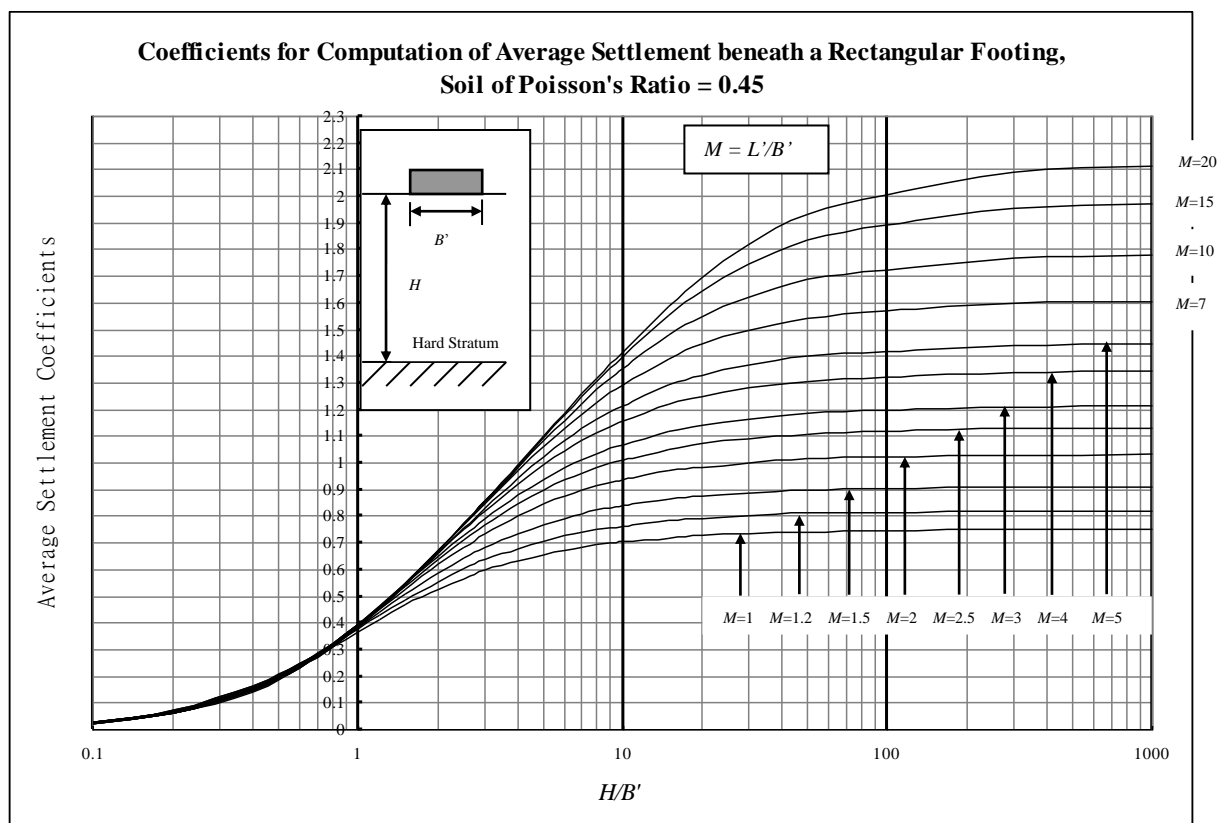


Figure HC-5(d) – Coefficients for Determination of Average Settlement of Rectangular Footing Resting on Top of an Elastic Half-space of Finite Depth to Hard Stratum, Soil of Poisson's ratio = 0.45

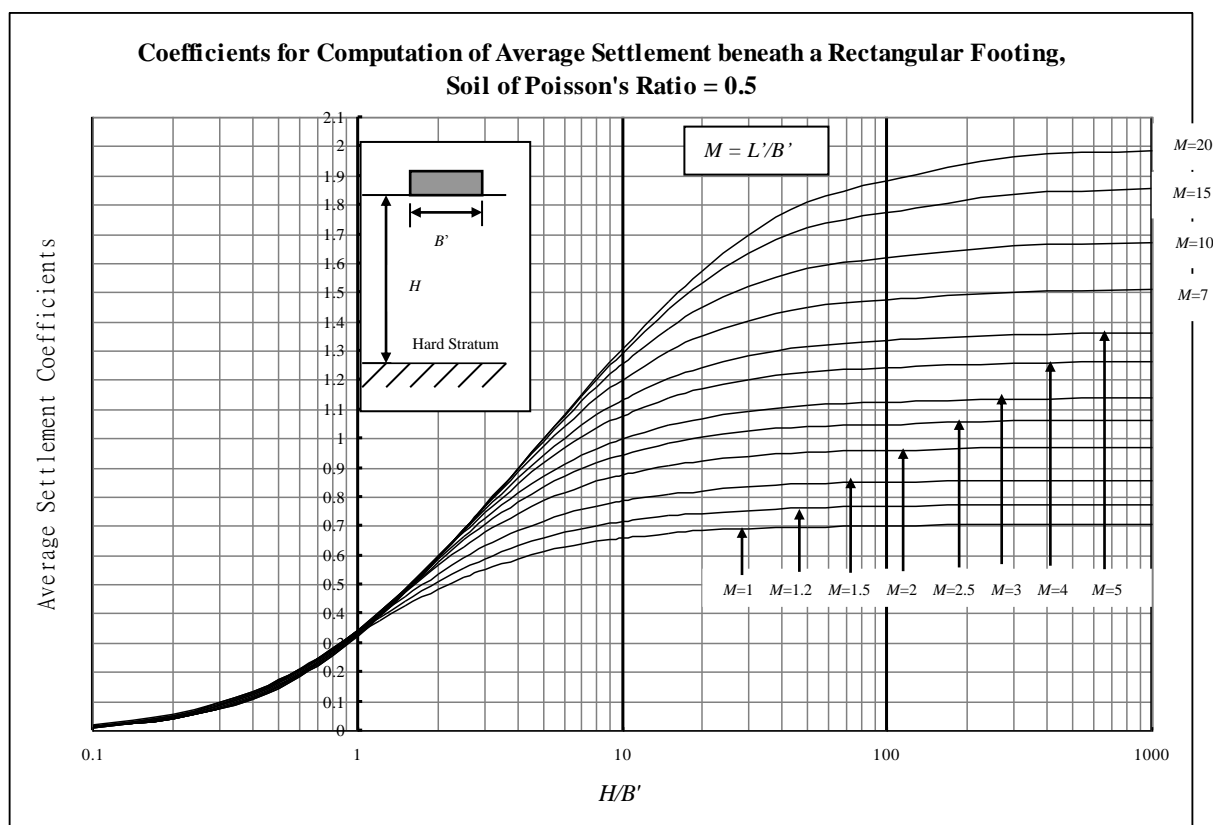


Figure HC-5(e) – Coefficients for Determination of Average Settlement of Rectangular Footing Resting on Top of an Elastic Half-space of Finite Depth to Hard Stratum, Soil of Poisson's ratio = 0.5

Figure HC-5(e) matches very well with that similarly produced by the National Research Council of Canada which has been reproduced by Azizi F. (2000) pp200 for $\nu = 0.5$.

For the Worked Example HC-1 where $M = 3/2 = 1.5$ and $N = 10/2 = 5$. With $\nu = 0.35$, the average settlement coefficient is estimated to be 0.85 by Figure HC-5(b).

So the average settlement is $I \times \frac{q_0 \times B'}{E_s} = 0.85 \times \frac{200 \times 2}{15000} = 0.0227 \text{ m}$ or 22.7mm which

is very close to the value by the more exact calculations in HC.2 of 22.9mm. The error arises from the reading of the charts.

HC.4 Sunken Footing

For footing buried below the ground surface at certain depths, the settlement can be simply multiplied by the coefficients calculated by (Eqn HC-2) or read from Figure HC-1.

HC.5 Non-rectangular Plan Shaped Footing

The approach discussed in the previous sections can be extended to estimation of the settlements of footings of non-rectangular plan shapes on a subgrade, so far as the plan shape of the footing can be divided into a number of rectangles, each carrying uniformly distributed loads. The estimation will involve estimating the settlement of

points outside rectangles by the process which can be explained in Figure HC-6. By averaging an adequate number of point settlements, the average settlement of the non-rectangular plan shaped footing can be estimated.

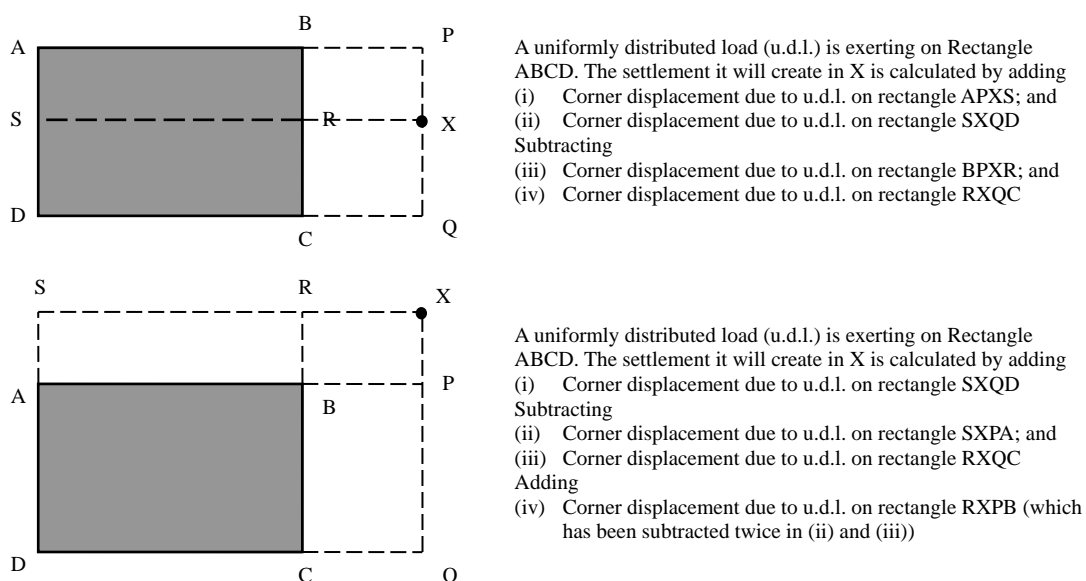


Figure HC-6 – Estimation of Settlement outside Rectangle Plan Footing carrying u.d.l.

Take an example of a footing of cruciform plan shape carrying a uniformly distributed load which can be divided into 3 nos. of rectangles ABMN, CEJL and FGHI as shown in Figure HC-7, the settlement of a point X inside the footing can be estimated in accordance with the principles illustrated in the Figure. By working out the settlements of a number of points similar to that of X and carrying out averaging, the average settlement can be calculated.

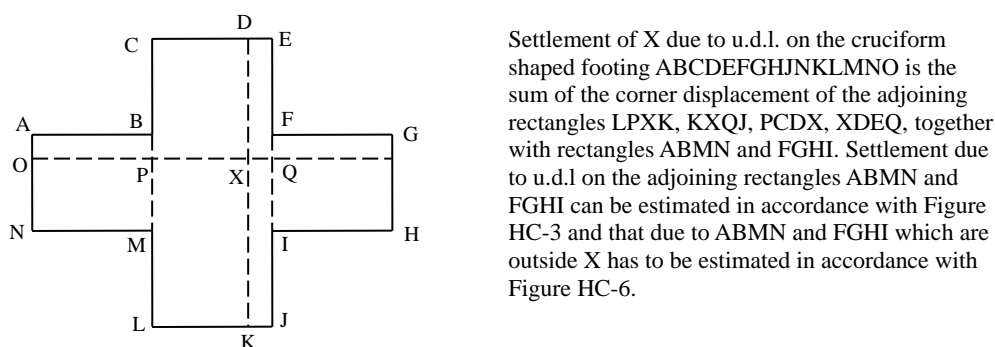
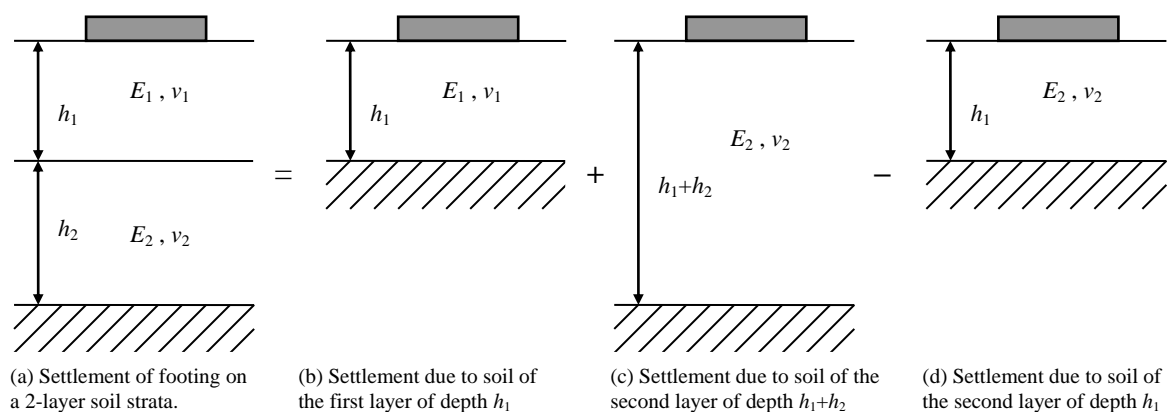


Figure HC-7 – Estimation of Settlement inside Non-rectangular Plan Shaped Footing

HC.6 Multi-Layer Subgrade

Equation (Eqn HC-1) applies to uniform subgrade of constant E_s and ν . However, for multi-layer subgrades of different properties, the settlement of the footing can be

estimated by the principle explained in Figure HC-8. Though Figure HC-8 demonstrates a 2 layers subgrade, the same principle can be extended to more than 2 layers of subgrade.



The settlement of the footing on the 2 layer subgrade will be the settlement calculated in (b) plus that in (c) minus that in (d).

Figure HC-8 – Illustration of Calculation of Footing Settlement in 2 Layered Subgrade

HC.7 Worked Example HC-2

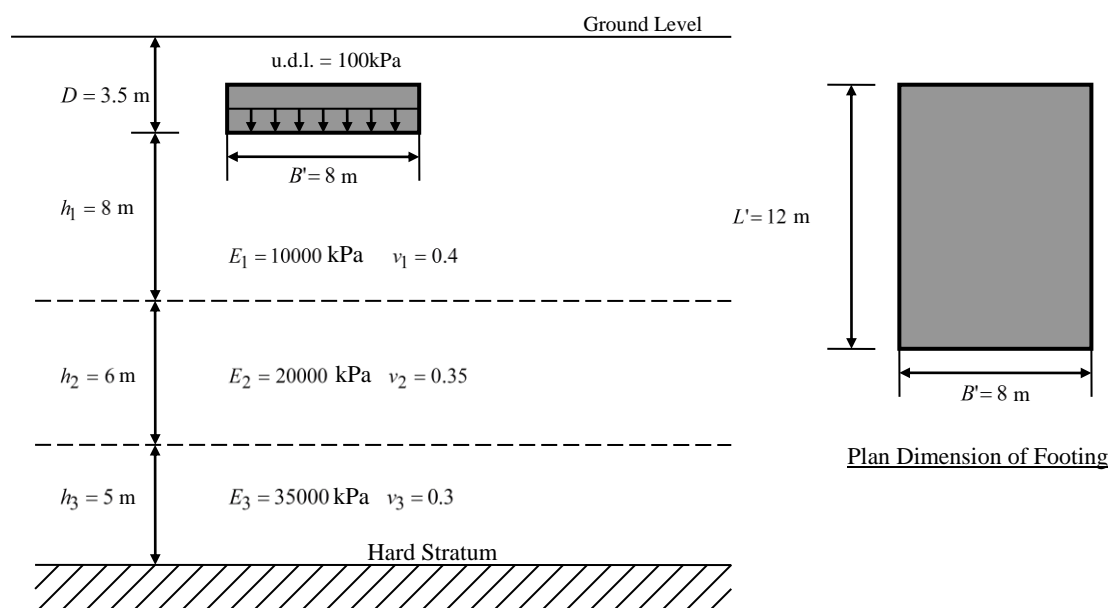


Figure HC-9 – Worked Example HC-2

To find the average settlement of a sunken Footing on a 3 layered strata as shown in Figure HC-9, the following procedures can be adopted:

- (i) Average settlement of the first layer of soil

$$M = \frac{L'}{B'} = \frac{12}{8} = 1.5; \quad N = \frac{h}{B'} = \frac{8}{8} = 1.0, \quad \nu = 0.4$$

Average settlement coefficient is 0.43 from Figure HC-5(c), so average settlement is

$$I \times \frac{q_0 B'}{E} = 0.43 \times \frac{100 \times 8}{10000} = 0.0344 \text{ m} = 34.4 \text{ mm}$$

- (ii) Average settlement of the second layer of soil

From bottom level of footing to bottom level of the second layer of soil

$$M = 1.5 \quad N = \frac{h}{B'} = \frac{8+6}{8} = 1.75, \quad \nu = 0.35$$

Average settlement coefficient is 0.63 from Figure HC-5(b), so average settlement is

$$I \times \frac{q_0 B'}{E} = 0.63 \times \frac{100 \times 8}{20000} = 0.0252 \text{ m} = 25.2 \text{ mm}$$

From bottom level of footing to top level of the second layer of soil

$$M = 1.5, \quad N = \frac{h}{B'} = \frac{8}{8} = 1.0; \quad \nu = 0.35$$

Average settlement coefficient is 0.46 from Figure HC-5(b), so average settlement is

$$I \times \frac{q_0 B'}{E} = 0.46 \times \frac{100 \times 8}{20000} = 0.0184 \text{ m} = 18.4 \text{ mm}$$

So the net average settlement of the second layer of soil is

$$25.2 - 18.4 = 6.8 \text{ mm}$$

- (iii) Average settlement of the third layer of soil

From bottom level of footing to bottom level of the third layer of soil

$$M = 1.5 \quad N = \frac{h}{B'} = \frac{8+6+5}{8} = 2.375, \quad \nu = 0.3$$

Average settlement coefficient is 0.75 from Figure HC-5(a), so average settlement is

$$I \times \frac{q_0 B'}{E} = 0.75 \times \frac{100 \times 8}{35000} = 0.0171 \text{ m} = 17.1 \text{ mm}$$

From bottom level of footing to top level of the third layer of soil

$$M = 1.5, \quad N = \frac{h}{B'} = \frac{8+6}{8} = 1.75; \quad \mu = 0.3$$

Average settlement coefficient is 0.67 from Figure HC-5(a), so average settlement is

$$I \times \frac{q_0 B'}{E} = 0.67 \times \frac{100 \times 8}{35000} = 0.0153 \text{ m} = 15.3 \text{ mm}$$

So the net average settlement of the third layer of soil is

$$17.1 - 15.3 = 1.8 \text{ mm}$$

I_F as determined from (Eqn HC-2) or estimated from Figure HC-1(b) (based on

$$\frac{D}{B'} = \frac{3.5}{8} = 0.4375) \text{ is } 0.86$$

So the total average settlement is $0.86 \times (34.4 + 6.8 + 1.8) = 36.98 \text{ mm}$.

HC.8 Support Stiffness of Footing

Sometimes it is required to input “support stiffness” in the Winkler’s spring mathematical model for the analysis of footings. The support stiffness is the pressure creating unit average settlement. The stiffness is therefore simply

$$\text{Support Stiffness} = \frac{\text{applied pressure}}{\text{average settlement}}$$

In Worked Example HC-1, the support stiffness of the footing is

$$\frac{200}{0.0229} = 8734 \text{ kN/m}^2/\text{m};$$

In Worked Example HC-2, the support stiffness of the footing is

$$\frac{100}{0.03698} = 2704 \text{ kN/m}^2/\text{m}.$$

The support stiffnesses can be used as “surface springs” to 2-dimensional mathematical models for analysis. These “surface springs” are actually “Winkler’s springs” as discussed in Section 4.2 of this Handbook.

HC.9 Footing Carrying Non-uniformly Distributed Loads

Theoretically the above approach can be extended to determine settlements of various points beneath a footing (rectangular or non-rectangular plan shapes) carrying a non-uniformly distributed load so far the load can be approximated by being divided into a number of rectangular portions each carrying different uniformly distributed loads. The settlement of any point is the summation of all such rectangles each carrying a u.d.l. The approach can be tedious. In fact, it may be simpler to use the primary forms of the Boussinesq or Mindlin Equations in which effects due to single point loads can be estimated and the footing loads be approximated as a number of point loads. However, it should be noted that the primary form of the Boussinesq or Mindlin Equations are for semi-finite subgrade. If finite depths of subgrade are encountered, it might be necessary to use the stress equations to find out the strain and then use integration to calculate the settlements of the subgrade subsequently. Alternatively, the Finite Element Method may be used. The design method and equations as given apply to the case of a flexible footing where the bending stiffness of the footing structure can be neglected. To account for the stiffness of the footing where the differential settlements will be smaller, the Finite Element Method should be used.

Appendix HD

Design of General Flexural Reinforcement in a R.C.

Plate Bending Structure

Design of General Flexural Reinforcement in a R.C. Plate Bending Structure

Rigorous analysis of a plate bending structure generally reveals a “twisting moment” at points of the structure, as in addition to bending moments in any mutually two perpendicular directions. However, design to resist a twisting moment is not as straightforward as it is for the bending moments. The existence and nature of the twisting moment are demonstrated in the rest of this appendix.

Figure HD-1 shows a small right-angled triangular element cut from a plate bending structure with its short sides parallel to the pre-determined x and y axes. The triangular element generally sustains bending moments (per unit width) M_x and M_y about the x and y axes as shown. The vectors representing the moments are also shown.

For the triangular element to be in equilibrium, the direction (vector direction) of the bending moment M_b about the hypotenuse, in general, does not align with that of the vector sum of M_x and M_y . So M_b alone cannot achieve equilibrium for the triangular element and another moment M_t , whose direction being perpendicular to the hypotenuse must exist to perform the function. However, this M_t (the direction of which is shown in Figure HD-1 taken from Lam and Law (2009)) is actually “twisting” the section, creating “complementary shear stress” (in contrast to pure flexural tensile and compressive stresses) which are in-plane shear flows on the structure as shown on the right half of the Figure.

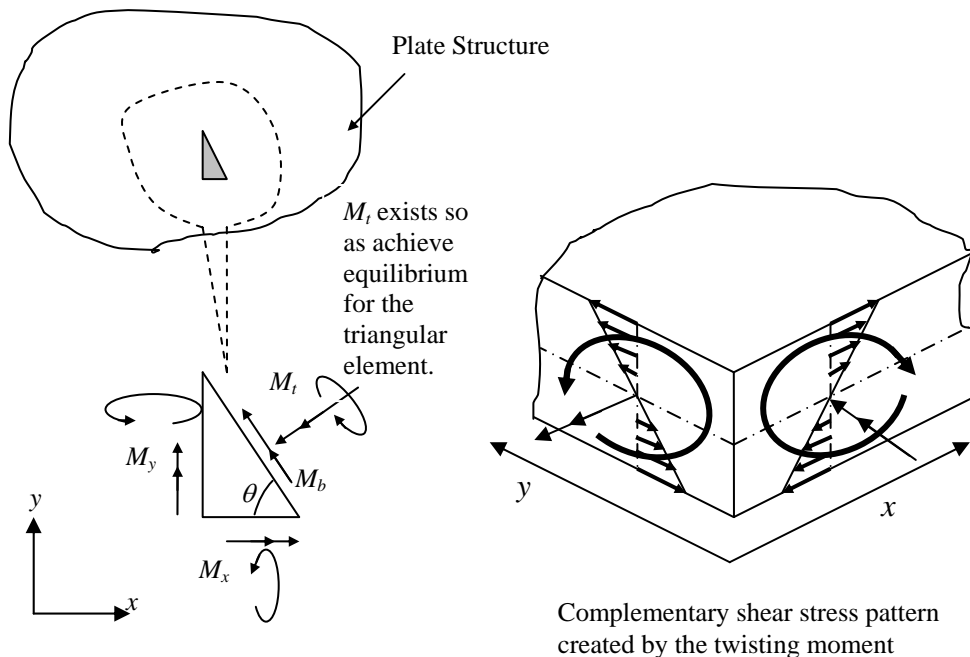


Figure HD-1 – Derivation and Nature of the “Twisting Moment”

As the hypotenuse can be in any orientation, it follows that a twisting moment exists, in general at any orientations, including the global X and Y directions. So at any point in a plate bending

structure, there exists a set of moments comprising two bending moments at mutually perpendicular directions and a twisting moment as summarized in Figure HD-2. In Figure HD-2, M_x , M_y and M_{xy} (the twisting moment) form a complete set of “moments” at a point with respect to the orientation θ .

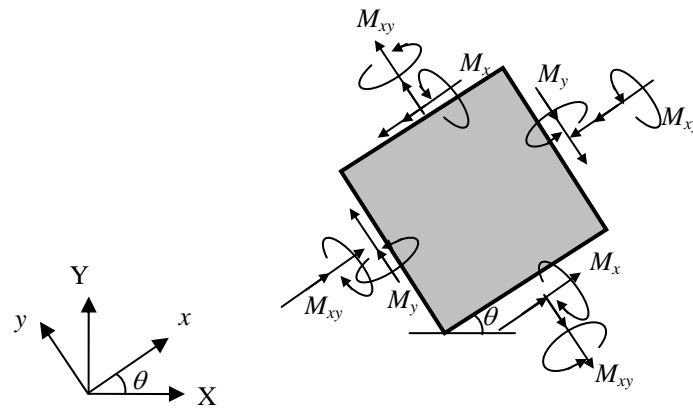


Figure HD-2 – General Moments at a Point in a Plate Bending Structure

It should be noted that the three moments change magnitudes as θ varies. At the orientation where $M_{xy} = 0$, the moments M_x , M_y become the “principal moments” and the orientation becomes the “principal directions”. The phenomenon is entirely analogous to the in-plane stress problem such that the variation of moments with orientation can be represented on a “Mohr Circle” as shown in Figure HD-3. In Figure HD-3, the moments M_x , M_y and M_{xy} at a point in the structure exist at an orientation θ to one principal direction and when $\theta = 0$, the bending moments at the point will become M_1 and M_2 (principal moments) and the twisting moment is zero.

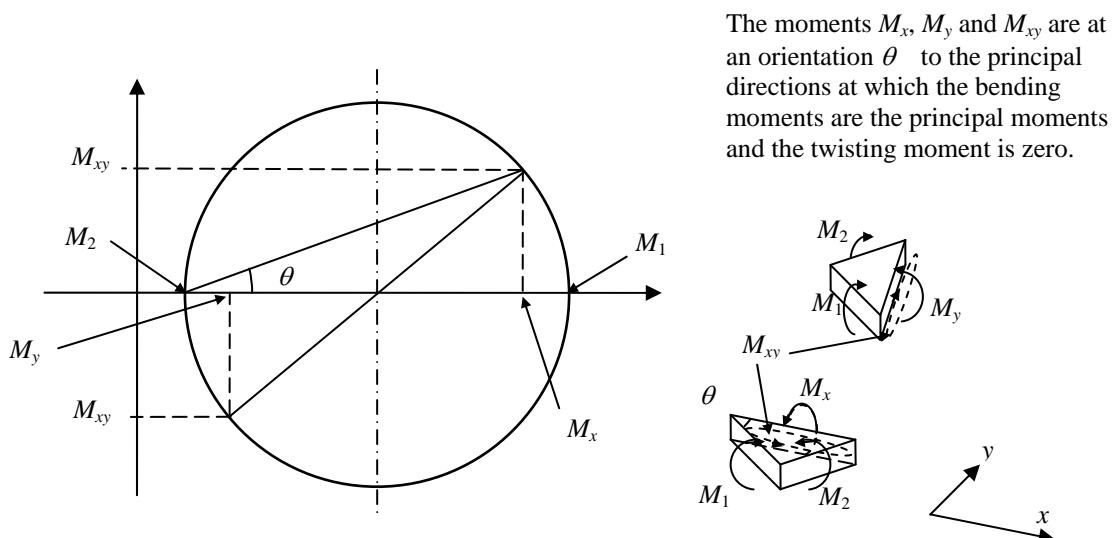


Figure HD-3 – Bending and Twisting Moment as Represented by the Mohr Circle

Theoretically it is sufficient to design the structure to resist the principal moments in the principal directions. However, in practice it is impossible to do so for reinforced concrete slabs as the principal directions change from point to point and from load case to load case. So if it is the intention that the reinforcing bars are in pre-determined directions where the twisting moments are in general not zero, it is necessary to cater for the twisting moments. The Wood Armer Equations by Wood (1968) for the reinforced concrete design of plate structures are to work out the “design moments” M_x^* and M_y^* in selected directions so that they incorporate effects due to M_x , M_y and M_{xy} . The underlying principle of the Wood-Armer Equations is that structural design based on M_x^* and M_y^* can resist bending moments in any directions while leaving the twisting moments to be resisted by the concrete. This is known as the “Normal Yield Criterion” which can be mathematically expressed as follows :

$$M_x^* \cos^2 \theta + M_y^* \sin^2 \theta \geq M_x \cos^2 \theta + M_y \sin^2 \theta + 2M_{xy} \cos \theta \sin \theta \quad (\text{Eqn HD-1})$$

The left hand side of the above inequality represents the flexural strengths of the plate structure in the direction θ upon the provision of flexural strengths of M_x^* and M_y^* in the x and y directions as derived by the Johansen’s Criterion (1962) whilst the right side represents the ‘normal moment’ which is the bending moment in the direction θ .

The Wood Armer Equations from Wood (1968) are reproduced as follows, with the convention that sagging moments are positive and hogging moment are negative:

For sagging moment:

$$\text{Generally} \quad M_x^* = M_x + |M_{xy}|; \quad M_y^* = M_y + |M_{xy}| \quad (\text{Eqn HD-2})$$

If either M_x^* or M_y^* is found to be negative, then such a value is changed to zero as follows :

$$\text{Either } M_x^* = M_x + \frac{|M_{xy}|^2}{M_y} \text{ with } M_y^* = 0 \text{ or } M_y^* = M_y + \frac{|M_{xy}|^2}{M_x} \text{ with } M_x^* = 0 \quad (\text{Eqn HD-2a})$$

If, in these changed formulae, the wrong algebraic sign results for M_x^* or M_y^* , then no such reinforcement is required. If both M_x^* and M_y^* are negative, no bottom reinforcement is required.

Similarly for hogging moment:

$$\text{Generally} \quad M_x^* = M_x - |M_{xy}|; \quad M_y^* = M_y - |M_{xy}| \quad (\text{Eqn HD-3})$$

If either M_x^* or M_y^* is found to be positive, then such a value is changed to zero as follows :

$$\text{Either } M_x^* = M_x - \frac{|M_{xy}|^2}{M_y} \text{ with } M_y^* = 0 \text{ or } M_y^* = M_y - \frac{|M_{xy}|^2}{M_x} \text{ with } M_x^* = 0 \quad (\text{Eqn HD-3a})$$

If, in these changed formulae, the wrong algebraic sign results for M_x^* or M_y^* , then no such

reinforcement is required. If both M_x^* and M_y^* are positive, no top reinforcement is required.

The following 2 examples demonstrate the use of the Wood-Armer Equations and their fulfillment of the “normal yield criterion”.

Worked Example HD-1 – (bending moments of equal sign)

$$M_x = 7; M_y = 23; M_{xy} = 9$$

For sagging :

$$M_x^* = M_x + |M_{xy}| = 7 + 9 = 16 > 0, \text{ so } M_x^* = 16;$$

$$M_y^* = M_y + |M_{xy}| = 23 + 9 = 32 > 0, \text{ so } M_y^* = 32;$$

For hogging :

$$M_x^* = M_x - |M_{xy}| = 7 - 9 = -2 < 0, \text{ so } M_x^* = -2;$$

$$M_y^* = M_y - |M_{xy}| = 23 - 9 = 14 > 0, \text{ so } M_y^* = 0, \quad M_x^* = M_x - \left| \frac{M_{xy}^2}{M_y} \right| = 7 - \left| \frac{9^2}{23} \right| = 3.478 > 0$$

(wrong algebraic sign, $M_x^* = 0$)

So for sagging : $M_x^* = 16;$ $M_y^* = 32;$

for hogging : $M_x^* = 0;$ $M_y^* = 0$

A plot of the strengths provided by M_x^* and M_y^* (sagging only) as determined by the left side of (Eqn HD-1) and the normal bending moments based on $M_x = 7; M_y = 23; M_{xy} = 9$ as determined by the right hand side of (Eqn HD-1) have been done for orientations from 0° to 360° and presented in Figure HD-4. It can be seen that the moment capacity curve (only sagging) envelops the normal bending moment for all orientations.

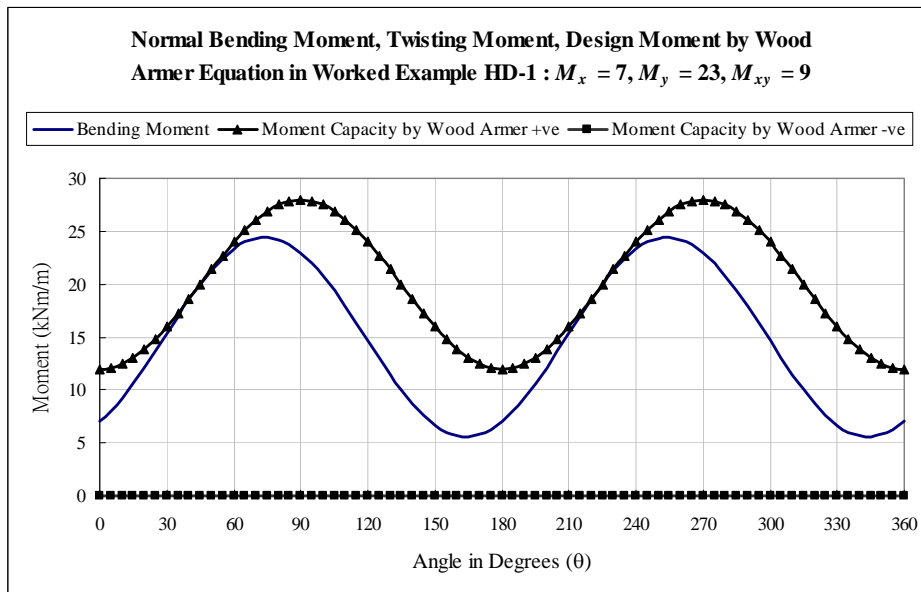


Figure HD-4 – Plots of Normal Moments and Strengths by Wood Armer Equation for Worked Example HD-1

Worked Example HD-2 – (bending moments of different signs)

$$M_x = 7; M_y = -23; M_{xy} = 9$$

For sagging :

$$M_x^* = M_x + |M_{xy}| = 7 + 9 = 16 > 0, \text{ so } M_x^* = 16;$$

$$M_y^* = M_y + |M_{xy}| = -23 + 9 = -14 < 0, \text{ so } M_y^* = 0 \text{ and } M_x^* = M_x + \left| \frac{M_{xy}^2}{M_y} \right| = 7 + \left| \frac{9^2}{-23} \right| = 10.522$$

For hogging :

$$M_x^* = M_x - |M_{xy}| = 7 - 9 = -2 < 0, \text{ so } M_x^* = -2;$$

$$M_y^* = M_y - |M_{xy}| = -23 - 9 = -32 < 0,$$

$$\text{So for sagging } M_x^* = 10.522; \quad M_y^* = 0$$

$$\text{for hogging } M_x^* = -2 \quad M_y^* = -32$$

Plots of the strengths provided by M_x^* and M_y^* (for both sagging and hogging) as determined by the left hand side of (Eqn HD-1) and the normal moments worked out by $M_x = 7$; $M_y = -23$; $M_{xy} = 9$ as determined by the right hand side of (Eqn HD-1) for orientations from 0° to 360° are presented in Figure HD-5. It can be seen that the moment capacity curves (sagging and hogging) envelop the normal bending moment for all orientations.

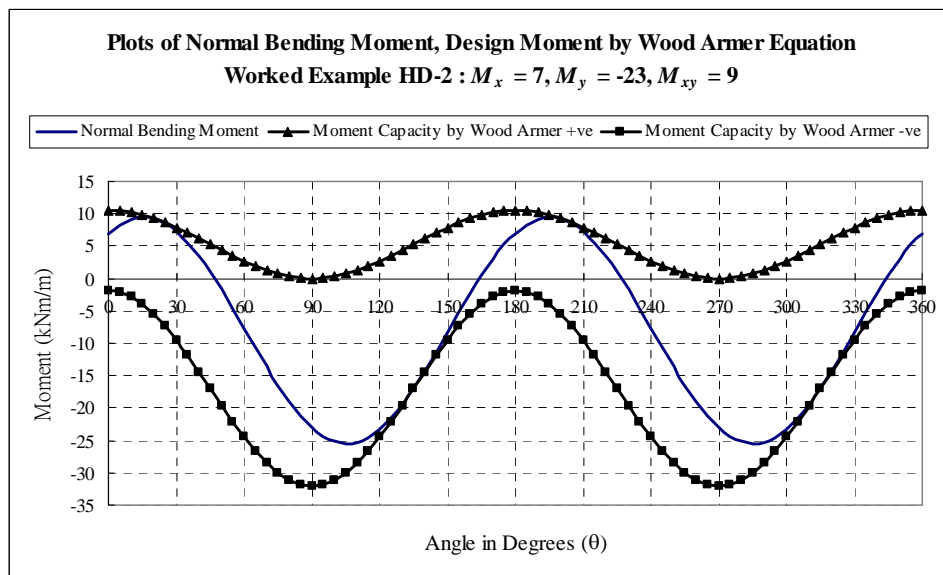


Figure HD-5 – Plots of Normal Moments and Strengths by Wood Armer Equation for Worked Example HD-2

Appendix HE

A Worked Example on Determination of the Group Reduction Factor (Geotechnical Capacity) of Pile Group in Cohesionless Soil

A Worked Example on Determination of the Group Reduction Factor (Geotechnical Capacity) of a Pile Group in Cohesionless Soil

Worked Example HE-1

Consider a pile group of 30 nos. S450 305×305×223kg/m driven piles capped by a pile cap and arranged as shown in Figure HE-1. The pile group with the soil mass embedded among the piles is “idealized” as a sunken footing at the average pile tip level which is 24m below ground.

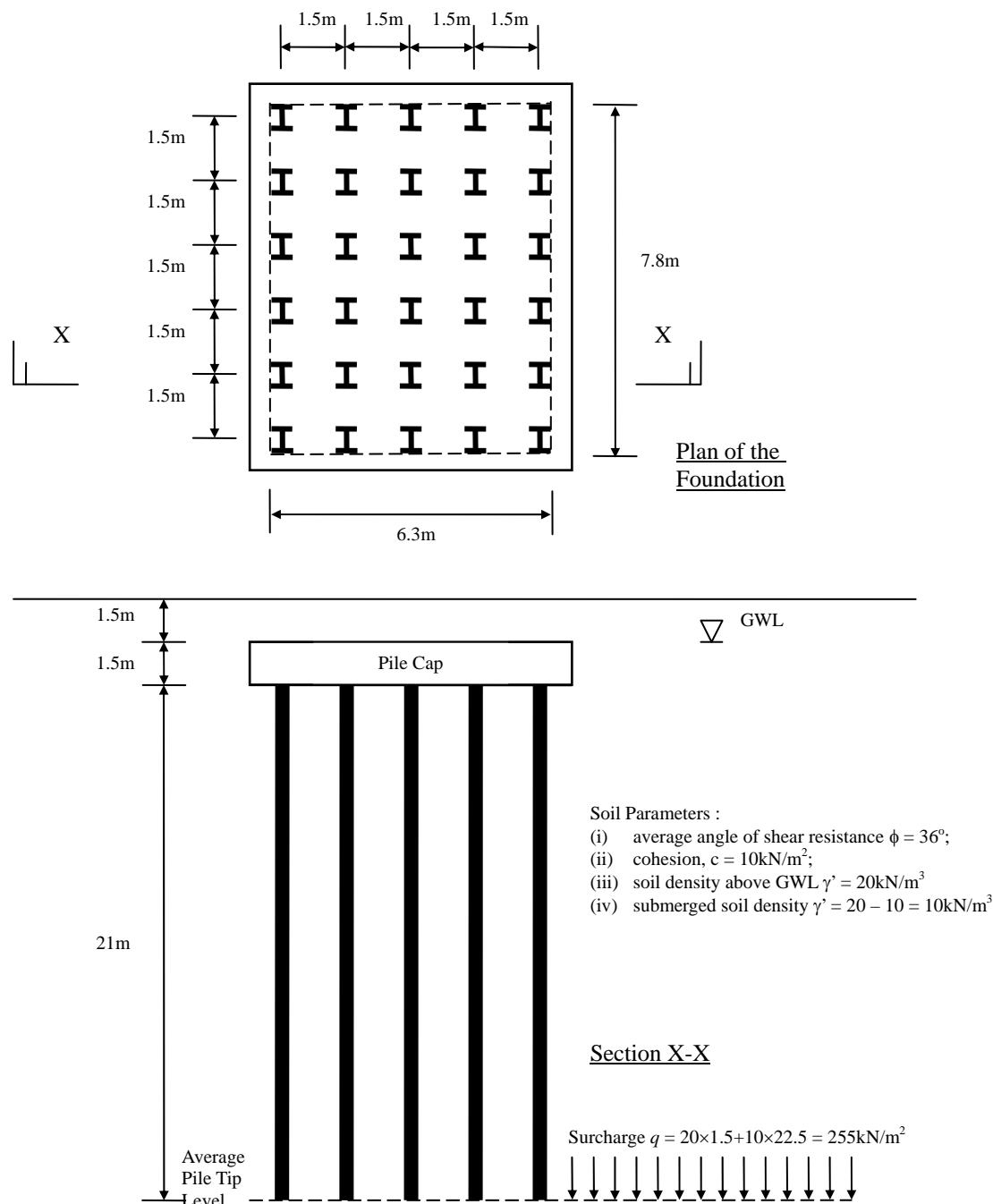


Figure HE-1 – Worked Example HE-1 for Pile Group Reduction Factor

The ultimate bearing capacity of the “idealized footing” is determined by the equation

$$q_u = cN_c\zeta_{cs} + 0.5B_f\gamma_s N_\gamma\zeta_{\gamma s} + qN_q\zeta_{qs} \quad (\text{Eqn HE-1})$$

where c is the cohesion of the soil, B_f is the effective width of the idealized footing, γ_s is the effective density of the soil, q is the surcharge on the area adjacent to the footing, the N factors are the bearing capacity factors and the ζ factors are those same factors which relate to the plan length to breadth ratio of the “idealized footing”. The equations for determination of the ζ factors can be found in clause 2.2.4 of the Code and GEOGUIDE 1 (2000) Figure A1.

The following parameters are listed as :

Soil Parameters

$\phi = 36^\circ$; $c = 10 \text{ kN/m}^2$; $\gamma' = 20 \text{ kN/m}^3$ above GWL; $\gamma' = 20 - 10 = 10 \text{ kN/m}^3$ below GWL

Effective width and Lengths of the “Idealized Footing”

$B_f = 6.3 \text{ m}$; $L_f = 7.8 \text{ m}$

Bearing Capacity Factors

$$N_q = e^{\pi \tan \phi} \tan^2 \left(\frac{\phi}{2} + 45^\circ \right) = 37.752; \quad N_c = (N_q - 1) \cot \phi = 50.585;$$

$$N_\gamma = 2(N_q + 1) \tan \phi = 56.311$$

Shape Factors

$$\zeta_{cs} = 1 + \frac{B_f}{L_f} \frac{N_q}{N_c} = 1.603; \quad \zeta_{\gamma s} = 1 - 0.4 \frac{B_f}{L_f} = 0.677; \quad \zeta_{qs} = 1 + \frac{B_f}{L_f} \tan \phi = 1.587$$

So the ultimate bearing capacity is

$$q_u = cN_c\zeta_{cs} + 0.5B_f\gamma_s N_\gamma\zeta_{\gamma s} + qN_q\zeta_{qs} = 810.88 + 1200.86 + 15277.67 = 17289.41 \text{ kN/m}^2,$$

but capped at 15MPa as per GEO 1/2006 clause 6.4.4.4. (It can readily be seen that the most significant component is $qN_q\zeta_{qs}$ which is due to the overburden soil.)

Taking a factor of safety = 3, the allowable bearing capacity is

$$q_{allowable} = \frac{q_u}{3} = \frac{15000}{3} = 5000 \text{ kN/m}^2.$$

The allowable load of the pile group based on the “idealized footing” is

$$q_{allowable} \times B_f \times L_f = 245700 \text{ kN}.$$

Comparing with the load carrying capacity calculated as the summation of the individual load carrying capacity of each pile, which is at most $30 \times 3663.6 = 109908 \text{ kN}$, the ratio is

$$\frac{245700}{109908} = 2.24 > 1.0$$

So the pile group reduction factor can remain as unity which is governed by the “structural capacity” of the pile group.

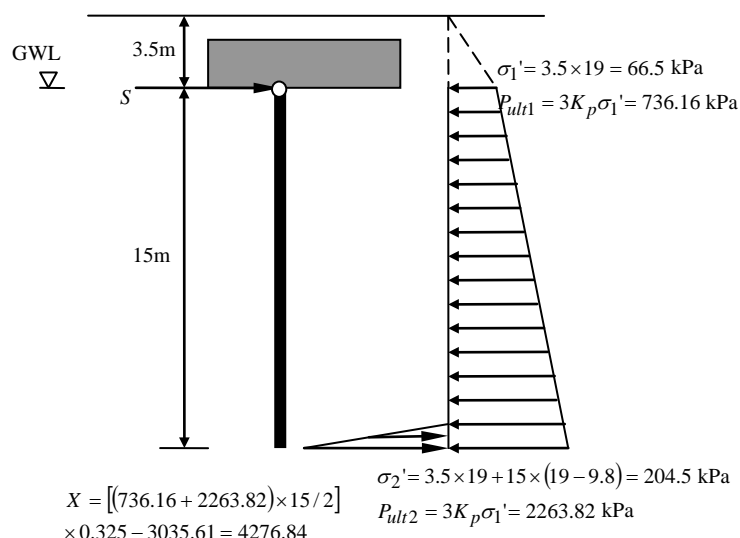
Appendix HF

Worked Examples for Determination of Ultimate Lateral Shear Resistances of Piles

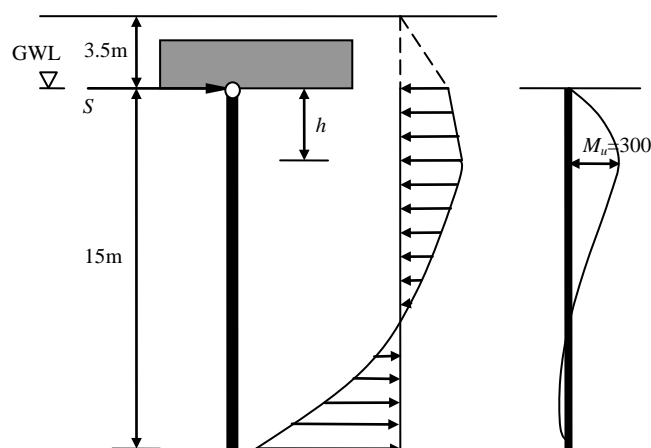
Worked Examples for Determination of Ultimate Lateral Shear Resistances of Piles

Worked Example HF-1

A 305×305×180kg/m S450 floating pile is embedded in cohesionless soil of $\phi' = 35^\circ$ as shown with pinned connection at the Pile Cap, with flexural capacity of 300kNm under the ultimate axial load. The ultimate shear resistance of the pile due to soil is to be determined.



- (i) Preliminary Check by Considering the Pile to be a "Short Pile", i.e. no reverse of Bending along the Pile Shaft



- (ii) Revised Check by Allowing the Pile to have Reversed Moments along the Pile Shaft and Limiting to Flexural Strength of the Pile, i.e. the Pile becomes a "Long Pile"

$$\text{Passive Pressure Coeff. } K_p = \frac{1 + \sin 35^\circ}{1 - \sin 35^\circ} = 3.69$$

Width of the Pile is $D = 0.325\text{m}$

The ultimate soil lateral resistance according to Broms (1964b) is $3K_p \sigma'$.

For rotational equilibrium of the pile, there must be a reversed direction of soil pressure at the pile tip. Assuming the reversed soil load is at a single pile tip level and taking moment about the tip level of the pile,

$$S \times 15 = [736.19 \times 15 \times 7.5 + 0.5 \times (2263.92 - 736.19) \times 15 \times (15/3)] \times 0.325$$

$$\Rightarrow S = 3035.74 \text{ kN.}$$

Let the level of zero shear be at h below the cap.

$$\left[736.19h + \frac{(2263.92 - 736.19)h}{15} \times \frac{h}{2} \right] \times 0.325 - 3035.61 = 0$$

$$\Rightarrow h = 8.123 \text{ m}$$

The maximum moment of the pile at the level 8.123m below the pile cap is

$$(736.19 \times 8.123^2 / 2 + 1527.73 \times 8.123^3 / 15 / 6) \times 0.325 - 3035.74 \times 8.123 = 13808 \text{ kNm} > 300 \text{ kNm}$$

As the flexural capacity is only 300kNm, the level of maximum moment (zero shear) has to be raised and h re-calculated as in (ii). At depth h , the ultimate lateral soil pressure is

$$736.19 + \frac{(2263.92 - 736.19)h}{15}$$

$$= 736.19 + 101.849h$$

The lateral shear provided by soil from top level of pile to the new depth h is

$$[736.19 + 101.849h + 736.19] \div 2 \times h \times 0.325$$

$$= 16.550423h^2 + 239.26155h$$

As zero shear exists in this level, the lateral soil shear balances the applied shear S

$$S = 16.55042h^2 + 239.2615h \quad (a)$$

Listing the moment equation as follows and limiting it to 300kNm

$$S \times h - \left(736.19 \times \frac{h^2}{2} + 101.849h \times \frac{h}{2} \times \frac{h}{3} \right) \times 0.325$$

$$= 300 \quad (b)$$

Solving equations (a) and (b) (involving solution of cubic equation), $h = 1.485 \text{ m}$ and

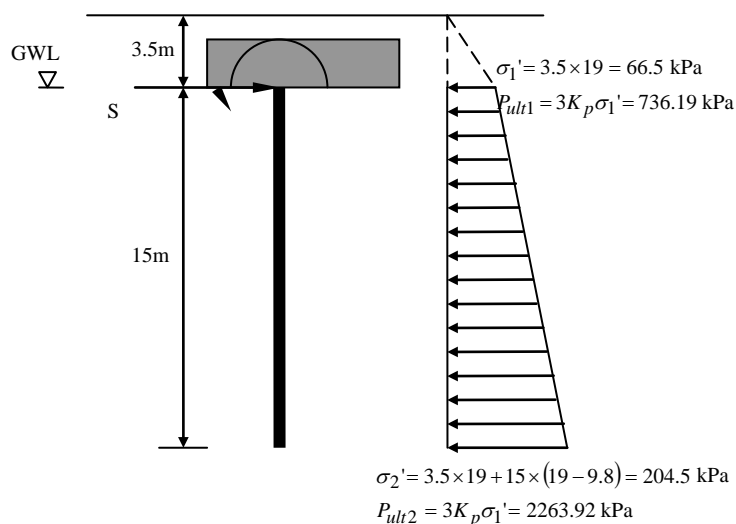
$$S = 16.55042h^2 + 239.2615h = 391.84 \text{ kN}$$

So the ultimate shear capacity required is 391.84kN

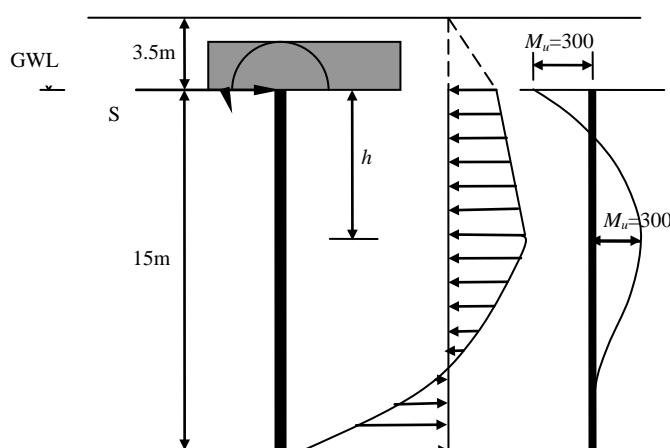
Figure HF-1 – Worked Example HF-1 for Determination of Ultimate Lateral Shear Resistances of Piles Pinned at Pile Cap

Worked Example HF-2

The pile in Worked Example HF-1 is now rigidly connected to the pile cap and its ultimate shear resistance of the pile due to soil is to be re-worked.



- (i) Preliminary Check by Considering the Pile to be a “Short Pile”,
i.e. no reverse of Bending along the Pile Shaft



- (ii) Revised Check by Allowing the Pile to have Reversed Moments
along the Pile Shaft and Limiting to Flexural Strength of the Pile,
i.e. the Pile becomes a “Long Pile”

Passive Pressure Coeff.

$$K_p = \frac{1 + \sin 35^\circ}{1 - \sin 35^\circ} = 3.69$$

Width of the Pile is $D = 0.325\text{m}$

The ultimate soil lateral resistance according to Broms (1964b) is $3K_p \sigma'$.

Assuming “short pile” by which the full ultimate lateral soil resistance is mobilized, to achieve equilibrium, the total shear and moment at top level of pile are respectively

$$S = (736.19 + 2263.92) / 2 \times 15 \times 0.325 = 7312.77 \text{ kN}$$

$$M = [736.19 \times 15 \times 7.5 + 1527.73 \times 15 / 2 \times 10] \times 0.325 = 64155.38 \text{ kNm} > 300 \text{ kNm}$$

As the flexural capacity is only 300kNm, the level of zero moment has to be raised to h below pile cap. This is based on the assumption that the maximum moment of 300kNm occurs at some depths of the pile, as equal to that at top level but in reversed direction and at this level, the shear is zero. At depth h , the ultimate lateral soil pressure is

$$736.19 + \frac{(2263.92 - 736.19)h}{15}$$

$$= 736.19 + 101.849h$$

The lateral shear provided by soil from top level of pile to the new depth h is

$$[736.19 + 101.849h + 736.19] \div 2 \times h \times 0.325$$

$$= 16.55042h^2 + 239.2615h$$

As zero shear exists at this level, the lateral shear by soil should balance the applied shear at cut-off level of the pile. So we can list

$$S = 16.55042h^2 + 239.2615h \quad (c)$$

Listing the moment equation as follows and limiting it to 300kNm at the zero shear location

$$S \times h - \left(736.19 \times \frac{h^2}{2} + 101.849h \times \frac{h}{2} \times \frac{h}{3} \right) \times 0.325 - 300 = 300 \quad (d)$$

Solving equations (c) and (d) (involving solution of cubic equation), $h = 2.053 \text{ m}$ and

$$S = 16.5504h^2 + 239.2615h = 561.11 \text{ kN}$$

So the ultimate shear capacity is 561.11kN

Figure HF-2 – Worked Example HF-2 for Determination of Ultimate Lateral Shear Resistances of Piles Rigidly Connected at Pile Cap

Appendix HG

Checking of Piles against Uplift, Overturning and Buoyancy of a Hypothetical Pile Group

Checking of Piles against Uplift, Overturning and Buoyancy of a Hypothetical Pile Group

Worked Example HG-1

The pile group comprises 26 nos. of 305×305×223 Grade S450J0 H-piles. No piles have adverse live load (i.e. uplift due to live load). The R_u values are derived from cohesion ($c = 20$ kPa as the ultimate value being twice the allowable value of 10kPa) on the pile shaft.

Pile No.	D_{min} (kN)	TL (DL+LL) (kN)	Wind Axial Load			Critical Load Combination		Uplift Checking						
			Wind X (kN)	Wind Y (kN)	W_{max} (kN)	TL (kN)	TL + W_{max} (kN)	Uphrust U_a (kN)	D_{min} - W_{max} + U_a (kN)	R_a (kN)	R_u (kN)	$D_{min}-W_{max}$ + $U+R_a$ (kN)	$D_{min}-1.5W_{max}$ + U_a (kN)	$D_{min}+0.9R_u-1.5(U_a+W_{max})$ (kN)
P1	1566	2211	-483	-987	987	2211	3198	-70	509	633	1227	1142	16	1085
P2	1450	2030	-83	-1033	1033	2030	3063	-69	348	633	1227	981	-169	901
P3	1438	2007	338	-1148	1148	2007	3155	-66	224	633	1227	857	-350	721
P4	1581	2217	982	-1407	1407	2217	3624	-58	116	633	1227	749	-588	488
P5	1671	2366	-808	-870	870	2366	3236	-70	731	633	1227	1364	296	1365
P6	1732	2458	-1154	-743	1154	2458	3612	-68	510	633	1227	1143	-67	1003
P7	1462	2036	986	-1131	1131	2036	3167	-58	273	633	1227	906	-293	783
P8	1641	2308	-1238	-513	1238	2308	3546	-68	335	633	1227	968	-284	786
P9	1389	1923	1029	-863	1029	1923	2952	-57	303	633	1227	936	-212	864
P10	1584	2207	-1365	-211	1365	2207	3572	-65	154	633	1227	787	-529	543
P11	1370	1890	1144	-455	1144	1890	3034	-53	173	633	1227	806	-399	679
P12	1429	1968	342	-62	342	1968	2310	-58	1029	633	1227	1662	858	1933
P13	1513	2096	-1469	143	1469	2096	3565	-60	-16	633	1227	617	-751	324
P14	1501	2068	-65	213	213	2068	2281	-58	1230	633	1227	1863	1124	2199
P15	1412	1951	1312	113	1312	1951	3263	-46	54	633	1227	687	-602	479
P16	1454	2008	878	399	878	2008	2886	-47	529	633	1227	1162	90	1171
P17	1473	2036	-1547	465	1547	2036	3583	-55	-129	633	1227	504	-903	174
P18	1518	2096	422	656	656	2096	2752	-49	813	633	1227	1446	485	1565
P19	1483	2054	1465	654	1465	2054	3519	-40	-22	633	1227	611	-755	330
P20	1530	2111	-1240	710	1240	2111	3351	-53	237	633	1227	870	-383	695
P21	1592	2199	-40	884	884	2199	3083	-50	658	633	1227	1291	216	1295
P22	1536	2127	985	934	985	2127	3112	-42	509	633	1227	1142	17	1100
P23	1451	2002	-1600	821	1600	2002	3602	-50	-199	633	1227	434	-999	80
P24	1596	2204	-893	995	995	2204	3199	-50	551	633	1227	1184	54	1133
P25	1603	2219	488	1177	1177	2219	3396	-43	383	633	1227	1016	-206	877
P26	1579	2194	1616	1258	1616	2194	3810	-35	-72	633	1227	561	-880	207

Table HG-1 – Example of Checking of Piles against Uplift, Overturning and Buoyancy of a Hypothetical Pile Group

Notes :

- As the values in the last column are all greater than zero, cl. 5.1.6 of the Code is fulfilled;
- The load factor for uplift U can be 1.1 instead of 1.5 if the ground water level is taken as the ground level in the determination of U ;
- A further check on the ultimate resistance R_u involving effective weight of soil mass/rock cone in accordance with cl. 5.3.3(b) should be required if the pile is in tension.

Appendix HH

Equivalent Raft Method

Equivalent Raft Method

HH.1 Principles of the Approach

The approach is for estimation of settlement of piled foundations in compressible soil as discussed by Tomlinson (2008). In principle, it assumes that the piled foundation behaves as a raft foundation with its founding level at $2/3$ of the average pile length below ground. Determination of the size of the equivalent raft is under the assumption of load spread of 1 in 4 above the assumed equivalent raft level and 30° below as shown in Figure HH-1 which is extracted from Tomlinson (2008). With the soil beneath treated as elastic materials, the settlement due to loads from the foundation can be estimated.

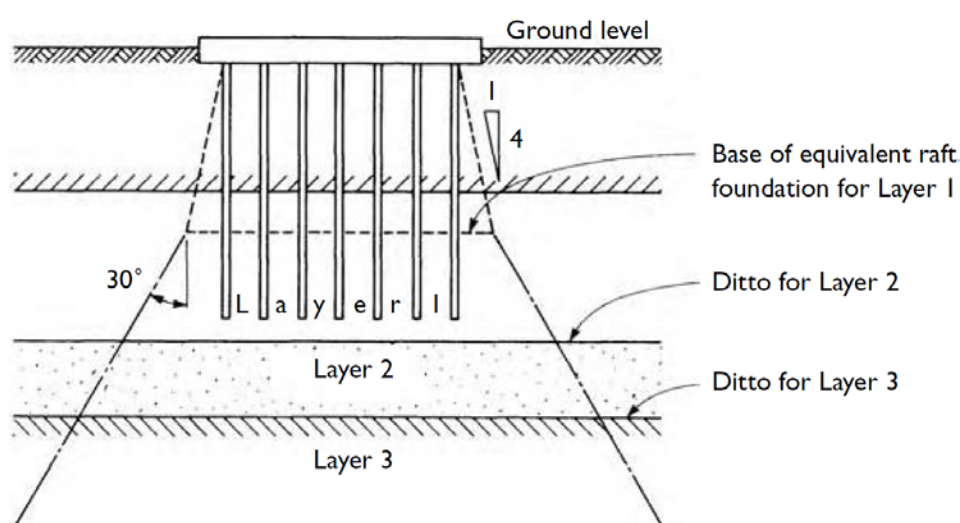


Figure 5.21 Load distribution beneath pile group in layered soil formation.

Figure HH-1 – Extract from Tomlinson (2008) Demonstrating the Principles of the Equivalent Raft Method

HH.2 Worked Example HH-1

Worked Example HH-1 illustrated by Figure HH-2 is used to demonstrate the equivalent raft method. In addition to the data given in the figure, the followings are added :

- (i) the plan dimensions of the pile group is $30\text{m} \times 40\text{m}$;
- (ii) E stands for the Young's Moduli of the soils;
- (iii) ν stands for their Poisson's ratios
- (iv) The load acting on the pile group is 100000 kN ;
- (v) The piles are $305 \times 305 \times 223$ H-piles, each with cross sectional area 0.0284m^2
- (vi) Total number of piles is 374.

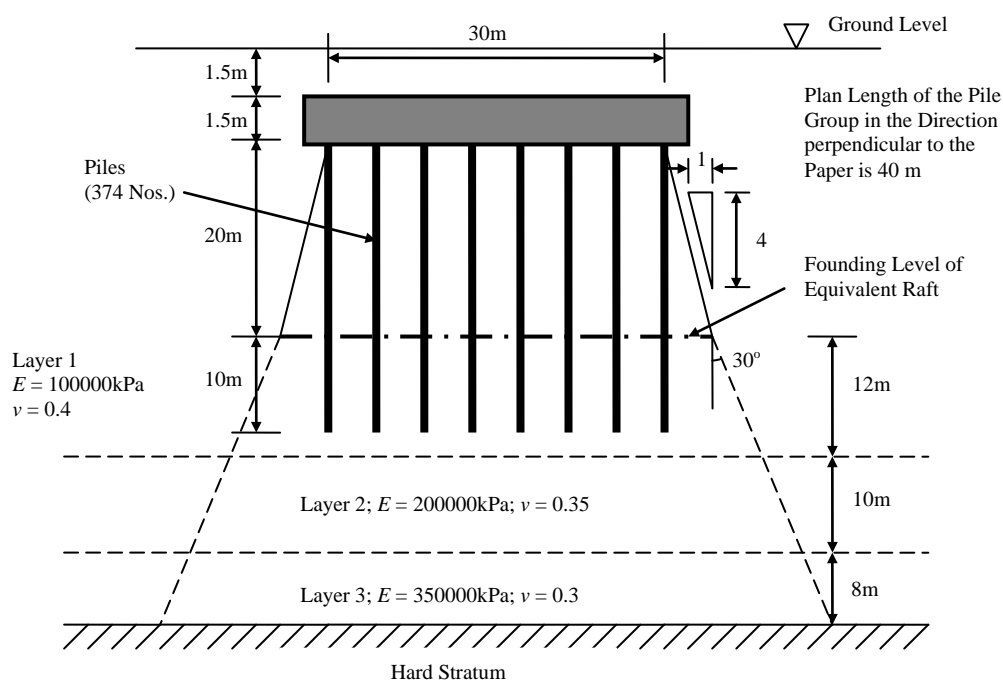


Figure HH-2 – Worked Example HH-1

The plan dimensions of the “Equivalent Raft” are worked out as

$$B_1 = 30 + 20/4 \times 2 = 40 \text{ m and } L_1 = 40 + 20/4 \times 2 = 50 \text{ m;}$$

The plan dimensions at the base level of Layer 1 are

$$B_2 = 40 + 12 \tan 30^\circ \times 2 = 53.856 \text{ m and } L_2 = 50 + 12 \tan 30^\circ \times 2 = 63.856 \text{ m;}$$

Similarly, the plan dimensions at base levels of Layer 2 and Layer 3 are

$$B_3 = 40 + 22 \tan 30^\circ \times 2 = 65.403 \text{ m and } L_3 = 50 + 22 \tan 30^\circ \times 2 = 75.403 \text{ m;}$$

$$B_4 = 40 + 30 \tan 30^\circ \times 2 = 74.641 \text{ m and } L_4 = 50 + 30 \tan 30^\circ \times 2 = 84.641 \text{ m.}$$

The average plan width and length of Layer 1 are $(40 + 53.856)/2 = 46.928 \text{ m}$ and $(50 + 63.856)/2 = 56.928 \text{ m}$ giving a plan area of $46.928 \times 56.928 = 2671.52 \text{ m}^2$.

Under the applied load of 100000 kN, treating the soil layer as an elastic material of height 12m with the load evenly exerted on the top of the layer, the settlement of Layer 1 is

$$\frac{PL}{AE} = \frac{100000 \times 12}{2671.52 \times 100000} = 0.00449.$$

Settlement of other layers are similarly worked out and summarized in Table HH-1.

Table HH-1 – Summary for Calculation for Worked Example HH-1

Layer	Average Width (m)	Average Length (m)	Average Plan Area (m ²)	Depth (m)	Young's Modulus of Soil (kN/m ²)	Settlement (mm)
1	46.928	56.928	2671.52	12	100000	4.49
2	59.630	69.630	4152.04	10	200000	1.20
3	70.022	80.022	5603.30	8	350000	0.41
					Sum	6.10

So the total settlement is 6.10mm.

Alternatively, a more accurate estimation is that by the approach outlined in Appendix HC as presented in Table HH-2. In the table, D' which is the depth of the “sunken footing” being simulated by the pile group is 23m and the applied pressure at the sunken footing level is $q_0 = 100000/40/50 = 50 \text{ kN/m}^2$. $B' = 40 \text{ m}$; $L' = 50 \text{ m}$; $D'/B' = 0.575$.

Table HH-2 – Calculation for Worked Example HH-2 by the Approach in Appendix HC (the I and I_F coefficients are read from Figures HC-1 and HC-5 of Appendix HC). $M = 50/40 = 1.25$. In the last column, the settlement is calculated by $(q_0 B'/E_s)I \times I_F$. The items with * are subtractive items.

Step	Description	E (MPa)	ν	M	H' (m)	N	D'/B'	I	I_F	Settlement (mm)
1	Due to 1 st layer,	100	0.4	1.25	12	0.3	0.575	0.139	0.806	2.241
2	Due to 1 st + 2 nd layers	200	0.35	1.25	22	0.55	0.575	0.285	0.785	2.234
3	Due to 1 st layer *	200	0.35	1.25	12	0.3	0.575	0.16	0.785	-1.254
4	Due to 1 st + 2 nd + 3 rd layers	350	0.3	1.25	30	0.75	0.575	0.395	0.765	2.725
5	Due to 1 st + 2 nd layers *	350	0.3	1.25	22	0.55	0.575	0.309	0.765	-1.352
										Sum
										4.594

The settlement determined is 4.594 mm which is significantly less than that by Tomlinson of 6.10 mm. This may be due to the assumption of 30° load spread in soil being too conservative by Tomlinson's approach. Another factor to account for the difference is due to the lack of consideration of the Poisson's effect of the soil which also helps reduce settlement.

Nevertheless, the above only caters for the settlement of the soil, additional settlement should also be allowed for the elastic shortening of the piles. Conservative estimation can be made through the elastic shortening (AE/L) approach which assumes the greatest shortening by ignoring skin friction along the pile shaft. As the cross sectional area of each of the pile is 0.0284m², conservatively ignoring the skin friction on the piles and assuming each pile have each share of the load from the pile cap, the elastic shortening of the piles are estimated as

$$\frac{PL}{AE} = \frac{100000 \times 30}{374 \times 0.0284 \times 205 \times 10^6} = 0.00138 \text{ m} = 1.38 \text{ mm}$$

This elastic shortening of the pile may be added to the settlement due to the compression of the soil.

Appendix HI

Buckling of Slender Piles – Embedded, Partially Exposed or Sleeved in Soil

Buckling of Slender Piles – Embedded, Partially Exposed or Sleeved in Soil

HI.1 Theoretical Background – based on Solution of the Basic Differential Equation by the Finite Difference Method

Assuming a pile as shown in Figure HI-1 is embedded in soil idealized as an elastic medium, buckling of the pile is based on the fundamental differential equation

$$E_p I_p \frac{d^4 v}{dz^4} + P \frac{d^2 v}{dz^2} + K_h v = 0 \quad (\text{Eqn HI-1})$$

where v is the lateral displacement of the pile at depth z

$E_p I_p$ is the flexural rigidity of the pile at depth z

P is the axial load of the pile at depth z

K_h is the elastic spring stiffness per unit length of the pile at depth z

The finite difference model for the analysis of (Eqn HI-1) is shown in Figure HI-2.

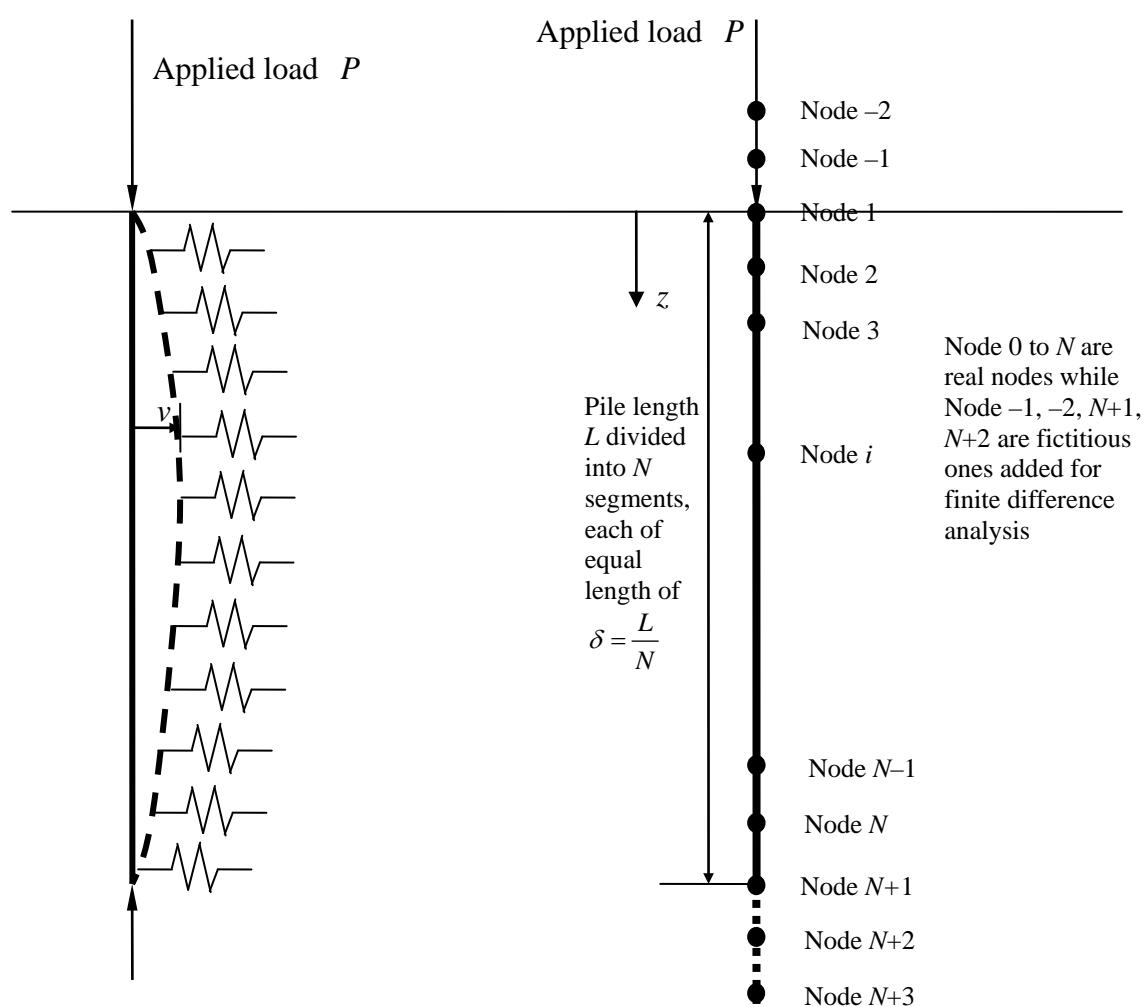


Figure HI-1 – Illustration of the Buckling Phenomenon of Pile in Elastic Soil

Figure HI-2 – The Finite Difference Model for the Simulation of a Pile

For cohesionless soil, the assessment of K_h can be based on Terzaghi (1955) on cohesionless soil which assumes lateral restraint by soil on the pile as follows :

$$K_h = k_h B \quad (\text{Eqn HI-2})$$

$$k_h = n_h \frac{z}{B} \quad (\text{Eqn HI-3})$$

where k_h is the “coefficient of horizontal subgrade reaction” of the soil defined as the pressure required to move the soil by unit length; and

z is the depth of the soil below ground;

B is the width of surface of contact of the pile and the soil which can be taken as the pile diameter;

n_h is the “constant of horizontal subgrade reaction” of the soil given in Table 5.1 of the Code which can be regarded as constant for a layer of soil.

It is obvious that

$$K_h = B \times k_h = B \times n_h \frac{z}{B} = n_h z \quad (\text{Eqn HI-4})$$

So (Eqn HI-1) can be written as

$$E_p I_p \frac{d^4 v}{dz^4} + P \frac{d^2 v}{dz^2} + n_h z v = 0 \quad (\text{Eqn HI-5})$$

Analytical solution for (Eqn HI-5) is difficult, taking into account the many different boundary conditions including end support conditions of piles, portions of pile length being sleeved or exposed. Nevertheless, they can be solved by a numerical method such as the finite difference method for the model shown in Figure HI-2.

HI.2 Solution by the Finite Difference Method

By the Finite Difference Method, the pile of length L is divided into N segments of equal length (each of segment length L/N with $N+1$ no. of “real nodes” and 4 “fictitious” nodes as shown in Figure HI-2. (Eqn HI-5) for the i^{th} node (z coordinate $= iL/N$) can be written as

$$\begin{aligned} E_p I_p \left[\frac{v_{i+2} - 4v_{i+1} + 6v_i - 4v_{i-1} + v_{i-2}}{(L/N)^4} \right] + P \left[\frac{v_{i+1} - 2v_i + v_{i-1}}{(L/N)^2} \right] + n_h \frac{i}{N} L v_i &= 0 \\ \Rightarrow (v_{i-1} - 2v_i + v_{i+1}) &= -\frac{E_p I_p N^2}{PL^2} \left[v_{i-2} - 4v_{i-1} + \left(6 + \frac{n_h L^5}{E_p I_p N^5} \right) v_i - 4v_{i+1} + v_{i+2} \right] \end{aligned} \quad (\text{Eqn HI-6})$$

By putting $T = \sqrt[5]{E_p I_p / n_h}$, (Eqn HI-6) becomes

$$\Rightarrow (v_{i-1} - 2v_i + v_{i+1}) = -\frac{E_p I_p N^2}{PL^2} \left[v_{i-2} - 4v_{i-1} + \left[6 + \left(\frac{L}{T} \right)^5 \frac{i}{N^5} \right] v_i - 4v_{i+1} + v_{i+2} \right] \quad (\text{Eqn HI-7})$$

Accuracy of the solution increases with increasing value of N . $N+1$ equations can be formulated by (Eqn HI-7) for the $N+1$ “real nodes” in the pile. However, to form equations at Nodes 1, 2, N and $N+1$, 4 additional fictitious nodes have to be added

which are numbered $-2, -1, N+2, N+3$ as shown in Figure HI-2. Thus 4 more equations are required which have to be derived from restraints at pile top and pile tip for solution of the problem. They are summarized in Table HI-1.

	Conditions	Pile Top	Pile Tip
Restraint from lateral movement	$v = 0$	$v_1 = 0$	$v_{N+1} = 0$
Restraint from Rotation	$\theta = \frac{dv}{dz} = 0$	$\frac{v_2 - v_{-1}}{2(L/N)} = 0$	$\frac{v_{N+2} - v_N}{2(L/N)} = 0$
Hinged Connections (moment = 0)	$M = E_p I_p \frac{d^2 v}{dz^2} = 0$	$E_p I_p \frac{v_2 - 2v_1 + v_{-1}}{(L/N)^2} = 0$	$E_p I_p \frac{v_{N+2} - 2v_{N+1} + v_N}{(L/N)^2} = 0$
Free end (Shear of pile to balance component of axial load)	$S = E_p I_p \frac{d^3 v}{dz^3};$ $E_p I_p \frac{d^3 v}{dz^3} + P \frac{dv}{dz} = 0$	$E_p I_p \frac{v_3 - 2v_2 + 2v_{-1} - v_{-2}}{2(L/N)^3}$ $+ P \frac{v_2 - v_{-1}}{2(L/N)} = 0$	$E_p I_p \frac{v_{N+3} - 2v_{N+2} + 2v_N - v_{N-1}}{2(L/N)^3}$ $+ P \frac{v_{N+2} - v_N}{2(L/N)} = 0$

Table HI-1 – Restraint Conditions on Lateral Load Analysis on Pile by the Finite Difference Method

With the boundary conditions at the pile ends added, (Eqn HI-7) can be written in a matrix form $[A][v] = -\frac{E_p I_p}{PL^2} N^2 [B][v]$ where $[A]$ and $[B]$ can be readily formulated and the expression can be written as

$$[B]^{-1}[A][v] = -\frac{E_p I_p}{PL^2} N^2 [v] \Rightarrow [C][v] = -\frac{E_p I_p}{PL^2} N^2 [v] \quad (\text{Eqn HI-8})$$

where $[C] = [B]^{-1}[A]$

(Eqn HI-8) is an eigen-value problem. The eigen-values $\lambda = -\frac{E_p I_p}{PL^2} N^2$ can be solved

$$\text{and } P = -\frac{E_p I_p N^2}{\lambda L^2} \quad (\text{Eqn HI-9})$$

(Eqn HI-9) gives the buckling loads and the eigen-vectors giving the relative values of v are the buckling mode shapes. Theoretically, there will be $N+1$ valid modes or buckling loads. The smallest load will be the fundamental buckling load or Euler load.

To find an equivalent length $R_{Leq}L$ as if the pile is a simple strut pinned at both ends and

free from restraints along its pile shaft, we may list $P = \frac{\pi^2 E_p I_p}{(R_{Leq}L)^2} = -\frac{E_p I_p N^2}{\lambda L^2}$, which

gives the equivalent length ratio as

$$R_{Leq} = \pi \sqrt{-\lambda} / N \quad (\text{Eqn HI-10})$$

By the above, Tables HI-2(a) to HI-2(f) which were extracted from Law (2013) with extension to $L/T = 40$ showing the equivalent length ratios against the L/T ratios for

end bearing piles are presented (where P is constant along the pile shaft) with different exposed length and sleeved length factors. Intermediate values can be interpolated. The exposed and sleeved length factors are the ratios of the lengths of the top part of the pile exposed above ground and sleeved below ground respectively as shown in Figure HI-3 (extracted from Law (2013)) to the total length of the pile. (Eqn HI-8) can easily be modified to account for the effects of these length factors. In addition, it can also be noted that the equivalent length ratios are almost independent of the pile tip support conditions at high L/T ratios, indicating that the pile tip support conditions become unimportant when the pile is long or the soil resistance is high.

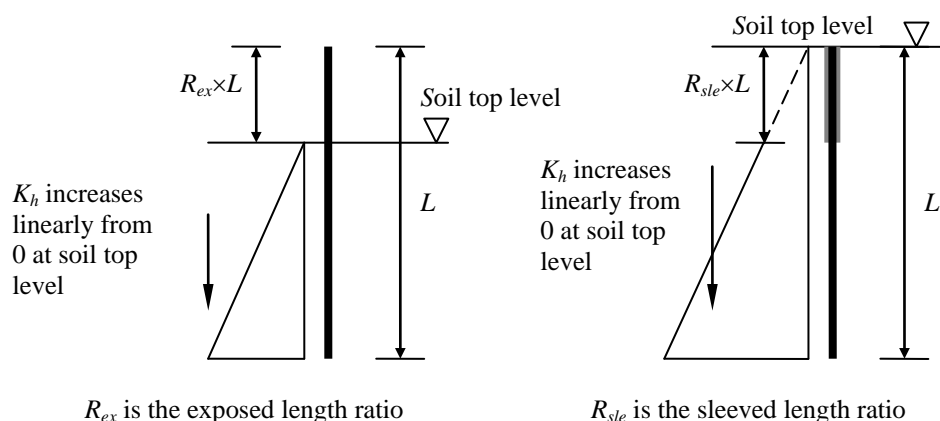


Figure HI-3 – Illustration of Exposed Length and Sleeved Length Factors

L/T Ratio	Top Pinned / Bottom Free					Top fixed / Bottom Free					Top Free / Bottom Free				
	Exposed Length Factor (R_{ex})					Exposed Length Factor (R_{ex})					Exposed Length Factor (R_{ex})				
	0	0.1	0.2	0.3	0.4	0	0.1	0.2	0.3	0.4	0	0.1	0.2	0.3	0.4
0	–	–	–	–	–	2.000	2.000	2.000	2.000	2.000	–	–	–	–	–
1	6.293	6.757	7.341	8.098	9.118	1.942	1.949	1.955	1.962	1.969	18.854	23.227	29.459	38.474	52.362
2	1.234	1.291	1.370	1.482	1.645	1.225	1.266	1.313	1.369	1.436	3.362	4.154	5.255	6.852	9.307
3	0.869	0.896	0.925	0.956	0.984	0.787	0.804	0.823	0.846	0.873	1.330	1.637	2.046	2.626	3.509
4	0.606	0.642	0.690	0.752	0.824	0.588	0.610	0.636	0.666	0.701	0.922	1.107	1.318	1.586	1.980
5	0.439	0.454	0.480	0.542	0.632	0.438	0.454	0.476	0.507	0.554	0.737	0.924	1.116	1.314	1.541
6	0.349	0.367	0.400	0.449	0.513	0.346	0.358	0.372	0.389	0.420	0.612	0.800	0.995	1.191	1.390
7	0.283	0.304	0.353	0.411	0.473	0.283	0.293	0.305	0.324	0.351	0.525	0.713	0.908	1.106	1.304
8	0.240	0.271	0.322	0.382	0.447	0.239	0.246	0.255	0.281	0.326	0.459	0.648	0.843	1.041	1.241
9	0.210	0.246	0.299	0.361	0.426	0.205	0.211	0.224	0.262	0.308	0.408	0.597	0.794	0.992	1.191
10	0.189	0.226	0.281	0.344	0.410	0.179	0.184	0.208	0.249	0.295	0.368	0.557	0.754	0.952	1.152
12	0.157	0.197	0.255	0.320	0.387	0.142	0.151	0.186	0.230	0.278	0.307	0.497	0.694	0.893	1.093
14	0.135	0.176	0.237	0.303	0.371	0.117	0.134	0.172	0.218	0.266	0.263	0.454	0.652	0.851	1.051
16	0.118	0.161	0.223	0.291	0.359	0.099	0.121	0.162	0.208	0.257	0.230	0.422	0.621	0.820	1.020
18	0.105	0.150	0.213	0.281	0.350	0.088	0.111	0.154	0.201	0.250	0.205	0.398	0.596	0.796	0.996
20	0.095	0.141	0.205	0.274	0.343	0.079	0.104	0.148	0.196	0.245	0.185	0.378	0.577	0.776	0.976
22	0.086	0.133	0.199	0.268	0.337	0.072	0.098	0.143	0.192	0.241	0.168	0.362	0.561	0.760	0.960
24	0.079	0.128	0.194	0.263	0.332	0.066	0.093	0.139	0.188	0.238	0.154	0.348	0.547	0.747	0.947
26	0.073	0.123	0.188	0.259	0.326	0.061	0.090	0.136	0.185	0.235	0.142	0.337	0.536	0.736	0.936
28	0.068	0.119	0.186	0.255	0.325	0.056	0.086	0.133	0.183	0.232	0.132	0.327	0.527	0.727	0.926
30	0.063	0.115	0.183	0.252	0.322	0.053	0.084	0.131	0.180	0.230	0.124	0.319	0.518	0.718	0.918
32	0.059	0.112	0.18	0.249	0.319	0.049	0.081	0.129	0.178	0.228	0.116	0.312	0.511	0.711	0.911
34	0.056	0.11	0.178	0.247	0.317	0.047	0.079	0.127	0.177	0.227	0.110	0.305	0.505	0.705	0.905
36	0.053	0.107	0.176	0.245	0.315	0.044	0.077	0.126	0.175	0.225	0.104	0.300	0.499	0.699	0.899
38	0.050	0.105	0.174	0.243	0.313	0.042	0.076	0.124	0.174	0.224	0.098	0.295	0.494	0.694	0.894
40	0.047	0.103	0.172	0.242	0.311	0.040	0.075	0.123	0.173	0.223	0.094	0.290	0.490	0.690	0.890

Table HI-2(a) – Table showing Variation of “Equivalent Length Factor” with L/T ratio and Pile Exposed Length Factor for End-bearing Piles with Bottom Free

L/T Ratio	Top Pinned / Bottom Pinned					Top fixed / Bottom Pinned					Top Free / Bottom Pinned				
	Exposed Length Factor (R_{ex})					Exposed Length Factor (R_{ex})					Exposed Length Factor (R_{ex})				
	0	0.1	0.2	0.3	0.4	0	0.1	0.2	0.3	0.4	0	0.1	0.2	0.3	0.4
0	1.000	1.000	1.000	1.000	1.000	0.699	0.699	0.699	0.699	0.699	–	–	–	–	–
1	0.997	0.998	0.998	0.999	0.999	0.698	0.699	0.699	0.699	0.699	10.906	13.461	17.030	22.236	30.256
2	0.927	0.940	0.954	0.967	0.979	0.674	0.678	0.682	0.686	0.690	2.076	2.529	3.156	4.066	5.468
3	0.671	0.711	0.759	0.813	0.869	0.557	0.575	0.595	0.617	0.640	1.187	1.360	1.570	1.857	2.307
4	0.461	0.490	0.533	0.595	0.674	0.388	0.406	0.434	0.473	0.521	0.922	1.102	1.280	1.459	1.663
5	0.381	0.411	0.450	0.498	0.554	0.323	0.337	0.353	0.372	0.402	0.735	0.922	1.116	1.306	1.489
6	0.314	0.348	0.394	0.449	0.507	0.261	0.280	0.308	0.337	0.371	0.612	0.799	0.994	1.191	1.387
7	0.270	0.303	0.352	0.410	0.473	0.226	0.242	0.267	0.303	0.345	0.525	0.713	0.907	1.105	1.304
8	0.236	0.271	0.322	0.382	0.446	0.197	0.214	0.242	0.279	0.323	0.459	0.648	0.843	1.041	1.240
9	0.210	0.246	0.299	0.360	0.426	0.175	0.193	0.223	0.262	0.307	0.408	0.597	0.794	0.992	1.191
10	0.189	0.226	0.281	0.344	0.410	0.158	0.176	0.208	0.249	0.295	0.368	0.557	0.754	0.952	1.152
12	0.157	0.197	0.255	0.320	0.387	0.131	0.151	0.186	0.230	0.278	0.307	0.497	0.694	0.893	1.093
14	0.135	0.176	0.237	0.303	0.371	0.113	0.134	0.172	0.218	0.266	0.263	0.454	0.652	0.851	1.051
16	0.118	0.161	0.223	0.291	0.359	0.099	0.121	0.162	0.208	0.257	0.230	0.422	0.621	0.820	1.020
18	0.105	0.150	0.213	0.281	0.350	0.088	0.111	0.154	0.201	0.250	0.205	0.398	0.596	0.796	0.996
20	0.095	0.141	0.205	0.274	0.343	0.079	0.104	0.148	0.196	0.245	0.185	0.378	0.577	0.776	0.976
22	0.086	0.133	0.199	0.268	0.337	0.072	0.098	0.143	0.192	0.241	0.168	0.362	0.561	0.760	0.960
24	0.079	0.128	0.194	0.263	0.332	0.066	0.093	0.139	0.188	0.238	0.154	0.348	0.547	0.747	0.947
26	0.073	0.123	0.190	0.259	0.328	0.061	0.090	0.136	0.185	0.235	0.142	0.337	0.536	0.736	0.931
28	0.068	0.119	0.186	0.255	0.325	0.056	0.086	0.133	0.183	0.232	0.132	0.327	0.527	0.727	0.926
30	0.063	0.115	0.183	0.252	0.322	0.053	0.084	0.131	0.180	0.230	0.124	0.319	0.518	0.718	0.918
32	0.059	0.112	0.180	0.249	0.319	0.049	0.081	0.129	0.178	0.228	0.116	0.312	0.511	0.711	0.911
34	0.056	0.110	0.178	0.247	0.317	0.047	0.076	0.127	0.177	0.227	0.110	0.305	0.505	0.705	0.905
36	0.053	0.107	0.176	0.245	0.315	0.044	0.077	0.126	0.175	0.225	0.104	0.300	0.499	0.699	0.899
38	0.050	0.105	0.174	0.243	0.313	0.042	0.076	0.124	0.174	0.224	0.098	0.295	0.494	0.694	0.894
40	0.047	0.103	0.172	0.242	0.311	0.040	0.075	0.123	0.173	0.223	0.094	0.290	0.490	0.690	0.890

Table HI-2(b) – Table showing Variation of “Equivalent Length Factor” with L/T ratio and Pile Exposed Length Factor for End-bearing Piles with Bottom Pinned

L/T Ratio	Top Pinned / Bottom Fixed					Top fixed / Bottom Fixed					Top Free / Bottom Fixed				
	Exposed Length Factor (R_{ex})					Exposed Length Factor (R_{ex})					Exposed Length Factor (R_{ex})				
	0	0.1	0.2	0.3	0.4	0	0.1	0.2	0.3	0.4	0	0.1	0.2	0.3	0.4
0	0.699	0.699	0.699	0.699	0.699	0.500	0.500	0.500	0.500	0.500	2.000	2.000	2.000	2.000	2.000
1	0.699	0.699	0.699	0.699	0.699	0.500	0.500	0.500	0.500	0.500	1.897	1.993	1.996	1.998	1.999
2	0.681	0.685	0.689	0.693	0.696	0.493	0.494	0.496	0.497	0.498	1.694	1.809	1.893	1.948	1.978
3	0.593	0.614	0.636	0.658	0.676	0.451	0.460	0.469	0.478	0.487	1.176	1.360	1.550	1.725	1.862
4	0.458	0.490	0.530	0.576	0.623	0.364	0.381	0.402	0.427	0.453	0.908	1.084	1.266	1.456	1.652
5	0.374	0.404	0.445	0.496	0.554	0.304	0.318	0.337	0.365	0.402	0.734	0.919	1.107	1.293	1.483
6	0.314	0.347	0.392	0.445	0.504	0.260	0.277	0.300	0.329	0.365	0.612	0.799	0.993	1.187	1.377
7	0.270	0.303	0.352	0.409	0.471	0.224	0.241	0.267	0.302	0.341	0.525	0.713	0.907	1.105	1.301
8	0.236	0.271	0.322	0.382	0.446	0.197	0.214	0.242	0.279	0.322	0.459	0.648	0.843	1.041	1.240
9	0.210	0.246	0.299	0.360	0.426	0.175	0.193	0.223	0.262	0.307	0.408	0.597	0.794	0.992	1.191
10	0.189	0.226	0.281	0.344	0.410	0.158	0.176	0.208	0.249	0.295	0.368	0.557	0.754	0.952	1.152
12	0.157	0.197	0.255	0.320	0.387	0.131	0.151	0.186	0.230	0.278	0.307	0.497	0.694	0.893	1.093
14	0.135	0.176	0.237	0.303	0.371	0.113	0.134	0.172	0.218	0.266	0.263	0.454	0.652	0.851	1.051
16	0.118	0.161	0.223	0.291	0.359	0.099	0.121	0.162	0.208	0.257	0.230	0.422	0.621	0.820	1.020
18	0.105	0.150	0.213	0.281	0.350	0.088	0.111	0.154	0.201	0.250	0.205	0.398	0.596	0.796	0.996
20	0.095	0.141	0.205	0.274	0.343	0.079	0.104	0.148	0.196	0.245	0.185	0.378	0.577	0.776	0.976
22	0.086	0.133	0.199	0.268	0.337	0.072	0.098	0.143	0.192	0.241	0.168	0.362	0.561	0.760	0.960
24	0.079	0.128	0.194	0.263	0.328	0.066	0.093	0.139	0.188	0.238	0.154	0.348	0.547	0.747	0.947
26	0.073	0.121	0.190	0.259	0.326	0.061	0.090	0.136	0.185	0.233	0.142	0.337	0.531	0.736	0.931
28	0.068	0.119	0.186	0.255	0.325	0.056	0.086	0.133	0.183	0.232	0.132	0.327	0.527	0.727	0.926
30	0.063	0.115	0.183	0.252	0.322	0.053	0.084	0.131	0.180	0.230	0.124	0.319	0.518	0.718	0.918
32	0.059	0.112	0.18	0.249	0.319	0.049	0.081	0.129	0.178	0.228	0.116	0.312	0.511	0.711	0.911
34	0.056	0.110	0.178	0.247	0.317	0.047	0.079	0.127	0.177	0.227	0.11	0.305	0.505	0.705	0.905
36	0.053	0.107	0.176	0.245	0.315	0.044	0.077	0.126	0.175	0.225	0.104	0.300	0.499	0.699	0.899
38	0.050	0.105	0.174	0.243	0.313	0.042	0.076	0.124	0.174	0.224	0.098	0.295	0.494	0.694	0.894
40	0.047	0.103	0.172	0.242	0.311	0.040	0.075	0.123	0.173	0.223	0.094	0.290	0.490	0.690	0.890

Table HI-2(c) – Table showing Variation of “Equivalent Length Factor” with L/T ratio and Pile Exposed Length Factor for End-bearing Piles with Bottom Fixed

L/T Ratio	Top Pinned / Bottom Free					Top fixed / Bottom Free					Top Free / Bottom Free				
	Sleeved Length Factor (R_{slc})					Sleeved Length Factor (R_{slc})					Sleeved Length Factor (R_{slc})				
	0	0.1	0.2	0.3	0.4	0	0.1	0.2	0.3	0.4	0	0.1	0.2	0.3	0.4
0	–	–	–	–	–	2.000	2.000	2.000	2.000	2.000	–	–	–	–	–
1	6.293	6.293	6.298	6.320	6.378	1.942	1.942	1.942	1.942	1.942	18.854	19.566	21.397	24.443	29.183
2	1.234	1.234	1.234	1.234	1.236	1.225	1.225	1.225	1.226	1.226	3.362	3.493	3.829	4.380	5.229
3	0.869	0.869	0.871	0.879	0.895	0.787	0.787	0.787	0.788	0.791	1.330	1.395	1.547	1.775	2.101
4	0.606	0.607	0.609	0.618	0.645	0.588	0.588	0.588	0.590	0.596	0.922	0.982	1.102	1.254	1.438
5	0.439	0.439	0.440	0.441	0.446	0.438	0.438	0.438	0.438	0.439	0.737	0.808	0.940	1.098	1.269
6	0.349	0.349	0.353	0.377	0.426	0.346	0.346	0.346	0.347	0.350	0.612	0.692	0.834	1.000	1.177
7	0.283	0.283	0.295	0.341	0.398	0.283	0.283	0.283	0.284	0.294	0.525	0.612	0.762	0.933	1.113
8	0.240	0.241	0.268	0.319	0.379	0.239	0.239	0.239	0.239	0.273	0.459	0.553	0.709	0.884	1.067
9	0.210	0.215	0.249	0.303	0.365	0.205	0.205	0.205	0.220	0.263	0.408	0.508	0.669	0.847	1.033
10	0.189	0.196	0.234	0.291	0.354	0.179	0.179	0.179	0.211	0.255	0.368	0.473	0.638	0.819	1.006
12	0.157	0.167	0.214	0.274	0.339	0.142	0.142	0.156	0.198	0.243	0.307	0.421	0.593	0.777	0.967
14	0.135	0.149	0.200	0.263	0.329	0.117	0.117	0.145	0.189	0.236	0.263	0.385	0.561	0.748	0.940
16	0.118	0.135	0.191	0.256	0.322	0.099	0.103	0.138	0.183	0.231	0.230	0.359	0.539	0.728	0.920
18	0.105	0.126	0.184	0.250	0.317	0.088	0.094	0.133	0.179	0.227	0.205	0.339	0.522	0.712	0.906
20	0.095	0.119	0.179	0.245	0.313	0.079	0.088	0.129	0.176	0.224	0.185	0.324	0.508	0.700	0.894
22	0.086	0.113	0.175	0.242	0.310	0.072	0.083	0.126	0.173	0.222	0.168	0.312	0.498	0.690	0.885
24	0.079	0.109	0.172	0.239	0.307	0.066	0.079	0.123	0.171	0.220	0.154	0.302	0.489	0.682	0.878
26	0.073	0.105	0.169	0.237	0.305	0.061	0.076	0.121	0.169	0.218	0.142	0.293	0.482	0.673	0.872
28	0.068	0.102	0.167	0.235	0.303	0.056	0.074	0.120	0.168	0.217	0.132	0.286	0.476	0.670	0.866
30	0.063	0.100	0.165	0.233	0.302	0.053	0.072	0.118	0.167	0.216	0.124	0.280	0.471	0.666	0.862
32	0.059	0.098	0.163	0.232	0.300	0.049	0.071	0.117	0.166	0.215	0.116	0.275	0.466	0.662	0.858
34	0.056	0.096	0.162	0.230	0.299	0.047	0.069	0.116	0.165	0.214	0.110	0.271	0.463	0.658	0.855
36	0.053	0.094	0.161	0.229	0.298	0.044	0.068	0.115	0.164	0.213	0.104	0.267	0.459	0.655	0.853
38	0.050	0.093	0.160	0.228	0.297	0.042	0.067	0.115	0.163	0.213	0.098	0.263	0.456	0.653	0.85
40	0.047	0.092	0.159	0.228	0.297	0.040	0.066	0.114	0.163	0.212	0.094	0.260	0.454	0.650	0.848

Table HI-2(d) – Table showing Variation of “Equivalent Length Factor” with L/T ratio and Pile Sleeved Length Factor for End-bearing Piles with Bottom Free

L/T Ratio	Top Pinned / Bottom Pinned					Top fixed / Bottom Pinned					Top Free / Bottom Pinned				
	Sleeved Length Factor (R_{slc})					Sleeved Length Factor (R_{slc})					Sleeved Length Factor (R_{slc})				
	0	0.1	0.2	0.3	0.4	0	0.1	0.2	0.3	0.4	0	0.1	0.2	0.3	0.4
0	1.000	1.000	1.000	1.000	1.000	0.699	0.699	0.699	0.699	0.699	–	–	–	–	–
1	0.997	0.997	0.998	0.998	0.998	0.698	0.698	0.698	0.698	0.698	10.906	11.232	12.108	13.604	15.965
2	0.927	0.927	0.928	0.932	0.939	0.674	0.674	0.674	0.674	0.676	2.076	2.142	2.313	2.592	3.017
3	0.671	0.671	0.674	0.686	0.714	0.557	0.557	0.557	0.558	0.564	1.187	1.232	1.329	1.459	1.623
4	0.461	0.461	0.468	0.488	0.523	0.388	0.388	0.388	0.388	0.389	0.922	0.982	1.099	1.240	1.391
5	0.381	0.382	0.392	0.421	0.465	0.323	0.323	0.324	0.331	0.350	0.735	0.806	0.939	1.098	1.268
6	0.314	0.316	0.333	0.372	0.425	0.261	0.262	0.264	0.280	0.312	0.612	0.691	0.834	0.999	1.176
7	0.270	0.273	0.295	0.340	0.397	0.226	0.226	0.231	0.252	0.288	0.525	0.612	0.762	0.933	1.113
8	0.236	0.240	0.268	0.319	0.378	0.197	0.197	0.205	0.234	0.273	0.459	0.553	0.709	0.884	1.067
9	0.210	0.215	0.249	0.303	0.365	0.175	0.176	0.187	0.220	0.263	0.408	0.508	0.669	0.847	1.033
10	0.189	0.196	0.234	0.291	0.354	0.158	0.158	0.174	0.211	0.255	0.368	0.473	0.638	0.819	1.006
12	0.157	0.167	0.214	0.274	0.339	0.131	0.133	0.156	0.198	0.243	0.307	0.421	0.593	0.777	0.967
14	0.135	0.149	0.200	0.263	0.329	0.113	0.116	0.145	0.189	0.236	0.263	0.385	0.561	0.748	0.940
16	0.118	0.135	0.191	0.256	0.322	0.099	0.103	0.138	0.183	0.231	0.230	0.359	0.539	0.728	0.920
18	0.105	0.126	0.184	0.250	0.317	0.088	0.094	0.133	0.179	0.227	0.205	0.339	0.522	0.712	0.906
20	0.095	0.119	0.179	0.245	0.313	0.079	0.088	0.129	0.176	0.224	0.185	0.324	0.508	0.700	0.894
22	0.086	0.113	0.175	0.242	0.310	0.072	0.083	0.126	0.173	0.222	0.168	0.312	0.498	0.690	0.885
24	0.079	0.109	0.172	0.239	0.307	0.066	0.079	0.123	0.171	0.220	0.154	0.302	0.489	0.682	0.878
26	0.073	0.105	0.168	0.237	0.305	0.061	0.076	0.121	0.169	0.218	0.142	0.293	0.482	0.676	0.872
28	0.068	0.102	0.167	0.235	0.303	0.056	0.074	0.12	0.168	0.217	0.132	0.286	0.476	0.67	0.866
30	0.063	0.100	0.165	0.233	0.302	0.053	0.072	0.118	0.167	0.216	0.124	0.280	0.471	0.666	0.862
32	0.059	0.098	0.163	0.232	0.300	0.049	0.071	0.117	0.166	0.215	0.116	0.275	0.466	0.662	0.858
34	0.056	0.096	0.162	0.230	0.299	0.047	0.069	0.116	0.165	0.214	0.110	0.271	0.463	0.658	0.855
36	0.053	0.094	0.161	0.229	0.298	0.044	0.068	0.115	0.164	0.213	0.104	0.267	0.459	0.655	0.853
38	0.050	0.093	0.160	0.228	0.297	0.042	0.067	0.115	0.163	0.213	0.098	0.263	0.456	0.653	0.850
40	0.047	0.092	0.159	0.228	0.297	0.040	0.066	0.114	0.163	0.212	0.094	0.260	0.454	0.650	0.848

Table HI-2(e) – Table showing Variation of “Equivalent Length Factor” with L/T ratio and Pile Exposed Length Factor for End-bearing Piles with Bottom Pinned

L/T Ratio	Top Pinned / Bottom Fixed					Top fixed / Bottom Fixed					Top Free / Bottom Fixed				
	Sleeved Length Factor (R_{slc})					Sleeved Length Factor (R_{slc})					Sleeved Length Factor (R_{slc})				
	0	0.1	0.2	0.3	0.4	0	0.1	0.2	0.3	0.4	0	0.1	0.2	0.3	0.4
0	0.699	0.699	0.699	0.699	0.699	0.500	0.500	0.500	0.500	0.500	2.000	2.000	2.000	2.000	2.000
1	0.699	0.699	0.699	0.699	0.699	0.500	0.500	0.500	0.500	0.500	1.897	1.988	1.991	1.994	1.997
2	0.681	0.681	0.682	0.684	0.687	0.493	0.493	0.493	0.493	0.494	1.694	1.721	1.778	1.844	1.905
3	0.593	0.593	0.596	0.606	0.625	0.451	0.451	0.451	0.453	0.459	1.176	1.224	1.326	1.459	1.608
4	0.458	0.459	0.466	0.487	0.523	0.364	0.364	0.364	0.369	0.384	0.908	0.966	1.082	1.222	1.378
5	0.374	0.375	0.387	0.416	0.460	0.304	0.304	0.306	0.315	0.337	0.734	0.805	0.936	1.092	1.258
6	0.314	0.316	0.333	0.372	0.424	0.260	0.260	0.263	0.279	0.310	0.612	0.691	0.834	0.999	1.175
7	0.270	0.272	0.295	0.340	0.397	0.224	0.224	0.229	0.252	0.288	0.525	0.612	0.762	0.933	1.113
8	0.236	0.240	0.268	0.319	0.378	0.197	0.197	0.205	0.233	0.273	0.459	0.553	0.709	0.884	1.067
9	0.210	0.215	0.249	0.303	0.365	0.175	0.176	0.187	0.220	0.263	0.408	0.508	0.669	0.847	1.033
10	0.189	0.196	0.234	0.291	0.354	0.158	0.158	0.174	0.211	0.255	0.368	0.473	0.638	0.819	1.006
12	0.157	0.167	0.214	0.274	0.339	0.131	0.133	0.156	0.198	0.243	0.307	0.421	0.593	0.777	0.967
14	0.135	0.149	0.200	0.263	0.329	0.113	0.116	0.145	0.189	0.236	0.263	0.385	0.561	0.748	0.940
16	0.118	0.135	0.191	0.256	0.322	0.099	0.103	0.138	0.183	0.231	0.230	0.359	0.539	0.728	0.920
18	0.105	0.126	0.184	0.250	0.317	0.088	0.094	0.133	0.179	0.227	0.205	0.339	0.522	0.712	0.906
20	0.095	0.119	0.179	0.245	0.313	0.079	0.088	0.129	0.176	0.224	0.185	0.324	0.508	0.700	0.894
22	0.086	0.113	0.175	0.242	0.310	0.072	0.083	0.126	0.173	0.222	0.168	0.312	0.498	0.690	0.885
24	0.079	0.109	0.172	0.239	0.307	0.066	0.079	0.123	0.171	0.220	0.154	0.302	0.489	0.682	0.878
26	0.073	0.105	0.169	0.237	0.305	0.061	0.076	0.121	0.169	0.218	0.142	0.293	0.482	0.676	0.872
28	0.068	0.102	0.167	0.235	0.303	0.056	0.074	0.120	0.168	0.217	0.132	0.286	0.476	0.670	0.866
30	0.063	0.100	0.165	0.233	0.302	0.053	0.072	0.118	0.167	0.216	0.124	0.280	0.471	0.666	0.862
32	0.059	0.098	0.163	0.232	0.300	0.049	0.071	0.117	0.166	0.215	0.116	0.275	0.466	0.662	0.858
34	0.056	0.096	0.162	0.230	0.299	0.047	0.069	0.116	0.165	0.214	0.110	0.271	0.463	0.658	0.855
36	0.053	0.094	0.161	0.229	0.298	0.044	0.068	0.115	0.164	0.213	0.104	0.267	0.459	0.655	0.853
38	0.050	0.093	0.160	0.228	0.297	0.042	0.067	0.115	0.163	0.213	0.098	0.263	0.456	0.653	0.850
40	0.047	0.092	0.159	0.228	0.297	0.040	0.066	0.114	0.163	0.212	0.094	0.260	0.454	0.650	0.848

Table HI-2(f) – Table showing Variation of “Equivalent Length Factor” with L/T ratio and Pile Exposed Length Factor for End-Bearing Piles with Bottom Fixed

HI.3 Brief Discussion on the “Buckling Phenomenon”

Law (2013) points out that the analytical results of “buckling” reveals only that a strut can take up the shape of any of the analyzed buckling modes, with any magnitude i.e. the “discrete buckling” loads. It is not the case, as discussed in some references and text books such as Coates et al (1980) that the Euler load is a threshold load above which the strut becomes unstable.

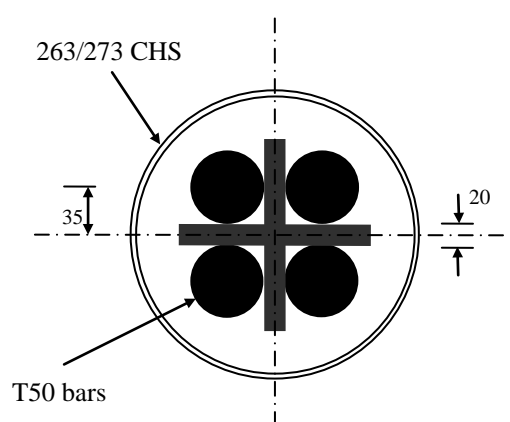
Nevertheless, a strut normally fails due to its own “initial imperfection” at loads well below the Euler load. By initial imperfection we refer to the initial “bowing” of the strut causing eccentric bending in the strut under applied pure axial load. The axial load will create further “bowing”, which may cause the strut to fail subsequently. It has, however, been proved that the Euler load is the absolute maximum, at which the imperfection (bowing) will increase to infinity, i.e. the strut will fail certainly.

It should also be noted that provisions in the steel and concrete codes (BS5950 and BS8110) for reduction of load capacity of a strut due to its length are actually not to cater for the theoretical “buckling phenomenon”. The provisions are to account for the extra bending caused by the initial imperfections assumed which lead to reduction of strut load capacity. The analysis for the Euler load, however, is useful in determining the effective length of the pile and the “buckling mode shape” which is the most critical initial imperfection shape leading to subsequent failure. Law (2013) has analyzed and provided design charts. Upon determination of the equivalent buckling length, it would

be acceptable, based on the approach outlined in HI.4, to determine the reduced load carrying capacity. Nevertheless, Law (2013) has, by assuming a sinusoidal deflected initial imperfection profile for the pile, developed an approach for determination of the moment due to the axial load and the imperfection for the pile under lateral restraint. The moment can then be taken into design.

HI.4 Numerical Example

Consider a 4-T50 mini-pile with cross section as shown in Figure HI-4 driven into soil of $n_h = 1300 \text{ kN/m}^3$ of total length 30m and the top 3m exposed. Its head is pinned at the underside of the pile cap and its other end socketed into rock which is considered as fixed.



$$I_{casing} = \frac{\pi 273^4}{64} - \frac{\pi 263^4}{64} = 37808149 \text{ mm}^4$$

$$I_{T50} = 4 \left(\frac{\pi 50^4}{64} + \frac{\pi 50^2}{4} \times 35^2 \right) = 10848312 \text{ mm}^4$$

$$I_{total} = 48656461 \text{ mm}^4$$

$$E_p I_p = 205 \times 10^6 \times 48656361 \times 10^{-12} = 9974.57 \text{ kNm}^2$$

$$\text{For } n_h = 1300 \text{ kN/m}^3$$

$$T = \sqrt[5]{E_p I_p / n_h} = 1.503 \text{ m}$$

Figure HI-4 – Numerical Example of a 4-T50 Mini-pile

Exposed length ratio is $3/30 = 0.1$, $L/T = 30/1.503 = 19.96$. By Table HI-2(c), the equivalent length factor is 0.1412 and the equivalent length is $L_{eq} = 0.1412 \times 30 = 4.236 \text{ m}$. So the “Euler” load is $\pi^2 E_p I_p / L_{eq}^2 = 5486 \text{ kN} >$ the structural capacity of the pile of $0.475 \times 500 \times 7854 \times 10^{-3} = 1865 \text{ kN}$. It can be seen that this theoretical “Euler” load is very high.

However, as discussed in HI.3, the codified design against “buckling” is not performed by checking against this Euler load. Instead, the codes including BS5950, the Code of Practice for Structural Use of Steel 2011 determine the reduced load carrying capacity of the strut based on its “initial imperfections”. The 2 steel codes are based on back-calculation from the experimental failure loads of struts of various types of sections and grades to determine the initial imperfections and provide formulae and tables for determination of the reduced strengths. To calculate the reduced strengths, we may assume the mini-pile to adopt the CHS section as no study has been carried out on the mini-pile section to determine initial imperfections. So according to Table 8.7 of the Code of Practice for Structural Use of Steel 2011, curve a) should be followed. The next step is to find the radius of gyration r of the section and subsequently the λ value which is L_{eq}/r .

$$\text{As } A_{steel} = (273^2 - 263^2)\pi / 4 + 4 \times \pi 25^2 = 12064 \text{ mm}^2;$$

$$r = \sqrt{I/A} = 63.51 \text{ mm}; \quad \lambda = L_{eq}/r = 4230/63.51 = 66.6$$

By Table 8.8 (a) of the Steel Code and assuming S460 (nearest to the grade of the T50 bars), the design strength of steel drops from 460N/mm² to 331N/mm², i.e. drops to 72% of its original value. So the load carrying capacity of the pile is $1689 \times 0.72 = 1216 \text{ kN}$.

However, if the pile is completely embedded, by Table HI-2(c), the equivalent length factor is 0.095 and the equivalent length is $L_{eq} = 0.095 \times 30 = 2.85 \text{ m}$. With $\lambda = 2850/63.51 = 44.87$ and by Table 8.8 (a) of the Steel Code, the design strength of steel drops from 460N/mm² to 415.26N/mm², i.e. drops to 90.3% of its original value. So the load carrying capacity of the pile is $1689 \times 0.903 = 1525 \text{ kN}$.

HI.5 Stiffness Method by the Use of the Geometric Matrix

The buckling phenomenon can also be solved by the stiffness method through the use of the “geometric matrix”. The stiffness matrix and the geometric matrix of a strut of length L and flexural stiffness EI are

$$[k_e] = \begin{bmatrix} \frac{12EI}{L^3} & \frac{6EI}{L^2} & \frac{-12EI}{L^3} & \frac{6EI}{L^2} \\ \frac{6EI}{L^2} & \frac{4EI}{L} & \frac{-6EI}{L^2} & \frac{2EI}{L} \\ \frac{-12EI}{L^3} & \frac{-6EI}{L^2} & \frac{12EI}{L^3} & \frac{-6EI}{L^2} \\ \frac{6EI}{L^2} & \frac{2EI}{L} & \frac{-6EI}{L^2} & \frac{4EI}{L} \end{bmatrix} \quad \text{and} \quad [k_G] = \frac{-1}{30L} \begin{bmatrix} 36 & 3L & -36 & 3L \\ 3L & 4L^2 & -3L & -L^2 \\ -36 & -3L & 36 & -3L \\ 3L & -L^2 & -3L & 4L^2 \end{bmatrix}$$

(Eqn HI-11)

It can be proven that the stiffness of the strut under an axial P becomes

$$[k_e] + P[k_G] \quad \text{(Eqn HI-12)}$$

It should be noted that P carries a positive value if in compression representing a reduction in the overall stiffness of the strut. Conversely P increases the stiffness if in tension. The mathematical model for Figure HI-1 can then be formed by assembling the matrices k_e and k_G for individual struts in the usual manner to form the entire stiffness matrix for the pile with the soil restraints as “point springs” in the following formula

$$[K_e] + P[K_G] \quad \text{(Eqn HI-13)}$$

If P is so chosen that when the matrix $[K_e] + P[K_G]$ diminishes implying zero stiffness of the pile, the buckling of the pile takes place and P becomes the buckling load, with $[v]$ as the lateral displacement matrix. So we may list

$$\begin{aligned}
[K_e] + P[K_G] = 0 &\Rightarrow \{[K_e] + P[K_G]\}[v] = 0 \Rightarrow [K_e][v] = -P[K_G][v] \\
&\Rightarrow [K_e]^{-1}[K_G][v] = \frac{-1}{P}[v]
\end{aligned}
\tag{Eqn HI-14}$$

Again (Eqn HI-14) is an eigen-value problem for the matrix $[K_e]^{-1}[K_G]$ and the eigen-values $\lambda = \frac{-1}{P}$ by which the buckling load can be determined as

$$P = \frac{-1}{\lambda} \tag{Eqn HI-15}$$

The lowest value of P represents the fundamental buckling load.

And the eigen vectors $[v]$ analyzed represent the buckling modes (shapes).

HI.6 P-Δ Effects

Both the finite difference approach and the stiffness method described above can be used directly to calculate lateral displacements with inclusion of P-Δ effects. Further details are discussed in Appendix HP.

Appendix HJ

Principle and Derivation of the Hiley Formula

Principle and Derivation of the Hiley Formula

HJ.1 Theoretical Background

The Hiley Formula, like most of the pile dynamic formulae is based on an energy approach by which the energy injected from the driving hammer into the pile is set equal to the work done by the pile on the soil in the form of “set” (advancement of the pile into the soil) and temporary compression of the soil (quake) and the pile itself. The ultimate resistance on the pile is then solved by the principle of conservation of energy. The energy transfer process is demonstrated in Figure HJ-1.

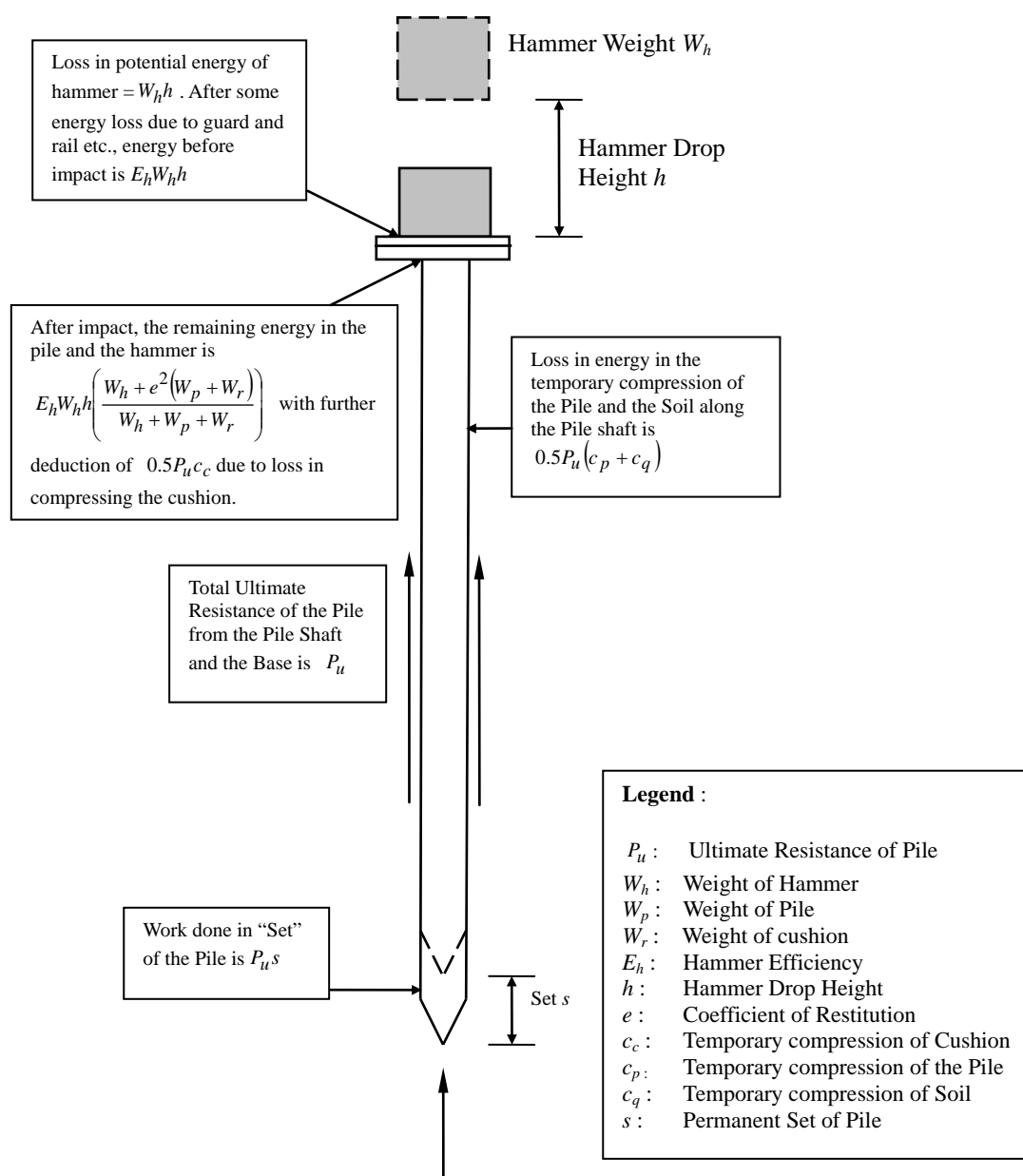


Figure HJ-1 – Energy Transfer Process as Assumed by the Hiley Formula

HJ.2 Detailed Derivation

Referring to Figure HJ-1, consider the drop hammer of weight W_h dropping from height h and impact on the pile of weight W_p and the weight of the helmet W_r . The loss of potential energy of the hammer is $W_h h$. After some loss due to hammer efficiency, the energy of the hammer just before impact is $E_h W_h h$, which is converted to the kinetic energy of the hammer $\frac{W_h U_h^2}{2g}$ where U_h is the velocity of the hammer before impact.

By equating the two energies,

$$U_h = \sqrt{E_h 2gh} \quad (\text{Eqn HJ-1})$$

Let V_h and V_p be the velocities of the hammer and the pile (and helmet) after impact, then during impact, by the Law of Conservation of Momentum (the contribution of the soil is ignored)

$$\frac{W_h U_h}{g} = \frac{W_h V_h}{g} + \frac{(W_p + W_r)}{g} V_p \Rightarrow W_h U_h = W_h V_h + (W_p + W_r) V_p \quad (\text{Eqn HJ-2})$$

Assuming the rigid body impact condition and applying Newton's Law of Restitution, we

$$\text{have } \frac{V_p - V_h}{0 - U_h} = -e \Rightarrow V_h = V_p - e U_h \quad (\text{Eqn HJ-3})$$

Substituting (Eqn HJ-3) into (Eqn HJ-2)

$$W_h U_h = W_h (V_p - e U_h) + (W_p + W_r) V_p \Rightarrow V_p = \frac{(1+e)W_h}{W_h + (W_p + W_r)} U_h \quad (\text{Eqn HJ-4})$$

$$\text{The kinetic energy of the pile and the cushion after impact is } \frac{(W_p + W_r)}{2g} V_p^2 \quad (\text{Eqn HJ-5})$$

Combining (Eqn HJ-5) with (Eqn HJ-1) and (Eqn HJ-4), the kinetic energy of the pile with the cushion after impact is

$$\frac{(W_p + W_r)}{2g} \left\{ \frac{(1+e)W_h}{W_h + W_p + W_r} \sqrt{E_h 2gh} \right\}^2 = E_h W_h h \left\{ \frac{(1+2e+e^2)W_h (W_p + W_r)}{(W_h + W_p + W_r)^2} \right\} \quad (\text{Eqn HJ-6})$$

$$\text{The kinetic energy of the hammer after impact is } \frac{W_h V_h^2}{2g}$$

Combining (Eqn HJ-3) with (Eqn HJ-4) and (Eqn HJ-1)

$$V_h = \frac{(1+e)W_h}{W_h + W_p + W_r} U_h - eU_h = \frac{W_h + eW_h - eW_h - eW_p - eW_r}{W_h + W_p + W_r} U_h = \frac{W_h - e(W_p + W_r)}{W_h + W_p + W_r} \sqrt{E_h 2gh}$$

So the kinetic energy of the hammer after impact is

$$\frac{W_h}{2g} V_h^2 = \frac{W_h}{2g} \left\{ \frac{W_h - e(W_p + W_r)}{W_h + W_p + W_r} \sqrt{E_h 2gh} \right\}^2 = E_h W_h H \left\{ \frac{W_h - e(W_p + W_r)}{W_h + W_p + W_r} \right\}^2 \quad (\text{Eqn HJ-7})$$

Adding the energies of the pile with cushion in (Eqn HJ-6) and that of the hammer in (Eqn HJ-7), the total energy $T.E.$ is

$$\begin{aligned} T.E. &= E_h W_h h \left\{ \frac{(1+2e+e^2)W_h(W_p + W_r)}{(W_h + W_p + W_r)^2} \right\} + E_h W_h h \left\{ \frac{W_h - e(W_p + W_r)}{W_h + W_p + W_r} \right\}^2 \\ &= E_h W_h h \left\{ \frac{W_h + e^2(W_p + W_r)}{W_h + W_p + W_r} \right\} \end{aligned} \quad (\text{Eqn HJ-8})$$

This total energy is eventually transferred to the pile and is dissipated through work done against soil resistances and elastic compression of the pile and cushion.

Assuming the soil is exhibiting elasto-plastic behaviour with elastic limit c_q (the quake) beyond which the soil resistance is constant at P_u and for a distance s which is the set, the work done on the soil is

$$0.5P_u c_q + P_u s \quad (\text{Eqn HJ-9})$$

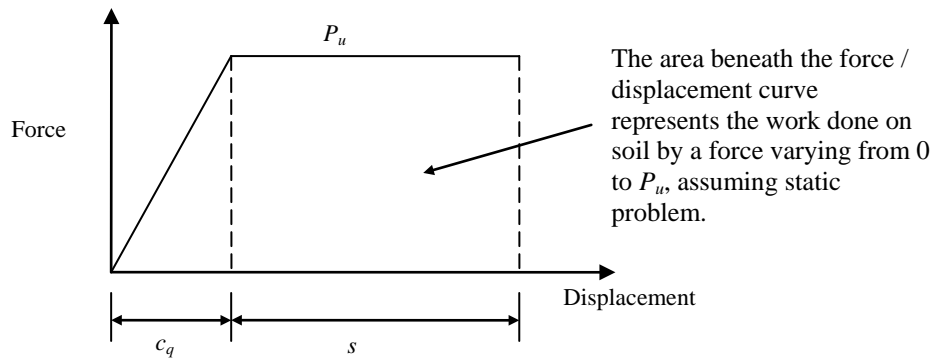


Figure HJ-2 – Work done in Quake and Set as Assumed by the Hiley Formula

Similarly, again assuming static behaviour, the work done on the elastic compression of the pile and the cushion is

$$0.5P_u c_p + 0.5P_u c_c \quad (\text{Eqn HJ-10})$$

where c_p and c_c are respectively the temporary compressions of the pile and the cushion.

So, equating the energy after impact to the work done on temporary compression of the pile / the soil and total “Set” of the Pile,

$$E_h W_h h \left\{ \frac{W_h + e^2(W_p + W_r)}{W_h + W_p + W_r} \right\} = 0.5 P_u c_q + P_u s + 0.5 P_u c_p + 0.5 P_u c_c = 0.5 P_u (c_c + c_p + c_q) + P_u s$$

$$\Rightarrow P_u = \frac{E_h W_h h}{s + 0.5(c_c + c_p + c_q)} \left\{ \frac{W_h + e^2(W_p + W_r)}{W_h + W_p + W_r} \right\} \quad (\text{Eqn HJ-11})$$

which is the Hiley Formula.

It should be noted that $c_p + c_q$ and s can be measured during the final set of the pile. c_c is small comparatively. It is often assumed to be constant, ranging from 4 to 6 mm. The value is either assumed or can be measured by video camera.

Appendix HK

Discussion on Limits of “Final Set” and Criteria for Formulation of the “Final Set” Table

Discussion of Limits of “Final Set” and Criteria for Formulation of the “Final Set” Table

HK.1 The “Final Set” Table

Other than piles driven to refusal achieving sets less than 10mm per 10 blows, the format of a final set table depends on the pile driving formula. The final set table relates the allowable maximum final set value S of a driven pile for a given design ultimate capacity to the elastic displacement of the pile head or other measurable quantities. The elastic displacement of the pile head is often regarded as the sum of the elastic compression of the piles c_p and the elastic settlement of the ground c_q when the pile is being driven. For the Hiley formula commonly used in Hong Kong, the actual final set s is related to c_p+c_q and the pile length L . A driven pile is considered to have achieved a sufficient ultimate pile capacity if s is smaller than S .

The ultimate pile capacity that can be developed by pile driving depends on the energy imparted to the pile. The same pile driving energy can be attained by using a lighter hammer with a larger drop height or a heavy hammer with a smaller drop height. Each combination of hammer weight and drop height produces a different final set table.

A higher drop height will tend to induce higher driving stress and thus a higher risk of damaging the pile. From a theoretical point of view, it is preferable to use a heavy hammer with a smaller drop height to limit the driving stress.

HK.2 Applicable Range of S

It is common to impose criteria limiting the applicable range of s . In Hong Kong, the most commonly used criteria in the past were that the combination of hammer weight and drop height should be such that s will not be higher than 50mm per 10 blows or less than 25mm per 10 blows. It was believed that the first criterion of requiring s to be more than 25mm per 10 blows was originated from the Civil Engineering Code of Practice 4 (ICE, 1954). There was a good reason for setting this limit. In the 1950s and 1960s, precast concrete piles were perhaps the most common type of driven piles. Imposing a lower limit is equivalent to discouraging the contractor from using a light hammer with a large drop height. This indirectly controls the driving stress and hence the potential for damaging precast concrete piles.

The setting of this lower bound limit of 25mm per 10 blows was later abandoned in the British standards CP2004 and BS8004 (BSI, 1972, 1986), but replaced by the second criterion of setting an upper limit of S not greater than 50mm per 10 blows. The reason for imposing such an upper limit is not explained in the British Standards nor discussed in the literature. From a theoretical point of view, this criterion is not reasonable. Imposing an upper limit will deter contractors from using a heavy hammer which is beneficial in reducing driving stresses.

If both of the above two criteria are imposed, the applicable range of S becomes very narrow. A driven pile which has attained a very small actual set value s will not be acceptable if the combination of measured c_p+c_q value and actual pile length is outside

the applicable range of S . The criteria for limiting the applicable range are developed so as to minimize the potential of pile damage. A driven pile with a small actual set value s that can achieve a higher pile capacity and has no apparent damage occurring during pile driving could be deemed not acceptable under such criteria. The contractors have to select a suitable combination of hammer weight and drop height that can meet the applicable range of S . They are often compelled to use drop hammers to perform final setting of piles even though the piles have been pitched by hydraulic hammers. With a drop hammer, the drop height can be varied much more easily than is the case with a hydraulic hammer to increase the chance of finding a suitable final set table that can fulfill the criteria.

HK.3 Criteria for Formulating the Final Set Table

In determining the criteria for formulating the Final Set Table, that the pile driving stress can now be measured directly by a Pile Driving Analyzer (PDA) is a consideration. According to recent studies by Lam (2007) and Li & Lam (2007) based on a large database of PDA test results, the driving stress is found to have no correlation with S . Fung *et al* (2004), Lam (2007) and Li & Lam (2007) further observed that the ratio of $(c_p+c_q)/L$ is a simple and useful indicator of pile driving stress. Lam (2007) and Li & Lam (2007) proposed that by limiting the ratio of $(c_p+c_q)/L$ to 1.15 where c_p+c_q is in millimetre and L is in metre, the driving stress in steel H-piles can generally be controlled to less than 80% of the yield stress of steel piles at which the risk of damage to the pile is considered to be acceptably small. Based on these findings, the following criteria were formulated for the final set table which are acceptable to the Buildings Department and finally incorporated into the Code.

- (i) The upper bound limit of S is relaxed to 100mm per 10 blows, but with the allowable value capped at 50mm. That is, if a calculated value of S between 50 and 100 is obtained, a value of 50 will still be used in the final set table;
- (ii) $(c_p+c_q)/L$ is limited to not greater than 1.15 where c_p+c_q is in millimetre and L is in metre.

The following Worked Example HK-1, of a final set table is developed using the above criteria based on the Hiley formula. It can be observed that the applicable range of S has become much wider, making it easier for compliance.

Data

Weight of Hammer :	16T
Type of Pile :	305×305×223 kg/m S450J0 Steel H-pile
Design Working Capacity	3053kN
Factor of Safety :	2
Design Ultimate Capacity	$R = 6106\text{kN}$
Weight of Hammer :	$W = 156.96\text{kN}$
Drop Height of Hammer:	$H = 1.5\text{m}$
Maximum Driving Energy:	$E = 235.44\text{kJ}$
Average Hammer Efficiency:	$\alpha = 0.7$
Pile Helmet Compression:	$c_c = 5\text{mm}$
Coefficient of Restitution:	$e = 0.32$
Weight of Pile Helmet:	$W_r = 30\text{kN}$

Weight of Pile:

$$W_p = 2.19 \text{ kN/m}$$

First of all, if no restriction on the S values at all, the set table is as shown in Table HK-1.

Pile Length (m)	Temporary Compression c_p+c_q																																
	6	7	8	9	10	11	12	13	14	15	16	17	18	19	20	21	22	23	24	25	26	27	28	29	30	31							
15	146	141	136	131	126	121	116	111	106	101	96	91	86	81	76	71	66	61	56	51	46	41	36	31	26	21							
16	144	139	134	129	124	119	114	109	104	99	94	89	84	79	74	69	64	59	54	49	44	39	34	29	24	19							
17	142	137	132	127	122	117	112	107	102	97	92	87	82	77	72	67	62	57	52	47	42	37	32	27	22	17							
18	141	136	131	126	121	116	111	106	101	96	91	86	81	76	71	66	61	56	51	46	41	36	31	26	21	16							
19	139	134	129	124	119	114	109	104	99	94	89	84	79	74	69	64	59	54	49	44	39	34	29	24	19	14							
20	137	132	127	122	117	112	107	102	97	92	87	82	77	72	67	62	57	52	47	42	37	32	27	22	17	12							
21	136	131	126	121	116	111	106	101	96	91	86	81	76	71	66	61	56	51	46	41	36	31	26	21	16	11							
22	134	129	124	119	114	109	104	99	94	89	84	79	74	69	64	59	54	49	44	39	34	29	24	19	14	9							
23	133	128	123	118	113	108	103	98	93	88	83	78	73	68	63	58	53	48	43	38	33	28	23	18	13	8							
24	131	126	121	116	111	106	101	96	91	86	81	76	71	66	61	56	51	46	41	36	31	26	21	16	11	6							
25	130	125	120	115	110	105	100	95	90	85	80	75	70	65	60	55	50	45	40	35	30	25	20	15	10	5							
26	129	124	119	114	109	104	99	94	89	84	79	74	69	64	59	54	49	44	39	34	29	24	19	14	9	4							
27	127	122	117	112	107	102	97	92	87	82	77	72	67	62	57	52	47	42	37	32	27	22	17	12	7	2							
28	126	121	116	111	106	101	96	91	86	81	76	71	66	61	56	51	46	41	36	31	26	21	16	11	6	1							
29	124	119	114	109	104	99	94	89	84	79	74	69	64	59	54	49	44	39	34	29	24	19	14	9	4	-1							
30	123	118	113	108	103	98	93	88	83	78	73	68	63	58	53	48	43	38	33	28	23	18	13	8	3	-2							
31	122	117	112	107	102	97	92	87	82	77	72	67	62	57	52	47	42	37	32	27	22	17	12	7	2	-3							
32	121	116	111	106	101	96	91	86	81	76	71	66	61	56	51	46	41	36	31	26	21	16	11	6	1	-4							
33	119	114	109	104	99	94	89	84	79	74	69	64	59	54	49	44	39	34	29	24	19	14	9	4	-1	-6							
34	118	113	108	103	98	93	88	83	78	73	68	63	58	53	48	43	38	33	28	23	18	13	8	3	-2	-7							
35	117	112	107	102	97	92	87	82	77	72	67	62	57	52	47	42	37	32	27	22	17	12	7	2	-3	-8							
36	116	111	106	101	96	91	86	81	76	71	66	61	56	51	46	41	36	31	26	21	16	11	6	1	-4	-9							
37	115	110	105	100	95	90	85	80	75	70	65	60	55	50	45	40	35	30	25	20	15	10	5	0	-5	-10							
38	113	108	103	98	93	88	83	78	73	68	63	58	53	48	43	38	33	28	23	18	13	8	3	-2	-7	-12							
39	112	107	102	97	92	87	82	77	72	67	62	57	52	47	42	37	32	27	22	17	12	7	2	-3	-8	-13							
40	111	106	101	96	91	86	81	76	71	66	61	56	51	46	41	36	31	26	21	16	11	6	1	-4	-9	-14							
41	110	105	100	95	90	85	80	75	70	65	60	55	50	45	40	35	30	25	20	15	10	5	0	-5	-10	-15							
42	109	104	99	94	89	84	79	74	69	64	59	54	49	44	39	34	29	24	19	14	9	4	-1	-6	-11	-16							
43	108	103	98	93	88	83	78	73	68	63	58	53	48	43	38	33	28	23	18	13	8	3	-2	-7	-12	-17							
44	107	102	97	92	87	82	77	72	67	62	57	52	47	42	37	32	27	22	17	12	7	2	-3	-8	-13	-18							

Table HK-1 – Final Set Values per 10 blows with No Restriction on the S values

If adopting the requirements that the applicable range of allowable set $S = 25$ to 100mm ; and $(c_p+c_q)/L \leq 1.15$ where c_p+c_q is in mm and L is in metre. Table HK-1 is reduced to Table HK-2.

Pile Length (m)	Temporary Compression c_p+c_q																															
	6	7	8	9	10	11	12	13	14	15	16	17	18	19	20	21	22	23	24	25	26	27	28	29	30	31						
15	-	-	-	-	-	-	-	-	-	-	96	91	-	-	-	-	-	-	-	-	-	-	-	-	-	-	-					
16	-	-	-	-	-	-	-	-	-	99	94	89	84	-	-	-	-	-	-	-	-	-	-	-	-	-	-					
17	-	-	-	-	-	-	-	-	-	97	92	87	82	77	-	-	-	-	-	-	-	-	-	-	-	-	-					
18	-	-	-	-	-	-	-	-	-	96	91	86	81	76	71	-	-	-	-	-	-	-	-	-	-	-	-					
19	-	-	-	-	-	-	-	-	99	94	89	84	79	74	69	64	-	-	-	-	-	-	-	-	-	-	-					
20	-	-	-	-	-	-	-	-	97	92	87	82	77	72	67	62	57	-	-	-	-	-	-	-	-	-	-					
21	-	-	-	-	-	-	-	-	96	91	86	81	76	71	66	61	56	51	46	-	-	-	-	-	-	-	-					
22	-	-	-	-	-	-	-	99	94	89	84	79	74	69	64	59	54	49	44	39	-	-	-	-	-	-	-					
23	-	-	-	-	-	-	-	98	93	88	83	78	73	68	63	58	53	48	43	38	33	-	-	-	-	-	-					
24	-	-	-	-	-	-	-	96	91	86	81	76	71	66	61	56	51	46	41	36	31	26	-	-	-	-	-					
25	-	-	-	-	-	-	100	95	90	85	80	75	70	65	60	55	50	45	40	35	30	-	-	-	-	-	-					
26	-	-	-	-	-	-	99	94	89	84	79	74	69	64	59	54	49	44	39	34	29	-	-	-	-	-	-					
27	-	-	-	-	-	-	97	92	87	82	77	72	67	62	57	52	47	42	37	32	27	-	-	-	-	-	-					
28	-	-	-	-	-	-	96	91	86	81	76	71	66	61	56	51	46	41	36	31	26	-	-	-	-	-	-					
29	-	-	-	-	-	99	94	89	84	79	74	69	64	59	54	49	44	39	34	29	-	-	-	-	-	-	-					
30	-	-	-	-	-	98	93	88	83	78	73	68	63	58	53	48	43	38	33	28	-	-	-	-	-	-	-					
31	-	-	-	-	-	97	92	87	82	77	72	67	62	57	52	47	42	37	32	27	-	-	-	-	-	-	-					
32	-	-	-	-	-	96	91	86	81	76	71	66	61	56	51	46	41	36	31	26	-	-	-	-	-	-	-					
33	-	-	-	-	99	94	89	84	79	74	69	64	59	54	49	44	39	34	29	-	-	-	-	-	-	-	-					
34	-	-	-	-	98	93	88	83	78	73	68	63	58	53	48	43	38	33	28	-	-	-	-	-	-	-	-					
35	-	-	-	-	97	92	87	82	77	72	67	62	57	52	47	42	37	32	27	-	-	-	-	-	-	-	-					
36	-	-	-	-	96	91	86	81	76	71	66	61	56	51	46	41	36	31	26	-	-	-	-	-	-	-	-					
37	-	-	-	100	95	90	85	80	75	70	65	60	55	50	45	40	35	30	-	-	-	-	-	-	-	-	-					
38	-	-	-	98	93	88	83	78	73	68	63	58	53	48	43	38	33	28	-	-	-	-	-	-	-	-	-					
39	-	-	-	97	92	87	82	77	72	67	62	57	52	47	42	37	32	27	-	-	-	-	-	-	-	-	-					
40	-	-	-	96	91	86	81	76	71	66	61	56	51	46	41	36	31	26	-	-	-	-	-	-	-	-	-					
41	-	-	-	95	90	85	80	75	70	65	60	55	50	45	40	35	30	25	-	-	-	-	-	-	-	-	-					
42	-	-	-	99	94	89	84	79	74	69	64	59	54	49	44	39	34	29	-	-	-	-	-	-	-	-	-					
43	-	-	-	98	93	88	83	78	73	68	63	58	53	48	43	38	33	28	-	-	-	-	-	-	-	-	-					

Finally, to be conservative, the values of S in excess of 50mm are capped at 50mm so that the final set table of Table HK-2 is modified as follows as Table HK-3:

Pile Length (m)	Temporary Compression c_p+c_q																															
	6	7	8	9	10	11	12	13	14	15	16	17	18	19	20	21	22	23	24	25	26	27	28	29	30	31						
15	-	-	-	-	-	-	-	-	-	-	50	50	-	-	-	-	-	-	-	-	-	-	-	-	-	-	-	-	-	-	-	
16	-	-	-	-	-	-	-	-	-	50	50	50	50	-	-	-	-	-	-	-	-	-	-	-	-	-	-	-	-	-	-	
17	-	-	-	-	-	-	-	-	-	50	50	50	50	50	-	-	-	-	-	-	-	-	-	-	-	-	-	-	-	-	-	
18	-	-	-	-	-	-	-	-	-	50	50	50	50	50	50	-	-	-	-	-	-	-	-	-	-	-	-	-	-	-	-	
19	-	-	-	-	-	-	-	-	50	50	50	50	50	50	50	50	-	-	-	-	-	-	-	-	-	-	-	-	-	-	-	
20	-	-	-	-	-	-	-	-	50	50	50	50	50	50	50	50	50	-	-	-	-	-	-	-	-	-	-	-	-	-	-	
21	-	-	-	-	-	-	-	-	50	50	50	50	50	50	50	50	50	50	-	-	-	-	-	-	-	-	-	-	-	-	-	
22	-	-	-	-	-	-	-	50	50	50	50	50	50	50	50	50	50	50	50	49	44	39	-	-	-	-	-	-	-	-	-	
23	-	-	-	-	-	-	-	50	50	50	50	50	50	50	50	50	50	50	50	48	43	38	33	-	-	-	-	-	-	-	-	
24	-	-	-	-	-	-	-	50	50	50	50	50	50	50	50	50	50	50	50	46	41	36	31	26	-	-	-	-	-	-	-	
25	-	-	-	-	-	-	50	50	50	50	50	50	50	50	50	50	50	50	50	45	40	35	30	-	-	-	-	-	-	-	-	
26	-	-	-	-	-	-	50	50	50	50	50	50	50	50	50	50	50	50	49	44	39	34	29	-	-	-	-	-	-	-	-	
27	-	-	-	-	-	-	50	50	50	50	50	50	50	50	50	50	50	50	47	42	37	32	27	-	-	-	-	-	-	-	-	
28	-	-	-	-	-	-	50	50	50	50	50	50	50	50	50	50	50	50	46	41	36	31	26	-	-	-	-	-	-	-	-	
29	-	-	-	-	-	-	50	50	50	50	50	50	50	50	50	50	50	49	44	39	34	29	-	-	-	-	-	-	-	-	-	
30	-	-	-	-	-	50	50	50	50	50	50	50	50	50	50	50	48	43	38	33	28	-	-	-	-	-	-	-	-	-	-	
31	-	-	-	-	-	50	50	50	50	50	50	50	50	50	50	50	47	42	37	32	27	-	-	-	-	-	-	-	-	-	-	
32	-	-	-	-	-	50	50	50	50	50	50	50	50	50	50	50	46	41	36	31	26	-	-	-	-	-	-	-	-	-	-	
33	-	-	-	-	50	50	50	50	50	50	50	50	50	50	50	49	44	39	34	29	-	-	-	-	-	-	-	-	-	-	-	
34	-	-	-	-	50	50	50	50	50	50	50	50	50	50	50	48	43	38	33	28	-	-	-	-	-	-	-	-	-	-	-	
35	-	-	-	-	50	50	50	50	50	50	50	50	50	50	50	47	42	37	32	27	-	-	-	-	-	-	-	-	-	-	-	
36	-	-	-	-	50	50	50	50	50	50	50	50	50	50	50	46	41	36	31	26	-	-	-	-	-	-	-	-	-	-	-	
37	-	-	-	50	50	50	50	50	50	50	50	50	50	50	45	40	35	30	25	-	-	-	-	-	-	-	-	-	-	-	-	
38	-	-	-	50	50	50	50	50	50	50	50	50	50	50	48	43	38	33	28	-	-	-	-	-	-	-	-	-	-	-	-	
39	-	-	-	50	50	50	50	50	50	50	50	50	50	50	47	42	37	32	27	-	-	-	-	-	-	-	-	-	-	-	-	
40	-	-	-	50	50	50	50	50	50	50	50	50	50	50	46	41	36	31	26	-	-	-	-	-	-	-	-	-	-	-	-	
41	-	-	-	50	50	50	50	50	50	50	50	50	50	50	45	40	35	30	25	-	-	-	-	-	-	-	-	-	-	-	-	
42	-	-	50	50	50	50	50	50	50	50	50	50	50	49	44	39	34	29	-	-	-	-	-	-	-	-	-	-	-	-	-	
43	-	-	50	50	50	50	50	50	50	50	50	50	50	48	43	38	33	28	-	-	-	-	-	-	-	-	-	-	-	-	-	
44	-	-	50	50	50	50	50	50	50	50	50	50	50	47	42	37	32	27	-	-	-	-	-	-	-	-	-	-	-	-	-	

Table HK-3 – Final Set Values per 10 blows (i) with limits between 25mm and 100mm per 10 blows; (ii) $(c_p+c_q)/L \leq 1.15$ where c_p+c_q is in mm; and L is in m; and (iii) S capped at 50mm

By Table HK-3, only Zones D and E are applicable zones. The controlling criteria in Zones A to E are described as follows :

- Zone A : $S > 100$;
- Zone B : $S < 25$;
- Zone C including Zone C1 and C2 is for $(c_p+c_q)/L > 1.15$. Zone C1 is with $S > 50$ and Zone C2 is with $50 \geq S \geq 25$. Zone C2 is acceptable in the previous practice when the new restraint $(c_p+c_q)/L \leq 1.15$ is not imposed;
- Zone D is for $50 \geq S \geq 25$ and $(c_p+c_q)/L \leq 1.15$;
- Zone E is for $100 \geq S > 50$ and $(c_p+c_q)/L \leq 1.15$.

To conclude, comparing with the previous practice, an additional large area of Zone D is added where the calculated value of S is relaxed to 100mm but capped at 50mm but a Zone C2 is excluded due to the imposition of the restraint $(c_p+c_q)/L \leq 1.15$ to avoid overstressing the pile.

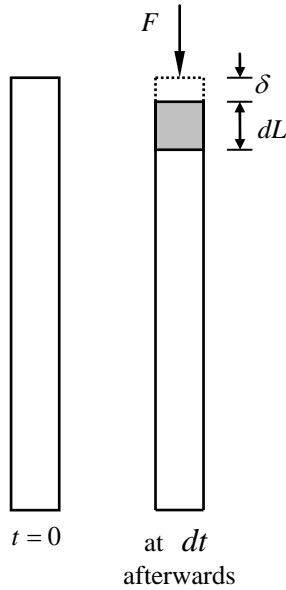
Appendix HL

**More Details and Examples in Wave Equation, the
Case Method and CAPWAP for Analysis of Pile
Capacities**

More Details and Examples in Wave Equation, the Case Method and CAPWAP for Analysis of Pile Capacities

HL.1 Wave Speed in a Pile

The speed of wave in a pile is an important parameter in the determination of pile load capacity by making use of the Wave Equation on the Case Method and CAPWAP analysis. This parameter can be derived as in follows:



Consider a pile being suddenly hit by a force F at time t as shown in Figure HL-1. At the first instant, all of its particles are at rest. But after a short time dt , a certain short rod element of length dL has been compressed which implies the wave has travelled a distance dL . Because of the compression, the end face of the pile has moved a distance δ as shown in the figure:

If the cross sectional area of the Pile is A , its Young's Modulus is E , then $\delta = \varepsilon \cdot dL = \left(\frac{P}{AE} \right) dL$

The change of particle velocity is

$$dv = \frac{\delta}{dt} = \frac{PdL}{AE dt} = \frac{P}{AE} \frac{dL}{dt} = \frac{P}{AE} c$$

where $\frac{dL}{dt} = c$, the wave speed.

Figure HL-1 – Derivation of Wave Speed in Pile

The acceleration is $a = \frac{dv}{dt} = \frac{P}{AE} \frac{c}{dt}$;

As by Newton's Law $F = ma$ and $m = AdL\rho$ where ρ is the density of the pile, so

$$a = \frac{P}{m} = \frac{P}{AdL\rho} \Rightarrow \frac{P}{AE} \frac{c}{dt} = \frac{P}{AdL\rho} \Rightarrow c \frac{dL}{dt} = c^2 = \frac{E}{\rho} \Rightarrow c = \sqrt{\frac{E}{\rho}} \quad (\text{Eqn HL-1})$$

The speed of force wave is therefore about 4000 to 5100m/sec in concrete and steel respectively. The wave speed should not be confused with the actual particle velocity which is comparatively very small, of the order of a few metres per second.

HL.2 The Basic Wave Equation

The Basic Wave Equation is derived as follows :

Consider an element of length ∂x in a pile of cross sectional area A and material density ρ as shown in Figure HL-2. The pile is struck by an external force so that a force acting on the element's upper face is F and that at its lower face is $F + \partial F$.

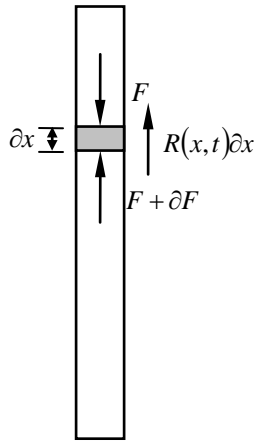


Figure HL-2 – Derivation of the Basic Wave Equation

Further, if u is the displacement of the element and the side friction per unit length is $R(x, t)$ which can also be the end resistance at the pile tip. By Newton's second Law in which Force = mass \times acceleration, we can list:

$$(F + \Delta F) - F + R(x, t)\Delta x = -\rho A \Delta x \frac{\partial^2 u}{\partial t^2}$$

$$\Rightarrow \frac{\partial F}{\partial x} = -\rho A \frac{\partial^2 u}{\partial t^2} - R(x, t) \quad (\text{Eqn HL-2})$$

However, F is also related to the deformation of the pile as

$$F = -AE\varepsilon = -AE \frac{\partial u}{\partial x} \Rightarrow \frac{\partial F}{\partial x} = -AE \frac{\partial^2 u}{\partial x^2} \quad (\text{Eqn HL-3})$$

Combining (Eqn HL-1), (Eqn HL-2) and (Eqn HL-3), we have

$$\frac{\partial^2 u}{\partial t^2} = \frac{E}{\rho} \frac{\partial^2 u}{\partial x^2} + S(x, t) \Rightarrow \frac{\partial^2 u}{\partial t^2} = c^2 \frac{\partial^2 u}{\partial x^2} + S(x, t) \quad (\text{Eqn HL-4})$$

where $S(x, t) = -R(x, t) / \rho A$ is a term related to the shaft and end-bearing resistance of the pile.

The pile driving force will be a boundary condition of (Eqn HL-4) and if $S(x, t)$ is known (even if it is related to the particle movement and velocity of the pile), the particle movement of the pile including the “Set” can be determined. Nevertheless, the equation is often used to back-calculate the pile shaft and end-bearing resistance with known values of measurable quantities such as forces, particle movements, velocities and set.

HL.3 Case Method

The Case Method is based on the basic wave equation (Eqn HL-4). The basic assumptions are as follows :

- (i) The pile is uniform in section and construction material, i.e. the impedance $Z = AE / c$ is constant;
- (ii) The stress wave experiences no energy loss in its transmission through the pile shaft and there are no distortions of signals;
- (iii) The resistance to the dynamic component of the force is at the pile toe only whilst that of the pile shaft is ignored;
- (iv) The resistance to the dynamic component is proportional to the particle velocity;

The following contains derivation of the formulae used in the Method with reference to 王杰賢(2001). If the reader is not interested, he may go directly to HL.3.2 where the symbols used in the formula are fully defined and the application is demonstrated.

HL.3.1 Derivation of the Formula for the Case Method

(Eqn HL-4) describes the particle displacement of the pile at any position x and time t ,

the general solution of the wave equation is given by mathematics as :

$$u(x, t) = h(x - ct) + f(x + ct) \quad (\text{Eqn HL-5})$$

where h and f are arbitrary functions determined by the initial boundary conditions.

Physically h and f may respectively be regarded as the downward and upward waves travelling in opposite directions but with the same speed c as derived in (Eqn HL-1). h and f cannot be measured directly, but the sum of these two waves which is the actual wave in the pile can be measured by the strain gauges and accelerometers in such tests as PDA tests. The shapes of the two waves remain unchanged in their course of transmission. However, at any level of the pile the side resistance R will de-generate into two resistance waves (both of magnitude $0.5R$), one of which is an upward compressive wave and the other is a downward tension wave. The resistance wave serves to increase the resistance and decrease the velocity of the pile at its top. As the total resistance of the pile is the sum of the static and dynamic resistance generated by the striking hammer, the Case Method is to determine the static resistance which is the true resistance of the pile in the course of its service life by wave analysis with a number of assumptions. The following sets out the detailed derivation of the formula to be used.

For the downward particle velocity (the actual moving velocity of the section)

$$v_d = \frac{\partial h(x - ct)}{\partial t} = \frac{\partial h(x - ct)}{\partial x} \cdot \frac{\partial x}{\partial t} = \frac{\partial h(x - ct)}{\partial x} \cdot (-c)$$

$$\text{As strain } \varepsilon_d = \frac{-\partial h(x - ct)}{\partial x} = \frac{v_d}{c}$$

$$\text{the downward force } F_d = AE\varepsilon_d = AE\left(\frac{v_d}{c}\right) = \frac{AE}{c}v_d = Zv_d, \quad (\text{Eqn HL-6})$$

by putting $Z = AE/c$, called the impedance as a mechanical property of the pile.

$$\text{Similarly, it can be deduced that the upward force is } F_u = -Zv_u \quad (\text{Eqn HL-7})$$

where v_u is the upward particle velocity.

So generally, it can be described that the velocity and force at any section of the pile shaft are made up of the upward and downward components as illustrated in Figure HL-3(a). That is:

$$v = v_u + v_d \quad (\text{Eqn HL-8})$$

$$F = F_u + F_d \quad (\text{Eqn HL-9})$$

The individual upward or downward components of the wave cannot be measured directly. Instead, the total sum v and F are measured by the PDA. If the measured velocity and force at any section M are respectively v_M and F_M , by replacing v and F by v_M and F_M and re-arranging (Eqn HL-6) to (Eqn HL-9), we can write :

$$v_d = \frac{1}{2}\left(v_M + \frac{F_M}{Z}\right) \quad (\text{Eqn HL-10})$$

$$v_u = \frac{1}{2}\left(v_M - \frac{F_M}{Z}\right) \quad (\text{Eqn HL-11})$$

$$F_d = \frac{1}{2}(F_M + Zv_M) \quad (\text{Eqn HL-12})$$

$$F_u = \frac{1}{2}(F_M - Zv_M) \quad (\text{Eqn HL-13})$$

At the pile base, if it is free without any base resistance as illustrated in Figure HL-3(b),
 $F = 0$ i.e. $F_u = -F_d$ (Eqn HL-14)

$$v_u = v_d; \quad v = v_u + v_d = 2v_d \quad (\text{Eqn HL-15})$$

At the pile base, if it is restrained from movement as illustrated in Figure HL-3(c)
 $v = 0$ i.e. $v_u + v_d = 0 \Rightarrow v_u = -v_d$ (Eqn HL-16)

$$F_u = F_d; \quad F = F_u + F_d = 2F_d \quad (\text{Eqn HL-17})$$

(Eqn HL-17) is important as it shows by theory that the pile tip penetration force is at most twice the pile axial force during driving. Without this dynamic effect, driving of pile will require a much higher driving force which may damage the pile.

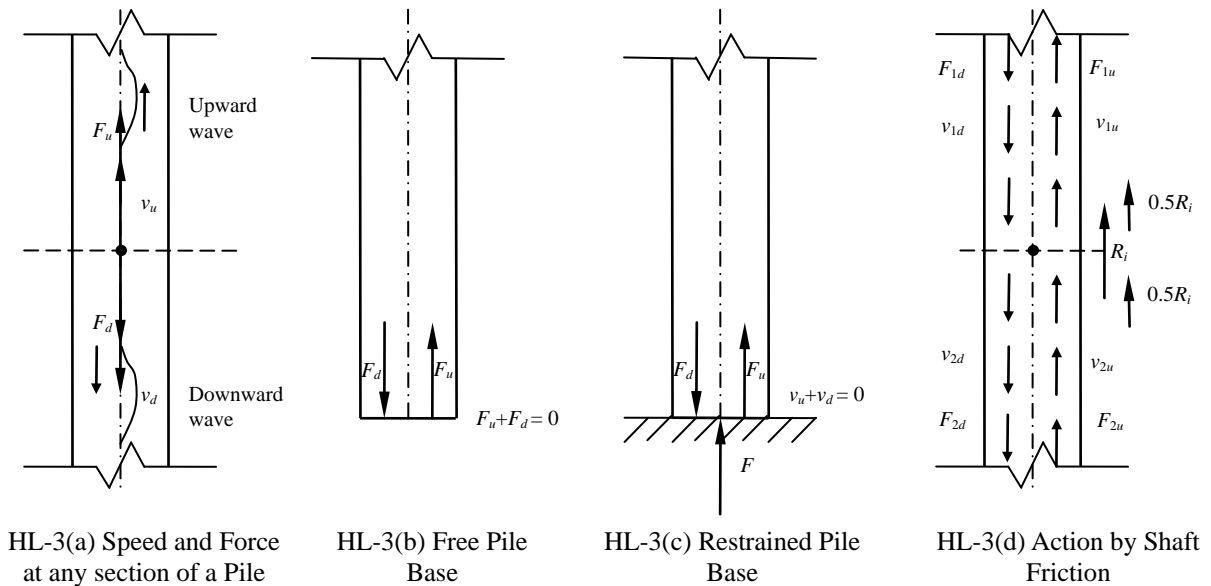


Figure HL-3 – Pile Forces and Velocities

The actual pile base condition will be between “free” and “restrained”, depending on the stiffness of the pile base subgrade. Reference is now made to Figure HL-3(d) for the analysis of side friction. Above and below the section i , the forces and velocities can be formulated as:

$$\text{Above the section:} \quad F_1 = F_{1u} + F_{1d}; \quad v_1 = v_{1u} + v_{1d}; \quad F_1 = -Zv_1 \quad (\text{Eqn HL-18})$$

$$\text{Below the section:} \quad F_2 = F_{2u} + F_{2d}; \quad v_2 = v_{2u} + v_{2d}; \quad F_2 = Zv_2 \quad (\text{Eqn HL-19})$$

$$\text{For equilibrium and compatibility} \quad R_i = F_1 - F_2; \quad v_1 = v_2 \quad (\text{Eqn HL-20})$$

As $R_i = F_1 - F_2 = (F_{1u} + F_{1d}) - (F_{2u} + F_{2d}) = (F_{1u} - F_{2u}) + (F_{1d} - F_{2d})$, and solving (Eqn HL-18) to (Eqn HL-20), $(F_{1u} - F_{2u}) = 0.5R_i$ and $(F_{1d} - F_{2d}) = 0.5R_i$ (Eqn HL-21) implying that R_i is split into 2 equal parts, each of $0.5R_i$. One generates an upward compressive wave and the other a downward tension wave.

Consider Figure HL-4, illustrating the transmission of waves in the pile shaft with particular reference to a section at x_i below ground. The pile is of length L below ground, and its head at height H above ground, cross sectional area A , Young's Modulus E and density ρ (the last two are for determination of wave speed c by (Eqn HL-1)). A sensor is installed at ground level.

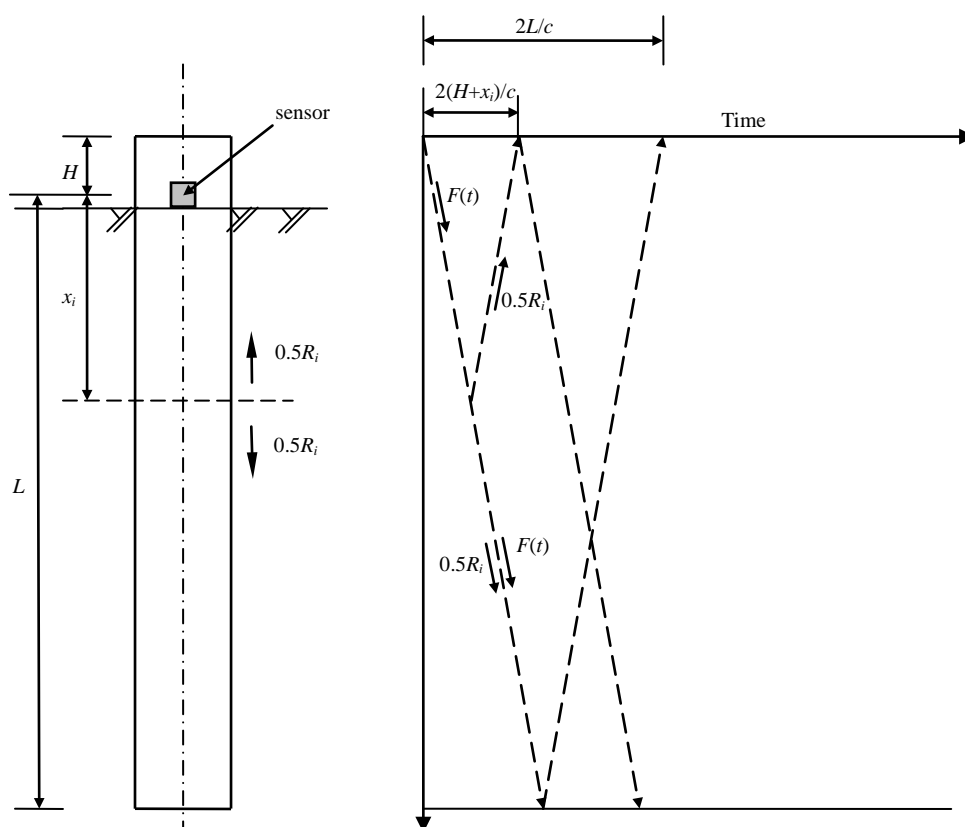


Figure HL-4 – Wave Transmission in Pile Shaft

When the hammer strikes the pile at its top, only a compressive downward wave is created with particle velocity $v_M(t) = F_M(t)/Z$ where $v_M(t)$ and $F_M(t)$ are recorded by the sensor.

When the compressive wave is transmitted to the pile tip which is assumed to be free after time L/c , a reflective wave (tension wave by which $F_u = -F_d = -F$ and $v_u = v_d = v$) is generated and reaches the sensor after time $2L/c$. The wave then subsequently reaches the top level of the pile at which it is reflected back to the sensor at $2(L+H)/c$. So the velocity and force detected by the sensor at time t is due to the wave reaching the sensor at time t and all the previous waves (n numbers) reaching the sensor after reflections at top level and tip of the pile as listed in (Eqn HL-22) and

(Eqn HL-23),

$$v_{MF}(t) = \frac{1}{Z} \left[F(t) + F\left(t - \frac{2L}{c}\right) + F\left(t - \frac{2L}{c} - \frac{2H}{c}\right) + F\left(t - \frac{4L}{c} - \frac{2H}{c}\right) + F\left(t - \frac{4L}{c} - \frac{4H}{c}\right) + \dots \right]$$

$$= \frac{1}{Z} \left[F(t) + \sum_{j=1}^n F\left[t - \frac{2jL}{c} - \frac{2jH}{c}(j-1)\right] + \sum_{j=1}^n F\left[t - \frac{2jL}{c} - \frac{2jH}{c}\right] \right] \quad (\text{Eqn HL-22})$$

$$F_{MF}(t) = F(t) - \sum_{j=1}^n F\left[t - \frac{2jL}{c} - \frac{2jH}{c}(j-1)\right] + \sum_{j=1}^n F\left[t - \frac{2jL}{c} - \frac{2jH}{c}\right] \quad (\text{Eqn HL-23})$$

As for the side friction R at x_i as indicated in Figure HL-4, similar to the generated upward waves, we can put down

$$v_{MRu}(t) = \frac{1}{Z} \left[\left(-\frac{1}{2}\right) \sum_{j=0}^n R_i \left[t - \frac{2x_i}{c} - \frac{2jL}{c} - \frac{2jH}{c}\right] + \left(-\frac{1}{2}\right) \sum_{i=0}^n R_i \left[t - \frac{2x_i}{c} - \frac{2jL}{c} - \frac{2jH}{c}(j-1)\right] \right] \quad (\text{Eqn HL-24})$$

$$F_{MRu}(t) = \frac{1}{2} \left[\sum_{j=0}^n R_i \left[t - \frac{2x_i}{c} - \frac{2jL}{c} - \frac{2jH}{c}\right] - \sum_{i=0}^n R_i \left[t - \frac{2x_i}{c} - \frac{2jL}{c} - \frac{2jH}{c}(j-1)\right] \right] \quad (\text{Eqn HL-25})$$

If there are N segments each giving friction forces R_1, R_2, \dots, R_N , then

$$v_{MRu}(t) = \frac{-1}{2Z} \left[\sum_{i=1}^N \sum_{j=0}^n R_i \left[t - \frac{2x_i}{c} - \frac{2jL}{c} - \frac{2jH}{c}\right] + \sum_{i=1}^N \sum_{j=0}^n R_i \left[t - \frac{2x_i}{c} - \frac{2jL}{c} - \frac{2jH}{c}(j-1)\right] \right] \quad (\text{Eqn HL-26})$$

$$F_{MRu}(t) = \frac{1}{2} \left[\sum_{i=1}^N \sum_{j=0}^n R_i \left[t - \frac{2x_i}{c} - \frac{2jL}{c} - \frac{2jH}{c}\right] - \sum_{i=1}^N \sum_{j=0}^n R_i \left[t - \frac{2x_i}{c} - \frac{2jL}{c} - \frac{2jH}{c}(j-1)\right] \right] \quad (\text{Eqn HL-27})$$

Similarly for the downward waves,

$$v_{MRd}(t) = \frac{-1}{2Z} \left[\sum_{i=1}^N \sum_{j=0}^n R_i \left[t - \frac{2x_i}{c} - \frac{2jL}{c} - \frac{2jH}{c}(j-1)\right] + \sum_{i=1}^N \sum_{j=0}^n R_i \left[t - \frac{2x_i}{c} - \frac{2jL}{c} - \frac{2jH}{c}\right] \right] \quad (\text{Eqn HL-28})$$

$$F_{MRd}(t) = \frac{1}{2} \left[\sum_{i=1}^N \sum_{j=0}^n R_i \left[t - \frac{2x_i}{c} - \frac{2jL}{c} - \frac{2jH}{c}(j-1)\right] - \sum_{i=1}^N \sum_{j=0}^n R_i \left[t - \frac{2x_i}{c} - \frac{2jL}{c} - \frac{2jH}{c}\right] \right] \quad (\text{Eqn HL-29})$$

The signal v_M and F_M as detected by the sensor is the sum of the above.

$$v_M = v_{MF} + v_{MRu} + v_{MRd} \quad (\text{Eqn HL-30})$$

$$F_M = F_{MF} + F_{MRu} + F_{MRd} \quad (\text{Eqn HL-31})$$

Energy loss in the form of radiating damping to the surrounding has been ignored in the above derivation. So error can be more significant if the testing time is long involving many time steps.

Consider only times at t_1 and $t_1 + \frac{2L}{c}$ where the signals $v_M(t_1)$, $F_M(t_1)$, $v_M\left(t_1 + \frac{2L}{c}\right)$, $F_M\left(t_1 + \frac{2L}{c}\right)$ are taken are added up (with the v_M multiplied by Z for matching of units) and by (Eqn HL-22) to (Eqn HL-29), we can arrive at

$$F_M(t_1) + F_M\left(t_1 + \frac{2L}{c}\right) + Zv_M(t_1) - Zv_M\left(t_1 + \frac{2L}{c}\right) = \sum_{i=1}^N R_i(t_1) + \sum_{i=1}^N R_i\left(t_1 + \frac{2L}{c} - \frac{2x_i}{c}\right) \quad (\text{Eqn HL-32})$$

Assuming R_i is constant, i.e. $R_i(t_1) = R_i\left(t_1 + \frac{2L}{c} - \frac{2x_i}{c}\right)$

So the total pile shaft resistance $R_T = \frac{1}{2} \left[\sum_{i=1}^N R_i(t_1) + \sum_{i=1}^N R_i\left(t_1 + \frac{2L}{c} - \frac{2x_i}{c}\right) \right]$

$$\Rightarrow R_T = \frac{1}{2} \left[F_M(t_1) + F_M\left(t_1 + \frac{2L}{c}\right) \right] + \frac{Z}{2} \left[v_M(t_1) - v_M\left(t_1 + \frac{2L}{c}\right) \right] \quad (\text{Eqn HL-33})$$

(Eqn HL-33) represents the basic equation for the Case Method. However, R_T comprises both the static and dynamic components, i.e.

$$R_T = R_{static} + R_{dynamic} \Rightarrow R_{static} = R_T - R_{dynamic} \quad (\text{Eqn HL-34})$$

R_{static} is to be found, which is the capacity of the pile during its service life.

Assuming $R_{dynamic}$ originated from the pile tip and that $R_{dynamic}$ is directly proportional to the velocity where the constant of proportionality is a “damping coefficient” J_p . That is

$$R_{dynamic}(t) = J_p v_{toe}(t) \quad (\text{Eqn HL-35})$$

When the wave generated by the blow at top reaches the pile tip, we can write

$$F_{toe} = F_M(t) - \frac{1}{2} \sum_{i=1}^N R_i(t) = F_M(t) - \frac{1}{2} R_T(t) \quad (\text{Eqn HL-36})$$

$$v_{toe} = 2v_d = 2 \frac{F_{toe}}{Z} = \frac{2}{Z} \left[F_M(t) - \frac{1}{2} R_T(t) \right] = \frac{1}{Z} [2F_M(t) - R_T(t)] \quad (\text{Eqn HL-37})$$

Putting $J_c = J_p / Z$ which is called the “Lumped Case Damping Factor” and substituting (Eqn HL-33), (Eqn HL-35) and (Eqn HL-37) into (Eqn HL-34)

$$R_{static}(t_1) = \frac{1}{2} \left[F_M(t_1) + F_M\left(t_1 + \frac{2L}{c}\right) \right] + \frac{Z}{2} \left[v_M(t_1) - v_M\left(t_1 + \frac{2L}{c}\right) \right]$$

$$- J_c Z \times \frac{1}{Z} \left[2F_M(t) - \frac{1}{2} \left[F_M(t_1) + F_M\left(t_1 + \frac{2L}{c}\right) \right] - \frac{Z}{2} \left[v_M(t_1) - v_M\left(t_1 + \frac{2L}{c}\right) \right] \right]$$

After simplifying, the static component of resistance of the pile at time t_1 is

$$R_{static}(t_1) = \frac{(1 - J_c)}{2} [F_M(t_1) + Zv_M(t_1)] + \frac{(1 + J_c)}{2} \left[F_M\left(t_1 + \frac{2L}{c}\right) - Zv_M\left(t_1 + \frac{2L}{c}\right) \right] \quad (\text{Eqn HL-38})$$

HL.3.2 Application of the Case Formula

The Case Formula for the ultimate static resistance of the Pile is as follows :

$$R_{static}(t_1) = \frac{(1-J_c)}{2} [F_M(t_1) + Zv_M(t_1)] + \frac{(1+J_c)}{2} \left[F_M\left(t_1 + \frac{2L}{c}\right) - Zv_M\left(t_1 + \frac{2L}{c}\right) \right] \quad (\text{Eqn HL-38})$$

By (Eqn HL-38), the ultimate static resistance of the pile at time t_1 can be estimated if the Pile Driving Analyzer (PDA) can produce readings of forces and velocities at time t_1 (any chosen time) and $t_1 + \frac{2L}{c}$ which are $F_M(t_1)$, $v_M(t_1)$; $F_M\left(t_1 + \frac{2L}{c}\right)$, $v_M\left(t_1 + \frac{2L}{c}\right)$ and with the assumed values of J_c . In the equation, the following symbols are re-iterated :

R_{static}	is the static resistance of the pile at pile at time t_1 ;
J_c	is the “Lumped Case Damping Factor” which need to be assumed or calibrated;
L	is the length of the pile below ground;
c	is the wave velocity in the pile shaft and can be determined by $c = \sqrt{E/\rho}$ where E and ρ are respectively the Young’s Modulus and density (mass, not weight per unit volume) of the pile material;
Z	is the impedance of the pile determined by $Z = AE/c$ where A is the cross sectional area of the pile;
$F_M(t_1)$	is the force reading detected by the PDA sensor at time t_1 ;
$v_M(t_1)$	is the velocity reading detected by the PDA sensor at time t_1 ;
$F_M\left(t_1 + \frac{2L}{c}\right)$	is the force reading detected by the PDA sensor at time $t_1 + \frac{2L}{c}$;
$v_M\left(t_1 + \frac{2L}{c}\right)$	is the velocity reading detected by the PDA sensor at time $t_1 + \frac{2L}{c}$

A worked example to demonstrate the use of the formula using a hypothetical pile is as follows :

Data :

The pile is 305×305×223 S450 H-pile

Cross section area of pile : $A = 284.8 \text{ cm}^2$;

Length of the Pile below ground : $L = 46.8 \text{ m}$;

Young’s Modulus of Steel : $E = 205000 \text{ MPa}$

Density of Pile : 78.5 kN/m^3 which is actually $78500 \div 9.807 = 8010 \text{ kg/m}^3$

Wave velocity in pile shaft is $c = \sqrt{E/\rho} = \sqrt{205000 \times 10^6 / 8010} = 5060.6 \text{ m/sec}$;

Impedance $Z = AE/c = 0.02848 \times 205000000 / 5060.6 = 1153.7 \text{ kNsec/m}$

Time interval $2L/c = 2 \times 46.8 / 5060.6 = 0.0184 \text{ sec} = 18.4 \text{ ms}$;

The following graph in Figure HL-5 shows the plot of the measured forces and velocities at the top level of a pile (length 46.8m) by a typical PDA test during a particular blow by a hammer. The first peaks of force and velocity indicate the peak values upon the arrival of the wave at the top without reflection and the later wave forms are results of superimposition of the upward and downward waves comprising reflected waves. The second peak in the force wave after time 18.40msec is likely due to superimposition of the reflected wave generated at the pile tip.

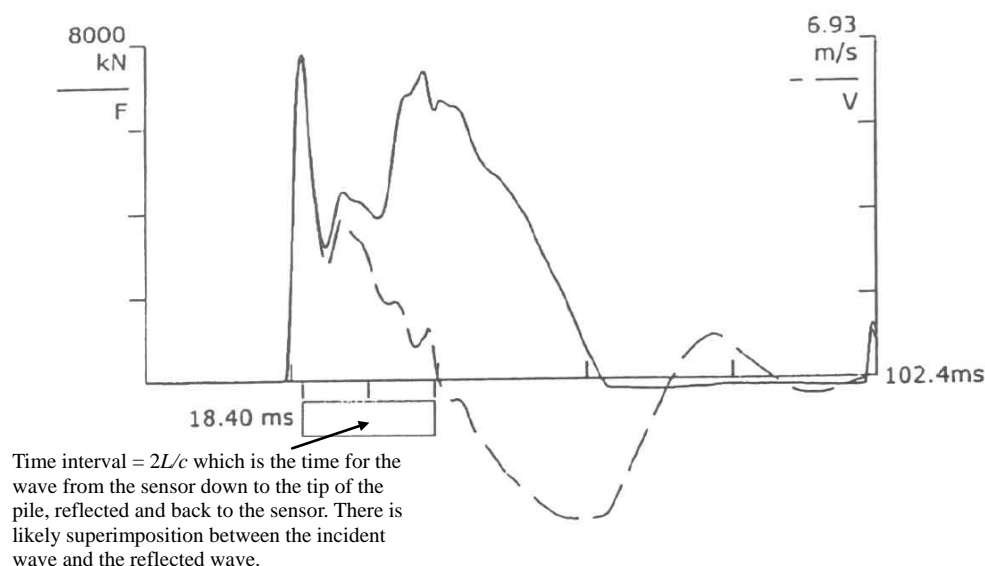


Figure HL-5 – Typical Plot of Measured Forces and Velocities of a Pile by PDA Test

The recorded values are tabulated in the following table and the ultimate static resistances of the pile for J_c varying from 0.4 to 0.9 are calculated in accordance with (Eqn HL-38).

In the table, $t_{c1} = t_1 + 2L/c = t_1 + 18.4$ msec.

Time after 1 st max Force (t_1) (msec)	$F_M(t_1)$ (kN)	$v_M(t_1)$ (m/sec)	$F_M(t_{c1})$ (kN)	$v_M(t_{c1})$ (m/sec)	Static Resistance (kN)					
					$J_c = 0.4$	$J_c = 0.5$	$J_c = 0.6$	$J_c = 0.7$	$J_c = 0.8$	$J_c = 0.9$
0	7750	6.66	6400	0.53	8682.07	8199.82	7717.56	7235.30	6753.05	6270.79
3.68	3200	2.45	6350	-0.43	6600.23	6641.21	6682.19	6723.16	6764.14	6805.12
7.36	4185	2.88	4923	-1.52	6925.93	6884.38	6842.83	6801.28	6759.73	6718.18
11.04	4050	1.6	3125	-2.17	5708.75	5695.38	5682.01	5668.64	5655.27	5641.90
14.72	6875	0.87	3125	-2.60	6650.85	6563.15	6475.44	6387.74	6300.03	6212.33
18.40	6400	0.53	1750	-2.92	5686.60	5591.97	5497.34	5402.70	5308.07	5213.44
Maximum Resistance					8682.07	8199.82	7717.56	7235.30	6764.14	6805.12

Table HL-1 – Estimation of Ultimate Static Resistance of a Hypothetical Pile by the Case Method

The appropriate value of J_c is dependent on the type of soil at the pile toe. GEO Publication 1/2006 quotes values ranging from 0.05 for clean sand to 1.1 for clay in its Table 9.2. For an appropriate chosen value of J_c , the ultimate static resistance of the

pile should be the maximum value identified for choices of t_1 as listed in the last row of Table HL-1.

HL.4 CAPWAP (Case Pile Wave Analysis Programme)

Figure HL-6 shows schematically the “Smith Model” for dynamic analysis of a pile. In the model the pile is idealized into a series of “lumped masses” connected by elastic springs. In the wave equation analysis, the set and the ultimate static resistance of the pile can be calculated under the assumed values of various parameters during driving.

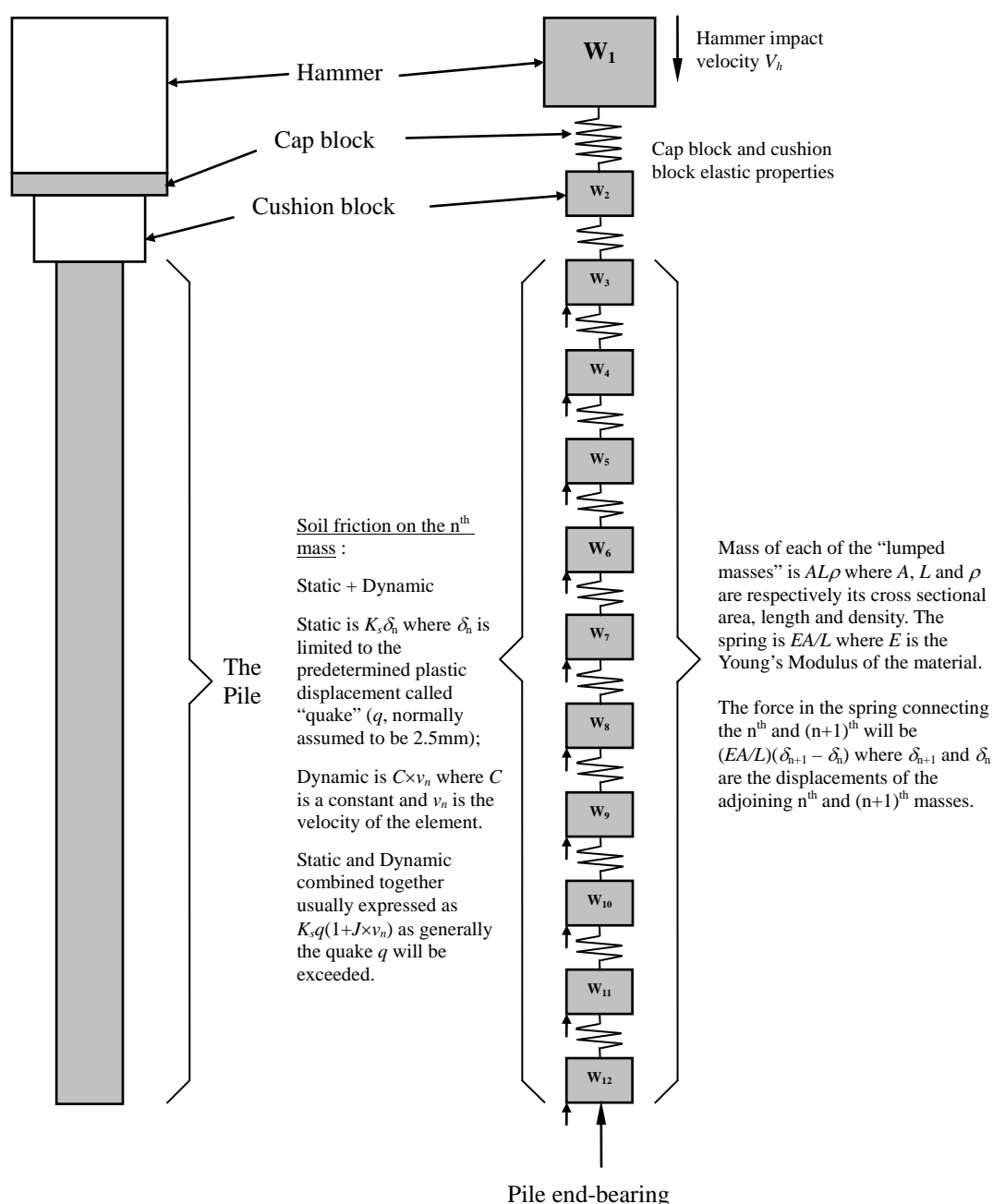


Figure HL-6 – Smith’s Idealization of Pile

The Smith's idealization can be applied by solving (Eqn HL-4) mathematically, by technique such as the finite difference method. If the soil parameters are given, (Eqn HL-4) can be solved directly to give the pile particle displacements and subsequently the particle velocity, set and axial force during pile driving. This is an alternative to the use of Hiley's formula in determining the set before pile driving. On site, the pile driving force and velocity of the wave (combined downward and upward component) can be measured by techniques such as PDA.

In the CAPWAP analysis, the matching of forces and velocities with time between the measured values and those calculated values by the wave equation (transformed into a numerical approach developed by Smith (1960)) under various sets of assumed parameters can be done for a pre-determined hammer blow. Good matching can justify the validity of the assumed parameters and thus the ultimate static resistance of the pile can be calculated. The following Figure HL-7 shows good matching between the measured force and the calculated force and measured velocity with computed velocity using the wave equation (in numerical form) for an actual blow on a pile.

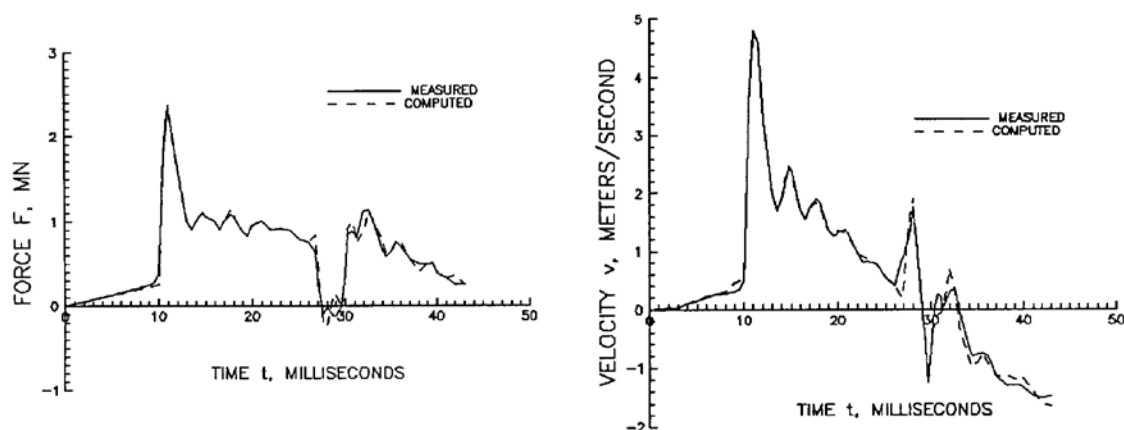


Figure HL-7 – Typical Graphs showing Good Matching between the Measured Forces and Calculated Forces with Time

HL.5 Pile Integrity as Revealed by the PDA Test

Another function of the PDA test is the assessment of pile shaft integrity through the examination of anomalies in the wave forms. Figure HL-8 displays the wave forms of a force wave (the P wave) and a $Z \cdot v$ wave (impedance as defined by (Eqn HL-6) times wave velocity which is a force generated by the wave where the particle velocity is v) obtained in a PDA test of a steel H-pile. The crossing of the P curve and $Z \cdot v$ curves indicates an anomaly and the integrity number is estimated to be 0.8. The depth of the anomaly below ground can also be located which is the arithmetic product of the wave speed and the time between the start of the test and the time when the reflected wave has reached the sensor at the top. The wave speed is a constant for a material which is 5060 m/sec in steel.

The pile is finally extracted from the ground and it is noticed that it is bent as shown in the photograph also in Figure HL-8, the location of which agrees with the assessment described above.

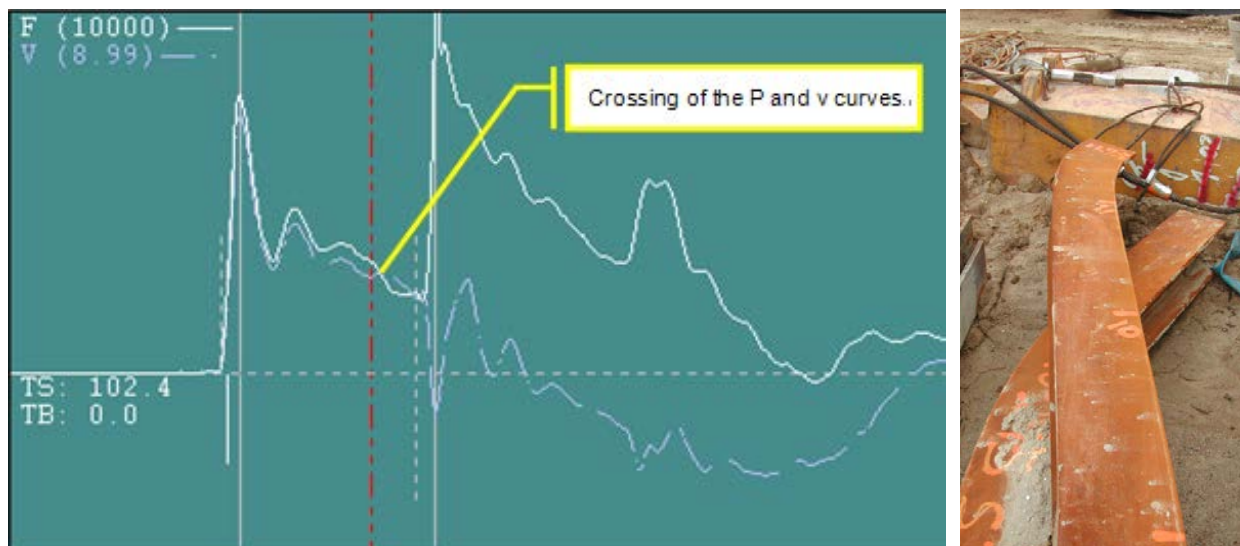


Figure HL-8 – Wave Forms of P and $Z \cdot v$ of a Pile undergoing PDA Test and Photograph showing the Defected Portion

Appendix HM

Closed Form Solution for the Bearing Capacity

Factor N_q in accordance with Berezantsev

Closed Form Solution for the Bearing Capacity Factor N_q in accordance with Berezantsev

HM.1 General Review of Bearing Capacity Factors for End Bearing Piles

As a well known phenomenon, a pile can develop very substantial end bearing capacity in soil at depth due to the high surcharge by the weight of the surrounding soil. As a common design approach by most of the researchers, the ultimate bearing capacity of pile in cohesionless soil is related to the effective overburden pressure at the pile base and the pile base area as

$$Q_b = N_q \sigma'_v A_b \quad (\text{Eqn HM-1})$$

where σ'_v is the effective overburden pressure at the pile base

A_b is the pile base area

N_q is the bearing capacity factor

While it is easy to determine σ'_v and A_b , the determination of N_q is much more difficult. Researchers including Terzaghi, Meyerhof, Vesic and Berezantsev had put forward different formulae, charts for determination of N_q as shown in Figure HM-1 based on different failure modes with some of which shown in Figure HM-2.

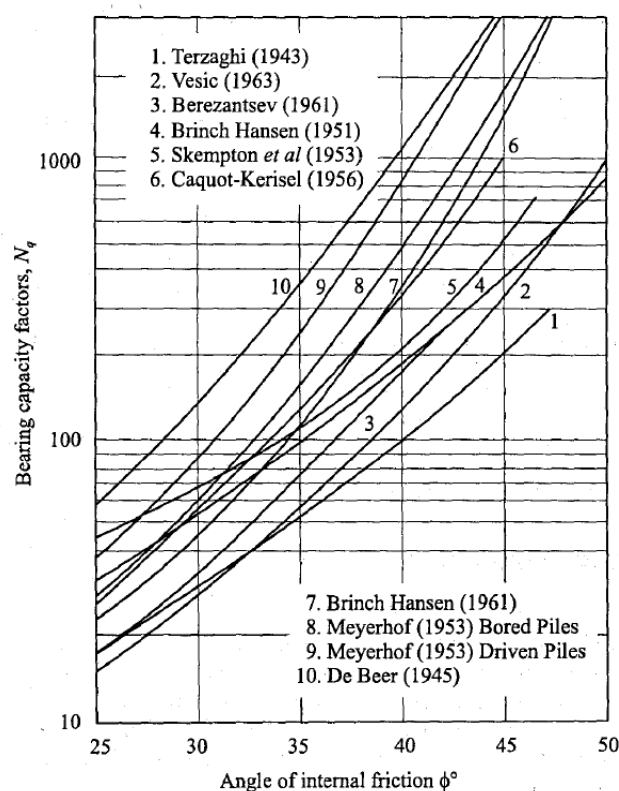


Figure HM-1 – Bearing Capacity Factor N_q for Circular Foundations
(after Kezdi, 1975)

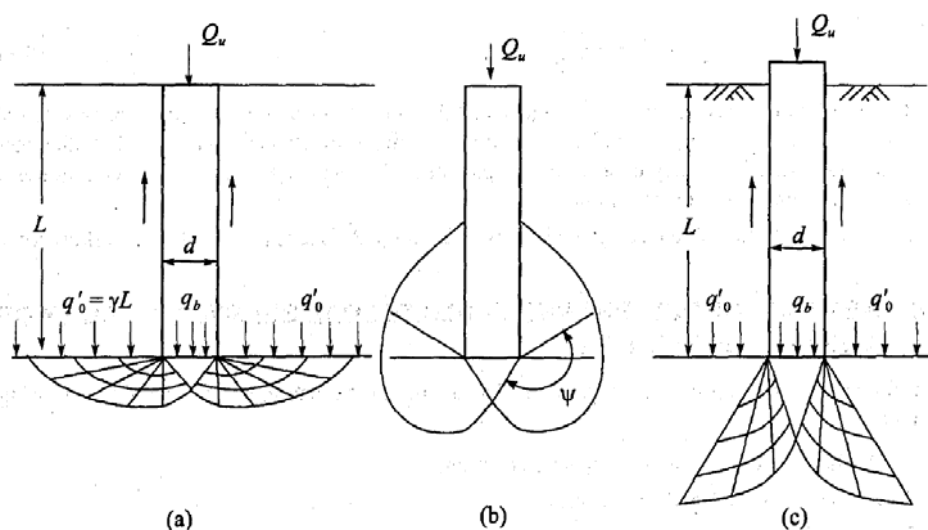


Figure HM-2 – The Shapes of Failure Modes at the Pile Tips as assumed by (a) Terzaghi and Berezantsev; (b) Meyerhof; (c) Vesic

The N_q depends on ϕ which is the angle of shearing resistance of soil, as adopted by all researchers. But in fact, N_q also depends on the L/d ratio which is ratio of the depth of penetration of the pile to its diameter, though the parameter L/d has been ignored in many design charts including Figure HM-1. Nevertheless, Tomlinson (2008) has included the L/d values for the work by Berezantsev and Brinch Hansen as indicated in Figure HM-3.

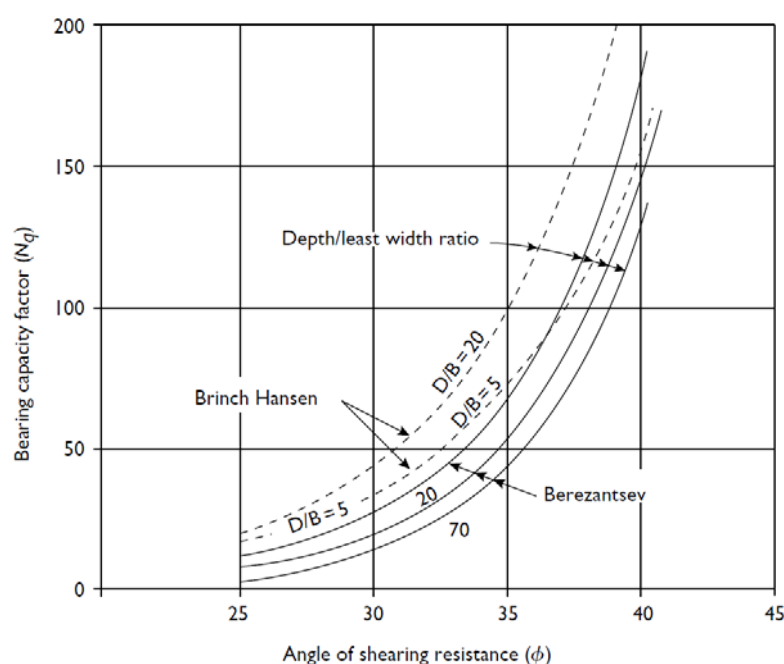


Figure HM-3 –Bearing Capacity Factors of Berezantsev and Brinch Hansen (after Tomlinson 2008)

As the original derivation of the formulae for determination of N_q were usually lengthy and complicated, use of these charts was comparatively convenient before the era of computers. However, it should be even more convenient and accurate to use computer to calculate the N_q values based on the original formulae nowadays. Law & Li (2017) has outlined the analytical procedure for determination of N_q by Berezantsev (1961) which is reproduced as follows. The analysis is easy to perform on spreadsheets.

HM.2 Analytical Procedure for N_q to Berezantsev's Approach

Law & Li (2017) has referred to 鄭大同 (1979) which was based on Berezantsev et al (1961) to derive the following procedures for the determination of N_q a function of ϕ and L/d ratio. The detailed derivations of the equations are omitted.

(i) Determine the l/a ratio as $l/a = \sqrt{2}e^{\left(\frac{\pi}{4} - \frac{\phi}{2}\right)\tan\frac{\phi}{2}} / \sin\left(\frac{\pi}{4} - \frac{\phi}{2}\right)$ (Eqn HM-2)

where $a = 0.5d$

(ii) Determine $k_1 = l_o/d = l/d + 0.5$ where $l_o = l + a$ (Eqn HM-3)

(iii) Determine $\lambda = 2 \tan \phi \tan\left(\frac{\pi}{4} + \frac{\phi}{2}\right)$ (Eqn HM-4)

(iv) Determine

$$E_D = \frac{1}{\lambda - 1} \left[\tan\left(\frac{\pi}{4} - \frac{\phi}{2}\right) k_1 + \frac{\tan^2\left(\frac{\pi}{4} - \frac{\phi}{2}\right) \left(\frac{L}{d} + k_1 \cot\left(\frac{\pi}{4} - \frac{\phi}{2}\right)\right)^2}{\left(\frac{1}{k_1} \tan\left(\frac{\pi}{4} - \frac{\phi}{2}\right) \frac{L}{d} + 1\right)^\lambda (\lambda - 2) \left(\frac{L}{d}\right)} - \frac{k_1^2}{(\lambda - 2) \left(\frac{L}{d}\right)} \right] \quad (\text{Eqn HM-5})$$

(v) Determine $\alpha_T = \left(\frac{k_1^2 - 0.25 - E_D 2k_1 \tan \phi}{k_1^2 - 0.25} \right)$ (Eqn HM-6)

(vi) Determine $M = \frac{\left[\sin\left(\frac{\pi}{4} - \frac{\phi}{2}\right) + \sqrt{2}e^{\left(\frac{\pi}{2} - \frac{\phi}{2}\right)\tan\left(\frac{\phi}{2}\right)} \right] \cos\left(\frac{\phi}{2}\right)}{\left[\cos\left(\frac{\phi}{2}\right) + e^{\left(\frac{\pi}{2} - \frac{\phi}{2}\right)\tan\left(\frac{\phi}{2}\right)} \right] \sin\left(\frac{\pi}{4} - \frac{\phi}{2}\right)}$ (Eqn HM-7)

(vii) Determine $\omega = 2 \tan \phi \tan\left(\frac{\pi}{4} - \frac{\phi}{2}\right)$ (Eqn HM-8)

$$(viii) \text{ Determine } A_k = \frac{1 + \sin \phi}{3} \left\{ \begin{aligned} & \frac{\cos(0.5\phi) + e^{(0.5\pi - 0.5\phi)\tan(0.5\phi)}}{(\omega + 1)\cos\phi\cos(0.5\phi)} (M^{\omega+1} - 1) e^{1.5\pi\tan\phi} \\ & - 0.77 \cot\phi \left[\left(\frac{\pi}{4} - \frac{\phi}{2} \right) e^{1.5\pi\tan\phi} - \left(\frac{3\pi}{4} - \frac{\phi}{2} \right) \right] \\ & + \cot\phi (1.2 - 0.26 \cot\phi) (e^{1.5\pi\tan\phi} - 1) \end{aligned} \right\} \quad (\text{Eqn HM-9})$$

$$(ix) \text{ Determine } B_k = \frac{1}{3} \times \frac{1 + \sin \phi}{1 - \sin \phi} e^{\pi \tan \phi} (1.5 + M^{\omega} e^{\pi \tan \phi}) \quad (\text{Eqn HM-10})$$

$$(x) \text{ Finally, } N_q = \left(\frac{1}{L/d} \right) \left(\frac{1}{2} A_k + B_k \alpha_T \frac{L}{d} \right) \quad (\text{Eqn HM-11})$$

Nevertheless, it should be noted that E_D in (Eqn HM-5) cannot be directly calculated when $\phi = 30^\circ$ which will lead to $\lambda = 2$ by (Eqn HM-4) and subsequently the sum of the last 2 terms of E_D becomes zero divided by zero which is indeterminate. A good approximation is to calculate N_q as average of $\phi = 30.05^\circ$ and $\phi = 29.95^\circ$. An exact approach is to find the limit of the sum of the last 2 terms (for $\phi = 30^\circ$ only) so that

$$E_D = \frac{1}{\lambda - 1} \left[\tan \left(\frac{\pi}{4} - \frac{\phi}{2} \right) k_1 + \frac{Y + Z \ln(X)}{X^3 (L/d) (\lambda - 1)} \right]$$

where $X = 3.464101615(L/d) + 15.050157522$

$$Y = 58155.992 + 40157.374(L/d) + 9243.041(L/d)^2 + 709.158(L/d)^3$$

$$Z = -21448.787 - 14810.631(L/d) - 3408.97(L/d)^2 - 261.548(L/d)^3$$

Using the above, Figure HM-4 as follows is constructed which agrees very well with Tomlinson (2008).

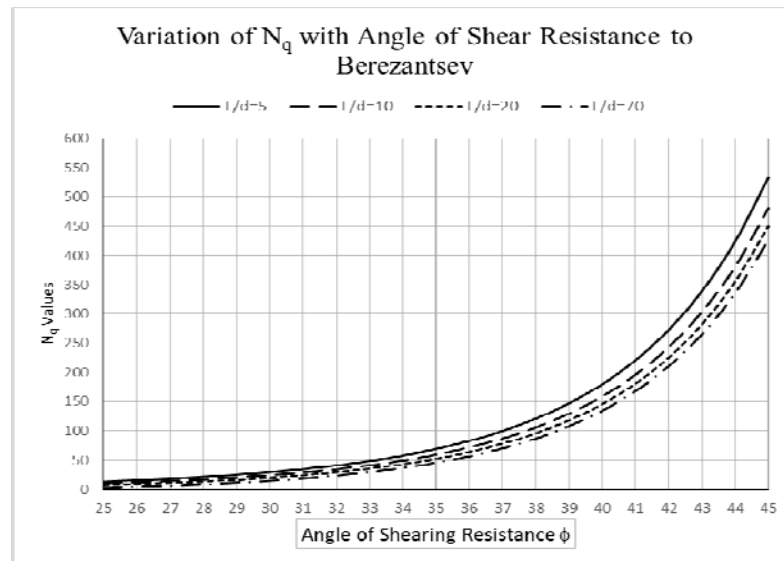


Figure HM-4 – Variation of N_q with ϕ at Different L/d ratios to Berezantsev

HM.5 Worked Example HM-1

Find N_q if $\phi = 35^\circ$ and $L/d = 10$

$$l/a = \sqrt{2} e^{\left(\frac{\pi}{4} - \frac{\phi}{2}\right) \tan \frac{\phi}{2}} / \sin\left(\frac{\pi}{4} - \frac{\phi}{2}\right) = 4.564$$

$$l/d = 0.5(l/a) = 2.282$$

$$k_1 = l/d + 0.5 = 2.782$$

$$\lambda = 2 \tan \phi \tan\left(\frac{\pi}{4} + \frac{\phi}{2}\right) = 2.690$$

$$E_D = \frac{1}{\lambda - 1} \left[\tan\left(\frac{\pi}{4} - \frac{\phi}{2}\right) k_1 + \frac{\tan^2\left(\frac{\pi}{4} - \frac{\phi}{2}\right) \left(\frac{L}{d} + k_1 \cot\left(\frac{\pi}{4} - \frac{\phi}{2}\right)\right)^2}{\left(\frac{1}{k_1} \tan\left(\frac{\pi}{4} - \frac{\phi}{2}\right) \frac{L}{d} + 1\right)^\lambda (\lambda - 2) \left(\frac{L}{d}\right)} - \frac{k_1^2}{(\lambda - 2) \left(\frac{L}{d}\right)} \right]$$

$$= 0.514$$

$$\alpha_T = \left(\frac{k_1^2 - 0.25 - E_D 2k_1 \tan \phi}{k_1^2 - 0.25} \right) = 0.733$$

$$M = \frac{\left[\sin\left(\frac{\pi}{4} - \frac{\phi}{2}\right) + \sqrt{2} e^{\left(\frac{\pi}{2} - \frac{\phi}{2}\right) \tan\left(\frac{\phi}{2}\right)} \right] \cos\left(\frac{\phi}{2}\right)}{\left[\cos\left(\frac{\phi}{2}\right) + e^{\left(\frac{\pi}{2} - \frac{\phi}{2}\right) \tan\left(\frac{\phi}{2}\right)} \right] \sin\left(\frac{\pi}{4} - \frac{\phi}{2}\right)} = 2.171$$

$$\omega = 2 \tan \phi \tan\left(\frac{\pi}{4} - \frac{\phi}{2}\right) = 0.729$$

$$A_k = \frac{1 + \sin \phi}{3} \left\{ \frac{\cos(0.5\phi) + e^{(0.5\pi - 0.5\phi) \tan(0.5\phi)}}{(\omega + 1) \cos \phi \cos(0.5\phi)} (M^{\omega+1} - 1) e^{1.5\pi \tan \phi} \right. \\ \left. - 0.77 \cot \phi \left[\left(\frac{\pi}{4} - \frac{\phi}{2}\right) e^{1.5\pi \tan \phi} - \left(\frac{3\pi}{4} - \frac{\phi}{2}\right) \right] \right. \\ \left. + \cot \phi (1.2 - 0.26 \cot \phi) (e^{1.5\pi \tan \phi} - 1) \right\} = 82.454$$

$$B_k = \frac{1}{3} \times \frac{1 + \sin \phi}{1 - \sin \phi} e^{\pi \tan \phi} (1.5 + M^\omega e^{\pi \tan \phi}) = 75.319$$

$$\therefore N_q = \left(\frac{1}{L/d} \right) \left(\frac{1}{2} A_k + B_k \alpha_T \frac{L}{d} \right) = 59.313$$

Appendix HN

Worked Examples for Determination of Ultimate Uplift Resistance of Piles

Worked Examples for Determination of Ultimate Uplift Resistance of Piles

HN.1 Useful Mathematical Expressions for Determination of Geometry of Anchorages by Soil and Rock against Uplift of Piles

Due to overlapping of the soil columns and rock cones for piles against uplift as illustrated by Figures 5.1 and 5.2 of the Code, the shaded portions of the soil column and rock cone on the top right portion of Figure HN-1 should be deducted from calculation of effective weight for a pile against uplift. Mathematical expressions for the determination of the geometric volumes of the overlapped portions are presented in the first part of this appendix.

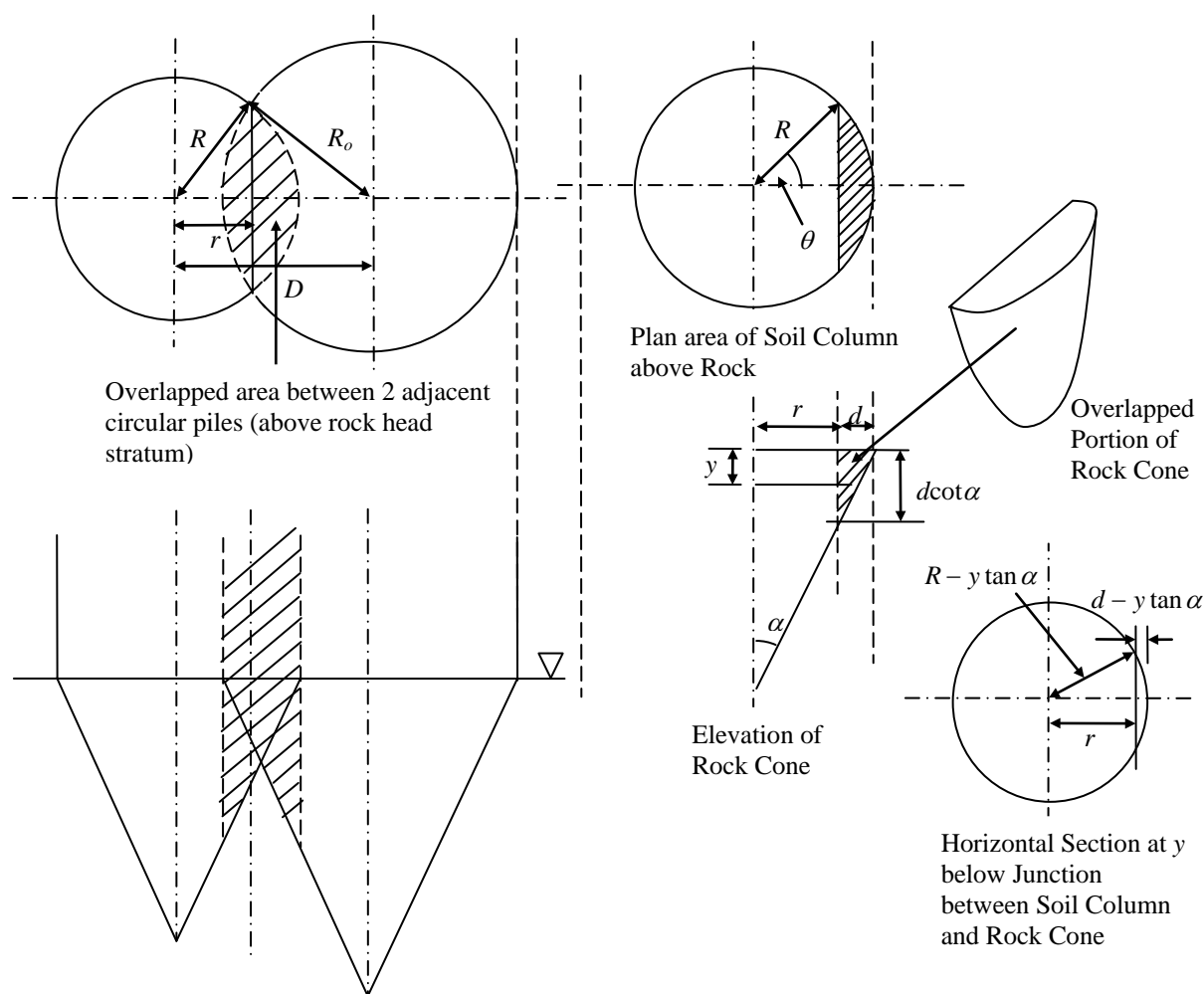


Figure HN-1 – Geometrical Shapes due to Overlapping of Soil Columns and Rock Cones of Two Adjacent Circular Piles

Consider a circular pile with R as its radius of the soil column as shown in Figure 5.1 of the Code. If its soil column overlaps with another pile of radius of soil column R_o with centre to centre distance D as shown in the top left portion of Figure HN-1, the distance r can be determined through the application of the cosine rule as

$$r = R \cos \theta = \frac{R^2 + D^2 - R_o^2}{2D} \quad (\text{Eqn HN-1})$$

Referring to the top right portion of Figure HN-1, the area of shaded portion is

$$A_s = \frac{1}{2} R^2 (2\theta) - r \sqrt{R^2 - r^2} = R^2 \sin^{-1} \left(\frac{\sqrt{R^2 - r^2}}{R} \right) - r \sqrt{R^2 - r^2} \quad (\text{Eqn HN-2})$$

The volume of the overlapped portion of the soil column is

$$V_s = A_s L \quad (\text{Eqn HN-3})$$

Below the rock head level, the overlapped portion will be that beyond a vertical plane at r from the centre a height of $d \cot \alpha$ as illustrated in Figure HN-2, with α limited to 30° by the Code. Consider an “elementary slice” at depth y beneath rock head stratum, the radius of the elementary slice is $R - y \tan \alpha$ and the width beyond “touching line” with the adjacent circular pile is $d - y \tan \alpha$ as illustrated in Figure HN-2. So the area of the overlapped portion by (Eqn HN-2) for one pile is

$$A(y) = [R - y \tan \alpha]^2 \sin^{-1} \left(\frac{\sqrt{(R - y \tan \alpha)^2 - r^2}}{R - y \tan \alpha} \right) - r \sqrt{(R - y \tan \alpha)^2 - r^2}$$

The volume of the elementary slice will be $A(y)dy$. Integrating over the height of overlapping of $d \cot \alpha$, the volume of the overlapping portion of the rock cone is

$$V_r = \int_0^{d \cot \alpha} A(y) dy$$

Analytically, the result is

$$V_r = \frac{\cot \alpha}{3} \left[r^3 \ln \left(\frac{r}{R - \sqrt{R^2 - r^2}} \right) + R^3 \sin^{-1} \left(\frac{\sqrt{R^2 - r^2}}{R} \right) - 2Rr \sqrt{R^2 - r^2} \right] \quad (\text{Eqn HN-4})$$

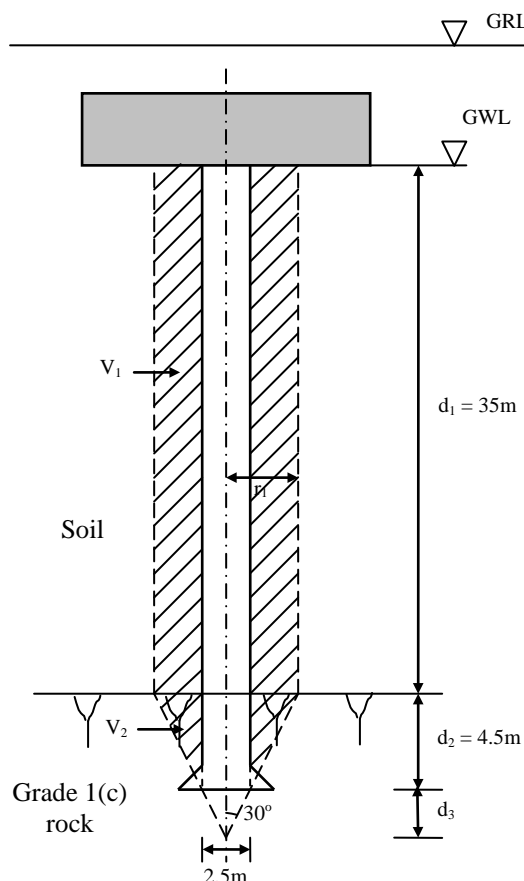
Nevertheless, an estimate can be obtained by treating the overlapping portion as a pyramid which results in a smaller value and subsequently a smaller deduction for the final effective weight, so

$$V_r \approx \frac{d \cot \alpha}{3} A_s \quad (\text{Eqn HN-5})$$

where A_s is taken from (Eqn HN-2).

The above geometric expressions can be used to evaluate the volume of soil columns and rock cones as required by clause 5.3.3 of the Code.

HN.2 Worked Example HN-1 – Ultimate Uplift Resistance of a Single Large Diameter Bored Pile by Weight of Rock Cone and Soil Column



Pile Loading

D.L. =	30000kN
D _{min} =	26000kN
LL =	12000kN
Wind W =	12000kN
Uplift, U =	14500kN

Density of Soil taken as 19kN/m^3
 Density of Rock taken as 22 kN/m^3
 Density of concrete taken as 24.5kN/m^3
 Density of water taken as 9.8kN/m^3

Ground Water Level : at Underside of
Pile Cap

Rock anchoring the pile is Grade 1(c)

Figure HN-2 – Worked Example for Checking Uplift of a Large Diameter Bored Pile

Check for Allowable Bond Resistance to Table 2.2 of the Code (under permanent tension condition)

Allowable Bond Resistance from Rock $R_{\text{bond}} = 2.5 \times \pi \times 4.5 \times 350 = 12370.02 \text{ kN}$

Check for Ground Resistance to Figure H5.3(a)

From the above Figure HN-2 $d_3 = 2500 \div 2 \div \tan 30^\circ = 2165.06\text{mm}$

$$r_1 = (4500 + 2165.06) \times \tan 30^\circ = 3848 \text{ mm}$$

Soil Column Volume $V_1 = (3.848^2 - 1.25^2) \times \pi \times 35 = 1456.32 \text{ m}^3$

Rock Cone Net Volume

$$V_2 = [(3.848^2 \times (4.5 + 2.165) - 1.25^2 \times 2.165)] / 3 \times \pi - 1.25^2 \times 4.5 \times \pi = 77.72 \text{ m}^3$$

Buoyant Weight of Soil Column $W'_1 = V_1 \times (19 - 9.8) = 13398.14 \text{ kN}$

Buoyant Weight of Rock Cone $W'_2 = V_2 \times (22 - 9.8) = 948.18 \text{ kN}$

$$\text{Buoyant Weight of Pile } W'_p = 1.25^2 \times \pi \times (35 + 4.5) \times (24.5 - 9.8) = 2850.26 \text{ kN}$$

$$W'_1 + W'_2 = 14346.32 \text{ kN}$$

$$\text{Ultimate Anchorage Resistance } R_u = W'_1 + W'_2 + W'_p = 17197 \text{ kN}$$

Check for Ultimate Anchorage and Allowable Anchorage to Cl. 5.1.6 of the Code

$$D_{\min} + 0.9R_u - 2.0I_a - 1.5U_a - 1.5W = 26000 + 0.9 \times 17197 - 2 \times 0 - 1.5 \times 14500 - 1.5 \times 12000 = 1727 \text{ kN} > 0$$

HN.3 Worked Example HN-2 – Ultimate Uplift Resistance of Group of Large Diameter Bored Piles by Effective Weight of Soil Column and Rock Cone

Consider a group of 4 large diameter bored piles, each of same geometry as in Worked Example HN-2 with centre to centre 6.0m as shown in Figure HN-3.

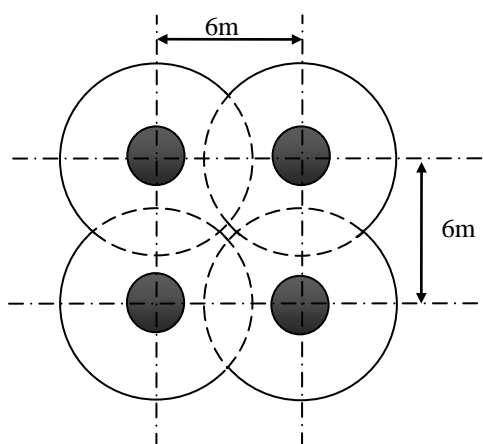


Figure HN-3 – Overlapping of Soil Columns and Rock Cones of 4 Large Diameter Bored Piles for Worked Example HN-2

Consider one single pile, the volumes of the overlapped portion of the soil column and rock cone of a pile are to be worked out.

By (Eqn HN-1), the distance r is calculated as (the radius of the soil column is $r_1 = R = 3.848 \text{ m}$ as per calculation in Worked Example HN-1)

$$r = \frac{R^2 + D^2 - R_o^2}{2D} = \frac{3.848^2 + 6^2 - 3.848^2}{2 \times 6} = 3 \text{ m}$$

(the symbols being defined in Figure HN-1. It can readily be seen that $r = 0.5D$ if $R = R_o$)

By (Eqn HN-2), the area of the overlapped portion in the soil column is

$$A_s = R^2 \sin^{-1} \left(\frac{\sqrt{R^2 - r^2}}{R} \right) - r\sqrt{R^2 - r^2} = 2.791 \text{ m}^2;$$

By (Eqn HN-3), the volume of an overlapped portion soil column is

$$V_s = A_s L = 2.791 \times 35 = 97.685 \text{ m}^3;$$

As there are 2 overlaps, the total volume of soil to be deducted is $97.685 \times 2 = 195.37 \text{ m}^3$ and the weight of the soil column is

$$W_s = 195.37 \times (19 - 9.8) = 1797.404 \text{ kN}$$

By (Eqn HN-4), volume of an overlapped portion of the rock cone is

$$V_r = \frac{\cot \alpha}{3} \left[r^3 \ln \left(\frac{r}{R - \sqrt{R^2 - r^2}} \right) + R^3 \sin^{-1} \left(\frac{\sqrt{R^2 - r^2}}{R} \right) - 2Rr\sqrt{R^2 - r^2} \right] = 1.6 \text{ m}^3;$$

Or by (Eqn HN-5),

$$V_r \approx \frac{d \cot \alpha}{3} A_s = 1.366 \text{ m}^3$$

The weight of the rock cone to be deducted (again 2 no.) is

$$W_r = 1.6 \times (22 - 9.8) \times 2 = 39.04 \text{ kN}.$$

So total weight to be deducted as the anchorage of a pile becomes

$$W_s + W_r = 1797.404 + 39.04 = 1836.444 \text{ kN}$$

So the corrected weight for anchorage by soil and rock is

$$17197 - 1836 = 15361 \text{ kN}$$

HN.4 Worked Example HN-3 – Uplift Resistance of Driven H-Pile by Frictional Resistance between Soil and Pile Surface – Effective Stress Method

A driven H-pile (305×305×223 kg/m) 46m long encounters soil of N-values as shown in Table HN-1. Adopting the Effective Stress Method $\tau_s = \beta \sigma_v'$ capped at 120kPa in accordance with clause 5.3.3(3)(ii) of the Code, Without trial pile, $\beta = 0.2$, the ultimate skin friction against uplift under transient tension worked out is worked out by Table HN-1.

Depth of Pile Below Ground (m)	N-value	σ_v' (kPa)	Unit Skin Friction $\tau_s = \beta\sigma_v'$ (kPa)	Friction Force per unit Perimeter of Pile (kN/m)
0	0	0.0	0.00	0.00
2	0	18.4	0.00	0.00
4	11	36.8	0.00	0.00
6	11	55.2	0.00	0.00
8	51	73.6	14.72	29.44
10	50	92.0	18.40	36.80
12	15	110.4	0.00	0.00
14	41	128.8	25.76	51.52
16	48	147.2	29.44	58.88
18	54	165.6	33.12	66.24
20	62	184.0	36.80	73.60
22	69	202.4	40.48	80.96
24	75	220.8	44.16	88.32
26	60	239.2	47.84	95.68
28	58	257.6	51.52	103.04
30	59	276.0	55.20	110.40
32	68	294.4	58.88	117.76
34	71	312.8	62.56	125.12
36	73	331.2	66.24	132.48
38	77	349.6	69.92	139.84
40	81	368.0	73.60	147.20
42	80	386.4	77.28	154.56
44	83	404.8	80.96	161.92
46	82	423.2	84.64	169.28
Sum				1943.04

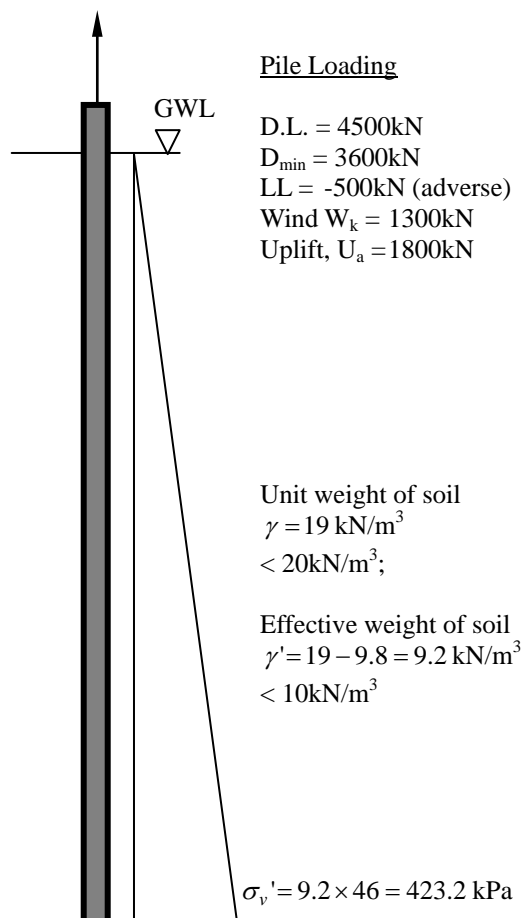


Table HN-1 – Computation of Ultimate Uplift Resistance of a Driven Pile (Effective Stress Method)

As the perimeter of the pile is 1.326m (the enclosing rectangle for the pile section), the total ultimate tension capacity against uplift for transient load on the pile is $R_{u-transient} = 1943.04 \text{ kN/m} \times 1.326 \text{ m} = 2576 \text{ kN}$.

The ultimate tension capacity against uplift for permanent load is $R_{u-permanent} = 2576/2 = 1288 \text{ kN}$.

Taking a factor of safety = 3, the allowable uplift resistance of the pile is $R_{a-transient} = 2576/3 = 859 \text{ kN}$ for transient load and $R_{a-permanent} = 1288/3 = 429 \text{ kN}$ for permanent load.

Check for Ultimate Anchorage and Allowable Anchorage to Cl. 5.1.6 of the Code

$$\text{By } [2.0I_a + 1.5U_a(\text{or } 1.1U_p) - D_{min}]/R_{u-permanent} + 1.5W_k/R_{u-transient} = 0.83 < 0.9$$

$$\text{By } [I_a + U_a - D_{min}]/R_{a-permanent} + W_k/R_{a-transient} = -1.51 < 1$$

So both conditions are satisfied.

HN.5 Worked Example HN-4 – Uplift Resistance of Driven H-Pile by Frictional Resistance between Soil and Pile Surface – Empirical Method by SPT N-values

A driven H-pile (305×305×223 kg/m) 46m long encounters soil of N-values as shown in Table HN-2. Without trial pile, the empirical correlation with SPT N-values as the ultimate value $\tau_s = 0.75N$ is adopted in accordance with clause 5.3.3(3)(iii) of the Code with τ_s capped at 60kPa (or SPT N capped at 80), the ultimate skin friction against uplift under transient tension is worked out by Table HN-2.

Depth of Pile Below Ground (m)	Actual N-Value	Design N-value	Unit Skin Friction (kPa)	Friction Force per unit Perimeter of Pile (kN/m)
0	0	0	0	0
2	0	0	0	0
4	11	11	8.25	16.5
6	11	11	8.25	16.5
8	51	51	38.25	76.5
10	50	50	37.5	75
12	15	15	11.25	22.5
14	41	41	30.75	61.5
16	48	48	36	72
18	54	54	40.5	81
20	62	62	46.5	93
22	69	69	51.75	103.5
24	75	75	56.25	112.5
26	60	60	45	90
28	58	58	43.5	87
30	59	59	44.25	88.5
32	68	68	51	102
34	71	71	53.25	106.5
36	73	73	54.75	109.5
38	77	77	57.75	115.5
40	81	80	60	120
42	80	80	60	120
44	83	80	60	120
46	82	80	60	60
Sum				1849.5

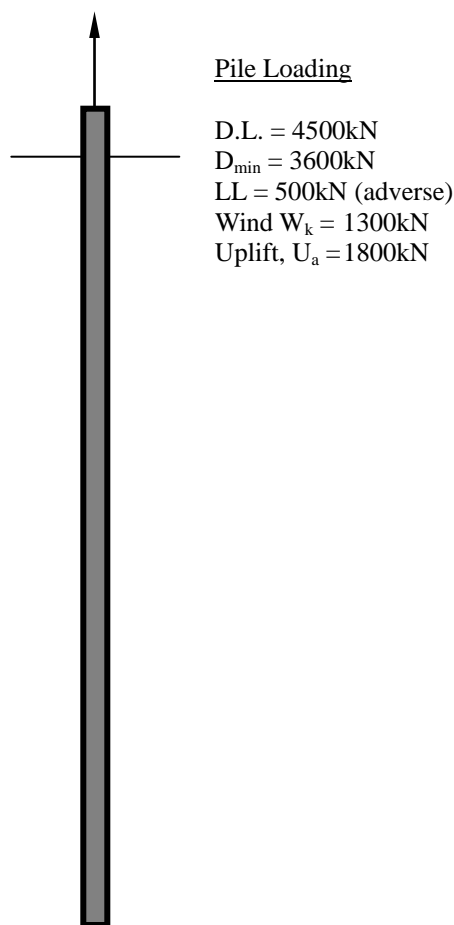


Table HN-2 – Computation of Ultimate Uplift Resistance of a Driven Pile (SPTN Values)

As the perimeter of the pile is 1.326m, the total ultimate tension capacity against uplift for transient load on the pile is $R_{u\text{-transient}} = 1849.5\text{kN/m} \times 1.326\text{m} = 2452.44\text{kN}$.

The ultimate tension capacity against uplift for permanent load is $R_{u\text{-permanent}} = 2452.44/2 = 1226.22\text{kN}$.

Taking a factor of safety = 3, the allowable uplift resistance of the pile is $R_{a\text{-transient}} = 2452.44/3 = 817.48\text{kN}$ for transient load and $R_{a\text{-permanent}} = 1226.22/3 = 407.74\text{kN}$ for permanent load.

Check for Ultimate Anchorage and Allowable Anchorage to Cl. 5.1.6 of the Code

$$\text{By } [2.0I_a + 1.5U_a(\text{or } 1.1U_p) - D_{\min}]/R_{u-\text{permanent}} + 1.5W_k/R_{u-\text{transient}} = 0.88 < 0.9$$

$$\text{By } [I_a + U_a - D_{\min}]/R_{a-\text{permanent}} + W_k/R_{a-\text{transient}} = -1.59 < 1$$

So both conditions are satisfied.

HN.6 Worked Example HN-5 – Effective weight of the Soil Columns and Cones of a Group of Floating Piles

The effective weight of the soil columns and cones of a pile group comprising 9 driven H-piles (305×305×223 kg/m) against uplift is as shown in Figure HN-4. The piles are 4m centre to centre apart. With the B and D dimension of the H-pile as B = 325.7mm and D = 337.9mm, the plan dimensions of the overlapping rectangles and circles are as shown in Figure HN-4.

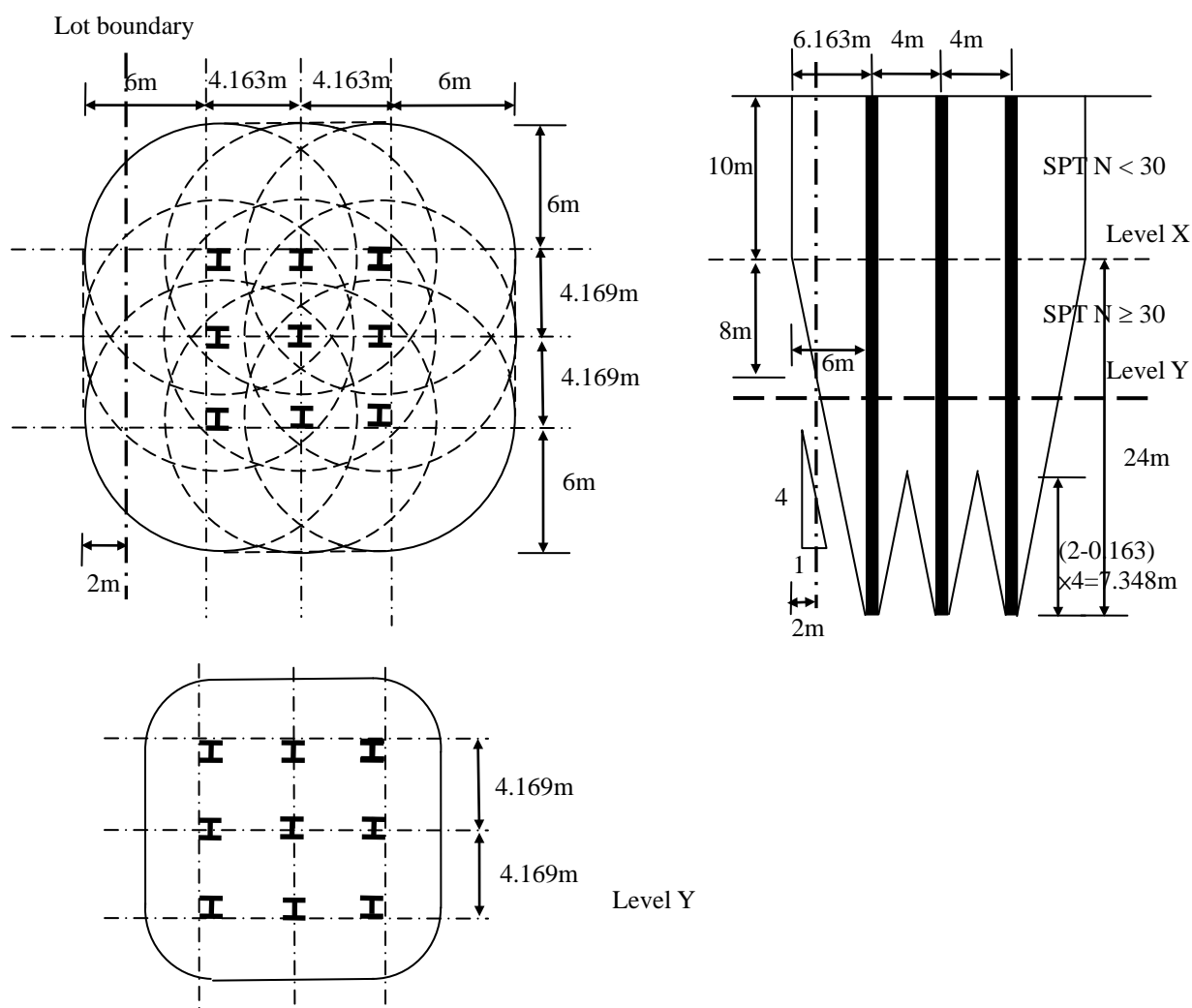


Figure HN-4 – Pile Layout for Worked Example HN-5

Ignoring the lot boundary first, the plan area of the soil column at ground level is

$$8.326 \times 8.338 + 2 \times 8.326 \times 6 + 2 \times 8.338 \times 6 + 4 \times \frac{\pi \times 6^2}{4} = 382.488 \text{ m}^2$$

So volume of the soil column above Level X is $382.488 \times 10 = 3824.88 \text{ m}^3$.

The soil volume beneath Level X can be regarded as comprising a square cylinder, 4 prisms and 4 quadrant circular cones at the corners as shown in Level Y in Figure HN-4. So the volume is

$$\begin{aligned} & 8.326 \times 8.338 \times 24 + 2 \times \frac{1}{2} \times 6 \times 8.326 \times 24 + 2 \times \frac{1}{2} \times 6 \times 8.338 \times 24 + 4 \times \frac{1}{4} \times \frac{1}{3} \times \pi \times 6^2 \times 24 \\ & = 1666.133 + 1198.944 + 1200.672 + 904.779 \\ & = 4970.528 \text{ m}^3 \end{aligned}$$

However, there are 4 “pyramids” of plan area $(4 - 0.326)(4 - 0.338) = 13.454 \text{ m}^2$ and height 7.348m among the pile tip that need to be deducted. The volume of these 4 “pyramids” is

$$4 \times \frac{1}{3} \times 13.454 \times 7.348 = 131.813 \text{ m}^3$$

Adding up, volume of soil without consideration of the lot boundary is $3824.88 + 4970.528 - 131.813 = 8663.587 \text{ m}^3$

If the lot boundary is considered, volume beyond the lot boundary is to be determined for deduction. The plan area of the portion is (with the use of (Eqn HN-2))

$$\begin{aligned} & 8.338 \times 2 + 6^2 \sin^{-1} \left(\frac{\sqrt{6^2 - 4^2}}{6} \right) - 4\sqrt{6^2 - 4^2} = 29.066 \text{ m}^2, \text{ giving a volume of} \\ & 29.066 \times 10 = 290.66 \text{ m}^3 \text{ above Level X.} \end{aligned}$$

For the portion below Level X comprising a prism and a cut cone with volume that can be calculated by (Eqn HN-4), the volume is

$$\begin{aligned} & \frac{1}{2} \times 8.338 \times 2 \times 8 + \frac{4}{3} \left[4^3 \ln \left(\frac{4}{6 - \sqrt{6^2 - 4^2}} \right) + 6^3 \sin^{-1} \left(\frac{\sqrt{6^2 - 4^2}}{6} \right) - 2 \times 6 \times 4\sqrt{6^2 - 4^2} \right] \\ & = 104.842 \text{ m}^3. \end{aligned}$$

So volume of soil beyond lot boundary to be deducted is $290.66 + 104.842 = 395.502 \text{ m}^3$.

Net soil volume after deduction of the portion beyond lot boundary is $8663.587 - 395.502 = 8268.085 \text{ m}^3$.

If the buoyant unit weight of soil is $19 - 9.8 = 9.2 \text{ kN/m}^3$, the total soil weight for balancing uplift is $8268.085 \times 9.2 = 76066.392 \text{ kN}$.

Shared among the 9 identical piles, the effective weight available for each pile against uplift is $76066.392/9 = 8541.82 \text{ kN}$.

As the effective weight available for each pile is greater than the structural capacity of the pile, the bond friction of soil on pile shaft is the controlling factor in this case.

Appendix HO

Determination of Horizontal Displacement of Pile Cap under Lateral Loads in accordance with the Elastic Continuum Theory

Determination of Horizontal Displacement of Pile Cap under Lateral Loads in accordance with the Elastic Continuum Theory

HO.1 Theoretical Background

In determining the horizontal displacement of a pile cap under lateral loads in accordance with Elastic Theory, the following assumptions are made :

- (i) Mindlin's Equations and their integrated forms (Vaziri et al 1982) which are applicable to calculations of displacements inside a semi-infinite homogeneous elastic medium due to loads applied in the medium are adopted for estimating pile cap lateral displacement due to lateral loads. The use of Mindlin's Equations are considered to give conservative estimations as long as parameters of the upper layer of soil embedding the pile cap only are used in the estimation, as the deeper and generally harder soil beneath will tend to reduce the soil movement;
- (ii) Basically the original form of Mindlin's Equation which calculates horizontal displacement ρ_x at any point in a horizontal direction in a semi-infinite homogeneous elastic medium due to a horizontal point load Q acting in the same direction and in the same medium is used. By considering the vertical face of the pile cap as exerting a series of point loads on soil idealized as an elastic medium, and as we are only interested in the displacement of the soil immediately at the wall face, we can simplify Mindlin's Equation as follows :

$$\rho_x = \frac{Q}{16\pi G(1-\mu)} \left[\frac{3-4\mu}{R_1} + \frac{1}{R_2} + \frac{2cz}{R_2^3} + \frac{4(1-\mu)(1-2\mu)}{R_2+z+c} \right] \quad (\text{Eqn HO-1})$$

where G and μ are the shear modulus and Poisson's ratio of the soil and the other dimensional symbols are explained in Figure HO-1.

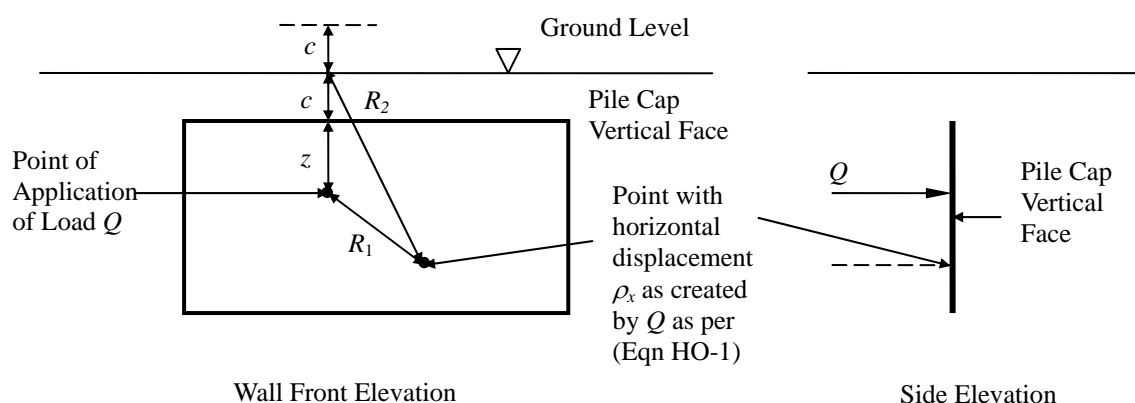


Figure HO-1 – Illustration of the Use of (Eqn HO-1)

Using the coordinate system as shown in Figure HO-2, the lateral deflection at

any point (u, v) due to load from the rectangular pile cap face can be expressed as summation of effects due to all points (x, y) on the face as

$$\rho_{u,v} = \int_{c_2-0.5b}^{c_1} \int_{-0.5b}^{0.5b} \frac{q dx dy}{16\pi G(1-\mu)} \left[\frac{3-4\mu}{R_1} + \frac{1}{R_2} + \frac{2cz}{R_2^3} + \frac{4(1-\mu)(1-2\mu)}{R_2+z+c} \right] \quad (\text{Eqn HO-2})$$

where q is the load per unit area at the point (x, y)

$$c = 0.5(c_1 + c_2) - y; \quad z = 0.5(c_1 + c_2) - v$$

$$R_1 = \sqrt{(x-u)^2 + (y-v)^2}; \quad R_2 = \sqrt{(x-u)^2 + (c_1 + c_2 - y - v)^2}$$

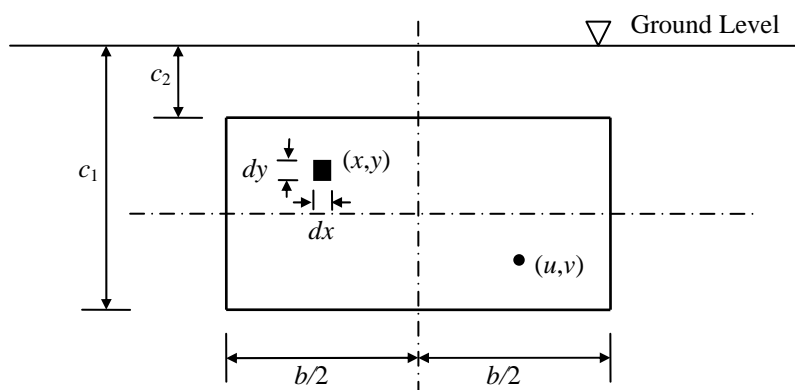
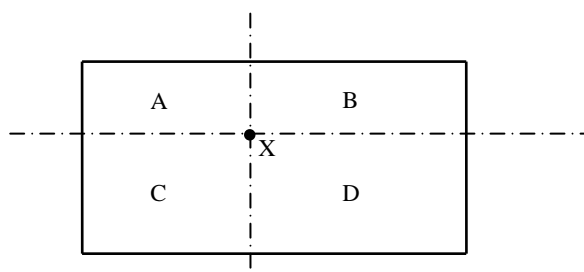


Figure HO-2 – Coordinate System for Calculation of Lateral Displacement of Pile Cap

HO.2 Calculation of Lateral Displacement of any point due to a Uniformly Distributed Horizontal Load

(Eqn HO-2) can be used to calculate the lateral deflections due to a rectangular patch of lateral load of any load intensity as long as the elastic limits of the soil medium are not exceeded. If the load is a uniformly distributed load, q in (Eqn HO-2) is a constant. Poulos and Davis (1980) have quoted the closed form solutions by Douglas and Davis (1964) for the upper and lower corners of a rectangular patch of a uniformly distributed load. The deflection of any point X within the rectangular patch can therefore be determined by the summation of effects due to the 4 rectangles as demonstrated in Figure HO-3 which is extracted from Law & Cheng (2014).



Horizontal Displacement of X is

$$\rho_X = \rho_{XL(A)} + \rho_{XL(B)} + \rho_{XU(C)} + \rho_{XU(D)}$$

where $\rho_{XL(A)}$ is the displacement at the lower corner of rectangle A due to u.d.l. acting on A etc.

Figure HO-3 – Calculation of Horizontal Displacement of a point X on the Front Face of a Uniformly Distributed Load acting on a Vertical Plane within a Semi-infinite Homogenous Elastic medium

Yet the algebraic expressions for the solutions are very lengthy. So instead Law & Cheng (2014) have evaluated the double integral in (Eqn HO-2) directly by numerical methods with the aid of modern computers which is simpler in formulation.

HO.3 Worked Example HO-1

As demonstrated by the following Worked Example HO-1, the method is applied to calculate the lateral deflections at various points due to a rectangular patch of load 8m wide and 2m deep with a uniformly distributed load intensity of 50kPa acting in an elastic medium of Young's modulus 5000kPa and Poisson's ratio 0.35. The rectangular patch is divided into 21 equally spaced grids in both the horizontal and vertical direction and the deflections of the 441 nodes in total are calculated and the deflection contours are plotted in Figure HO-4. The deflections are in mm. The displacement is a maximum at 20.93mm at 14.4mm above the centre, a minimum at the lower corners at 11.39mm and the overall average value is 18.19mm. Greater deflections are found near the centre which is obvious as it is the area under greater superimposition of stresses.

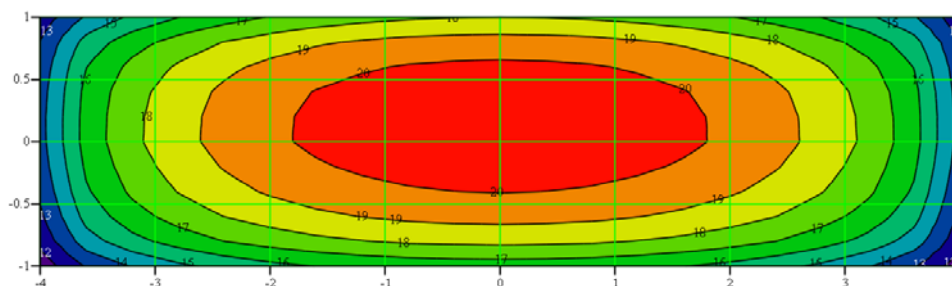


Figure HO-4 – Lateral Deflection Contour of a Vertical Plane Exerting u.d.l. in a Semi-infinite Homogenous Elastic Medium

HO.4 “Rigid Face” Analysis

However, a pile cap exerting a horizontal load on the soil medium normally has a very large in-plane stiffness such that its front face cannot deform as discussed in HO.2 and HO.3. Effectively the plane section containing the front face of the pile cap should remain plane after soil movement named by Law & Cheng as “rigid face”. In order to satisfy Mindlin's Equations, it follows that the horizontal pressures on the front face of the pile cap should vary such that the horizontal movements of the soil remain intact with the cap in a vertical plane.

The proposed approach is based on numerical analysis. The vertical face of the pile cap confronting the soil is divided into a number of equal rectangular elements each of width b' and depth d' , centre at (y_i, z_i) and each having a uniform pressure p_i to be determined as shown in Figure HO-5 extracted from Law & Cheng (2014). The displacement at the centre of the element ρ_i will be the summation of effects from loads of itself and all other elements.

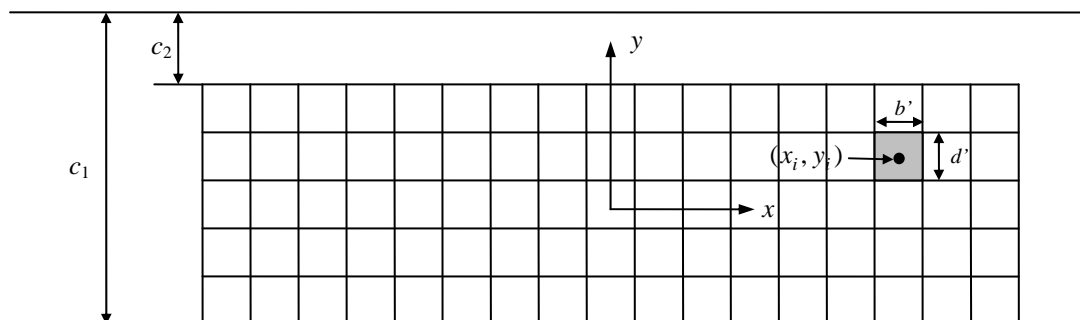


Figure HO-5 – Front face of a Pile Cap divided into a Number of Equal Rectangular Elements

The reduced form of the Mindlin's Equation as listed in (Eqn HO-1) in Figure HO-1 for a point load will be used to calculate the contribution to the displacement of element i due to an element j by considering the element j to be exerting a point load of magnitude $p_j b' d'$.

$$\rho_{ij} = \frac{p_j b' d'}{16\pi G(1-\mu)} \left[\frac{3-4\mu}{R_1} + \frac{1}{R_2} + \frac{2z_i z_j}{R_2^3} + \frac{4(1-\mu)(1-2\mu)}{R_2 + z_i + z_j} \right] \quad (\text{Eqn HO-3})$$

$$\text{where } z_i = 0.5(c_1 + c_2) - y_i; \quad z_j = 0.5(c_1 + c_2) - y_j$$

$$R_1 = \sqrt{(x_i - x_j)^2 + (y_i - y_j)^2}; \quad R_2 = \sqrt{(x_i - x_j)^2 + (c_1 + c_2 - y_i - y_j)^2}$$

(Eqn HO-3) can be re-written as

$$\rho_{ij} = f_{ij} p_j \quad (\text{Eqn HO-4})$$

$$\text{where } f_{ij} = \frac{b' d'}{16\pi G(1-\mu)} \left[\frac{3-4\mu}{R_1} + \frac{1}{R_2} + \frac{2z_i z_j}{R_2^3} + \frac{4(1-\mu)(1-2\mu)}{R_2 + z_i + z_j} \right] \quad (\text{Eqn HO-5})$$

is the interaction coefficient between the two elements i and j .

However, direct application of (Eqn HO-4) to calculate effect on element i due to the load on itself cannot be carried out as R_1 will be zero. So the integrated forms of the equations (Eqn HO-2) and (Eqn HO-3) in Figure HO-2 have to be used with the average displacement approach as discussed in para. HO.2 with the approximation that the pressure is uniform within the small area represented by the joint. By this approach, the displacements at the four corners and the centre of the element i are calculated by the integrated forms of the equation and the weighted mean value is then taken as ρ_{ii} due to a unit load applied to the element. The coefficient f_{ii} is

$$\text{obtained from } f_{ii} = \frac{\rho_{ii}}{p_i}$$

So the total deflection at the centre of an element i is

$$\rho_i = f_{ii} p_i + \sum_{i \neq j} f_{ij} p_j$$

$$\Rightarrow f_{ii}p_i + \sum_{i \neq j} f_{ij}p_j - \rho_i = 0 \quad (\text{Eqn HO-6})$$

However, ρ_i follows a linear deflection. Let the deflection at the centre of the front face of the cap be ρ_0 , then the deflection of the centre of element i is $\rho_0 + my_i$ where m is a constant. So (Eqn HO-6) can be re-written as

$$f_{ii}p_i + \sum_{i \neq j} f_{ij}p_j - \rho_0 - my_i = 0 \quad (\text{Eqn HO-7})$$

N equations will be formulated if the pile cap front face is divided into N elements. For summation of the total force, under the application of the total external force P

$$\sum p_i b' d' = P \Rightarrow \sum p_i = \frac{P}{b' d'} \quad (\text{Eqn HO-8})$$

For summation of the total moment about the centre under the action of the external moment (torsional about a vertical axis through the centre of the pile cap face)

$$\sum p_i b' d' y_i = M \Rightarrow \sum p_i y_i = \frac{M}{b' d'} \quad (\text{Eqn HO-9})$$

From (Eqn HO-7) to (Eqn HO-9), there will be $N+2$ equations solving $N+2$ unknowns which comprise the N nos. of p_i , the centre deflection ρ_0 and the constant m . With determination of ρ_0 and m , the deflection profile of the whole pile cap vertical face can be determined. Re-arranging (Eqn HO-7) to (Eqn HO-9) in matrix form, (Eqn HO-10) is formulated as follows :

$$\begin{bmatrix} y_1 & y_2 & y_3 & \cdot & \cdot & \cdot & y_{N-1} & y_N & 0 & 0 \\ 1 & 1 & 1 & \cdot & \cdot & \cdot & 1 & 1 & 0 & 0 \\ f_{1,1} & f_{1,2} & f_{1,3} & \cdot & \cdot & \cdot & f_{1,N-1} & f_{1,N} & -1 & y_1 \\ f_{2,1} & f_{2,2} & f_{2,3} & \cdot & \cdot & \cdot & f_{2,N-1} & f_{2,N} & -1 & y_2 \\ \cdot & \cdot & \cdot & \cdot & \cdot & \cdot & \cdot & \cdot & \cdot & \cdot \\ \cdot & \cdot & \cdot & \cdot & \cdot & \cdot & \cdot & \cdot & \cdot & \cdot \\ \cdot & \cdot & \cdot & \cdot & \cdot & \cdot & \cdot & \cdot & \cdot & \cdot \\ f_{N,1} & f_{N,2} & f_{N,3} & \cdot & \cdot & \cdot & f_{N,N-1} & f_{N,N} & -1 & y_N \end{bmatrix} \begin{bmatrix} p_1 \\ p_2 \\ p_3 \\ \cdot \\ \cdot \\ \cdot \\ p_N \\ \rho_0 \\ m \end{bmatrix} = \frac{1}{b' d'} \begin{bmatrix} M \\ P \\ 0 \\ 0 \\ 0 \\ 0 \\ 0 \\ 0 \\ 0 \end{bmatrix} \quad (\text{Eqn HO-10})$$

HO.5 Worked Example HO-2

The approach as described in HO.4 is applied to the solution of the pile cap face as described in Worked Example HO-1. For comparison purpose, the applied load on the face is first set to $50 \times 8 \times 2 = 800 \text{ kN}$ which is the same as the applied load on the “flexible face”.

The deflection becomes a unique value of 16.72mm which is smaller than the average value of 18.19mm arrived in Worked Example HO-1.

However, very high pressures at the corners and edges result and the pressures increase with an increasing number of “meshes” (division of the face in a number of

grids). Law & Cheng (2014) points out that the pressures should be at infinity which is a common phenomenon in the application of continuum theory. However, in actual practice, the soil would “yield” at certain stress levels and therefore another parameter, which is the yield stress of soil, should be introduced into the calculation. As an acceptable approach, the passive resistance of the soil which is dependent on the vertical effective stresses in the soil can be used to determine the yield stress.

The next consideration is on the on-plan rotation of the cap. For a “rigid face”, to resist a pure torsional moment, the pressures on different halves of the face (the two halves being formed by a vertical line through the centre of the face) are in opposite directions. While soil cannot sustain tensile stresses, the opposite pressures have to be derived from compression on the far end of the cap. As it is unlikely that there are interactions between the pressures at the opposite faces of the cap as they are far apart through a solid cap structure, the $f_{i,j}$ coefficients in (Eqn HO-10) should be set to zero if point i and point j belong to different faces. By this modification, applying a torsional moment of $M = 1200$ kNm to the face, the rotation is $m = 0.002297$ rad. This is obtained by setting $M = 1200$ in (Eqn HO-10) and $P = 0$ in addition to modification of the f coefficients. Again peak stresses occur at the edges of the face. Law & Cheng (2014) however conclude that the elastic analysis as described above is the most conservative approach.

HO.6 Parametric Studies of Pile Cap Displacement

In order to eliminate the use of yield stresses of the soil so as to simplify the problem, Law & Cheng (2014) discuss that conservative results for the cap movements comprising translation and rotation can be achieved by (i) adopting the average deflection due to a uniformly distributed pressure on a vertical face as the cap moves laterally; (ii) adopting the rigid face approach for the determination of rotation despite the occurrence of the high stresses along the edges and the corners. Based on this approach and the assumptions, Law & Cheng (2014) prepared tables containing coefficients for determination of translational and on-plan rotational stiffnesses of a pile cap which are reproduced in Tables HO-1(a) to (e) and HO-2(a) to (e). By the term “translational stiffness” of a pile cap, we refer to the horizontal shear acting on a pile cap required to produce unit translation and similarly for the rotational stiffness, it is the on-plan moment required to produce unit rotation. In these tables, the notations for determination of the depth and dimensions of the pile cap face by Poulos & Davis (1980) are used by which $K_1 = \frac{2c_1}{b}$ and $K_2 = \frac{2c_2}{b}$ where c_1, c_2 are defined in Figure HO-2 and b is the width of the cap. In Tables HO-1(a) to (e), the coefficients obtained should be multiplied by bG to arrive at the estimated translation stiffness while those for Tables HO-2(a) to (e) be multiplied by b^3G to obtain the rotational stiffness.

As a check, for Worked Example HO-1, $K_1 = \frac{2 \times 3.5}{8} = 0.875$, $K_2 = \frac{2 \times 1.5}{8} = 0.375$, the coefficient for translation as interpolated in Figure HO-1(b) is 2.960. When this

coefficient is multiplied by bG , where $G = \frac{E}{2(1+\mu)} = \frac{5000}{2 \times (1+0.35)} = 1851.85 \text{ kN/m}^2$, the translation stiffness is $2.960 \times 8 \times 1851.85 = 43851.85 \text{ kN/m}$. Upon application of the horizontal shear of $8 \times 2 \times 50 = 800 \text{ kN}$, a lateral deflection of $\frac{800}{43851.85} = 0.01824 \text{ m}$ or 18.24 mm is obtained, which is very close to the value obtained by direct analysis of 18.19 mm . For rotation, the coefficient interpolated in Table HO-2(b) is 0.5446 for Worked Example HO-2. When this coefficient is multiplied by b^3G , the rotational stiffness is $0.5446 \times 8^3 \times 1851.85 = 516361 \text{ kNm}$. Upon application of the torsional moment of 1200 kNm , the rotation is $\frac{1200}{516361} = 0.002324 \text{ rad}$ which is again close to the value obtained by direct analysis of 0.002297 rad .

$K_1 \backslash K_2$	0	0.1	0.2	0.3	0.4	0.5	0.6	0.7	0.8	0.9	1.0	1.1
0.1	1.356	—	—	—	—	—	—	—	—	—	—	—
0.2	1.674	1.615	—	—	—	—	—	—	—	—	—	—
0.3	1.929	1.903	1.745	—	—	—	—	—	—	—	—	—
0.4	2.154	2.139	2.039	1.832	—	—	—	—	—	—	—	—
0.5	2.359	2.351	2.276	2.137	1.896	—	—	—	—	—	—	—
0.6	2.551	2.546	2.487	2.378	2.211	1.946	—	—	—	—	—	—
0.7	2.735	2.732	2.681	2.591	2.458	2.270	1.986	—	—	—	—	—
0.8	2.912	2.909	2.864	2.786	2.674	2.523	2.319	2.019	—	—	—	—
0.9	3.080	3.081	3.040	2.970	2.871	2.742	2.576	2.359	2.046	—	—	—
1.0	3.245	3.245	3.210	3.145	3.056	2.942	2.800	2.622	2.393	2.070	—	—
1.1	3.406	3.406	3.373	3.315	3.232	3.129	3.002	2.848	2.660	2.423	2.090	—
1.2	3.563	3.563	3.532	3.478	3.404	3.306	3.191	3.053	2.890	2.694	2.448	2.107

Table HO-1(a) Coefficient of Translation Soil Poisson's Ratio $\mu = 0.3$

$K_1 \backslash K_2$	0	0.1	0.2	0.3	0.4	0.5	0.6	0.7	0.8	0.9	1.0	1.1
0.1	1.426	—	—	—	—	—	—	—	—	—	—	—
0.2	1.755	1.686	—	—	—	—	—	—	—	—	—	—
0.3	2.018	1.984	1.818	—	—	—	—	—	—	—	—	—
0.4	2.250	2.229	2.123	1.908	—	—	—	—	—	—	—	—
0.5	2.462	2.448	2.369	2.223	1.974	—	—	—	—	—	—	—
0.6	2.661	2.651	2.587	2.474	2.300	2.026	—	—	—	—	—	—
0.7	2.850	2.842	2.788	2.694	2.556	2.362	2.067	—	—	—	—	—
0.8	3.033	3.026	2.978	2.896	2.780	2.624	2.413	2.102	—	—	—	—
0.9	3.209	3.204	3.160	3.087	2.985	2.851	2.680	2.455	2.131	—	—	—
1.0	3.379	3.375	3.336	3.268	3.177	3.058	2.911	2.727	2.491	2.155	—	—
1.1	3.545	3.541	3.506	3.445	3.359	3.252	3.121	2.962	2.768	2.522	2.176	—
1.2	3.707	3.704	3.670	3.614	3.537	3.436	3.317	3.175	3.007	2.803	2.549	2.195

Table HO-1(b) Coefficient of Translation Soil Poisson's Ratio $\mu = 0.35$

$K_1 \backslash K_2$	0	0.1	0.2	0.3	0.4	0.5	0.6	0.7	0.8	0.9	1.0	1.1
0.1	1.505	—	—	—	—	—	—	—	—	—	—	—
0.2	1.847	1.768	—	—	—	—	—	—	—	—	—	—
0.3	2.119	2.078	1.905	—	—	—	—	—	—	—	—	—
0.4	2.360	2.332	2.222	1.998	—	—	—	—	—	—	—	—
0.5	2.579	2.560	2.477	2.326	2.067	—	—	—	—	—	—	—
0.6	2.786	2.770	2.704	2.586	2.407	2.122	—	—	—	—	—	—
0.7	2.982	2.970	2.912	2.816	2.673	2.473	2.167	—	—	—	—	—
0.8	3.171	3.160	3.110	3.026	2.907	2.745	2.527	2.204	—	—	—	—
0.9	3.355	3.344	3.299	3.224	3.119	2.982	2.805	2.572	2.235	—	—	—
1.0	3.532	3.524	3.482	3.414	3.319	3.198	3.046	2.856	2.611	2.261	—	—
1.1	3.705	3.697	3.660	3.596	3.510	3.400	3.265	3.101	2.899	2.644	2.284	—
1.2	3.874	3.867	3.831	3.774	3.693	3.592	3.469	3.322	3.149	2.937	2.673	2.304

Table HO-1(c) Coefficient of Translation Soil Poisson's Ratio $\mu = 0.4$

$K_1 \backslash K_2$	0	0.1	0.2	0.3	0.4	0.5	0.6	0.7	0.8	0.9	1.0	1.1
0.1	1.596	—	—	—	—	—	—	—	—	—	—	—
0.2	1.952	1.865	—	—	—	—	—	—	—	—	—	—
0.3	2.235	2.188	2.009	—	—	—	—	—	—	—	—	—
0.4	2.485	2.453	2.339	2.108	—	—	—	—	—	—	—	—
0.5	2.715	2.691	2.606	2.451	2.183	—	—	—	—	—	—	—
0.6	2.930	2.911	2.843	2.723	2.539	2.243	—	—	—	—	—	—
0.7	3.135	3.119	3.062	2.963	2.817	2.610	2.292	—	—	—	—	—
0.8	3.333	3.319	3.268	3.183	3.061	2.895	2.669	2.333	—	—	—	—
0.9	3.525	3.512	3.466	3.390	3.284	3.143	2.960	2.719	2.367	—	—	—
1.0	3.711	3.700	3.657	3.589	3.493	3.370	3.214	3.017	2.762	2.397	—	—
1.1	3.891	3.882	3.845	3.780	3.693	3.581	3.443	3.274	3.065	2.799	2.422	—
1.2	4.069	4.060	4.025	3.967	3.885	3.782	3.657	3.507	3.327	3.107	2.832	2.445

Table HO-1(d) Coefficient of Translation Soil Poisson's Ratio $\mu = 0.45$

$K_1 \backslash K_2$	0	0.1	0.2	0.3	0.4	0.5	0.6	0.7	0.8	0.9	1.0	1.1
0.1	1.702	—	—	—	—	—	—	—	—	—	—	—
0.2	2.074	1.983	—	—	—	—	—	—	—	—	—	—
0.3	2.371	2.321	2.138	—	—	—	—	—	—	—	—	—
0.4	2.633	2.599	2.485	2.248	—	—	—	—	—	—	—	—
0.5	2.874	2.849	2.764	2.608	2.332	—	—	—	—	—	—	—
0.6	3.101	3.081	3.014	2.893	2.706	2.399	—	—	—	—	—	—
0.7	3.317	3.300	3.244	3.146	2.999	2.786	2.455	—	—	—	—	—
0.8	3.525	3.511	3.462	3.379	3.256	3.087	2.854	2.502	—	—	—	—
0.9	3.727	3.714	3.671	3.597	3.492	3.349	3.162	2.911	2.542	—	—	—
1.0	3.925	3.912	3.873	3.807	3.713	3.588	3.429	3.226	2.961	2.577	—	—
1.1	4.116	4.107	4.070	4.009	3.924	3.812	3.672	3.498	3.282	3.004	2.607	—
1.2	4.303	4.295	4.263	4.205	4.127	4.025	3.898	3.745	3.559	3.331	3.042	2.633

Table HO-1(e) Coefficient of Translation Soil Poisson's Ratio $\mu = 0.5$

$K_1 \backslash K_2$	0	0.1	0.2	0.3	0.4	0.5	0.6	0.7	0.8	0.9	1.0	1.1
0.1	0.188	—	—	—	—	—	—	—	—	—	—	—
0.2	0.260	0.229	—	—	—	—	—	—	—	—	—	—
0.3	0.326	0.299	0.247	—	—	—	—	—	—	—	—	—
0.4	0.387	0.362	0.320	0.258	—	—	—	—	—	—	—	—
0.5	0.443	0.419	0.384	0.333	0.265	—	—	—	—	—	—	—
0.6	0.502	0.477	0.442	0.398	0.342	0.270	—	—	—	—	—	—
0.7	0.554	0.534	0.501	0.458	0.408	0.348	0.273	—	—	—	—	—
0.8	0.616	0.589	0.558	0.516	0.467	0.415	0.353	0.276	—	—	—	—
0.9	0.665	0.639	0.613	0.574	0.528	0.475	0.421	0.357	0.278	—	—	—
1.0	0.721	0.693	0.663	0.630	0.586	0.536	0.481	0.425	0.360	0.280	—	—
1.1	0.763	0.746	0.717	0.680	0.642	0.595	0.543	0.486	0.429	0.362	0.281	—
1.2	0.804	0.799	0.770	0.733	0.692	0.651	0.602	0.548	0.490	0.431	0.364	0.282

Table HO-2(a) Coefficient of Rotation for Soil Poisson's Ratio $\mu = 0.3$

$K_1 \backslash K_2$	0	0.1	0.2	0.3	0.4	0.5	0.6	0.7	0.8	0.9	1.0	1.1
0.1	0.196	—	—	—	—	—	—	—	—	—	—	—
0.2	0.270	0.238	—	—	—	—	—	—	—	—	—	—
0.3	0.338	0.311	0.257	—	—	—	—	—	—	—	—	—
0.4	0.401	0.375	0.333	0.268	—	—	—	—	—	—	—	—
0.5	0.460	0.434	0.398	0.346	0.275	—	—	—	—	—	—	—
0.6	0.520	0.495	0.458	0.414	0.356	0.281	—	—	—	—	—	—
0.7	0.575	0.554	0.519	0.475	0.424	0.362	0.284	—	—	—	—	—
0.8	0.639	0.611	0.579	0.536	0.486	0.432	0.367	0.287	—	—	—	—
0.9	0.690	0.663	0.636	0.596	0.548	0.494	0.438	0.371	0.289	—	—	—
1.0	0.747	0.719	0.688	0.654	0.609	0.557	0.501	0.442	0.374	0.291	—	—
1.1	0.791	0.773	0.744	0.706	0.666	0.618	0.565	0.506	0.446	0.377	0.293	—
1.2	0.834	0.828	0.798	0.762	0.719	0.676	0.626	0.570	0.510	0.449	0.379	0.294

Table HO-2(b) Coefficient of Rotation for Soil Poisson's Ratio $\mu = 0.35$

$K_1 \backslash K_2$	0	0.1	0.2	0.3	0.4	0.5	0.6	0.7	0.8	0.9	1.0	1.1
0.1	0.205	—	—	—	—	—	—	—	—	—	—	—
0.2	0.282	0.248	—	—	—	—	—	—	—	—	—	—
0.3	0.352	0.324	0.269	—	—	—	—	—	—	—	—	—
0.4	0.418	0.391	0.347	0.281	—	—	—	—	—	—	—	—
0.5	0.479	0.453	0.416	0.362	0.289	—	—	—	—	—	—	—
0.6	0.542	0.516	0.479	0.433	0.372	0.294	—	—	—	—	—	—
0.7	0.599	0.578	0.542	0.497	0.444	0.380	0.298	—	—	—	—	—
0.8	0.665	0.637	0.604	0.561	0.508	0.452	0.385	0.301	—	—	—	—
0.9	0.719	0.692	0.664	0.623	0.574	0.518	0.459	0.389	0.304	—	—	—
1.0	0.779	0.750	0.719	0.683	0.637	0.584	0.525	0.464	0.393	0.306	—	—
1.1	0.825	0.807	0.777	0.738	0.697	0.647	0.591	0.530	0.468	0.396	0.307	—
1.2	0.870	0.864	0.834	0.796	0.752	0.708	0.656	0.598	0.535	0.471	0.398	0.309

Table HO-2(c) Coefficient of Rotation for Soil Poisson's Ratio $\mu = 0.4$

$K_1 \backslash K_2$	0	0.1	0.2	0.3	0.4	0.5	0.6	0.7	0.8	0.9	1.0	1.1
0.1	0.216	—	—	—	—	—	—	—	—	—	—	—
0.2	0.296	0.261	—	—	—	—	—	—	—	—	—	—
0.3	0.370	0.340	0.283	—	—	—	—	—	—	—	—	—
0.4	0.438	0.410	0.366	0.297	—	—	—	—	—	—	—	—
0.5	0.503	0.476	0.438	0.382	0.305	—	—	—	—	—	—	—
0.6	0.569	0.542	0.504	0.456	0.394	0.312	—	—	—	—	—	—
0.7	0.628	0.607	0.571	0.524	0.469	0.402	0.316	—	—	—	—	—
0.8	0.698	0.669	0.636	0.591	0.537	0.479	0.408	0.320	—	—	—	—
0.9	0.755	0.728	0.699	0.657	0.606	0.548	0.486	0.413	0.323	—	—	—
1.0	0.818	0.789	0.757	0.720	0.673	0.617	0.556	0.492	0.417	0.325	—	—
1.1	0.867	0.849	0.818	0.779	0.736	0.684	0.626	0.562	0.496	0.420	0.327	—
1.2	0.915	0.909	0.879	0.840	0.795	0.748	0.694	0.633	0.567	0.500	0.422	0.328

Table HO-2(d) Coefficient of Rotation for Soil Poisson's Ratio $\mu = 0.45$

$K_1 \backslash K_2$	0	0.1	0.2	0.3	0.4	0.5	0.6	0.7	0.8	0.9	1.0	1.1
0.1	0.228	—	—	—	—	—	—	—	—	—	—	—
0.2	0.313	0.277	—	—	—	—	—	—	—	—	—	—
0.3	0.391	0.361	0.302	—	—	—	—	—	—	—	—	—
0.4	0.463	0.435	0.390	0.318	—	—	—	—	—	—	—	—
0.5	0.532	0.505	0.466	0.409	0.328	—	—	—	—	—	—	—
0.6	0.602	0.575	0.537	0.488	0.422	0.335	—	—	—	—	—	—
0.7	0.665	0.644	0.608	0.559	0.503	0.432	0.341	—	—	—	—	—
0.8	0.740	0.711	0.678	0.632	0.576	0.514	0.439	0.345	—	—	—	—
0.9	0.802	0.774	0.744	0.702	0.649	0.588	0.522	0.445	0.348	—	—	—
1.0	0.868	0.839	0.808	0.769	0.720	0.662	0.597	0.529	0.449	0.351	—	—
1.1	0.920	0.904	0.873	0.833	0.788	0.734	0.673	0.605	0.534	0.453	0.353	—
1.2	0.974	0.967	0.937	0.898	0.852	0.802	0.745	0.681	0.611	0.539	0.456	0.355

Table HO-2(e) Coefficient of Rotation for Soil Poisson's Ratio $\mu = 0.5$

The translational stiffness and rotational stiffness of the pile cap are useful as input to analysis of the pile group against lateral shear as demonstrated in the worked example in Appendix HQ. They can also be inputted into computer mathematical models for analysis.

Appendix HP

Lateral Restraint on a Pile by the Winkler's Spring

Assumption – Cohesionless Soil

Lateral Resistance on a Pile by the Winkler's Spring Assumption – Cohesionless Soil

HP.1 Theoretical Background

The basic equation governed by elastic beam theory is used, by which the pile is treated as a beam and the lateral deflection of the pile v , as related to the elastic support, can be described by the differential equation as follows, without consideration of P- δ effect :

$$E_p I_p \frac{d^4 v}{dz^4} = -K_h v \quad (\text{Eqn HP-1})$$

(Eqn HP-1) is in fact a particular case of (Eqn HI-1) of Appendix HI for study of the buckling of a pile with the axial load P set to zero, i.e. the axial load effect is ignored. Using also Terzaghi (1955)'s theory for the coefficient of horizontal subgrade reaction and the finite difference method, (Eqn HP-1) can be similarly formulated as (Eqn HI-7) by setting $P = 0$ leading to

$$v_{i-2} - 4v_{i-1} + \left[6 + \left(\frac{L}{T} \right)^5 \frac{i}{N^5} \right] v_i - 4v_{i+1} + v_{i+2} = 0 \quad (\text{Eqn HP-2})$$

The formulation of the support conditions of the pile ends are also identical to that in Appendix HI except that for the free conditions as summarized in Table HP-1.

	Conditions	Pile Head	Pile Tip
Restraint from lateral movement	$v = 0$	$v_1 = 0$	$v_{N+1} = 0$
Restraint from Rotation	$\theta = \frac{dv}{dz} = 0$	$\frac{v_2 - v_{-1}}{2(L/N)} = 0$	$\frac{y_{N+2} - y_N}{2(L/N)} = 0$
Hinged Connections (moment = 0)	$M = E_p I_p \frac{d^2 v}{dz^2} = 0$	$E_p I_p \frac{v_2 - 2v_1 + v_{-1}}{(L/N)^2} = 0$	$E_p I_p \frac{v_{N+2} - 2v_{N+1} + v_N}{(L/N)^2} = 0$
Free end	$S = E_p I_p \frac{d^3 v}{dz^3} = 0$	$E_p I_p \frac{v_3 - 2v_2 + 2v_{-1} - v_{-2}}{2(L/N)^3} = 0$	$E_p I_p \frac{y_{N+3} - 2y_{N+2} + 2y_N - y_{N-1}}{2(L/N)^3} = 0$

Table HP-1 – Restraint Conditions on Lateral Load Analysis on Pile by the Finite Difference Method

The formulation of moments and lateral shears in the finite difference method is as follows at the pile head are as follow :

$$M = E_p I_p \frac{d^2 v}{dz^2} = E_p I_p \left[\frac{v_2 - 2v_1 + v_{-1}}{(L/N)^2} \right] \Rightarrow v_2 - 2v_1 + v_{-1} = \left[\frac{1}{N^2} \left(\frac{L}{T} \right)^2 \right] \frac{MT^2}{E_p I_p} \quad (\text{Eqn HP-3})$$

$$S = E_p I_p \frac{d^3 v}{dz^3} = E_p I_p \left[\frac{v_3 - 2v_2 + 2v_{-1} - v_{-2}}{2(L/N)^3} \right] \Rightarrow v_3 - 2v_2 + 2v_{-1} - v_{-2} = \left[\frac{2}{N^3} \left(\frac{L}{T} \right)^3 \right] \frac{ST^3}{E_p I_p} \quad (\text{Eqn HP-4})$$

Thus 4 additional equations comprising 2 at pile head (for support condition and / or application of external shear or moment) and 2 at pile tip (both support conditions) can be

formed by the equations listed in Table HP-1 and (Eqn HP-2) to (Eqn HP-4) in regards to the end restraint conditions at the head and tip of the pile, making up altogether $N + 5$ equations for solving all the $N + 5$ nos. of v values. Subsequently, the rotation, moment and shear at the i^{th} node can be back-calculated respectively as $\theta_i = \frac{v_{i+1} - v_{i-1}}{2(L/N)}$;

$$M_i = EI \frac{d^2 y}{dz^2} = EI \left[\frac{v_{i+1} - 2v_i + v_{i-1}}{(L/N)^2} \right] \text{ and } S_i = EI \frac{d^3 y}{dz^3} = EI \left[\frac{v_{i+2} - 2v_{i+1} + 2v_{i-1} - v_{i-2}}{2(L/N)^3} \right].$$

The lateral or rotational stiffnesses at the pile head can be determined by dividing the applied shear or moments by the lateral displacement or rotation respectively obtained by solving the $N + 5$ equations.

HP.2 Design Charts and Tables based on the Finite Difference Method

Design charts based on the solution of the equations described in HP.1 have, however, been given in various publications including DM-7 (1971), Tomlinson (2001). In the preparation of these charts, the equations for applied moment and shear used for analysis were transformed from (Eqn HP-3) and (Eqn HP-4) to (Eqn HP-5) and (Eqn HP-6) as follows with the incorporation of $E_p I_p$ and n_h into T as $T = \sqrt[3]{E_p I_p / n_h}$ so that the whole set of equations is based on L/T and N only where N dictates accuracy.

$$v_2 - 2v_1 + v_{-1} = \frac{1}{N^2} \left(\frac{L}{T} \right)^2 \quad (\text{for applied shear at pile head}) \quad (\text{Eqn HP-5})$$

$$v_3 - 2v_2 + 2v_{-1} - v_{-2} = \frac{2}{N^3} \left(\frac{L}{T} \right)^3 \quad (\text{for applied moment at pile head}) \quad (\text{Eqn HP-6})$$

Direct solution of the equations gives v as the “deflection coefficients” are to be multiplied by $MT^2 / E_p I_p$ or $ST^3 / E_p I_p$ as appropriate to obtain the actual deflection. Formulation of the rotation, shear and moment coefficients and the corresponding parameters multiplied by these coefficients to obtain the respective true values of the rotation, shear and moment are summarized in Table HP-2:

	Expressions for the True Value of Lateral deflection, Rotation, Lateral Shear and Moment	Coefficients related to L/T and N only	Parameters Multiplied to Coefficient to obtain True Value of Lateral deflection, Rotation, Lateral Shear and Moment	
			Shear S at Pile Head	Moment M at Pile Head
Lateral Deflection	v_i	v_i	$\frac{ST^3}{E_p I_p}$	$\frac{MT^2}{E_p I_p}$
Rotation	$\frac{v_{i+1} - v_{i-1}}{2(L/N)}$	$\frac{v_{i+1} - v_{i-1}}{2(L/T)/N}$	$\frac{ST^3}{E_p I_p} \times \frac{1}{T} = \frac{ST^2}{E_p I_p}$	$\frac{MT^2}{E_p I_p} \times \frac{1}{T} = \frac{MT}{E_p I_p}$
Lateral Shear	$E_p I_p \left[\frac{v_{i+2} - 2v_{i+1} + 2v_{i-1} - v_{i-2}}{2(L/N)^3} \right]$	$\left[\frac{v_{i+2} - 2v_{i+1} + 2v_{i-1} - v_{i-2}}{2(L/T)^3 / N^3} \right]$	$\frac{ST^3}{E_p I_p} \times \frac{E_p I_p}{T^3} = S$	$\frac{MT^2}{E_p I_p} \times \frac{E_p I_p}{T^3} = \frac{M}{T}$
Moment	$E_p I_p \frac{v_{i+1} - 2v_i + v_{i-1}}{(L/N)^2}$	$\frac{v_{i+1} - 2v_i + v_{i-1}}{(L/T)^2 / N^2}$	$\frac{ST^3}{E_p I_p} \times \frac{E_p I_p}{T^2} = ST$	$\frac{MT^2}{E_p I_p} \times \frac{E_p I_p}{T^2} = M$

Table HP-2 – Use of Coefficients for Determination of Displacements, Rotations, Shears and Moments in Piles by the Finite Difference Method

Samples of these design charts are reproduced in Figure HP-1 :

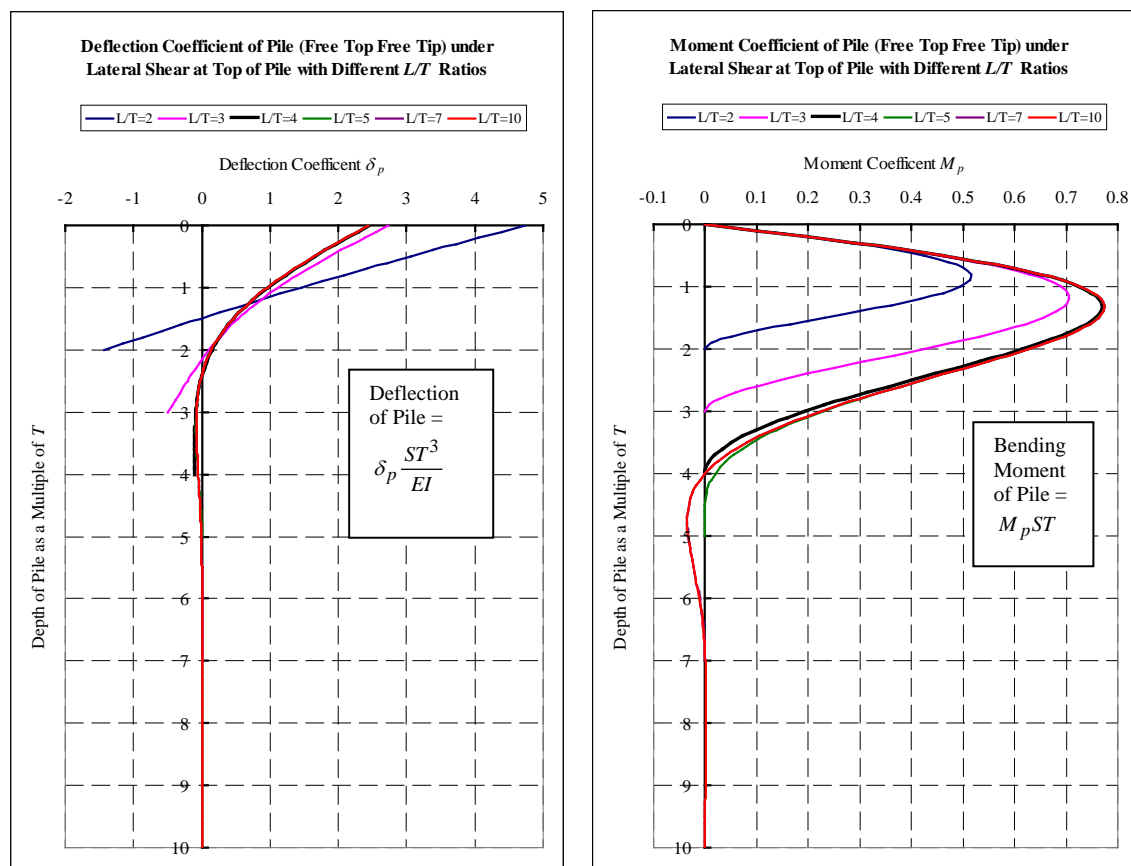


Figure HP-1 – Illustrative Plots of Deflection and Moment Coefficients of Pile under Lateral Load

However, these design charts are all for piles (i) whose cut-off levels are at ground level and (ii) which are ‘floating’, i.e. unrestrained from lateral deflection and rotation at their tips; and (iii) with constant n_h values along the whole length of the pile. As most piles have cut-off levels below ground, where the initial soil stiffness is not zero, these charts under-estimate the stiffness for piles with cut-off below ground level because the actual lateral soil restraint is obviously higher. In addition, restraint of the pile tip against lateral movement (e.g. a large diameter bored pile with short socket into rock) and restraint against both lateral deflection and rotation (e.g. a socketed pile with long socket into rock) may also considerably increase the pile stiffness, especially for short piles.

In this Appendix, analysis by the Finite Difference Method as described in HP.1 and HP.2 has been carried out which takes into account the cases where the pile cut-offs are below ground and the pile tip is either free or restrained from rotation or translation. Similar coefficients are obtained which need to be multiplied by the constants listed in the last 2 columns of Table HP-2 to obtain the true values of deflections, rotations, shears and moments as appropriate. Coefficients for the lateral deflections and moments for pile cut-off levels at certain depths beneath ground and under lateral shear at the cut-off level with different pile tip restraint conditions are listed in Tables HP-3(a) to (f), for various L/T values. Intermediate values can be interpolated. It should be noted that the moment coefficient is for determination of the maximum moment along the pile shaft

which takes place at the pile head if the pile head is restrained from rotation and at certain depth below the pile head if the pile head is free to rotate.

Pile Length as Multiple of L/T	Lateral Deflection Coefficient at Cut-off Level (δ_p)							Coefficient for Maximum Moment (M_p)						
	Ratio of Depth between Ground and the Cut-off Level of the Pile to the Total Pile Length							Ratio of Depth between Ground and the Cut-off Level of the Pile to the Total Pile Length						
	0.00	0.05	0.10	0.15	0.20	0.25	0.30	0.00	0.05	0.10	0.15	0.20	0.25	0.30
2	4.739	3.850	3.247	2.812	2.482	2.224	2.016	0.513	0.468	0.438	0.416	0.399	0.386	0.375
3	2.728	2.218	1.878	1.635	1.452	1.310	1.195	0.704	0.628	0.577	0.539	0.511	0.488	0.469
4	2.442	1.933	1.611	1.388	1.224	1.098	0.998	0.768	0.659	0.589	0.541	0.505	0.477	0.455
5	2.433	1.837	1.489	1.260	1.098	0.976	0.881	0.772	0.640	0.564	0.513	0.477	0.450	0.428
7	2.431	1.676	1.299	1.070	0.916	0.805	0.720	0.772	0.606	0.522	0.472	0.437	0.411	0.391
10	2.431	1.488	1.097	0.881	0.742	0.645	0.573	0.772	0.564	0.478	0.429	0.396	0.373	0.355
15	2.431	1.260	0.881	0.69	0.573	0.493	0.435	0.772	0.514	0.429	0.384	0.355	0.334	0.318
20	2.431	1.097	0.742	0.573	0.472	0.404	0.356	0.772	0.478	0.396	0.355	0.328	0.309	0.295
30	2.431	0.881	0.573	0.435	0.356	0.303	0.266	0.772	0.429	0.355	0.318	0.295	0.278	0.265
40	2.431	0.742	0.472	0.356	0.290	0.246	0.216	0.772	0.396	0.328	0.295	0.273	0.258	0.246

Table HP-3(a) – Deflection and Moment Coefficients for Pile with Free Head and Tip Unrestrained from both Lateral Movement and Rotation due to Horizontal Shear at Cut-off Level

Pile Length as Multiple of L/T	Lateral Deflection Coefficient at Cut-off Level (δ_p)							Moment Coefficient (M_p)						
	Ratio of Depth between Ground and the Cut-off Level of the Pile to the Total Pile Length							Ratio of Depth between Ground and the Cut-off Level of the Pile to the Total Pile Length						
	0.00	0.05	0.10	0.15	0.20	0.25	0.30	0.00	0.05	0.10	0.15	0.20	0.25	0.30
2	1.102	0.999	0.915	0.846	0.787	0.736	0.692	1.064	1.009	0.963	0.924	0.89	0.86	0.834
3	1.028	0.891	0.788	0.707	0.643	0.590	0.546	0.967	0.893	0.836	0.792	0.756	0.726	0.700
4	0.940	0.792	0.687	0.609	0.548	0.499	0.459	0.926	0.847	0.789	0.745	0.709	0.681	0.656
5	0.929	0.757	0.642	0.560	0.498	0.450	0.411	0.927	0.832	0.767	0.719	0.682	0.652	0.627
7	0.928	0.706	0.574	0.487	0.425	0.378	0.342	0.927	0.803	0.727	0.675	0.636	0.606	0.581
10	0.928	0.642	0.498	0.410	0.351	0.309	0.276	0.927	0.767	0.682	0.627	0.588	0.558	0.534
15	0.928	0.560	0.410	0.328	0.276	0.240	0.213	0.927	0.719	0.627	0.572	0.534	0.506	0.484
20	0.928	0.498	0.351	0.276	0.230	0.198	0.175	0.927	0.682	0.588	0.534	0.498	0.472	0.451
30	0.928	0.410	0.276	0.213	0.175	0.150	0.132	0.927	0.627	0.534	0.484	0.451	0.427	0.408
40	0.928	0.351	0.230	0.175	0.143	0.122	0.107	0.927	0.588	0.498	0.451	0.420	0.397	0.379

Table HP-3(b) – Deflection and Moment Coefficients for Pile with Head Restrained from Rotation and Tip Unrestrained from both Lateral Movement and Rotation due to Horizontal Shear at Cut-off Level

Pile Length as Multiple of L/T	Deflection Coefficient at Cut-off Level (δ_p)							Moment Coefficient (M_p)						
	Ratio of Depth between Ground and the Cut-off Level of the Pile to the Total Pile Length							Ratio of Depth between Ground and the Cut-off Level of the Pile to the Total Pile Length						
	0.00	0.05	0.10	0.15	0.20	0.25	0.30	0.00	0.05	0.10	0.15	0.20	0.25	0.30
2	3.384	2.833	2.442	2.149	1.922	1.741	1.237	0.605	0.560	0.528	0.503	0.484	0.468	0.674
3	2.407	2.005	1.727	1.522	1.366	1.242	1.140	0.768	0.685	0.626	0.582	0.548	0.520	0.497
4	2.421	1.923	1.606	1.386	1.223	1.098	0.998	0.776	0.663	0.592	0.543	0.506	0.478	0.455
5	2.429	1.836	1.489	1.260	1.098	0.976	0.881	0.773	0.640	0.564	0.514	0.478	0.450	0.429
7	2.431	1.676	1.299	1.070	0.916	0.805	0.720	0.772	0.606	0.522	0.472	0.437	0.411	0.391
10	2.431	1.488	1.097	0.881	0.742	0.645	0.573	0.772	0.564	0.478	0.429	0.396	0.373	0.355
15	2.431	1.260	0.881	0.690	0.573	0.493	0.435	0.772	0.514	0.429	0.384	0.355	0.334	0.318
20	2.431	1.097	0.742	0.573	0.472	0.404	0.356	0.772	0.478	0.396	0.355	0.328	0.309	0.295
30	2.431	0.881	0.573	0.435	0.356	0.303	0.266	0.772	0.429	0.355	0.318	0.295	0.278	0.265
40	2.431	0.742	0.472	0.356	0.290	0.246	0.216	0.772	0.396	0.328	0.295	0.273	0.258	0.246

Table HP-3(c) – Deflection and Moment Coefficients for Pile with Free Head and Tip Restrained from Lateral Movement but Free to Rotate due to Horizontal Shear at Cut-off Level

Pile Length as Multiple of L/T	Deflection Coefficient at Cut-off Level (δ_p)							Moment Coefficient (M_p)						
	Ratio of Depth between Ground and the Cut-off Level of the Pile to the Total Pile Length							Ratio of Depth between Ground and the Cut-off Level of the Pile to the Total Pile Length						
	0.00	0.05	0.10	0.15	0.20	0.25	0.30	0.00	0.05	0.10	0.15	0.20	0.25	0.30
2	1.096	0.997	0.915	0.846	0.786	0.735	0.691	1.099	1.030	0.973	0.925	0.884	0.848	0.817
3	0.965	0.841	0.747	0.673	0.614	0.565	0.524	0.919	0.855	0.806	0.767	0.736	0.709	0.686
4	0.924	0.782	0.681	0.604	0.545	0.497	0.457	0.925	0.847	0.790	0.746	0.711	0.682	0.657
5	0.928	0.757	0.642	0.560	0.498	0.449	0.411	0.928	0.832	0.767	0.719	0.682	0.652	0.627
7	0.928	0.706	0.574	0.487	0.425	0.378	0.342	0.927	0.803	0.727	0.675	0.636	0.606	0.581
10	0.928	0.642	0.498	0.410	0.351	0.309	0.276	0.927	0.767	0.682	0.627	0.588	0.558	0.534
15	0.928	0.560	0.410	0.328	0.276	0.240	0.213	0.927	0.719	0.627	0.572	0.534	0.506	0.484
20	0.928	0.498	0.351	0.276	0.230	0.198	0.175	0.927	0.682	0.588	0.534	0.498	0.472	0.451
30	0.928	0.410	0.276	0.213	0.175	0.150	0.132	0.927	0.627	0.534	0.484	0.451	0.427	0.408
40	0.928	0.351	0.230	0.175	0.143	0.122	0.107	0.927	0.588	0.498	0.451	0.420	0.397	0.379

Table HP-3(d) – Deflection and Moment Coefficients for Pile with Head Restrained from Rotation and Tip Restrained from Lateral Movement but Free to Rotate due to Horizontal Shear at Cut-off Level

Pile Length as Multiple of L/T	Deflection Coefficient at Cut-off Level (δ_p)							Moment Coefficient (M_p)						
	Ratio of Depth between Ground and the Cut-off Level of the Pile to the Total Pile Length							Ratio of Depth between Ground and the Cut-off Level of the Pile to the Total Pile Length						
	0.00	0.05	0.10	0.15	0.20	0.25	0.30	0.00	0.05	0.10	0.15	0.20	0.25	0.30
2	1.842	1.701	1.581	1.477	1.387	1.307	1.237	1.180	1.066	0.969	0.886	0.813	0.749	0.693
3	2.387	1.998	1.725	1.522	1.366	1.241	1.139	0.781	0.691	0.628	0.583	0.548	0.520	0.496
4	2.402	1.910	1.596	1.377	1.216	1.092	0.994	0.778	0.666	0.595	0.546	0.509	0.480	0.458
5	2.427	1.834	1.487	1.259	1.097	0.976	0.881	0.773	0.641	0.565	0.514	0.478	0.450	0.429
7	2.431	1.676	1.299	1.070	0.916	0.805	0.720	0.772	0.606	0.522	0.472	0.437	0.411	0.391
10	2.431	1.488	1.097	0.881	0.742	0.645	0.573	0.772	0.564	0.478	0.429	0.396	0.373	0.355
15	2.431	1.260	0.881	0.690	0.573	0.493	0.435	0.772	0.514	0.429	0.384	0.355	0.334	0.318
20	2.431	1.097	0.742	0.573	0.472	0.404	0.356	0.772	0.478	0.396	0.355	0.328	0.309	0.295
30	2.431	0.881	0.573	0.435	0.356	0.303	0.266	0.772	0.429	0.355	0.318	0.295	0.278	0.265
40	2.431	0.742	0.472	0.356	0.290	0.246	0.216	0.772	0.396	0.328	0.295	0.273	0.258	0.246

Table HP-3(e) – Deflection and Moment Coefficients for Pile with Head Pinned and Tip Restrained from both Lateral Movement and Rotation due to Horizontal Shear at Cut-off Level

Pile Length as Multiple of L/T	Deflection Coefficient at Cut-off Level (δ_p)							Moment Coefficient (M_p)						
	Ratio of Depth between Ground and the Cut-off Level of the Pile to the Total Pile Length							Ratio of Depth between Ground and the Cut-off Level of the Pile to the Total Pile Length						
	0.00	0.05	0.10	0.15	0.20	0.25	0.30	0.00	0.05	0.10	0.15	0.20	0.25	0.30
2	0.545	0.525	0.506	0.488	0.471	0.456	0.442	0.888	0.865	0.843	0.823	0.805	0.788	0.772
3	0.898	0.796	0.716	0.652	0.599	0.554	0.516	0.938	0.875	0.825	0.785	0.751	0.723	0.698
4	0.924	0.782	0.680	0.604	0.544	0.496	0.457	0.924	0.845	0.788	0.744	0.709	0.680	0.656
5	0.927	0.756	0.641	0.559	0.498	0.449	0.410	0.927	0.832	0.767	0.719	0.682	0.652	0.627
7	0.928	0.706	0.574	0.487	0.425	0.378	0.342	0.927	0.803	0.727	0.675	0.636	0.606	0.581
10	0.928	0.642	0.498	0.410	0.351	0.309	0.276	0.927	0.767	0.682	0.627	0.588	0.558	0.534
15	0.928	0.560	0.410	0.328	0.276	0.240	0.213	0.927	0.719	0.627	0.572	0.534	0.506	0.484
20	0.928	0.498	0.351	0.276	0.230	0.198	0.175	0.927	0.682	0.588	0.534	0.498	0.472	0.451
30	0.928	0.410	0.276	0.213	0.175	0.150	0.132	0.927	0.627	0.534	0.484	0.451	0.427	0.408
40	0.928	0.351	0.230	0.175	0.143	0.122	0.107	0.927	0.588	0.498	0.451	0.420	0.397	0.379

Table HP-3(f) – Deflection and Moment Coefficients for Pile with Head Restrained from Rotation and Tip Restrained from both Lateral Movement and Rotation due to Horizontal Shear at Cut-off Level

Similarly, coefficients for rotation due to moments applied at the cut-off level are determined and tabulated in Table HP-4(a) to (c). Again the coefficients should be multiplied by the constants as listed in Table HP-2 for the determination of rotation.

Pile Length as Multiple of L/T	Rotation Coefficient for Pile Restrained from Translation at Head							Rotation Coefficient for Pile Free to Translate at Head						
	Ratio of Depth between Ground and the Cut-off Level of the Pile to the Total Pile Length							Ratio of Depth between Ground and the Cut-off Level of the Pile to the Total Pile Length						
	0.00	0.05	0.10	0.15	0.20	0.25	0.30	0.00	0.05	0.10	0.15	0.20	0.25	0.30
2	0.747	0.727	0.709	0.693	0.679	0.666	0.654	3.213	2.801	2.516	2.305	2.142	2.012	1.905
3	0.686	0.669	0.654	0.640	0.627	0.616	0.605	1.819	1.666	1.559	1.479	1.417	1.366	1.324
4	0.674	0.652	0.633	0.616	0.601	0.588	0.576	1.751	1.592	1.484	1.405	1.344	1.294	1.252
5	0.668	0.642	0.621	0.602	0.586	0.571	0.558	1.750	1.559	1.439	1.355	1.291	1.240	1.198
7	0.667	0.633	0.605	0.582	0.563	0.546	0.532	1.747	1.504	1.369	1.279	1.213	1.162	1.120
10	0.667	0.621	0.585	0.558	0.536	0.517	0.501	1.747	1.438	1.291	1.197	1.131	1.080	1.038
15	0.667	0.601	0.557	0.525	0.500	0.480	0.464	1.747	1.349	1.196	1.103	1.038	0.988	0.949
20	0.667	0.585	0.535	0.501	0.475	0.454	0.437	1.747	1.290	1.131	1.038	0.974	0.926	0.888
30	0.667	0.558	0.501	0.464	0.437	0.417	0.400	1.747	1.197	1.038	0.949	0.888	0.843	0.807
40	0.667	0.536	0.475	0.437	0.411	0.391	0.375	1.747	1.131	0.975	0.888	0.830	0.787	0.753

Table HP-4(a) – Rotation Coefficients for Pile Tip Unrestrained from both Lateral Movement and Rotation due to Moment at Pile Head

Pile Length as Multiple of L/T	Rotation Coefficient for Pile Restrained from Translation at Head							Rotation Coefficient for Pile Free to Translate at Head						
	Ratio of Depth between Ground and the Cut-off Level of the Pile to the Total Pile Length							Ratio of Depth between Ground and the Cut-off Level of the Pile to the Total Pile Length						
	0.00	0.05	0.10	0.15	0.20	0.25	0.30	0.00	0.05	0.10	0.15	0.20	0.25	0.30
2	0.614	0.609	0.604	0.599	0.595	0.590	0.586	1.896	1.730	1.612	1.523	1.454	1.398	1.351
3	0.685	0.667	0.652	0.637	0.624	0.612	0.601	1.707	1.591	1.507	1.442	1.389	1.345	1.308
4	0.668	0.647	0.629	0.613	0.598	0.585	0.573	1.751	1.592	1.484	1.405	1.343	1.293	1.251
5	0.667	0.642	0.620	0.602	0.585	0.571	0.558	1.748	1.558	1.438	1.354	1.290	1.239	1.197
7	0.667	0.633	0.605	0.582	0.563	0.546	0.532	1.747	1.504	1.369	1.279	1.213	1.162	1.120
10	0.667	0.621	0.585	0.558	0.536	0.517	0.501	1.747	1.438	1.291	1.197	1.131	1.080	1.038
15	0.667	0.601	0.557	0.525	0.500	0.480	0.464	1.747	1.354	1.197	1.104	1.038	0.989	0.949
20	0.667	0.585	0.535	0.501	0.475	0.454	0.437	1.747	1.290	1.131	1.038	0.974	0.926	0.888
30	0.667	0.558	0.501	0.464	0.437	0.417	0.400	1.747	1.197	1.038	0.949	0.888	0.843	0.807
40	0.667	0.536	0.475	0.437	0.411	0.391	0.375	1.747	1.131	0.975	0.888	0.830	0.787	0.753

Table HP-4(b) – Rotation Coefficients for Pile Tip Restrained from Lateral Movement but Free to Rotation due to Moment at Pile Head

Pile Length as Multiple of L/T	Rotation Coefficient for Pile Restrained from Translation at Head							Rotation Coefficient for Pile Free to Translate at Head						
	Ratio of Depth between Ground and the Cut-off Level of the Pile to the Total Pile Length							Ratio of Depth between Ground and the Cut-off Level of the Pile to the Total Pile Length						
	0.00	0.05	0.10	0.15	0.20	0.25	0.30	0.00	0.05	0.10	0.15	0.20	0.25	0.30
2	0.487	0.485	0.484	0.482	0.48	0.479	0.477	1.645	1.573	1.512	1.459	1.413	1.372	1.336
3	0.636	0.625	0.615	0.605	0.596	0.587	0.579	1.691	1.569	1.481	1.413	1.360	1.315	1.278
4	0.666	0.646	0.628	0.612	0.598	0.585	0.573	1.733	1.578	1.474	1.397	1.337	1.288	1.247
5	0.667	0.642	0.620	0.602	0.585	0.571	0.558	1.747	1.557	1.438	1.354	1.290	1.239	1.197
7	0.667	0.633	0.605	0.582	0.563	0.546	0.532	1.747	1.504	1.369	1.279	1.213	1.162	1.120
10	0.667	0.621	0.585	0.558	0.536	0.517	0.501	1.747	1.438	1.291	1.197	1.131	1.080	1.038
15	0.667	0.601	0.557	0.525	0.500	0.480	0.464	1.747	1.354	1.197	1.104	1.038	0.989	0.949
20	0.667	0.585	0.535	0.501	0.475	0.454	0.437	1.747	1.290	1.131	1.038	0.974	0.926	0.888
30	0.667	0.558	0.501	0.464	0.437	0.417	0.400	1.747	1.197	1.038	0.949	0.888	0.843	0.807
40	0.667	0.536	0.475	0.437	0.411	0.391	0.375	1.747	1.131	0.975	0.888	0.830	0.787	0.753

Table HP-4(c) – Rotation Coefficients for Pile Tip Restrained from both Lateral Movement and Rotation due to Moment at Pile Head

The coefficients listed in Tables HP-4(a) to (c) are useful in determining the “rotational stiffness” of a pile embedded in soil so that rotational restraints can be applied to the pile cap for analysis in which the piles are assumed to be rigidly jointed to the pile cap. The assumption of rigid joint connections between the pile and the pile cap can often

significantly reduce lateral deflection of the pile cap. In addition, Tables HP-5(a) to (c) are given below for determination of the maximum shear forces on pile shafts due to a moment acting at the pile head. The maximum shears exist at the pile head when the pile is restrained from translation at the pile head. The coefficients are useful when assigning translation stiffnesses to piles during lateral load analysis.

Pile Length as Multiple of L/T	Shear Coefficient (S_p) for Pile Head Restrained from Translation							Shear Coefficient (S_p) for Pile Head Unrestrained from Translation						
	Ratio of Depth between Ground and the Cut-off Level of the Pile to the Total Pile Length							Ratio of Depth between Ground and the Cut-off Level of the Pile to the Total Pile Length						
	0.00	0.05	0.10	0.15	0.20	0.25	0.30	0.00	0.05	0.10	0.15	0.20	0.25	0.30
2	0.721	0.734	0.746	0.757	0.768	0.778	0.788	0.874	0.837	0.813	0.797	0.785	0.777	0.770
3	0.645	0.670	0.694	0.716	0.737	0.757	0.776	0.556	0.536	0.528	0.527	0.529	0.533	0.538
4	0.664	0.697	0.727	0.754	0.779	0.802	0.823	0.475	0.480	0.491	0.504	0.517	0.530	0.543
5	0.667	0.706	0.742	0.773	0.802	0.828	0.852	0.478	0.487	0.501	0.517	0.533	0.548	0.562
7	0.667	0.721	0.767	0.807	0.843	0.875	0.904	0.479	0.492	0.514	0.536	0.556	0.575	0.592
10	0.667	0.741	0.802	0.852	0.896	0.934	0.969	0.479	0.501	0.533	0.562	0.587	0.611	0.632
15	0.667	0.773	0.853	0.916	0.970	1.016	1.056	0.479	0.517	0.561	0.597	0.631	0.660	0.686
20	0.667	0.802	0.896	0.969	1.029	1.081	1.126	0.479	0.533	0.588	0.632	0.669	0.702	0.730
30	0.667	0.852	0.969	1.056	1.126	1.185	1.237	0.479	0.562	0.632	0.686	0.730	0.767	0.800
40	0.667	0.896	1.029	1.126	1.203	1.269	1.325	0.479	0.587	0.669	0.730	0.779	0.820	0.856

Table HP-5(a) – Shear Coefficients for Pile Tip Unrestrained from both Lateral Movement and Rotation due to Moment at Pile Head

Pile Length as Multiple of L/T	Shear Coefficient (S_p) for Pile Head Restrained from Translation							Shear Coefficient (S_p) for Pile Head Unrestrained from Translation						
	Ratio of Depth between Ground and the Cut-off Level of the Pile to the Total Pile Length							Ratio of Depth between Ground and the Cut-off Level of the Pile to the Total Pile Length						
	0.00	0.05	0.10	0.15	0.20	0.25	0.30	0.00	0.05	0.10	0.15	0.20	0.25	0.30
2	0.615	0.629	0.643	0.656	0.668	0.681	0.693	0.928	0.874	0.833	0.801	0.775	0.752	0.732
3	0.652	0.679	0.704	0.727	0.748	0.768	0.787	0.473	0.466	0.469	0.476	0.485	0.495	0.506
4	0.669	0.701	0.730	0.756	0.780	0.803	0.824	0.472	0.480	0.493	0.507	0.520	0.533	0.546
5	0.667	0.706	0.741	0.773	0.801	0.828	0.852	0.480	0.487	0.502	0.517	0.533	0.548	0.562
7	0.667	0.721	0.767	0.807	0.843	0.875	0.904	0.479	0.492	0.514	0.536	0.556	0.575	0.592
10	0.667	0.741	0.802	0.852	0.896	0.934	0.969	0.479	0.501	0.533	0.562	0.587	0.611	0.632
15	0.667	0.774	0.853	0.916	0.969	1.015	1.056	0.479	0.515	0.561	0.600	0.632	0.661	0.686
20	0.667	0.802	0.896	0.969	1.029	1.081	1.126	0.479	0.533	0.587	0.632	0.669	0.702	0.730
30	0.667	0.852	0.969	1.056	1.126	1.185	1.237	0.479	0.562	0.632	0.686	0.730	0.767	0.800
40	0.667	0.896	1.029	1.126	1.203	1.269	1.325	0.479	0.587	0.669	0.730	0.779	0.820	0.856

Table HP-5(b) – Shear Coefficients for Pile Tip Restrained from Lateral Movement but Free to Rotation due to Moment at Pile Head

Pile Length as Multiple of L/T	Shear Coefficient (S_p) for Pile Head Restrained from Translation							Shear Coefficient (S_p) for Pile Head Unrestrained from Translation						
	Ratio of Depth between Ground and the Cut-off Level of the Pile to the Total Pile Length							Ratio of Depth between Ground and the Cut-off Level of the Pile to the Total Pile Length						
	0.00	0.05	0.10	0.15	0.20	0.25	0.30	0.00	0.05	0.10	0.15	0.20	0.25	0.30
2	0.793	0.800	0.807	0.813	0.820	0.827	0.833	0.426	0.467	0.501	0.53	0.555	0.576	0.593
3	0.665	0.687	0.709	0.729	0.748	0.766	0.783	0.540	0.526	0.521	0.521	0.524	0.529	0.534
4	0.666	0.699	0.728	0.755	0.779	0.802	0.823	0.475	0.480	0.491	0.504	0.517	0.530	0.542
5	0.667	0.707	0.742	0.773	0.802	0.828	0.852	0.478	0.486	0.501	0.517	0.533	0.548	0.562
7	0.667	0.721	0.767	0.807	0.843	0.875	0.904	0.479	0.492	0.514	0.536	0.556	0.575	0.592
10	0.667	0.741	0.802	0.852	0.896	0.934	0.969	0.479	0.501	0.533	0.562	0.587	0.611	0.632
15	0.667	0.774	0.853	0.916	0.969	1.015	1.056	0.473	0.515	0.561	0.600	0.632	0.661	0.686
20	0.667	0.802	0.896	0.969	1.029	1.081	1.126	0.479	0.533	0.587	0.632	0.669	0.702	0.730
30	0.667	0.852	0.969	1.056	1.126	1.185	1.237	0.479	0.562	0.632	0.686	0.730	0.767	0.800
40	0.667	0.896	1.029	1.126	1.203	1.269	1.325	0.479	0.587	0.669	0.730	0.779	0.820	0.856

Table HP-5(c) – Shear Coefficients for Pile Tip Restrained from both Lateral Movement and Rotation due to Moment at Pile Head

HP.4 Application of the Method

For layered soils, different n_h values can be applied at respective levels of the pile for the determination of lateral restraint, for analysis purpose by the finite difference method using (Eqn HP-2) and others or the stiffness method. However, as the top level of the soil plays the most important part in lateral restraint, the result will be conservative if the whole mass of soil is taken as that of the top layer which generally has the smallest n_h values.

It can also be shown readily that the translational and rotational stiffness of a pile can be determined respectively by

$$K_T = \frac{E_p I_p}{\delta_p T^3} \quad (\text{Eqn HP-7})$$

$$K_\theta = \frac{E_p I_p}{M_p T} \quad (\text{Eqn HP-8})$$

HP.5 Illustration for the Use of the Tables HP-3 and HP-4

The use of the Tables HP-3 and HP-4 is illustrated by Worked Example HP-1 as follows :

Worked Example HP-1

Consider a driven H-pile 305×305×223 Section of length 20m embedded in loose fill and in the presence of closely spaced piles. The effective value of the constant of horizontal subgrade reaction is $n_h = 1300 \times 0.25 = 325 \text{ kN/m}^3$ (Table 5.2 of the Code). The cut-off level is at 3.5m below ground. Applied load at cut-off level is $S = 100 \text{ kN}$ in the direction to causing bending about the major axis of the pile. $E_p = 205 \times 10^6 \text{ kN/m}^2$; $I_p = 52700 \times 10^{-8} \text{ m}^4$ so that $E_p I_p = 205 \times 10^6 \times 52700 \times 10^{-8} = 108035 \text{ kN/m}^2$

$$T = \sqrt[5]{EI / n_h} = \sqrt[5]{108035 / 325} = 3.194 \text{ m};$$

$$L/T = 20 / 3.194 = 6.262$$

The depth factor representing cut-off level to total pile length is $3.5/20 = 0.175$

- (i) The pile is a floating pile, i.e. not driven to rock and hinged at top level to the pile cap.

From Table HP-3(a), the interpolated deflection coefficient is

$$\delta_p = 1.062.$$

Deflection at cut-off level due to the applied shear is

$$v_T = \delta_p \times \frac{ST^3}{E_p I_p} = 1.062 \times \frac{100 \times 3.194^3}{108035} = 0.03203 \text{ m} = 32.03 \text{ mm}$$

$$\text{So the shear stiffness of the pile is } \frac{S}{v_T} = \frac{100}{0.03203} = 3122 \text{ kN/m}$$

From Table HP-3(a), the interpolated moment coefficient is $M_p = 0.469$

Maximum moment on the pile shaft is

$$M_p \times ST = 0.469 \times 100 \times 3.194 = 149.80 \text{ kNm.}$$

- (ii) The pile is restrained from rotation at the cut-off level and restrained from rotation and lateral displacement at the tip

From Table HP-3(f), the interpolated deflection coefficient is

$$\delta_p = 0.483.$$

Deflection at cut-off level due to the horizontal shear is

$$\delta_p \times \frac{ST^3}{E_p I_p} = 0.483 \times \frac{100 \times 3.194^3}{108035} = 0.01457 \text{ m} = 14.57 \text{ mm}$$

From Table HO-3(f), the interpolated moment coefficient is $M_p = 0.672$

Maximum moment on the pile shaft is

$$M_p \times ST = 0.672 \times 100 \times 3.194 = 214.64 \text{ kNm.}$$

- (iii) Rotational stiffness of the floating pile in (i) restrained from translation at the pile head is to be found. The appropriate coefficient is interpolated from Table HP-4(a) which is 0.5804. So the rotation due to unit moment applied at the pile head is

$$0.5804 \times MT / E_p I_p = 0.5804 \times 1 \times 3.194 / 108035 = 17.159 \times 10^{-6} \text{ rad}$$

Thus the rotational stiffness is $1 / 17.159 \times 10^{-6} = 58278 \text{ kNm/rad.}$

HO.6 Frame Analysis Method

Alternatively, the pile can be idealized as a strut member carrying the $E_p I_p$ value of the pile laterally supported by a series of elastic “point springs” simulating the lateral support of the soil as shown in Figure HP-2. The structure can then be solved by the stiffness method as is included in many commercial softwares.

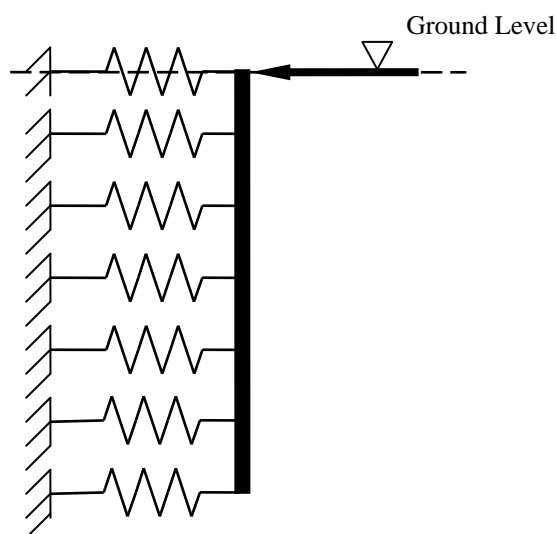


Figure HP-2 – The Winkler's Spring Model for Piles under Lateral Load

The frame method is used to analyze the pile in Worked Example HP-1. The elastic spring values worked out follow (Eqn HI-4) as $K_h = n_h z$. However, as (Eqn HI-4) in Appendix HI is the spring value per unit length, each of them has to be multiplied by the tributary length which is the sum of half the distance between the spring above and the spring below to obtain the value of a “point support” for stiffness method analysis. As a counter-check, the problems in Worked Example HP-1 are re-done below by the stiffness method.

Worked Example HP-2

The pile in Worked Example HP-1 is divided into 40 equal segments laterally supported by 41 elastic point springs. The point spring values are worked out using $K_h d = n_h z d$ where d is the tributary length equal to $d = 20/40 = 0.5$ m. So the spring value at z below ground is $325z \times 0.5 = 162.5z$ in which starting at $z = 3.5$ m for the first spring. The values at the first spring and the last spring are, however, halved as $162.5 \times 3.5 \times 0.5 = 284.375$ and $162.5 \times 23.5 \times 0.5 = 1909.375$ due to the halved tributary lengths.

Frame analysis is carried out accordingly to give the solution for comparison with results of Worked Example HP-1 as listed in Table HP-6. It can be seen that the two sets of results are very close.

Pile Head Connection	Parameter for Comparison	HP-1 From Tables 4 and 5	HP-2 By Frame Analysis
Pinned Pile Head Connection	Pile Head Deflection (mm)	32.02	31.52
	Pile Shaft Max Moment (kNm)	149.80	148.48
	Pile Head Rotation (rad) at unit Mt	17.16×10^{-6}	17.13×10^{-6}
Fixed Pile Head Connection	Pile Head Deflection (mm)	14.57	14.42
	Pile Head Moment (kNm)	214.64	213.71

Table HP-6 – Comparison of Results between Worked Examples HP-1 and HP-2

HP.7 P-Δ Effects

The 1st order linear analysis has ignored the effects of axial load on the lateral deflection as per the foregoing analysis in this appendix, both by the finite difference and stiffness approaches. However, for a pile under lateral load, the axial load in the pile can in fact create additional eccentric moments (axial load \times the lateral displacement of the pile) on the pile and subsequently further lateral displacements. Alternatively it can be regarded that the axial load decreases the stiffness of the pile thus produce greater lateral displacements.

Nevertheless, if the analysis is based on (Eqn HI-1) for the finite difference method in Appendix HI so that (Eqn HP-2) can be modified as follows, P-Δ effects can then be accounted for.

$$E_p I_p \left[\frac{v_{i+2} - 4v_{i+1} + 6v_i - 4v_{i-1} + v_{i-2}}{(L/N)^4} \right] + P \left[\frac{v_{i+1} - 2v_i + v_{i-1}}{(L/N)^2} \right] + n_h \frac{i}{N} L v_i = 0$$

$$\Rightarrow v_{i+2} - \left(4 - \frac{P_r}{N^2} \right) v_{i+1} + \left[6 - \frac{2P_r}{N^2} + \left(\frac{L}{T} \right)^5 \frac{i}{N^5} \right] v_i - \left(4 - \frac{P_r}{N^2} \right) v_{i-1} + v_{i-2} = 0 \quad (\text{Eqn HP-9})$$

Other equations for support conditions and application of loads and moments remain unchanged and the full set of equations can then be analyzed which would include the effects due to P-Δ. Similarly, for the stiffness method, if the combined stiffness (the conventional stiffness matrix + the geometric matrix) as listed in (Eqn HI-12) is used, P-Δ effects can also be accounted for.

Figure HP-3 shows the difference in deflection profiles and bending moments of a 40m long 305×305×223 pile with free head embedded in soil of $n_h = 1100 \text{ kN/m}^3$ under a horizontal shear of 90kN with and without an axial load of 5500kN. There are significant differences under such a comparatively high axial load.

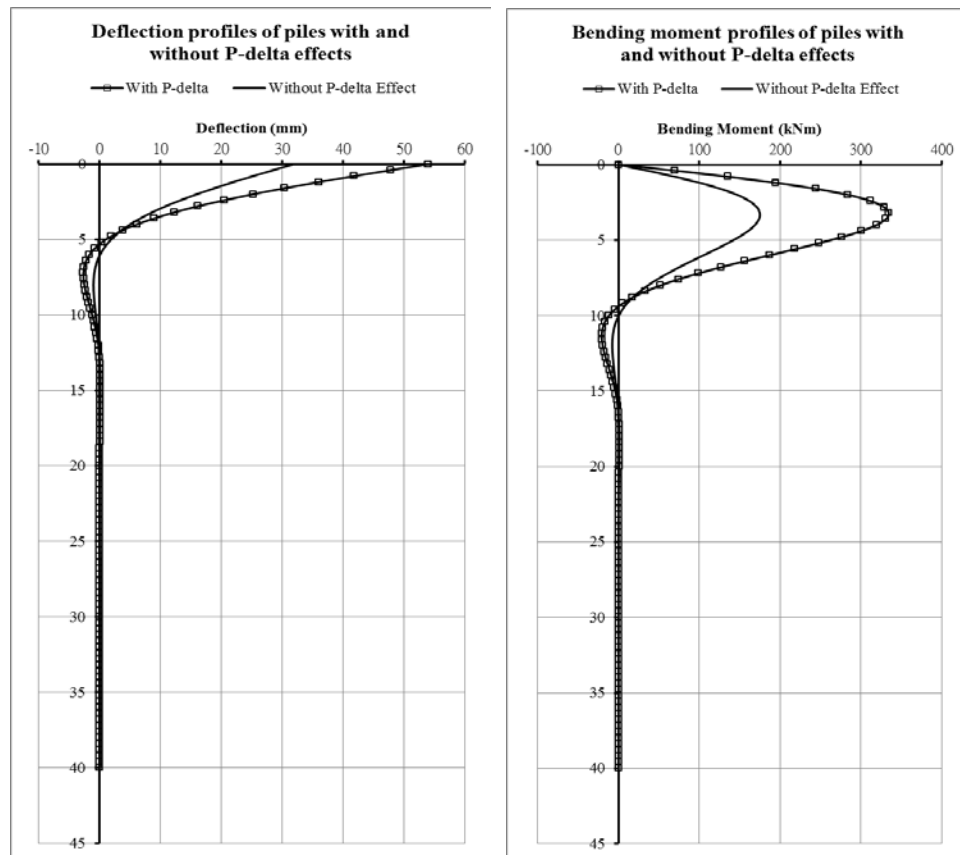


Figure HP-3 – An Example Demonstrating the Differences in Deflection and Bending Moment of a Pile with Free Head with and without P-Δ Effect

Nevertheless, the differences are significantly reduced when the pile head is restrained against rotation as shown in Figure HP-4. The proportion of stiffness reduction is smaller when the pile head is fixed.

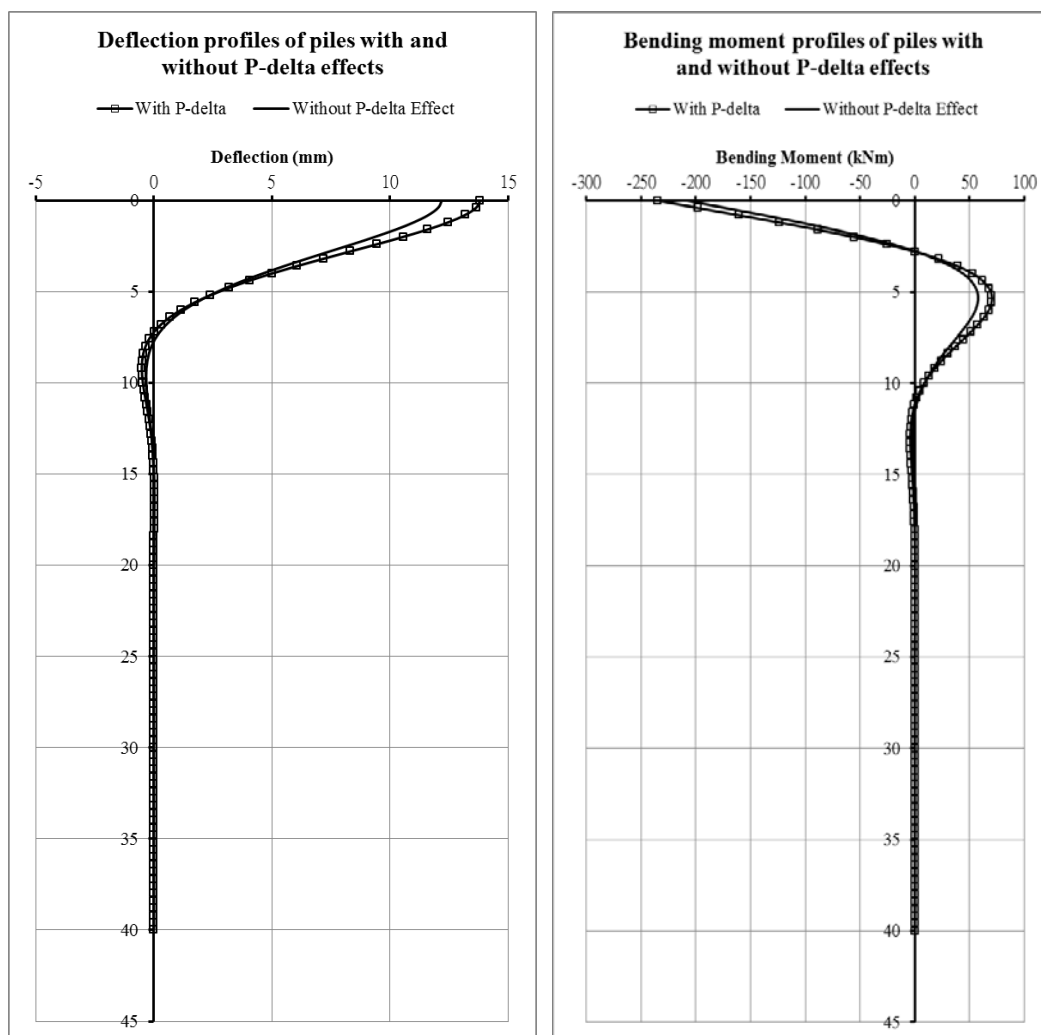


Figure HP-4 – An Example Demonstrating the Differences in Deflection and Bending Moment of a Pile with Fixed Head with and without P- Δ Effect

Analysis of P- Δ effects is available in many commercial softwares.

Appendix HQ

Lateral Resistance of a Piled Foundation – Distribution of Lateral Loads among the Piles and the Pile Cap

Lateral Resistance of a Piled Foundation – Distribution of Lateral Loads among the Piles and the Pile Cap

HQ.1 Theoretical Background

The determination of the distribution of lateral shear forces among the piles and the pile cap of a piled foundation is based on the compatibility of lateral deflections of the piles and the pile cap at the pile cut-off levels. To simplify calculation, infinite in-plane stiffness of the pile cap is usually assumed.

The elastic theory is adopted to determine the lateral load distribution among the piles and the pile cap. The lateral stiffness of the pile group (which is the load to produce unit displacement) is first determined based on the summation of the lateral stiffnesses of the individual piles. Consider a pile group of N piles no. 1, 2, 3, ..., i , ..., N located respectively at coordinates (x_1, y_1) , (x_2, y_2) , ..., (x_i, y_i) , ..., (x_N, y_N) with reference to a pre-determined rectangular co-ordinate system on X and Y axes. The lateral stiffness of each pile in each of the X and Y directions is pre-determined as K_{px1} , K_{px2} , ..., K_{pxi} , ..., K_{pxN} and K_{py1} , K_{py2} , ..., K_{pyi} , ..., K_{pyN} respectively in accordance with the approach discussed in Appendix HP.

The lateral stiffness of the pile cap, which may also experience restraint from the embedded soil can be pre-determined in accordance with the approach discussed in Appendix HO, if rectangular on plan. The pre-determined lateral stiffnesses and on-plan rotational stiffness of the cap with respect to the global X and Y axes are K_{capx} , K_{capy} , K_{capz} and the centroidal axes are at x_{cap} and y_{cap} .

The recommended approach and formulae for analysis are as follows:

- (i) The “shear centre” of the pile group and the pile cap is to be located with respect to the pre-determined coordinate system as

$$X_{cg} = \frac{\sum K_{pyi} x_i + K_{capy} x_{cap}}{\sum K_{pyi} + K_{capy}} \quad (\text{Eqn HQ-1})$$

$$Y_{cg} = \frac{\sum K_{pxi} y_i + K_{capx} y_{cap}}{\sum K_{pxi} + K_{capx}} \quad (\text{Eqn HQ-2})$$

- (ii) The external applied load in the directions parallel to the global X and Y directions are denoted by S_x and S_y respectively. Any unbalanced on plan torsion calculated about the shear centre is denoted by T which is taken as positive if it is acting anti-clockwise;

- (iii) The total lateral stiffness of the piled foundation system in the X and Y directions are respectively

$$K_x = \sum K_{pxi} + K_{capx} \quad (\text{Eqn HQ-3})$$

$$K_Y = \sum K_{pyi} + K_{capY} \quad (\text{Eqn HQ-4})$$

Physically the two stiffnesses are the forces required to produce unit displacements in the directions under consideration when the resultant external loads acts at the “shear centre”;

- (iv) The rotational stiffness of the system is:

$$J = \sum [K_{pxi} (y_i - Y_{cg})^2 + K_{pyi} (x_i - X_{cg})^2] + K_{capZ} \quad (\text{Eqn HQ-5})$$

Physically it is the moment required to produce unit rotation at the shear centre;

- (v) To ensure compatibility of the lateral displacements of the pile cap and the piles, the lateral shears of the pile i in the X and Y directions will respectively be

$$S_{pxi} = S_X \frac{K_{pxi}}{K_X} - T \frac{K_{pxi} (y_i - Y_{cg})}{J}; \quad (\text{Eqn HQ-6})$$

$$S_{pyi} = S_Y \frac{K_{pyi}}{K_Y} + T \frac{K_{pyi} (x_i - X_{cg})}{J}; \quad (\text{Eqn HQ-7})$$

- (vi) The lateral shears in the X and Y directions and torsion acting on the pile cap are respectively

$$S_{capX} = S_X \frac{K_{capX}}{K_X} - T \frac{K_{capX} (y_{cap} - Y_{cg})}{J}; \quad (\text{Eqn HQ-8})$$

$$S_{capY} = S_Y \frac{K_{capY}}{K_Y} + T \frac{K_{capY} (x_{cap} - X_{cg})}{J} \quad (\text{Eqn HQ-9})$$

$$M_{cap} = T \frac{K_{capZ}}{J} \quad (\text{Eqn HQ-10})$$

- (vii) As compatibility of displacements of the pile group and the pile cap is ensured, the lateral displacements (in the global X and Y directions) and rotation of the shear centre can be worked out as

$$\delta_X = \frac{S_X}{K_X}; \quad \delta_Y = \frac{S_Y}{K_Y}; \quad \theta_Z = \frac{T}{J} \quad (\text{Eqn HQ-11})$$

HQ.2 Worked Example HQ-1

The distribution of lateral loads on a piled foundation comprising a pile cap covering 26 nos. of H-piles of section 305×305×223 grade S450 piles is analyzed as Worked Example HQ-1. The piles are 30m long and assumed pinned at the cut-off levels to the pile cap. The pile cap is 1.5m thick, of plan size 10m by 10m and is buried 1.5m below the ground surface. Soil restraint on the pile cap can only be considered in the Y direction. In the X direction where there are foundations of adjacent buildings, there will be no restraint assumed by the soil on the pile cap. The layout is shown in Figure HQ-1.

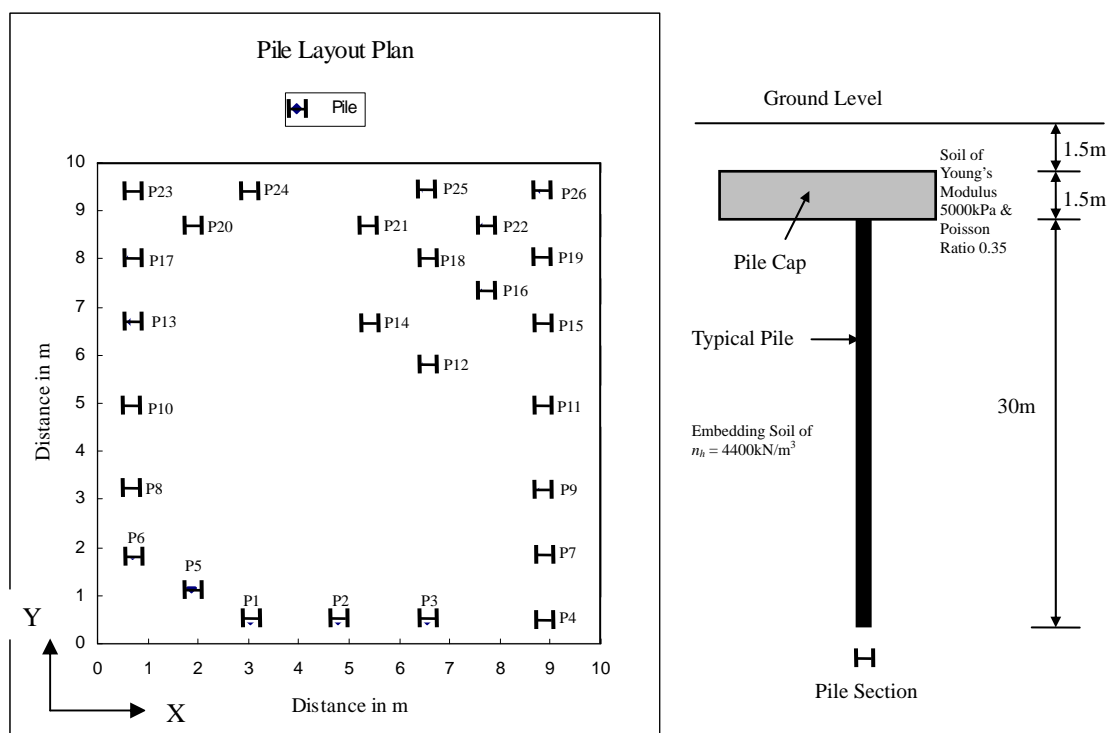


Figure HQ-1 – Piling Layout Plan and Details for Worked Example HQ-1

Design Data :

Pile 305×305×223 H-Pile (Grade S450) ; $E_{steel} = 205 \text{ GPa}$
 $I_{major} = 52700 \text{ cm}^4$; $I_{minor} = 17580 \text{ cm}^4$; $B = 325.7 \text{ mm}$; $D = 337.9 \text{ mm}$
 Soil parameters above pile cut-off level : $E_{soil} = 5000 \text{ kPa}$; $\mu = 0.35$;
 $G_{soil} = E_{soil} / [2(1 + \mu)] = 1851.85 \text{ kPa}$;
 Soil below cut-off level $n_h = 4400 \text{ kN/m}^3$; Cap width $b = 10 \text{ m}$

- (i) The lateral stiffness of the pile cap is determined by the approach discussed in Appendix HP. The lateral stiffness of the pile cap in the X-direction is taken as zero (no soil restraint in the X-direction) and $2.474 \times b G_{soil} = 45815 \text{ kN/m}$ in the Y direction (Table HO-1(b) with $K_1 = 2 \times 3 / 10 = 0.6$ and $K_2 = 2 \times 1.5 / 10 = 0.3$). The rotational stiffness is $0.414 \times b^3 G_{soil} = 766667 \text{ kNm/rad}$ (Table HO-2(b));
- (ii) The lateral stiffnesses of the individual piles are first determined in accordance with the method discussed in Appendix HP. As discussed the constant of horizontal subgrade reaction is to be discounted with respect to pile spacing in accordance with Table 5.2 of the Code. The values arrived at are tabulated in Table HQ-1. As the ratio of cut-off level depth to pile length is $3/30 = 0.1$ and the piles are floating piles with a pinned connection at the pile heads, Table HP-3(a) is used to find the lateral deflection coefficients δ_{px} and δ_{py} in accordance with the L/T ratios as tabulated in Table HQ-1. The determination of the pile shear stiffnesses is in accordance with (Eqn HP-7) in Appendix HP.

Pile No.	Coordinate (m)		Distance to Closest Pile (m)		n_b Discount Factor		T_{xi} (m)	T_{yi} (m)	L/T_{xi}	L/T_{yi}	δ_{pxi}	δ_{pyi}	Shear Stiffness (kN/m)	
	x_i	y_i	X-dir	Y-dir	X-dir	Y-dir							K_{pxi}	K_{pyi}
P1	3.040	0.500	1.748	8.890	0.605	1.000	2.097	1.523	14.304	19.700	0.911	0.750	12853.27	13599.28
P2	4.788	0.500	1.748	6.190	0.605	1.000	2.097	1.523	14.304	19.700	0.911	0.750	12853.27	13599.28
P3	6.536	0.500	1.748	5.317	0.605	1.000	2.097	1.523	14.304	19.700	0.911	0.750	12853.27	13599.28
P4	8.876	0.500	2.340	1.350	0.878	0.399	1.947	1.830	15.409	16.395	0.870	0.842	16832.95	6984.42
P5	1.870	1.175	10.000	7.540	1.000	1.000	1.897	1.523	15.816	19.700	0.858	0.750	18443.86	13599.28
P6	0.700	1.850	8.176	1.350	1.000	0.399	1.897	1.830	15.816	16.395	0.858	0.842	18443.86	6984.42
P7	8.876	1.850	8.176	1.350	1.000	0.399	1.897	1.830	15.816	16.395	0.858	0.842	18443.86	6984.42
P8	0.700	3.200	8.176	1.350	1.000	0.399	1.897	1.830	15.816	16.395	0.858	0.842	18443.86	6984.42
P9	8.876	3.200	8.176	1.350	1.000	0.399	1.897	1.830	15.816	16.395	0.858	0.842	18443.86	6984.42
P10	0.700	4.945	8.176	1.745	1.000	0.575	1.897	1.701	15.816	17.633	0.858	0.808	18443.86	9059.78
P11	8.876	4.945	8.176	1.745	1.000	0.575	1.897	1.701	15.816	17.633	0.858	0.808	18443.86	9059.78
P12	6.536	5.817	10.000	2.223	1.000	0.787	1.897	1.598	15.816	18.777	0.858	0.776	18443.86	11388.14
P13	0.700	6.690	4.666	1.350	1.000	0.399	1.897	1.830	15.816	16.395	0.858	0.842	18443.86	6984.42
P14	5.366	6.690	3.510	2.025	1.000	0.699	1.897	1.636	15.816	18.338	0.858	0.788	18443.86	10442.38
P15	8.876	6.690	3.510	1.350	1.000	0.399	1.897	1.830	15.816	16.395	0.858	0.842	18443.86	6984.42
P16	7.706	7.365	10.000	1.350	1.000	0.399	1.897	1.830	15.816	16.395	0.858	0.842	18443.86	6984.42
P17	0.700	8.040	5.836	1.350	1.000	0.399	1.897	1.830	15.816	16.395	0.858	0.842	18443.86	6984.42
P18	6.536	8.040	2.340	1.350	0.878	0.399	1.947	1.830	15.409	16.395	0.870	0.842	16832.95	6984.42
P19	8.876	8.040	2.340	1.350	0.878	0.399	1.947	1.830	15.409	16.395	0.870	0.842	16832.95	6984.42
P20	1.870	8.715	3.496	7.540	1.000	1.000	1.897	1.523	15.816	19.700	0.858	0.750	18443.86	13599.28
P21	5.366	8.715	2.340	2.025	0.878	0.699	1.947	1.636	15.409	18.338	0.870	0.788	16832.95	10442.38
P22	7.706	8.715	2.340	1.350	0.878	0.399	1.947	1.830	15.409	16.395	0.870	0.842	16832.95	6984.42
P23	0.700	9.390	2.340	1.350	0.878	0.399	1.947	1.830	15.409	16.395	0.870	0.842	16832.95	6984.42
P24	3.040	9.390	2.340	8.890	0.878	1.000	1.947	1.523	15.409	19.700	0.870	0.750	16832.95	13599.28
P25	6.536	9.390	2.340	1.350	0.878	0.399	1.947	1.830	15.409	16.395	0.870	0.842	16832.95	6984.42
P26	8.876	9.390	2.340	1.350	0.878	0.399	1.947	1.830	15.409	16.395	0.870	0.842	16832.95	6984.42

Table HQ-1 – Lateral Stiffness of the Piled Foundation of Worked Example HQ-1

(iii) The shear centre and stiffness of the piled foundation are worked out by Table HQ-2 as follows.

Pile No / Cap.	Shear Stiffness (kN/mm)		Coordinate (m)		$K_{pyi}x_i$ (kN)	$K_{pxi}y_i$ (kN)	Eccentricity from pile group (m)		$K_{pyi}x_{ci}^2$ (kNm)	$K_{pxi}y_{ci}^2$ (kNm)
	K_{pxi}	K_{pyi}	x_i	y_i			$x_{ci}=x_i-X_{cg}$	$y_{ci}=y_i-Y_{cg}$		
P1	12853	13599	3.040	0.500	41341.82	6426.637	-1.862	-5.159	47162.16	342075.2
P2	12853	13599	4.788	0.500	65113.37	6426.637	-0.114	-5.159	177.5237	342075.2
P3	12853	13599	6.536	0.500	88884.92	6426.637	1.634	-5.159	36298.22	342075.2
P4	16833	6984	8.876	0.500	61993.72	8416.474	3.974	-5.159	110288.6	447989.8
P5	18444	13599	1.870	1.175	25430.66	21671.53	-3.032	-4.484	125039.5	370814.1
P6	18444	6984	0.700	1.850	4889.095	34121.13	-4.202	-3.809	123337.4	267573
P7	18444	6984	8.876	1.850	61993.72	34121.13	3.974	-3.809	110288.6	267573
P8	18444	6984	0.700	3.200	4889.095	59020.34	-4.202	-2.459	123337.4	111511.6
P9	18444	6984	8.876	3.200	61993.72	59020.34	3.974	-2.459	110288.6	111511.6
P10	18444	9060	0.700	4.945	6341.848	91204.87	-4.202	-0.714	159986.1	9398.98
P11	18444	9060	8.876	4.945	80414.63	91204.87	3.974	-0.714	143059.9	9398.98
P12	18444	11388	6.536	5.817	74432.9	107287.9	1.634	0.158	30396.4	461.235
P13	18444	6984	0.700	6.690	4889.095	123389.4	-4.202	1.031	123337.4	19610.34
P14	18444	10442	5.366	6.690	56033.8	123389.4	0.464	1.031	2245.745	19610.34
P15	18444	6984	8.876	6.690	61993.72	123389.4	3.974	1.031	110288.6	19610.34
P16	18444	6984	7.706	7.365	53821.95	135839	2.804	1.706	54904.49	53688.33
P17	18444	6984	0.700	8.040	4889.095	148288.6	-4.202	2.381	123337.4	104573.3
P18	16833	6984	6.536	8.040	45650.18	135336.9	1.634	2.381	18642.31	95439.73
P19	16833	6984	8.876	8.040	61993.72	135336.9	3.974	2.381	110288.6	95439.73
P20	18444	13599	1.870	8.715	25430.66	160738.2	-3.032	3.056	125039.5	172265.2
P21	16833	10442	5.366	8.715	56033.8	146699.2	0.464	3.056	2245.745	157219.4
P22	16833	6984	7.706	8.715	53821.95	146699.2	2.804	3.056	54904.49	157219.4
P23	16833	6984	0.700	9.390	4889.095	158061.4	-4.202	3.731	123337.4	234338
P24	16833	13599	3.040	9.390	41341.82	158061.4	-1.862	3.731	47162.16	234338
P25	16833	6984	6.536	9.390	45650.18	158061.4	1.634	3.731	18642.31	234338
P26	16833	6984	8.876	9.390	61993.72	158061.4	3.974	3.731	110288.6	234338
Pile Cap	0	45815	5.000	5.000	229075	0	0.098	-0.659	437.7322	0
Sum	448270	282569			1385227	2536700			2144763	4454486

Table HQ-2 – Summary of Stiffness of the Piled Foundation of Worked Example HQ-1

From Table HQ-2, the total translational stiffnesses of the piled foundation in the X and Y directions are $K_x = 448270 \text{ kN/m}$ and $K_y = 282569 \text{ kN/m}$ respectively (as sum of the 2nd and 3rd columns respectively)

By (Eqn HQ-1) and (Eqn HQ-2), the shear centre is located at

$$X_{cg} = \frac{\sum K_{pyi} x_i + K_{capy} x_{cap}}{\sum K_{pyi} + K_{capy}} = \frac{1385227}{282569} = 4.902 \text{ m from the origin,}$$

$$Y_{cg} = \frac{\sum K_{pxi} y_i + K_{capx} y_{cap}}{\sum K_{pxi} + K_{capx}} = \frac{2536700}{448270} = 5.659 \text{ m from the origin.}$$

Based on the worked out location of the shear centre, the coordinates of the piles and the pile cap are shifted (the 8th and 9th columns) relative to the shear centre as the origin. The rotational stiffness of the pile cap is therefore worked out as

$$J = \sum [K_{pxi} (y_i - Y_{cg})^2 + K_{pyi} (x_i - X_{cg})^2] + K_{capz} = \sum [K_{pxi} y_{ci}^2 + K_{pyi} x_{ci}^2] + K_{capz}$$

$$= 2144763 + 4454486 + 766667 = 7365916 \text{ kNm/rad by (Eqn HQ-5)}$$

- (iv) The applied external lateral wind load about the shear centre are worked out as :

	Wind X (kN)	Wind Y (kN)	On-plan Moment (kNm)
Wind Load in X-direction	2260	0	1755.449
Wind Load in Y-direction	15	1890	680.7435

Table HQ-3 – Summary of External Lateral Load of Worked Example HQ-1

- (v) The shears and moments acting on the piles and the pile cap are worked out for two wind load cases in accordance with (Eqn HQ-6) to (Eqn HQ-10) and tabulated in Tables HQ-4(a) and HQ-4(b) as follows :

Pile No / Cap	Shear (kN)						Moment Coeff.		Max. Moment (kNm)	
	Due to Direct Shear		Due to Torsion		Total		M_{pxi}	M_{pyi}	along X-X	along Y-Y
	X-X	Y-Y	X-X	Y-Y	X-X	Y-Y				
P1	64.801	0.000	15.803	-6.036	80.604	-6.036	0.436	0.398	73.68	-3.66
P2	64.801	0.000	15.803	-0.370	80.604	-0.370	0.436	0.398	73.68	-0.22
P3	64.801	0.000	15.803	5.295	80.604	5.295	0.436	0.398	73.68	3.21
P4	84.865	0.000	20.695	6.614	105.560	6.614	0.426	0.420	87.61	5.08
P5	92.987	0.000	19.709	-9.827	112.696	-9.827	0.424	0.398	90.55	-5.96
P6	92.987	0.000	16.742	-6.995	109.729	-6.995	0.424	0.420	88.17	-5.37
P7	92.987	0.000	16.742	6.614	109.729	6.614	0.424	0.420	88.17	5.08
P8	92.987	0.000	10.808	-6.995	103.795	-6.995	0.424	0.420	83.40	-5.37
P9	92.987	0.000	10.808	6.614	103.795	6.614	0.424	0.420	83.40	5.08
P10	92.987	0.000	3.138	-9.073	96.124	-9.073	0.424	0.412	77.24	-6.35
P11	92.987	0.000	3.138	8.580	96.124	8.580	0.424	0.412	77.24	6.01
P12	92.987	0.000	-0.695	4.434	92.291	4.434	0.424	0.404	74.16	2.86
P13	92.987	0.000	-4.532	-6.995	88.454	-6.995	0.424	0.420	71.07	-5.37
P14	92.987	0.000	-4.532	1.154	88.454	1.154	0.424	0.407	71.07	0.77
P15	92.987	0.000	-4.532	6.614	88.454	6.614	0.424	0.420	71.07	5.08
P16	92.987	0.000	-7.499	4.667	85.487	4.667	0.424	0.420	68.69	3.58
P17	92.987	0.000	-10.466	-6.995	82.520	-6.995	0.424	0.420	66.31	-5.37
P18	84.865	0.000	-9.552	2.719	75.313	2.719	0.426	0.420	62.51	2.09
P19	84.865	0.000	-9.552	6.614	75.313	6.614	0.426	0.420	62.51	5.08
P20	92.987	0.000	-13.433	-9.827	79.553	-9.827	0.424	0.398	63.92	-5.96
P21	84.865	0.000	-12.260	1.154	72.605	1.154	0.426	0.407	60.26	0.77
P22	84.865	0.000	-12.260	4.667	72.605	4.667	0.426	0.420	60.26	3.58
P23	84.865	0.000	-14.968	-6.995	69.897	-6.995	0.426	0.420	58.01	-5.37
P24	84.865	0.000	-14.968	-6.036	69.897	-6.036	0.426	0.398	58.01	-3.66
P25	84.865	0.000	-14.968	2.719	69.897	2.719	0.426	0.420	58.01	2.09
P26	84.865	0.000	-14.968	6.614	69.897	6.614	0.426	0.420	58.01	5.08
Pile Cap	0.000	0.000	0.000	1.067	0.000	1.067	–	–	–	–
Sum	2260.00	0.000	0.000	0.000	2260.00	0.000				

Table HQ-4(a) – Summary of Pile and Pile Cap Reactions to Wind in X-direction

Pile No / Cap	Shear (kN)						Moment Coeff.		Max. Moment (kNm)	
	Due to Direct Shear		Due to Torsion		Total		M_{pxi}	M_{pyi}	along X-X	along Y-Y
	X-X	Y-Y	X-X	Y-Y	X-X	Y-Y				
P1	0.430	90.960	6.128	-2.341	6.558	88.620	0.436	0.398	5.99	53.71
P2	0.430	90.960	6.128	-0.144	6.558	90.817	0.436	0.398	5.99	55.04
P3	0.430	90.960	6.128	2.053	6.558	93.014	0.436	0.398	5.99	56.37
P4	0.563	46.716	8.025	2.565	8.589	49.281	0.426	0.420	7.13	37.85
P5	0.617	90.960	7.643	-3.811	8.260	87.149	0.424	0.398	6.64	52.82
P6	0.617	46.716	6.492	-2.712	7.110	44.004	0.424	0.420	5.71	33.80
P7	0.617	46.716	6.492	2.565	7.110	49.281	0.424	0.420	5.71	37.85
P8	0.617	46.716	4.191	-2.712	4.808	44.004	0.424	0.420	3.86	33.80
P9	0.617	46.716	4.191	2.565	4.808	49.281	0.424	0.420	3.86	37.85
P10	0.617	60.597	1.217	-3.518	1.834	57.079	0.424	0.412	1.47	39.97
P11	0.617	60.597	1.217	3.327	1.834	63.925	0.424	0.412	1.47	44.77
P12	0.617	76.171	-0.270	1.719	0.348	77.890	0.424	0.404	0.28	50.28
P13	0.617	46.716	-1.758	-2.712	-1.140	44.004	0.424	0.420	-0.92	33.80
P14	0.617	69.845	-1.758	0.448	-1.140	70.293	0.424	0.407	-0.92	46.80
P15	0.617	46.716	-1.758	2.565	-1.140	49.281	0.424	0.420	-0.92	37.85
P16	0.617	46.716	-2.908	1.810	-2.291	48.526	0.424	0.420	-1.84	37.27
P17	0.617	46.716	-4.059	-2.712	-3.442	44.004	0.424	0.420	-2.77	33.80
P18	0.563	46.716	-3.704	1.055	-3.141	47.771	0.426	0.420	-2.61	36.69
P19	0.563	46.716	-3.704	2.565	-3.141	49.281	0.426	0.420	-2.61	37.85
P20	0.617	90.960	-5.209	-3.811	-4.592	87.149	0.424	0.398	-3.69	52.82
P21	0.563	69.845	-4.754	0.448	-4.191	70.293	0.426	0.407	-3.48	46.80
P22	0.563	46.716	-4.754	1.810	-4.191	48.526	0.426	0.420	-3.48	37.27
P23	0.563	46.716	-5.804	-2.712	-5.241	44.004	0.426	0.420	-4.35	33.80
P24	0.563	90.960	-5.804	-2.341	-5.241	88.620	0.426	0.398	-4.35	53.71
P25	0.563	46.716	-5.804	1.055	-5.241	47.771	0.426	0.420	-4.35	36.69
P26	0.563	46.716	-5.804	2.565	-5.241	49.281	0.426	0.420	-4.35	37.85
Pile Cap	0.000	306.439	0.000	0.414	0.000	306.853	–	–	–	–
Sum	15.00	1890.00	0.000	0.000	15.00	1890.00				

Table HQ-4(b) – Summary of Pile and Pile Cap Reactions to Wind in Y-direction

The determination of maximum moment on the pile shaft is based on the coefficients from Table HP-3(a) in Appendix HP in accordance with the L/T ratios. The moments are determined by multiplying the coefficients by the shear and the T values according to Table HP-2.

The shear in the pile cap is given in the Table whilst the torsion on the pile cap has to be worked out using (Eqn HQ-10) as

$$M_{cap} = T \frac{K_{capz}}{J} = 1755.449 \times \frac{766667}{7365916} = 182.71 \text{ kNm for Wind in the X-direction}$$

$$M_{cap} = T \frac{K_{capz}}{J} = 680.74 \times \frac{766667}{7365916} = 70.85 \text{ kNm for Wind in the Y-direction}$$

- (vi) The displacement of the shear centre of the piled foundation is determined by (Eqn HQ-11) as

	Translation in X-direction (mm)	Translation in Y-direction (mm)	On-plan Rotation (Radian / Degrees)
Wind Load in X-direction	8.00	0	0.000238 / 0.014°
Wind Load in Y-direction	0.05	6.69	0.000092 / 0.0053°

Table HQ-5 – Summary of Pile and Pile Cap Displacements to Wind Loads

Lateral displacements of a pile i or any coordinate point (X_{ci}, Y_{ci}) with respect

to the coordinate system with the shear Centre as the origin and the axes parallel to the X and Y axes can be determined as

$$\text{Along the X-direction} \quad \Delta X_g - Y_{ci} \Delta \theta$$

$$\text{Along the Y-direction} \quad \Delta Y_g + X_{ci} \Delta \theta$$

where ΔX_g , ΔY_g and $\Delta \theta$ are respectively the translation of the shear centre in the X-direction, translation of the shear centre in the Y-direction and on-plan rotation of the shear centre. Take the Worked Example HQ-1 for the case of “Wind Load in X-direction” where the on-plan rotation of the shear centre is positive (i.e. anti-clockwise), the pile no. P26 (at 3.974m and 3.731m along X and Y respectively from the shear centre of the system) should therefore suffer the actual translation as

$$\text{Along the X-direction} \quad \Delta X_g - Y_{ci} \Delta \theta = 8.00 - 0.000238 \times 3731 = 7.11 \text{ mm}$$

$$\text{Along the Y-direction} \quad \Delta Y_g + X_{ci} \Delta \theta = 0 + 0.000238 \times 3974 = 0.95 \text{ mm}$$

HQ.3 Application in Mathematical Models

The approach as described above is for hand calculations with or without the use of spreadsheets. Nevertheless, with the inputs of the stiffnesses of the piles and the pile cap into computer mathematical models, the analysis can also be carried out by computer software. Nowadays analysis based on 3-dimensional mathematical models can analyze in-plane (due to shear) and out-of-plane loads simultaneously enabling load combinations to be carried out for structural design.

Appendix HR

**Assessment of Effects on Adjacent Structures due to
Loads from a New Structure by the Continuum
Theory based on Mindlin's Equation**

Assessment of Effects on Adjacent Structures due to Loads from a New Structure by the Continuum Theory based on Mindlin's Equations

HR.1 Theoretical Background

The Mindlin's Equations calculate stresses and deformations in various directions at a point within a semi-infinite elastic medium due to a point load acting in the same medium but at another point. Figure HR-1 indicates application of the equations for calculating direct and shear stresses at the point B due to a vertical point load P at A.

$R_1 = \sqrt{x^2 + y^2 + (z-c)^2}$
 $R_2 = \sqrt{x^2 + y^2 + (z+c)^2}$
 ν is the Poisson's ratio of the Medium

$$\sigma_x = \frac{-P}{8\pi(1-\nu)} \left[\frac{(1-2\nu)(z-c)}{R_1^3} - \frac{3x^2(z-c)}{R_1^5} + \frac{(1-2\nu)[3(z-c)-4\nu(z+c)]}{R_2^3} - \frac{3(3-4\nu)x^2(z-c)-6c(z+c)[(1-2\nu)z-2\nu c]}{R_2^5} - \frac{30cx^2z(z+c)}{R_2^7} - \frac{4(1-\nu)(1-2\nu)}{R_2(R_2+z+c)} \left(1 - \frac{x^2}{R_2(R_2+z+c)} - \frac{x^2}{R_2^2} \right) \right] \quad (\text{Eqn HR-1})$$

$$\sigma_y = \frac{-P}{8\pi(1-\nu)} \left[\frac{(1-2\nu)(z-c)}{R_1^3} - \frac{3y^2(z-c)}{R_1^5} + \frac{(1-2\nu)[3(z-c)-4\nu(z+c)]}{R_2^3} - \frac{3(3-4\nu)y^2(z-c)-6c(z+c)[(1-2\nu)z-2\nu c]}{R_2^5} - \frac{30cy^2z(z+c)}{R_2^7} - \frac{4(1-\nu)(1-2\nu)}{R_2(R_2+z+c)} \left(1 - \frac{y^2}{R_2(R_2+z+c)} - \frac{y^2}{R_2^2} \right) \right] \quad (\text{Eqn HR-2})$$

$$\sigma_z = \frac{-P}{8\pi(1-\nu)} \left[-\frac{(1-2\nu)(z-c)}{R_1^3} + \frac{(1-2\nu)(z-c)}{R_2^3} - \frac{3(z-c)^3}{R_1^5} - \frac{3(3-4\nu)z(z+c)^2-3c(z+c)(5z-c)}{R_2^5} - \frac{30cz(z+c)^3}{R_2^7} \right] \quad (\text{Eqn HR-3})$$

$$\tau_{yz} = \frac{-Py}{8\pi(1-\nu)} \left[-\frac{1-2\nu}{R_1^3} + \frac{1-2\nu}{R_2^3} - \frac{3(z-c)^2}{R_1^5} - \frac{3(3-4\nu)z(z+c)-3c(3z+c)}{R_2^5} - \frac{30cz(z+c)^2}{R_2^7} \right] \quad (\text{Eqn HR-4})$$

$$\tau_{zx} = \frac{-Px}{8\pi(1-\nu)} \left[-\frac{1-2\nu}{R_1^3} + \frac{1-2\nu}{R_2^3} - \frac{3(z-c)^2}{R_1^5} - \frac{3(3-4\nu)z(z+c)-3c(3z+c)}{R_2^5} - \frac{30cz(z+c)^2}{R_2^7} \right] \quad (\text{Eqn HR-5})$$

$$\tau_{xy} = \frac{-Pxy}{8\pi(1-\nu)} \left[-\frac{3(z-c)}{R_1^5} - \frac{3(3-4\nu)(z-c)}{R_2^5} + \frac{4(1-\nu)(1-2\nu)}{R_2^2(R_2+z+c)} \left(\frac{1}{R_2+z+c} + \frac{1}{R_2} \right) - \frac{30cz(z+c)}{R_2^7} \right] \quad (\text{Eqn HR-6})$$

Figure HR-1 – Illustration of Mindlin's Equations for Determination of Various Components of Stresses due to a Vertical Load in a Semi-infinite Elastic Medium

The effects due to loaded area can then be obtained by integrating the effects over the whole area which can be idealized as comprising a series of point loads. For example, if the exerting stress of an area of load at a location of coordinate (x, y) is $u_z(x, y)$ by which we can define a point load $dP = u_z(x, y)dxdy$ acting at the point and by applying the relevant formula in Figure HR-1, we can calculate the effect, say the vertical stress at another point X due to the point load as $d\sigma_z = dPI_z(x, y) = u_z(x, y)dxdyI_z(x, y)$ where $I_z(x, y)$ is the coefficient of P in (Eqn HR-3). The total effect due to the area load at X will then be $\int_A d\sigma_z = \int_A u_z(x, y)I_z(x, y)dxdy$.

HR.2 Worked Example HR-1

A rectangular footing of plan area 40m by 30m is exerting a linearly varying “net” ground pressures at 3m below ground. That is, the pressures are due to the weight of the structure minus the weight of soil displaced. The “net” pressures at the 4 corners of the footing are 125kPa, 155kPa, 45kPa and 75kPa as shown in Figure HR-2 in which a coordinate system with the origin at the centre of the footing is shown. The ground pressure at any point (x, y) within the footprint of the footing can then be defined by the equation $P(x, y) = 2x - y + 100$. The horizontal and shear stresses of a wall at location shown in Figure HR-2 with its top level at the ground and bottom level 15m below ground are to be determined.

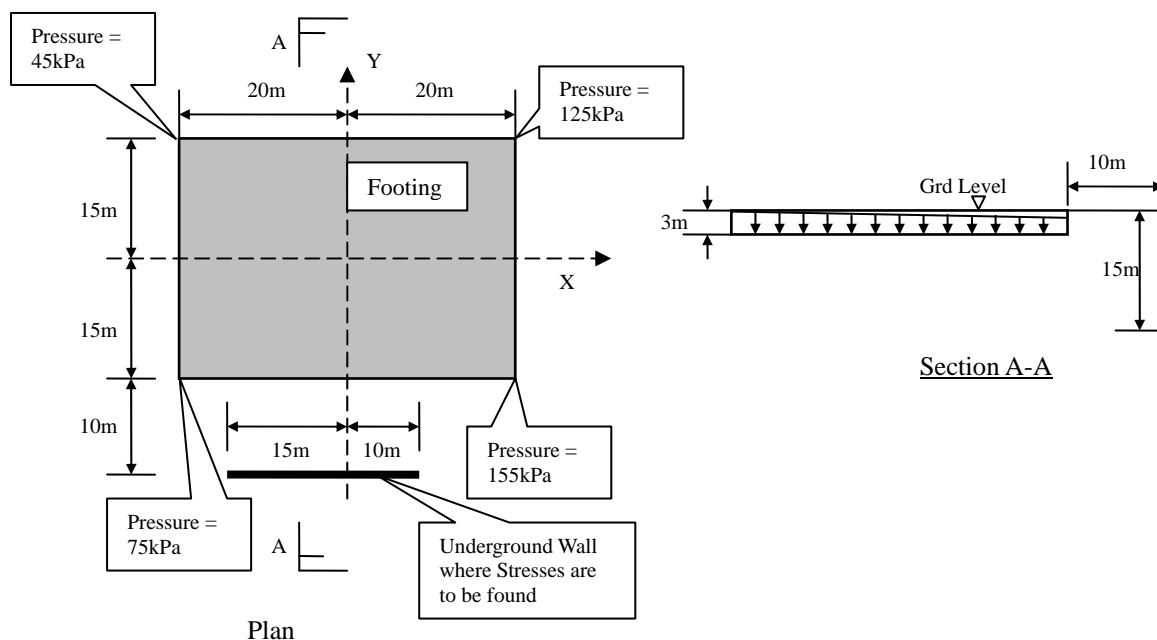


Figure HR-2 – Worked Example HR-1

The normal stresses of the wall (stresses in the global Y direction of Figure HR-2) are calculated for points in on the wall at 1m grid (in both global X and Z directions) and the stress contour is plotted in Figure HR-3. Analytical solutions have not been

found for the integrals. Instead numerical solutions based on the software Mathcad (2001) have been used for calculation and plotting. Alternatively, other software including Microsoft excel can be used.

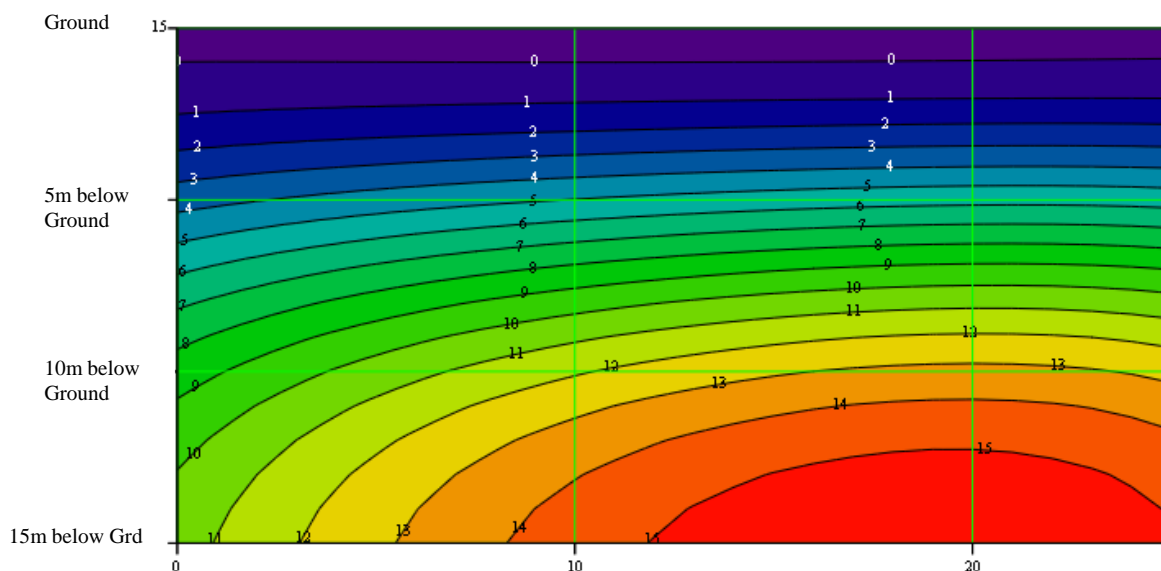


Figure HR-3(a) – Normal Stress Contours in kPa on the Wall of Worked Example HR-1

Similarly, the shear stresses on the wall are also calculated and plotted in Figure HR-3(b)

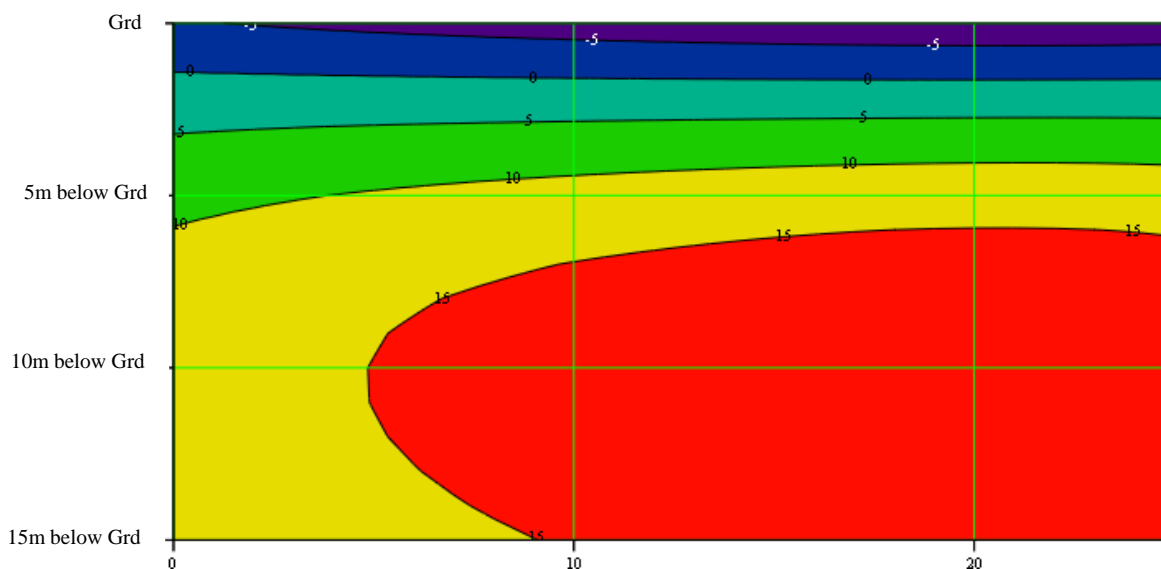


Figure HR-3(b) – Shear Stress Contours in kPa on the Wall of Worked Example HR-1

Appendix HS

Seepage Analysis of Excavation in a Homogeneous, Isotropic Soil Medium

Seepage Analysis of Excavation in a Homogeneous, Isotropic Soil Medium

HS.1 Theoretical Background

By the theory of water seepage through soil, the following governing differential equation can be derived which is found in many text books.

$$K_x \frac{\partial^2 h}{\partial x^2} + K_y \frac{\partial^2 h}{\partial y^2} = 0 \quad (\text{Eqn HS-1})$$

In the equation, h is the total head (the sum of elevation head and pressure head in the Bernoulli Theorem with the velocity head ignored due to its insignificant contribution, K_x and K_y are the coefficients of permeability of the soil in the X and Y directions defined by the Darcy Law as :

$$v_x = K_x \frac{\partial h}{\partial x}; \quad v_y = K_y \frac{\partial h}{\partial y} \quad (\text{Eqn HS-2})$$

where v_x and v_y are respectively the velocities of flow of water in the soil in the X and Y directions.

Though numerical methods can always be used to solve (Eqn HS-1), analytical solutions of the equation can also be found for certain cases where the geometries of excavations involving impermeable walls are simple. The following Worked Examples HS-1 and HS-2 illustrate the use of analytical solutions for two simple but common geometries by which water pressures on the wall and the “criticalities” of water seepage can be estimated. However, in these 2 examples, the ground water levels are assumed to be at constant levels on the upstream sides so that constant values of total head h can be prescribed at the levels as boundary conditions to the differential equation at (Eqn HS-1) for solution. The assumption in fact transforms the problem to a “confined flow” problem where the water is flowing through fixed boundary. On the other hand, if the assumption is not adopted where the flow becomes an “unconfined flow”, the ground water level is not constant but drops towards the sheetpile and the solution has to be based on a trial and error process which will be discussed in the later part of this appendix. Nevertheless, the analysis will be more critical in terms of water pressure and flow under the “confined flow” assumption which can be adopted as a conservative design for excavation supported by sheetpile.

HS.2 Worked Example HS-1 – Impermeable layer at depth at infinity

In the example, the head and criticalities of an excavation shown in Figure HS-1 where the flow is at steady stage are to be estimated. The impermeable soil layer is taken at depth infinity and the soil is homogeneous and isotropic. It is also intended to keep the water level at the downstream side constant at 0.5m (by pumping) below ground.

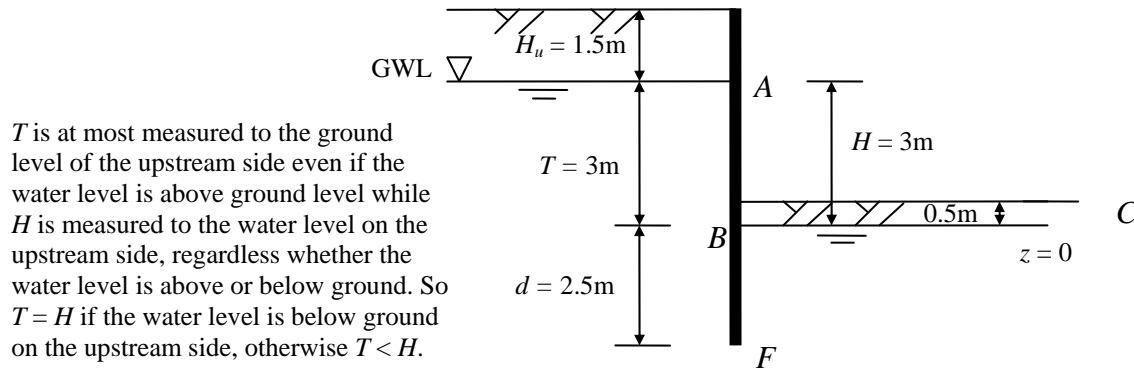


Figure HS-1 – Worked Example HS-1

If the soil is homogeneous and isotropic where $K_x = K_y$, (Eqn HS-1) can be reduced

$$\text{to } \frac{\partial^2 h}{\partial x^2} + \frac{\partial^2 h}{\partial y^2} = 0 \quad (\text{Eqn HS-3})$$

Analytical solutions for the geometry have been derived and are listed in Azizi (2000) and the following steps can be followed :

- (i) Determine η from (Eqn HS-4) listed below (by trial and error)

$$\tan(\pi\eta) - \pi\eta = \frac{\pi d}{T} \quad (\text{Eqn HS-4})$$

- (ii) Determine h_F (head at F which is the toe level of the impermeable wall) by

$$h_F = \eta H \quad (\text{Eqn HS-5})$$

- (iii) Determine $\lambda = \frac{H}{\pi}$; $\beta = \frac{T}{\pi}$; $\alpha = \frac{\beta}{\cos(h_F / \lambda)}$ (Eqn HS-6)

- (iv) The equation relating total head h_z along the wall and depth z is

$$z = \frac{\beta h_z}{\lambda} - \alpha \sin \frac{h_z}{\lambda} \quad (\text{Eqn HS-7})$$

where z is taken as zero at the downstream water level. It should be noted that the equation is applicable both upstream and downstream. When h_z increases along the flow from upstream to downstream, z will change from decreasing to increasing at the upstream course.

- (v) The average hydraulic gradient at the upstream side at the wall at level z is

$$i_{uz} = \frac{h_A - h_z}{T - z} \quad (\text{Eqn HS-8})$$

where h_A is the total head at the ground surface of the upstream side.

- (vi) The average hydraulic gradient at the upstream side at the wall at level z is

$$i_{ud} = \frac{h_z - h_B}{z} \quad (\text{Eqn HS-9})$$

where h_B is the total head at the water surface of the downstream side.

(vii) The actual pressure is $(h_z - z)\gamma_w$ where γ_w is the density of water.

For the numerical problem in Worked Example HS-1, by (Eqn HS-4)

$$\tan(\pi\eta) - \pi\eta = \frac{\pi d}{T} = \frac{\pi \times 2.5}{3} \Rightarrow \eta = 0.42089$$

$$h_F = \eta H = 0.42089 \times 3 = 1.26267$$

$$\lambda = \frac{H}{\pi} = \frac{3}{\pi} = 0.95493; \quad \beta = \frac{T}{\pi} = \frac{3}{\pi} = 0.95493; \quad \alpha = \frac{\beta}{\cos(h_F / \lambda)} = 3.882132$$

So the governing equation between z and h_z is

$$z = \frac{\beta h_z}{\lambda} - \alpha \sin \frac{h_z}{\lambda} = h_z - 3.882132 \sin 1.047198 h_z;$$

The calculated results at the various levels on the upstream and downstream sides are tabulated as :

Head h_z (m)	Depth z (m)	Average Hydraulic Gradient i_{zu}	Hydraulic Pressure $(h_z - z)\gamma_w$ (kPa)
3	3	0	0.00
2.75	1.7452	0.1992	10.05
2.5	0.5589	0.2048	19.41
2.25	-0.4951	0.2146	27.45
2	-1.3620	0.2293	33.62
1.75	-1.9999	0.2500	37.50
1.625	-2.2239	0.2632	38.49
1.5	-2.3821	0.2787	38.82
1.45	-2.4268	0.2856	38.77
1.4	-2.4609	0.2930	38.61
1.272	-2.5000	0.3142	37.72

Table HS-1(a) – Summary of Upstream Side

Head h_z (m)	Depth z (m)	Average Hydraulic Gradient i_{zd}	Hydraulic Pressure $(h_z - z)\gamma_w$ (kPa)
0	0.0000	0	0.00
0.25	-0.7548	-0.3312	10.05
0.5	-1.4411	-0.3470	19.41
0.75	-1.9951	-0.3759	27.45
1	-2.3620	-0.4234	33.62
1.25	-2.4999	-0.5000	37.50
1.272	-2.5000	-0.5088	37.72

Table HS-1(b) – Summary of Downstream Side

Table HS-1 – Summary of Heads/Pressures of Worked Example HS-1

The calculated hydrostatic pressure profiles are plotted in Figure HS-2 as follows :

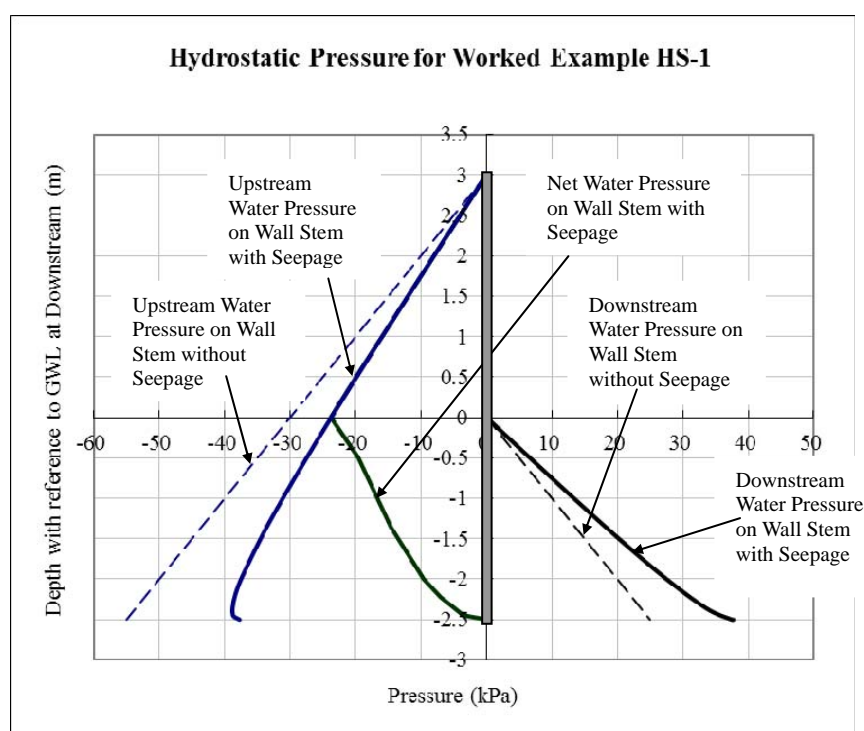


Figure HS-2 – Hydrostatic Pressures on Wall in Worked Example HS-1

The total forces and moments on the wall due to the seeping water on both sides are summed and tabulated as :

Force (kN) per metre width			Moment (kNm) about wall toe per metre width		
Up Stream	Down Stream	Net	Up Stream	Down Stream	Net
116.8	42.99	73.81	218.33	35.19	183.14

The average hydraulic gradient at downstream is 0.5. The “Quick sand” effect can be assumed not to take place as the gradient is less than the critical value of the ratio of buoyant density of soil over density of water divided by 1.5 which is $(19-10)/10/1.5 = 0.6$. It should be pointed out that the water pressures at both sides at the wall toe must be equal. Thus adoption of the “No seepage” hydrostatic pressure for design will be very conservative.

HS.3 Worked Example HS-2 – Impermeable layer at finite depth

Worked Example HS-1 is modified with the impermeable layer at finite depth as shown in Figure HS-3 and re-analyzed as Worked Example HS-2.

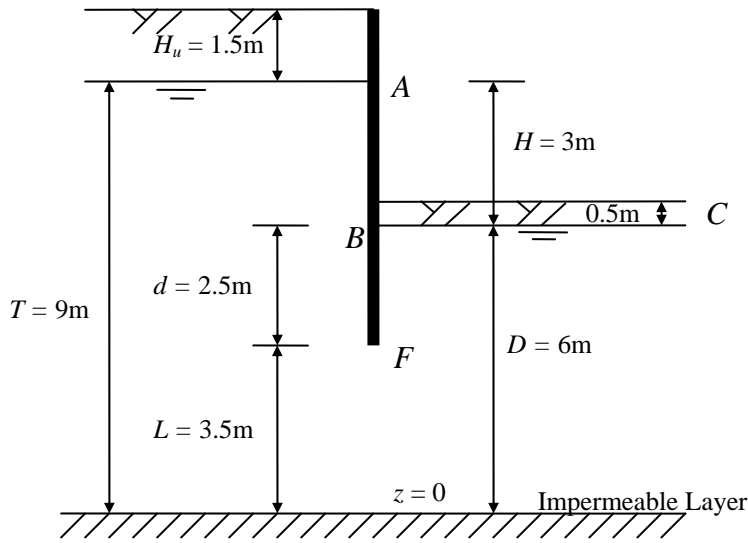


Figure HS-3 – Worked Example HS-2

The analytical formulae are different from those of Worked Example HS-1 which are listed as follows. $z = 0$ is set at the level of the impermeable layer.

(i) Calculate $\xi = \frac{H}{\ln \left[\frac{T}{L} + \sqrt{\frac{T^2}{L^2} - 1} \right] + \ln \left[\frac{D}{L} + \sqrt{\frac{D^2}{L^2} - 1} \right]}$ (Eqn HS-9)

(ii) Along upstream side AF, the head is $h_z = \xi \ln \left[\frac{z}{L} + \sqrt{\frac{z^2}{L^2} - 1} \right]$ (Eqn HS-10)

(iii) Along downstream side AF, the head is $h_z = -\xi \ln \left[\frac{z}{L} + \sqrt{\frac{z^2}{L^2} - 1} \right]$ (Eqn HS-11)

(iv) Determine the head at A $h_A = \xi \ln \left[\frac{T}{L} + \sqrt{\frac{T^2}{L^2} - 1} \right]$; and head at B

$$h_B = -\xi \ln \left[\frac{D}{L} + \sqrt{\frac{D^2}{L^2} - 1} \right] \text{ and it can be shown that } h_A - h_B = H$$

(v) So the total head at z on wall upstream is $h_{Tuz} = h_z - h_A + T$ (Eqn HS-12)

and at z on the wall downstream is $h_{Tdz} = h_z - h_B + D$ (Eqn HS-13)

(vi) The water pressure at z on wall at upstream is $(h_{Tuz} - z)\gamma_w$ (Eqn HS-14)

and that at z on the wall downstream is $(h_{Tdz} - z)\gamma_w$ (Eqn HS-15)

For the numerical problem in Figure HS-3, $\xi = 1.0985$; $h_A = 1.7548$ m;

$$h_B = -1.2452 \text{ m}$$

The heads, hydraulic gradients, and water pressures are tabulated as follows :

Depth z (m)	Head h_z (m)	$h_{Tuz} = h_z - h_A + T$ (m)	Average Hydraulic Gradient i_{zu}	Water Pressure $(h_{Tuz} - z)\gamma_w$ (kPa)
9	1.7548	9.0000	0.0000	0.00
8.5	1.6863	8.9315	0.1370	4.31
8	1.6127	8.8579	0.1421	8.58
7.5	1.5332	8.7784	0.1477	12.78
7	1.4467	8.6919	0.1541	16.92
6.5	1.3514	8.5966	0.1614	20.97
6	1.2452	8.4904	0.1699	24.90
5.5	1.1246	8.3698	0.1801	28.70
5	0.9838	8.2290	0.1927	32.29
4.5	0.8118	8.0570	0.2096	35.57
4	0.5804	7.8256	0.2349	38.26
3.5	0.0000	7.2452	0.3191	37.45

Table HS-2(a) – Summary of Upstream Side

Depth z (m)	Head h_z (m)	$h_{Tdz} = h_z - h_B + D$ (m)	Average Hydraulic Gradient i_{zd}	Water Pressure $(h_{Tdz} - z)\gamma_w$ (kPa)
6	-1.2452	6.0000	0.0000	0.00
5.5	-1.1246	6.1206	-0.2412	6.21
5	-0.9838	6.2614	-0.2614	12.61
4.5	-0.8118	6.4334	-0.2889	19.33
4	-0.5804	6.6648	-0.3324	26.65
3.5	0.0000	7.2452	-0.4981	37.45

Table HS-2(b) – Summary of Downstream Side

Table HS-2 – Summary of Heads/Pressures of Worked Example HS-2

The calculated hydrostatic pressure profiles are plotted in Figure HS-4 as follows :

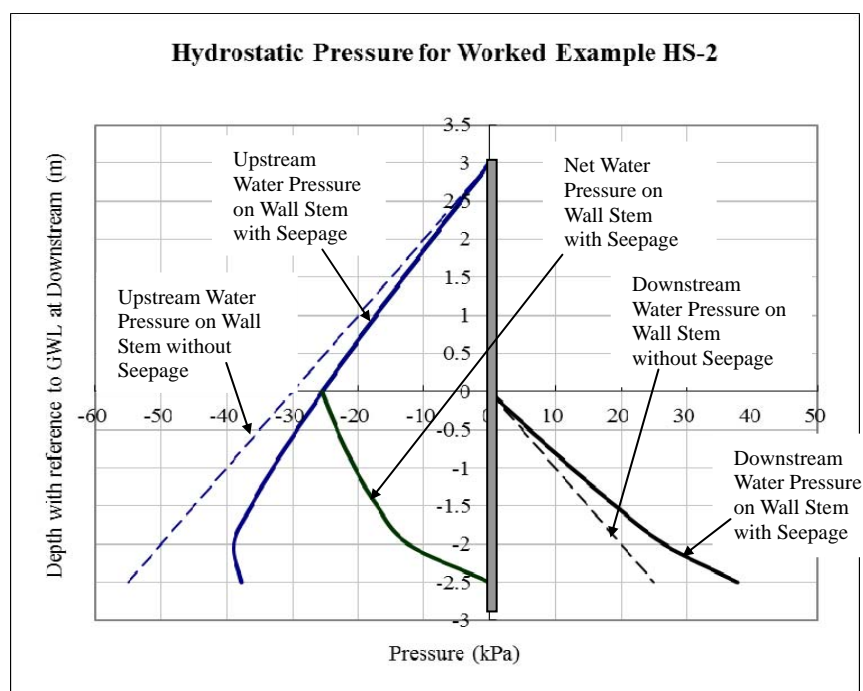


Figure HS-4 – Hydrostatic Pressures on Wall in Worked Example HS-2

Summing the total force and moments on the wall due to the seeping water on both sides :

Force (kN) per metre width			Moment (kNm) about wall toe per metre width		
Up Stream	Down Stream	Net	Up Stream	Down Stream	Net
121.0	41.76	79.24	229.67	33.56	196.12

As compared with Worked Example HS-1, there is a slight increase in the forces and moments.

The exercise is re-done by decreasing the depth between the wall toe and the impermeable layer to 1.5m as Worked Example HS-3 and the summation of force and moment become as follows which only slightly greater than Worked Example HS-2:

Force (kN) per metre width			Moment (kNm) about wall toe per metre width		
Up Stream	Down Stream	Net	Up Stream	Down Stream	Net
123.37	41.60	81.76	234.58	33.30	201.28

Again the average hydraulic gradient which is $0.5 < 0.6$ as in Worked Example HS-1.

HS.4 Solution by Numerical Method

(Eqn HS-1) can in fact be solved by the finite difference method. The 2-dimensional soil medium is first divided into a regular rectangular mesh with “nodes” at which the total head h as defined in para. HS.1 are to be determined. Formulation in accordance with (Eqn HS-1) in accordance with the h value of a point at the location (i, j) denoted as $h_{i,j}$ as illustrated in Figure HS-5 can be as follows :

$$K_x \frac{h_{i,j-1} - 2h_{i,j} + h_{i,j+1}}{\Delta x^2} + K_y \frac{h_{i-1,j} - 2h_{i,j} + h_{i+1,j}}{\Delta y^2} = 0 \quad (\text{Eqn HS-16})$$

where Δx and Δy are the intervals between adjacent points in the X and Y directions along the rectangular mesh as shown in Figure HS-5.

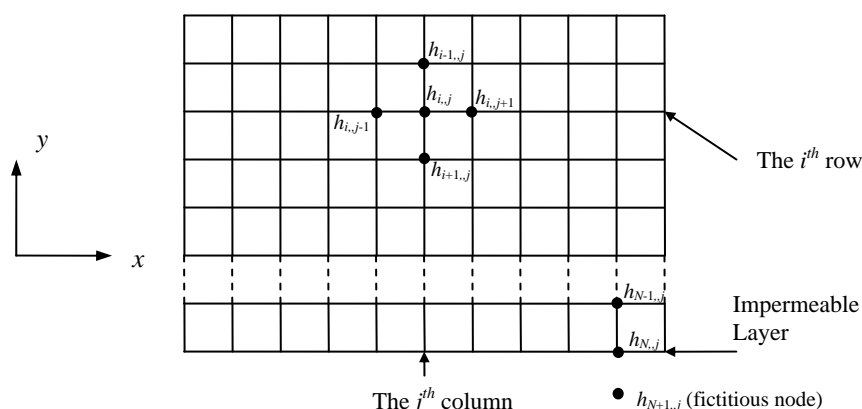


Figure HS-5 – Soil Medium Idealized into a Regular Rectangular Mesh

If setting $K_x = K_y$, $\Delta x = \Delta y$, (Eqn HS-16) can be simplified to

$$h_{i-1,j} + h_{i,j-1} - 4h_{i,j} + h_{i,j+1} + h_{i+1,j} = 0 \quad (\text{Eqn HS-17})$$

N number of equations can be formulated in accordance with (Eqn HS-17) for N number of nodes, together with the use of “fictitious nodes” outside the soil medium which is the usual assumption in finite difference analysis. To ensure the number of equations equals the sum of the N real nodes and the number of fictitious nodes, additional “boundary conditions” equations have to be included. For the Worked Example HS-2 where $\Delta x = \Delta y = 0.5$ m, these boundary conditions include :

- (i) Total head h remain constant at the nodes along the top “free surface” of the upstream and downstream sides which are respectively 9m and 6m;
- (ii) At the nodes along a vertical edge considerably far away from the wall, the hydrostatic conditions are considered normal without flow, i.e. the total head h remain constant. The total head at a node at z below the top surface along the far vertical edge at the upstream side, the elevation head is $9 - z$ and the pressure head is z so that the total head remains at $h = (9 - z) + z = 9$. Similarly for the downstream side the total head at the nodes along the far edge remains at $h = 6$. The far edges are taken as 10m from the wall;
- (iii) The speed of flow in (1) the vertical direction (Y-direction) at the impermeable layer and (2) the horizontal direction at the wall are 0, i.e. by (Eqn HS-2) for (1)

$$v_y = K_y \frac{\partial h}{\partial y} = 0 \Rightarrow \frac{h_{N+1,j} - h_{N-1,j}}{2\Delta y} = 0 \Rightarrow h_{N+1,j} = h_{N-1,j} \quad \text{where } h_{N+1,j} \text{ and } h_{N-1,j}$$
 are respectively the heads at the nodes just above the impermeable layer and at the “fictitious nodes” beneath the impermeable layer as illustrated in Figure HS-5 above. Similar boundary conditions can be formulated for (2).

The solution yields the total head contours (or equi-potential lines) in Figure HS-6. A set of “flow-lines” perpendicular to the total head contours are superimposed onto the total head contours to form the “flow net”.

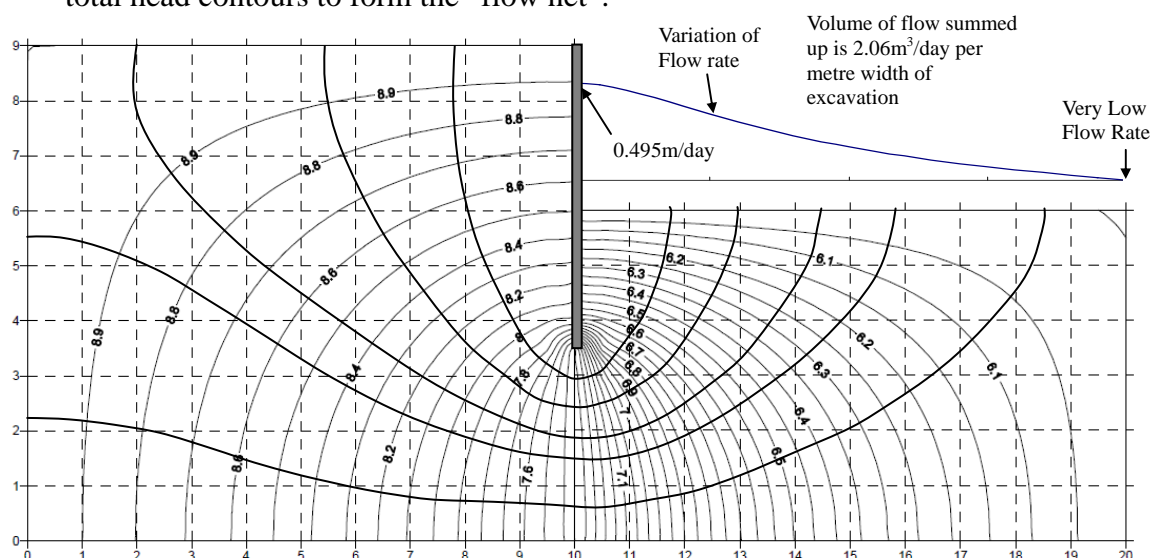


Figure HS-6 – “Flow net” Analysis of Worked Example HS-2 by the Finite Difference Method

In addition, the water flow rate at coordinate $y = j$ at the top level of the downstream side can be calculated by $v_y = K_y \frac{\partial h}{\partial y} \Big|_{y=M} = K_y \frac{h_{M,j} - h_{M-1,j}}{\Delta y}$ where $h_{M,j}$ is the head at the top of the downstream surface. Taking $K_y = 2 \times 10^{-5}$ m/sec, the flow rates at various points are calculated and plotted in Figure HS-6. The total seepage volume can be determined numerically at $2.06 \text{ m}^3/\text{day}$.

The “pressure head” can, however be obtained by subtracting the elevation head from the total head as determined previously. The hydrostatic pressure can then be determined by multiplying the pressure head by the density of water and the pressure contour is plotted in Figure HS-7.

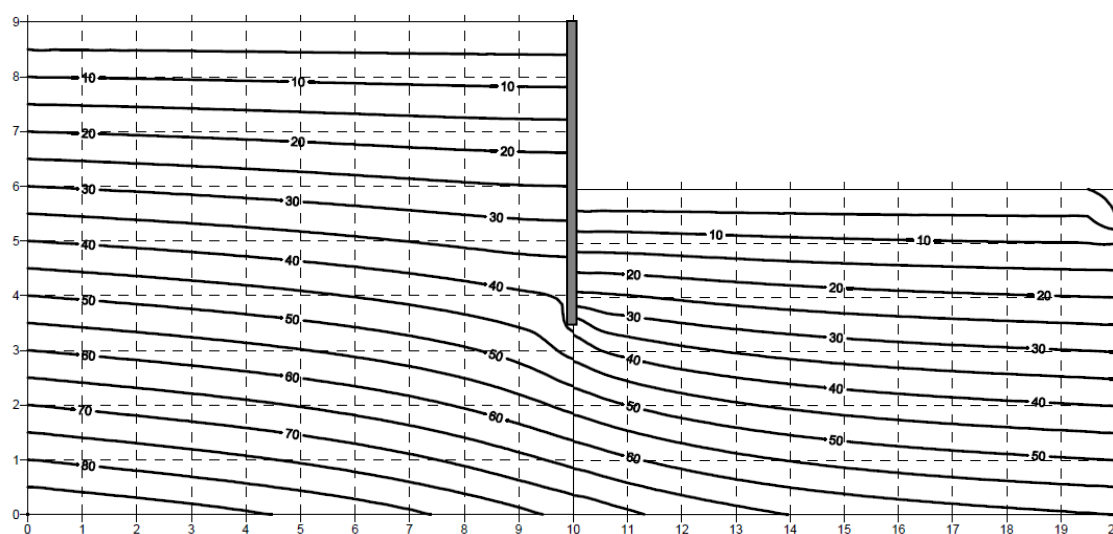


Figure HS-7 – Hydrostatic Pressure Contour of Worked Example HS-2

HS.5 Finite Element Approach

The flow can also be solved analytically by the finite element method in which the soil medium is “meshed” into an assembly of polygonal elements similar to that of structural analysis. The commonest elements are the triangular element and rectangular element and solution at the nodes are the total head. For a rectangular element of sides $2a$ and $2b$, the “seepage stiffness” matrix of isotropic material is

$$K_e = K_s \begin{bmatrix} \frac{a^2 + b^2}{3ab} & \frac{-2a^2 + b^2}{6ab} & \frac{a^2 - 2b^2}{6ab} & \frac{-a^2 - b^2}{6ab} \\ \frac{-2a^2 + b^2}{6ab} & \frac{a^2 + b^2}{3ab} & \frac{-a^2 - b^2}{6ab} & \frac{a^2 - 2b^2}{6ab} \\ \frac{6ab}{a^2 - 2b^2} & \frac{3ab}{-a^2 - b^2} & \frac{6ab}{a^2 + b^2} & \frac{6ab}{-2a^2 + b^2} \\ \frac{6ab}{-a^2 - b^2} & \frac{6ab}{a^2 - 2b^2} & \frac{3ab}{-2a^2 + b^2} & \frac{6ab}{a^2 + b^2} \\ \frac{6ab}{6ab} & \frac{6ab}{6ab} & \frac{6ab}{6ab} & \frac{3ab}{3ab} \end{bmatrix} \quad (\text{Eqn HS-18})$$

With the formulation of “seepage stiffness” matrix for each element and the entire

matrix for the soil mass can be assembled in the same manner as that for structural analysis. Conditions at boundaries can also be similarly prescribed for solution of the total head h at the joining nodes of the elements.

HS.6 Unconfined Flow

If the assumption of prescribed constant ground water level on the upstream side is not adopted resulting in “unconfined flow”, the upstream profile becomes another unknown to be solved. So the upstream top water level is not prescribed to a constant total head but instead only under the condition that the vertical flow velocity is zero as similar to the impermeable layer below. However, total head values less than the elevation heads resulting in negative hydraulic pressure heads will be resulted at certain nodes at the upper portion of the upstream side. In the finite difference approach, these nodes have to be eliminated for re-analysis as shown in Figure HS-8. The iterative process should go on until only one layer of negative hydraulic pressure heads are obtained and the zero hydraulic pressure head can be obtained by interpolation between the negative head nodes and the next positive head nodes. In the finite element approach, however, as any rectangular element with one or more negative hydraulic pressure head values have to be eliminated altogether resulting finally with all positive values, the zero hydraulic pressure head profile has to be obtained by extrapolation for the zero values. The zero hydraulic pressure head profile is obviously the final ground water level.

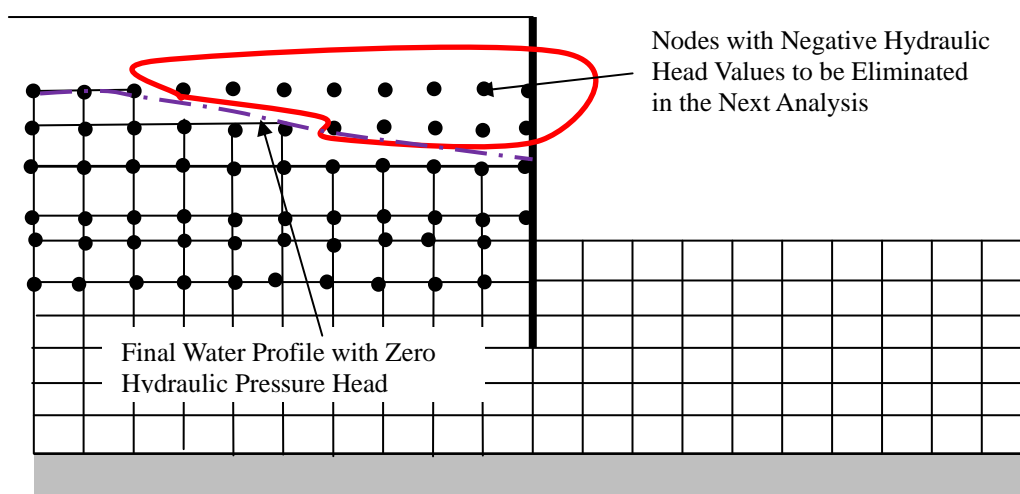


Figure HS-8 – Finite Difference Mesh after Elimination of Nodes of Negative Water Heads and Final Water Profile

Appendix HT

Trench Stability Calculation of Bentonite Slurry

Excavation

Trench Stability Calculation of Bentonite Slurry Excavation

The calculation is based on Schneebeli's Method as quoted by Hajinal I. et. al.'s "Construction of Diaphragm Walls". The method is applicable to both cohesive and cohesionless soils.

HT.1 Theoretical Background

The theoretical background and design parameters are summarized as follows :

- (i) Trench stability is ensured when the "net bentonite pressure" (which is the pressure exerted by the bentonite inside the trench less the ground water pressure outside) achieves a factor of safety 1.2 (in line with many temporary work practices) over the effective lateral soil pressure. Mathematically, it is expressed as :

$$\frac{P_b - P_w}{\sigma'_h} \geq FOS = 1.2 \quad (\text{Eqn HT-1})$$

- (ii) In (Eqn HT-1) above, P_b is the pressure exerted by the bentonite inside the trench. It varies with h_b (which is the depth below the top level of the bentonite) as

$$P_b = \gamma_b h_b \quad (\text{Eqn HT-2})$$

where γ_b is the density of the bentonite

Similarly P_w which is the pressure by the water outside the trench at depth h_w below the ground water level can be calculated by

$$P_w = \gamma_w h_w \quad (\text{Eqn HT-3})$$

where γ_w is the density of water.

- (iii) σ'_h is the lateral earth pressure to be supported by the net bentonite pressure. It is conventionally related to the coefficient of active soil pressure $K_a = \frac{1 - \sin \phi}{1 + \sin \phi}$, vertical effective stress σ'_v and cohesion c as

$$\sigma'_h = K_a \sigma'_v - 2c \sqrt{K_a} \quad (\text{Eqn HT-4})$$

Determination of σ'_v can take into account the "vertical arching effect" which is significant over the relatively short length of a barrette. The arching effect serves to reduce the effective vertical pressure from the pure overburden weight of the soil and surcharge by (Eqn HT-5) :

$$\sigma'_v = \frac{\gamma_s L}{\sin 2\phi} \left(1 - e^{-\sin 2\phi \cdot z / L} \right) + q_0 e^{-\sin 2\phi \cdot z / L} \quad (\text{Eqn HT-5})$$

The outstanding symbols in the above equations are defined as follows :

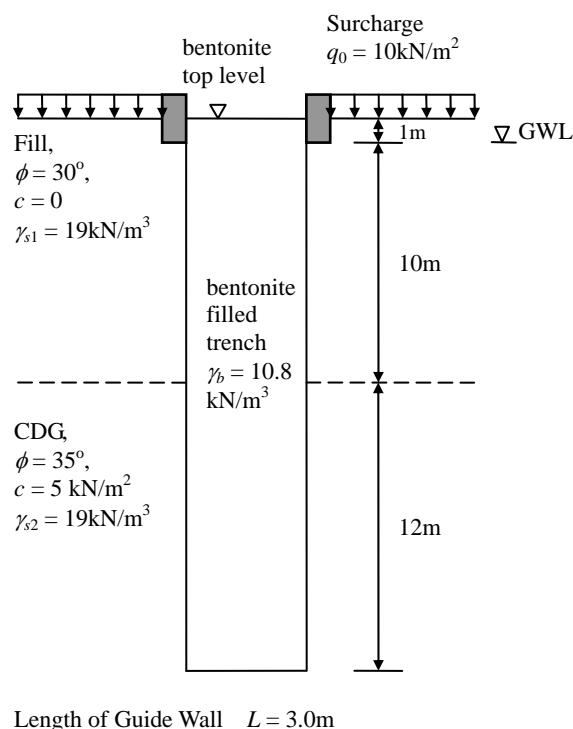
z is the depth under consideration;
 L is the length of the trench opening;
 ϕ is the soil friction angle;
 γ_s is the effective weight of soil;
 z is the depth of soil;
 c is cohesion of the soil;
 q_0 is the vertical surcharge.

It can be shown that the first term of (Eqn HT-5) will tend to $\gamma_s z$ and the second term tend to q_0 when L tends to infinity.

- (iv) The equations listed in (iii) are for homogeneous soil. For layered soil, σ'_v needs to be assessed layer by layer with q_0 being the vertical stress at the top level of the layer.

HT.2 Worked Example HT-1

The following worked example serves to demonstrate the use of the equations in HT.1.



Determinations of bentonite pressure and ground water pressure are straightforward. For example, at level 6m below ground :

Bentonite Pressure is $p_b = 10.8 \times 6 = 64.8 \text{ kN/m}^2$;

Ground Water Pressure is $p_w = 10 \times 5 = 50 \text{ kN/m}^2$.

Determination of Soil active pressure is more difficult as the effective vertical pressure takes "arching effect" into account :

- (i) For the fill above GWL;
 - $q_0 = 10 \text{ kN/m}^2$, the external surcharge,
 - $\gamma_s = 19 \text{ kN/m}^3$;
 - Using (Eqn HT-5), at $z = 1$,
 - $\sigma'_v = 23.996 \text{ kN/m}^2$;
 - Using (Eqn HT-4), $\sigma'_h = 7.999 \text{ kN/m}^2$.
- (ii) For the fill below GWL, $q_0 = 23.996 \text{ kN/m}^2$,
 - $\gamma_s = 19 - 10 = 9 \text{ kN/m}^3$; So, again using (Eqn HT-5) at the bottom level of the fill where $z = 10$; $\sigma'_v = 30.777 \text{ kN/m}^2$; and
 - by (Eqn HT-6), $\sigma'_h = 10.259 \text{ kN/m}^2$
- (iii) For the CDG, at top level, $\sigma'_v = 30.777 \text{ kN/m}^2$ as obtained in (ii); $\sigma'_h = 3.134 \text{ kN/m}^2$ by (Eqn HT-6) as $\phi = 35^\circ$ and $c = 5 \text{ kN/m}^2$
- (iv) For the CDG, at bottom level,
 - $q_0 = 30.777 \text{ kN/m}^2$; $z = 12 \text{ m}$;
 - $\sigma'_v = 28.78 \text{ kN/m}^2$ by (Eqn HT-5) and
 - $\sigma'_h = 2.594 \text{ kN/m}^2$ by (Eqn HT-6)

Figure HT-1 – Soil Profile for Worked Example HT-1

The results are tabulated in Table HT-1. The following observations can be drawn :

- (i) The vertical stresses and hence the horizontal pressures in the soil become more or less constant at greater depths instead of increasing linearly. The arching effect is thus very significant;
- (ii) The factor of safety of 1.2 can be achieved at all levels, except at the top first metre which is safeguarded by the existence of the guide walls.

Depth	ϕ	γ_s'	σ_v'	σ_h	σ_w	σ_b	$\sigma_b - \sigma_w$	FOS
0	30	19	10.000	3.333	0	0	0	0.00
1	30	19	23.996	7.999	0	10.8	10.8	1.35
1	30	9	23.996	7.999	0	10.8	10.8	1.35
2	30	9	25.797	8.599	10	21.6	11.6	1.35
3	30	9	27.146	9.049	20	32.4	12.4	1.37
4	30	9	28.156	9.385	30	43.2	13.2	1.41
5	30	9	28.914	9.638	40	54	14	1.45
6	30	9	29.481	9.827	50	64.8	14.8	1.51
7	30	9	29.906	9.969	60	75.6	15.6	1.56
8	30	9	30.225	10.075	70	86.4	16.4	1.63
9	30	9	30.464	10.155	80	97.2	17.2	1.69
10	30	9	30.643	10.214	90	108	18	1.76
11	30	9	30.777	10.259	100	118.8	18.8	1.83
11	35	9	30.777	3.134	100	118.8	18.8	6.00
12	35	9	30.227	2.986	110	129.6	19.6	6.57
13	35	9	29.825	2.877	120	140.4	20.4	7.09
14	35	9	29.531	2.797	130	151.2	21.2	7.58
15	35	9	29.317	2.739	140	162	22	8.03
16	35	9	29.160	2.696	150	172.8	22.8	8.46
17	35	9	29.045	2.665	160	183.6	23.6	8.85
18	35	9	28.961	2.642	170	194.4	24.4	9.23
19	35	9	28.900	2.626	180	205.2	25.2	9.60
20	35	9	28.855	2.614	190	216	26	9.95
21	35	9	28.822	2.605	200	226.8	26.8	10.29
22	35	9	28.798	2.598	210	237.6	27.6	10.62
23	35	9	28.780	2.594	220	248.4	28.4	10.95

Table HT-1 – Summary of Stresses in Worked Example HT-1

Graphical variations of the stresses are shown in Figure HT-2.

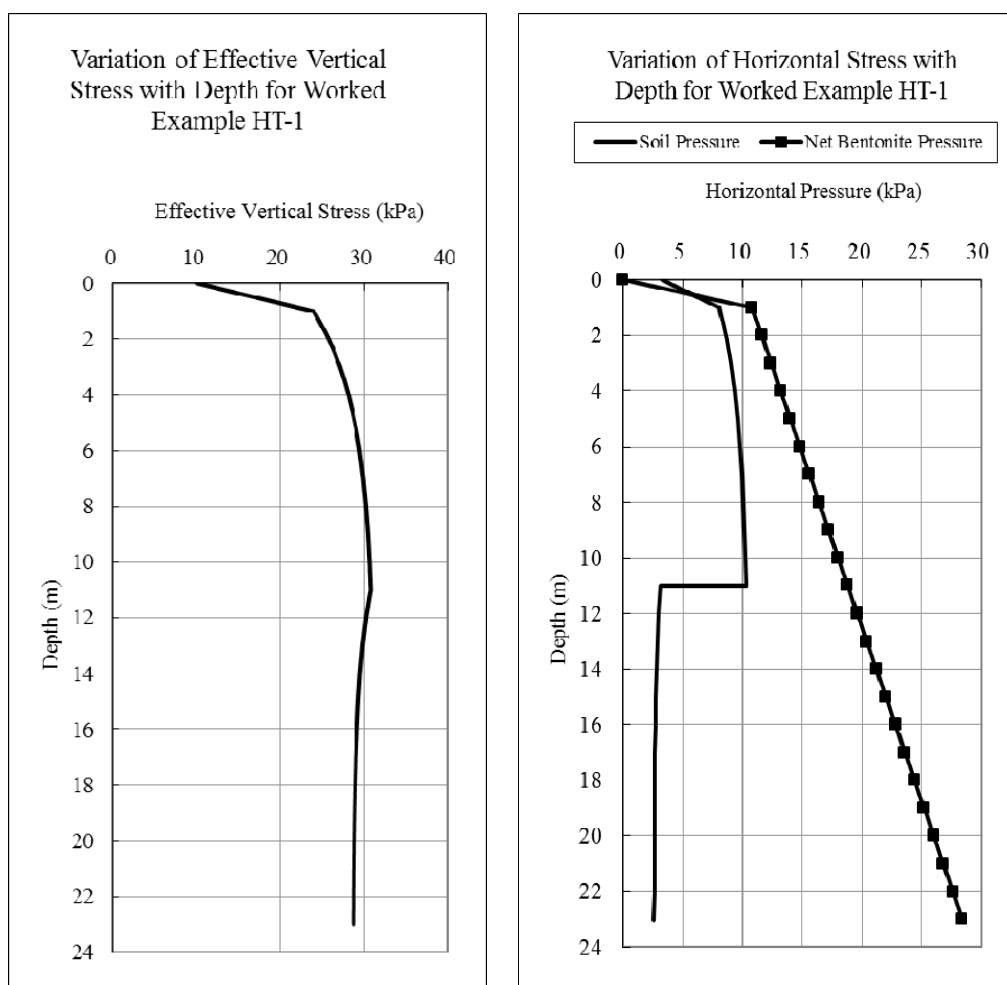


Figure HT-2 – Graphical Representation of Variation of Stresses with Depth in Worked Example HT-1

Appendix HU

Photographic Demonstration of Construction Procedures of Some Common Types of Foundations

Photographic Demonstration of Construction Procedures of Some Common Types of Piles

HU.1 Driven Steel H-Piles



Photo HU1.1 – Welding of Pile Shoes

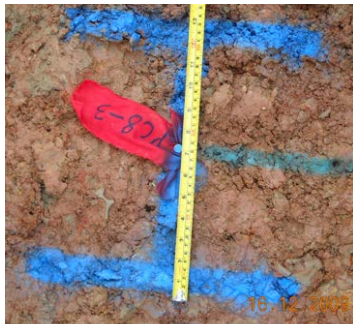


Photo HU1.2 – HU2.1



Photo HU1.3 – Installation of Pile in Correct Position



Photo HU1.4 – Checking Verticality

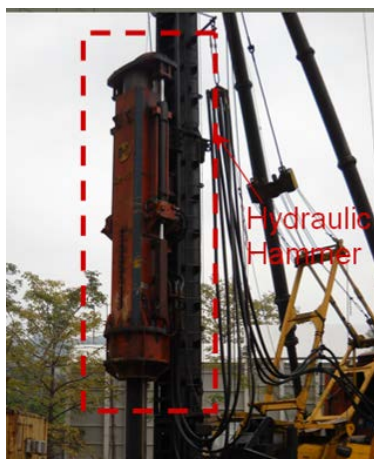


Photo HU1.5 – Pitching of Pile (by Hydraulic Hammer)



Photo HU1.6 – Connection of Pile by Welding



Photo HU1.7 – Test of Weld



Photo HU1.8 – Pitching to the Required Depth



Photo HU1.9 – Installing Transducers on Pile for the PDA Test



Photo HU1.10 – Pile Driving Analyzer Test Data Displayed on Screen



Photo HU1.11 – Final Set Measurement



Photo HU1.12 – Close-up of Final Set Measurement



Photo HU1.13 – Static Loading Test – Set-up with Kentledge



Photo HU1.14 – Static Loading Test – Close-up of Load Cell on Top of Pile

HU.2 Large Diameter Bored Pile



Photo HU2.1 – Setting-Out of Pile on Ground

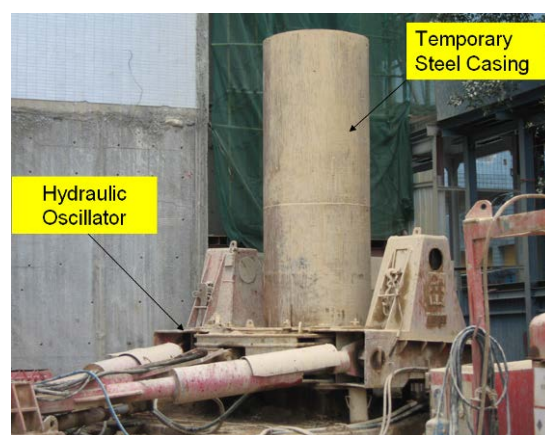
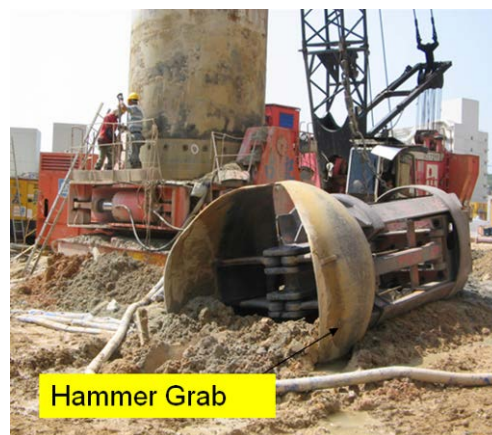


Photo HU2.2 – Set up the Hydraulic Oscillator with Crawler Crane and Drive the Temporary Steel Casing into the Ground



Hammer Grab

Photo HU2.3 – Excavation using Hammer Grab inside Temporary Steel Casing.



Bolt-connected Casing



Weld-connected Casing

Photo HU2.4 – Extending the Temporary Steel Casing by Bolting or Welding Connections



Reverse Circulation Drilling Rig



Tungsten Carbide Roller Cutter

Photo HU2.5 – Excavation of rock or similar hard material using Reverse Circulation Drilling Rig for Formation of the Rock Socket.

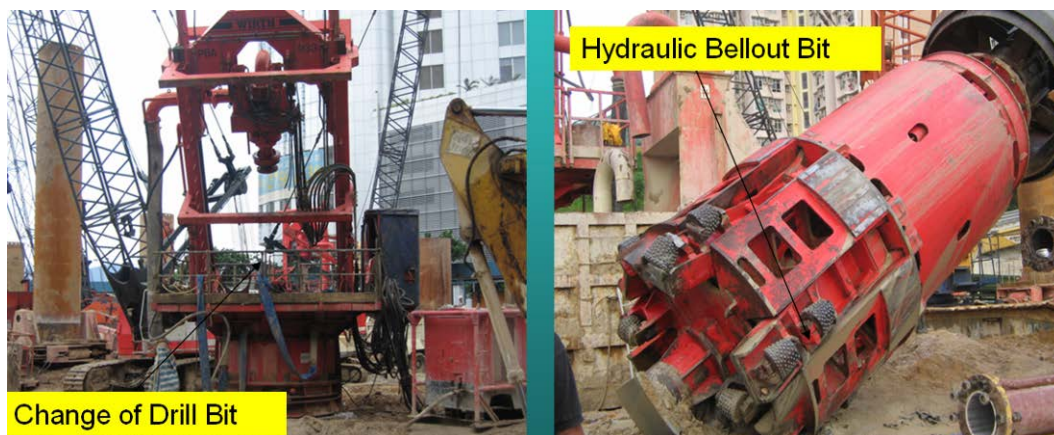


Photo HU2.6 – Formation of Bellout by Hydraulic Bellout Bit using Reverse Circulation Drilling Rig

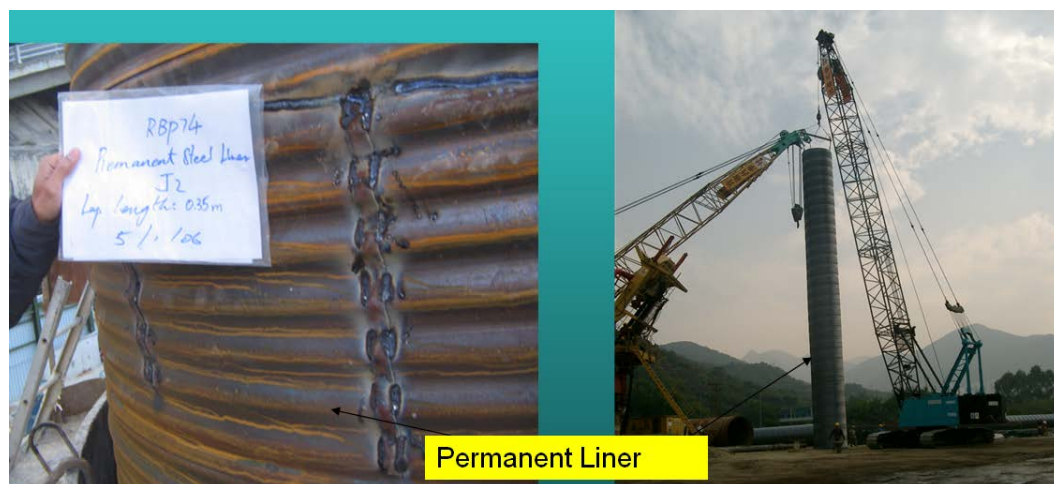


Photo HU2.7 – Installation of Permanent Liner (usually in Zone of Weak Soil) inside the Temporary Casing to Avoid “Necking”



Photo HU2.8 – Installation of Steel Reinforcement Cage inside the Bored Pile Shaft using Crawler Crane



Photo HU2.9 – Cleaning of Pile Base using Airlifting Method by Compressed Air



Photo HU2.10 – Placing Tremie Concrete with Gradual Extraction of the Temporary Steel Casing Concurrently



Photo HU2.11 – Rotary Drilling Rig for Concrete Core Test



Photo HU2.12 – Sonic Logging Test

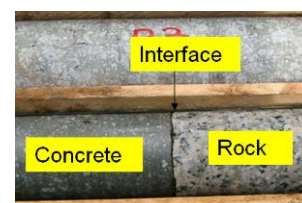


Photo HU2.13 – Sample of Concrete / Rock Interface

HU.3 Socketed Steel H-Pile



Photo HU3.1 – Drilling with the first Temporary Casing



Photo HU3.2 – Checking Alignment

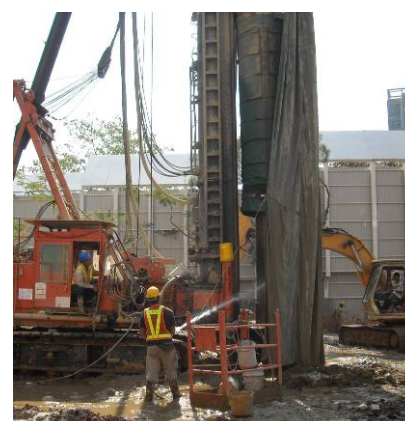


Photo HU3.3 – Drilling Works by ODEX Method



Photo HU3.4 – ODEX Drilling Bit



Photo HU3.5 – Prefabrication of Steel H-pile for Socket Length Portion



Photo HU3.6 – Double Shelter for Noise and Dust Reduction during Piling



Photo HU3.7 – Casing Joint Preparation



Photo HU3.8 – Splicing of Temporary Casing



Photo HU3.9 – Splicing of Steel H-pile



Photo HU3.10 – Obtaining Rock Sample after Completion of Drilling Operation



Photo HU3.11 – Preparation Works for Grouting Work



Photo HU3.12 – Air-lifting before Grouting Work



Photo HU3.13 – Cement Grouting for the Socketed H-Pile



Photo HU3.14 – Extracting Temporary Steel Casing by Vibrating Hammer



Photo HU3.15 – Extracting Temporary Steel Casing by Hydraulic Jack under Adverse Condition



Photo HU3.16 – Grout Testing Work

HU.4 Mini-pile



Photo HU4.1 – Drilling Rig for Mini-pile on Working Platform

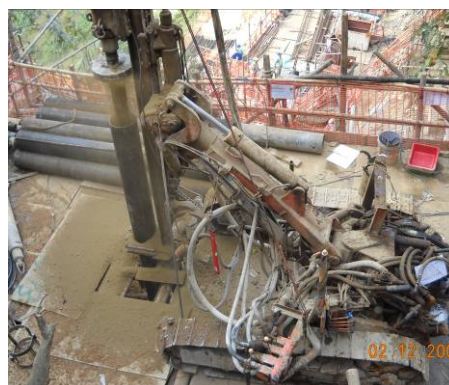


Photo HU4.2 – Drilling Work in Progress (Vertical Mini-pile)



Photo HU4.3 – Drilling Work in Progress (Raking Min-pile)



Photo HU4.4 – Checking Alignment of Mini-pile

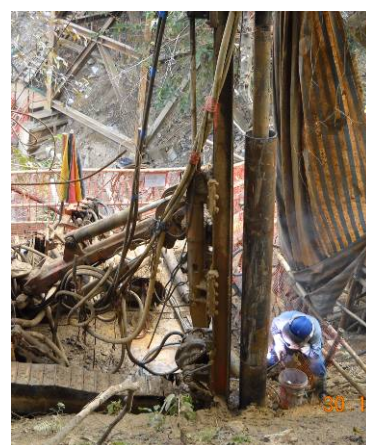


Photo HU4.5 – Splicing of Steel Casing



Photo HU4.6 – Collecting Rock Sample at Founding Level



Photo HU4.7 – Air Lifting at Completion of Drilling



Photo HU4.8 – Prefabrication of Steel Bars



Photo HU4.9 – Installation of Steel Bars



Photo HU4.10 – Completion of Pile by Cement Grouting

HU.5 PIP Pile



Photo HU5.1 – Setting Out of Pile



Photo HU5.2 – Auger Drilling Rod

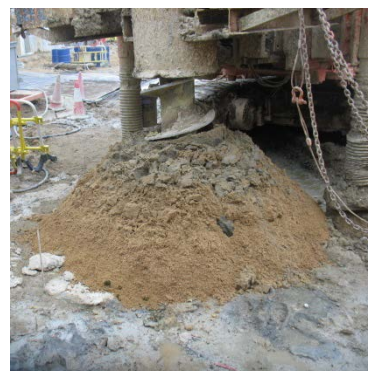


Photo HU5.3 – Drilling Work in Progress



Photo HU5.4 – Extension of Auger Drilling Rod



Photo HU5.5 – Drilling Completed to the Required Depth of Pile



Photo HU5.6 – Grouting Work of Pile



Photo HU5.7 – Flow Cone Test for Grout



Photo HU5.8 – Initial Setting Time Test for Grout



Photo HU5.9 – Grout Cube Compression Test



Photo HU5.10 – Completion of Grouting Work



Photo HU5.11 – Prefabricated Steel Cage



Photo HU5.12 – Installation of Steel Cage into the Pile Shaft



Photo HU5.13 – Surveying of the Top Level of Steel Bar



Photo HU5.14 – Stabilizing the Steel Cage (in Grout) by U-bolts



Photo HU5.15 – Inspection of Grout at Top Level of Pile before Backfill

HU.6 Barrette Construction



Photo HU6.1 – Shallow Trench formed and surrounded by Guide Walls and filled by Bentonite Slurry



Photo HU6.2 – Silos on Site for Re-circulation of Bentonite Slurry



Photo HU6.3 – The Hydromill Machine for Trench Excavation



Photo HU6.4 – Cutter at the bottom of The Hydromill Machine



Photo HU6.5 – Excavation by Hydromill within Guide Walls



Photo HU6.6 – Scrapers used to Clean Trench sides by Removing Excess Filter Cake



Photo HU6.7 – Reinforcement Cage Pre-fabricated on Site



Photo HU6.8 – Lifting Reinforcement Cage



Photo HU6.9 – Lowering Reinforcement Cage into Excavation Trench



Photo HU6.10 – Tremie Concreting for Barrette



Photo HU6.11 – Finished Barrette after Concreting / Grouting

HU.7 Hollow Box Footing



Photo HU7.1 – Open Excavation for Raft Footing Construction



Photo HU7.2 – Blinding the Bottom Level of the Raft Footing



Photo HU7.3 – Reinforcement Fixing for the Bottom Slab



Photo HU7.4 – Concreting for the Bottom Slab



Photo HU7.5 – Reinforcement Fixing for the Walls



Photo HU7.6 – Concreting for the Walls



Photo HU7.7 – Formwork Erection and Reinforcement Fixing for the Top Slab



Photo HU7.8 – Concreting for the Top Slab

Appendix HV

Estimation of Interactions of Piles in Close Proximity under Vertical Loads by Randolph's Approach

Estimation of Interactions of Piles in Close Proximity under Vertical Loads by Randolph's Approach

HV.1 Introduction

A pile under vertical load will settle and “drag” the soil around it downwards and thus will create further settlement on adjacent piles. So the settlement of a pile is that due to its own and the effects from others. The phenomenon is termed as “pile interactions”.

The mechanism is difficult to quantify even under the elastic theory by which the soil is idealized as an elastic continuum. Poulos & Davis (1980) has developed an approach based on Mindlin's Equations originated from effects due to point loads in an elastic continuum. However, the approach involves lengthy and tedious mathematical manipulations. Randolph (1977), nevertheless, has developed a much simplified approach which has been popularly used by designers and researchers.

HV.2 Description of Randolph's Approach

Basically, Randolph assumes the soil deforms by shear due to the shear stress on the pile shaft and that the effects on soil will be considered negligible beyond a distance r_m (defined below) for determination of pile settlement due to soil friction. The following Figure HV-1 and (Eqn HV-1) are extracted from GEO Publication 1/2006 (Figure 6.26) which explains the assumption. It should be noted that the formula is based on linearly varying shear modulus of soil with depth.

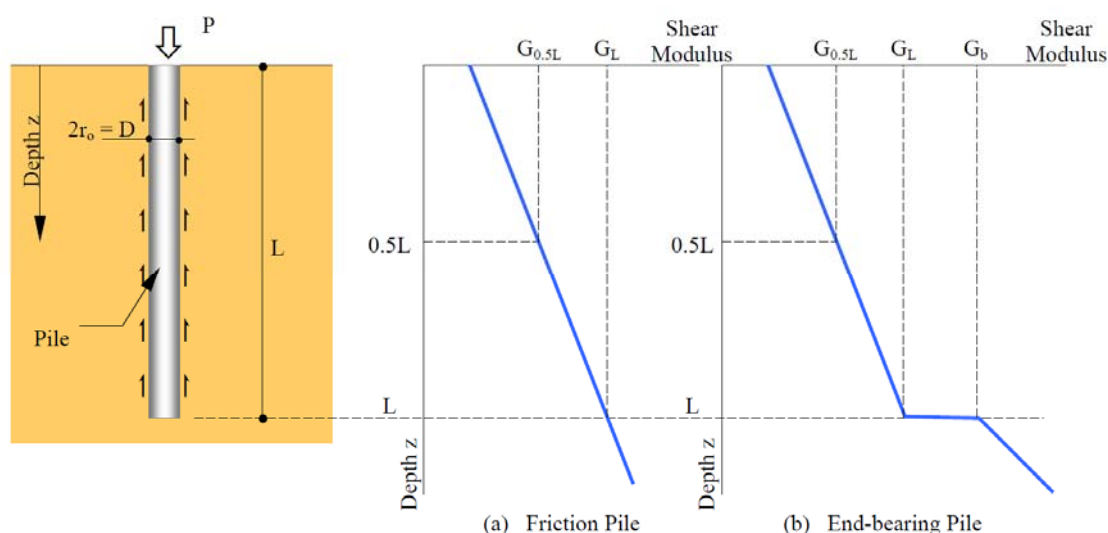


Figure HV-1 – Extract from GEO 1/2006 (Figure 6.26) to Explain Randolph's Approach in Settlement Determination

$$\frac{P}{\delta_i r_o G_L} = \frac{\frac{4\eta}{(1-v_s)\xi} + \frac{2\pi\rho \tanh(\mu L)}{\zeta} \frac{\mu L}{r_o}}{1 + \frac{4\eta}{\pi\lambda(1-v_s)\xi} \frac{\tanh(\mu L)}{\mu L} \frac{L}{r_o}} \quad (\text{Eqn HV-1})$$

where P is the load applied at the pile head
 δ_i is the settlement of the pile head
 r_o is the pile radius at the pile shaft
 r_b is the radius of the underream for underreamed pile
 L is the length of embedment of the pile
 $\eta_r = r_b/r_o$ (ratio of underream to pile radius for underreamed pile)
 G_L is the shear modulus of soil at the pile tip
 $G_{0.5L}$ is the shear modulus of soil at mid-depth
 G_b is the shear modulus of soil under the pile tip
 $\rho = G_{0.5L}/G_L$ (rate of variation of shear modulus of soil with depth)
 $\xi = G_L/G_b$
 E_p is Young's modulus of Pile
 $\lambda = E_p/G_L$ (pile-soil stiffness ratio)
 ν_s is the Poisson's ratio of the soil
 $r_m = [0.25 + (2.5\rho(1-\nu) - 0.25)\xi]L$
 $\zeta = \ln(r_m/r_o)$ (measure of radius of influence of pile)
 $\mu L = \sqrt{2/\zeta\lambda}(L/r_o)$ (measure of pile compressibility)

Re-writing (Eqn HV-1), we may list

$$\delta_i = \left(\frac{1 + \frac{4\eta_r}{\pi\lambda(1-\nu_s)\xi} \frac{\tanh(\mu L)}{\mu L} \frac{L}{r_o}}{\frac{4\eta_r}{(1-\nu_s)\xi} + \frac{2\pi\rho}{\zeta} \frac{\tanh(\mu L)}{\mu L} \frac{L}{r_o}} \right) \frac{P}{r_o G_L} \quad (\text{Eqn HV-2})$$

Again by Randolph's approach, the settlement at the soil surface at distance S_{pi} away is

$$\delta_i = \delta_t \frac{\ln(r_m/S_{pi})}{\zeta} \quad (\text{Eqn HV-3})$$

where $\zeta = \ln(r_m/r_o)$ as defined above.

By the elastic theory, this settlement can be imposed onto a pile at the same distance from the original pile. The phenomenon is explained by Figure HV-2 which is an extract of Figure 7.9 of GEO Publication 1/2006.

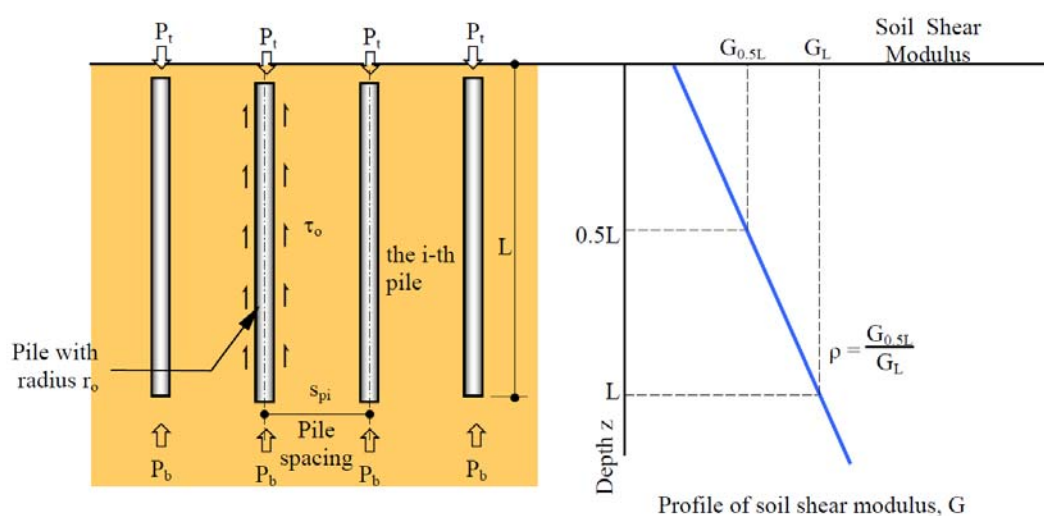


Figure HV-2 – Extract from GEO 1/2006 (Figure 7.9) to Explain Randolph's Approach in Pile Interaction of Settlement

So for the application to piles undergoing tension test, the settlement due to a test pile carrying a compression load created onto the test pile will be calculated which should be deducted from the up-rise of the pile.

HV.3 Worked Example HV-1

Consider a socketed H-pile of cross section undergoing tension load test in soil as indicated in Figure HV-3.

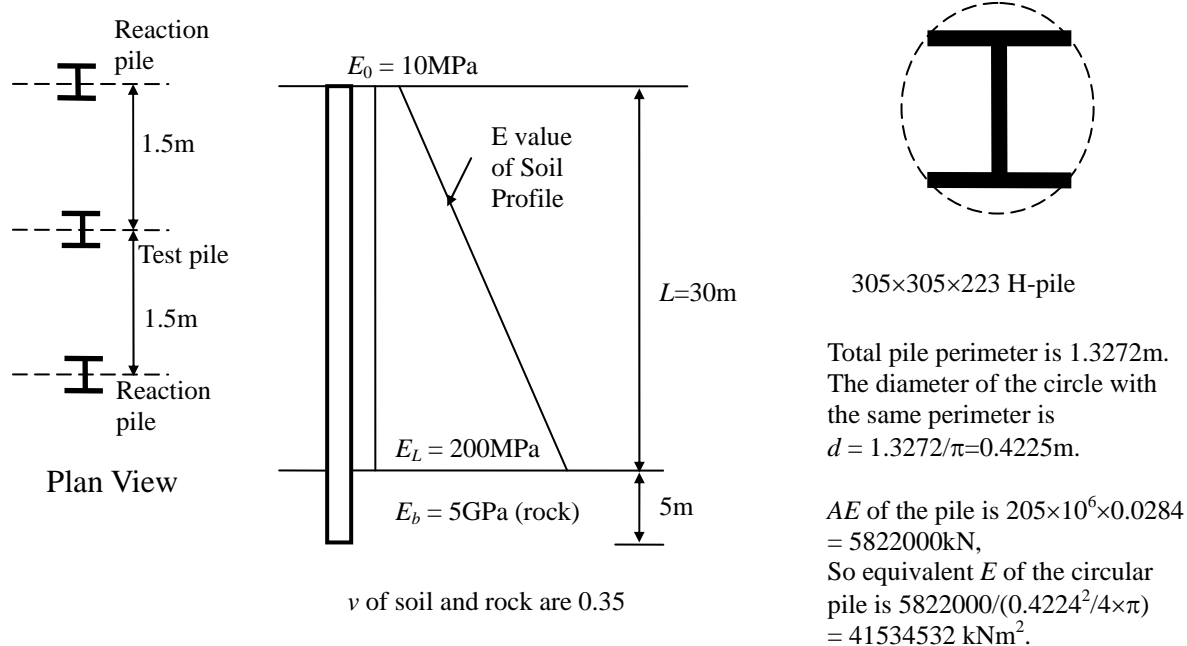


Figure HV-3 – Worked Example HV-1 for a Tension Loading Test

The maximum test tension load on the socketed pile is 6100kN so that each reaction pile carries 3050kN compression. The followings are calculated for estimation of settlement of the reaction pile by (Eqn HV-1) :

$$\eta_r = d_b/d = 1.0$$

$$E_0 = 10000 \text{ kPa} \Rightarrow G_0 = \frac{E_0}{2(1+\nu)} = \frac{10000}{2(1+0.35)} = 3703.7 \text{ kPa}$$

$$E_L = 200000 \text{ kPa} \Rightarrow G_L = \frac{E_L}{2(1+\nu)} = \frac{200000}{2(1+0.35)} = 74074.07 \text{ kPa}$$

$$E_b = 5000000 \text{ kPa} \Rightarrow G_b = \frac{E_b}{2(1+\nu)} = \frac{5000000}{2(1+0.35)} = 1851851.85 \text{ kPa}$$

$$\xi = G_L/G_b = 0.04 \text{ (ratio of soil and rock shear moduli at rock top level)}$$

$$\rho = \bar{G}/G_L = (3703.7 + 74074.07)/2/74074.07 = 0.525$$

$$\lambda = E_p/G_L = 41534532/74074.07 = 560.716$$

$$r_m = [0.25 + (2.5\rho(1-\nu) - 0.25)\xi]L$$

$$= [0.25 + (2.5 \times 0.525(1 - 0.35) - 0.25) \times 0.04]30 = 8.224 \text{ m}$$

$$\zeta = \ln(2r_m/d) = \ln(2 \times 8.224/0.4225) = 3.6618$$

$$\mu L = 2\sqrt{2/\zeta\lambda}(L/d) = 2\sqrt{2/(3.6618 \times 560.716)}(30/0.4225) = 4.4326$$

$$r_o = 0.5d$$

$$\text{So } \delta_t = \left(\frac{1 + \frac{4\eta_r}{\pi\lambda(1-\nu_s)\xi} \frac{\tanh(\mu L)}{\mu L} \frac{2L}{d}}{\frac{4\eta_r}{(1-\nu_s)\xi} + \frac{4\pi\rho}{\zeta} \frac{\tanh(\mu L)}{\mu L} \frac{L}{d}} \right) \frac{2P}{dG_L}$$

$$\text{So } \delta_t = \left(\frac{1 + \frac{8\eta_r}{\pi\lambda(1-\nu)\xi} \frac{\tanh(\mu L)}{\mu L} \frac{L}{d}}{\frac{2\eta_r}{(1-\nu)\xi} + \frac{2\pi\rho}{\zeta} \frac{\tanh(\mu L)}{\mu L} \frac{L}{d}} \right) \frac{P}{dG_L} = 0.00405 \text{ m}$$

By (Eqn HV-3), the settlement induced on the test pile at $S_{pi} = 1.5 \text{ m}$ away is

$$\delta_i = \delta_t \frac{\ln(r_m/S_{pi})}{\zeta} = 0.00405 \times \frac{\ln(8.224/1.5)}{3.6618} = 0.00405 \times 0.4647 = 0.00188 \text{ m}$$

As there are 2 reaction piles, a downward settlement of $1.88 \times 2 = 3.77 \text{ mm}$ would be induced to the test pile which would reduce the uplift displacement of the test pile. So this downward settlement should be added to the measured uplift displacement of the test pile to increase its upward displacement reflect the scenario of no pile interaction.

(Note : in reality the variation of the G values of soil is not linear. An approximation can be made by fitting a best line with least error through the G values measured at different levels by the mathematical technique of linear regression.)

References

1. Attewell, P.B. and Farmer, L.W. *Attenuation of Ground Vibrations from Pile Driving*. Ground Engineering, Vol. 6, No. 4, pp 26 – 29. (1973)
2. Azizi Fethi. *Applied analysis in geotechnics*, E & EN Spon Press, (2000).
3. Berezzantsev, V.G.; Khristoforov, V.S.; Golubkov, V.N. *Load Bearing Capacity and Deformation of Piled Foundation*, Proc, 5th Int. Conf. Soil Mechanics (1961). Vol. II pp11-15
4. Borowicka, H., *Druckverteilung unter elastischen Platten*. Ingenieur Archiv, Vol. X, No. 2, pp 113 – 125 (1939)
5. Bowles J.E. *Foundation Analysis and Design*. 5th Edition. The McGraw-Hill Companies, Inc. (1996)
6. Braja M. Das *Advanced Soil Mechanics Third Edition*. Taylor & Francis London and New York (2007)
7. British Standard Institute (BSI), *CP2004 : September 1972 – Code of Practice for Foundations*. (1972)
8. British Standard Institute. *BS5228-2:2009 Code of Practice for Noise and Vibration Control on Construction and Open Sites Part 2: Vibration*. (2009)
9. British Standard Institute. *BS8004:1986 Code of Practice for Foundations*. (1986)
10. British Standard Institute. *BSEN 1538:2010+A1:2015 Execution of special geotechnical works : Diaphragm Walls* (2000)
11. British Standard Institute *BSEN10025-1:2004 – Hot Rolled Product of Structural Steel* (2004)
12. British Standard Institute *BSEN14199-2005 – Execution of special geotechnical works – Micropile Annex D* (2005)
13. British Standard Institute *BSEN1997-1:2004 Eurocode 7 – Geotechnical design* (2004)
14. British Standard Institute *BSEN1997-2:2007 Eurocode 7 – Geotechnical design* (2007)
15. Broms, B.B. *Lateral Resistance of Piles in Cohesive Soils*, J.S.M.F.D., ASCE Vol. 90, SM2: 27 – 63 (1964a)
16. Broms, B.B. *Lateral Resistance of Piles in Cohesionless Soils*, J.S.M.F.D., ASCE Vol. 90, SM3: 123 – 156 (1964b)
17. Building (Construction) Regulations (2012) The Government of SAR. Hong Kong (2012)
18. Building (Construction) Regulations (1985) The Government of SAR. Hong Kong (1985)
19. Buildings Department. *Code of Practice for Foundations*. The Government of SAR. Hong Kong (2004).
20. Buildings Department. *Code of Practice for Structural Use of Concrete 2013*. The Government of SAR. Hong Kong (2013).
21. Buildings Department. *Code of Practice for Structural Use of Concrete 1987*. The Government of Hong Kong (1987).
22. Buildings Department. *Code of Practice for Dead and Imposed Loads 2011*. The Government of SAR. Hong Kong (2011).
23. Buildings Department. *Code of Practice for Structural Use of Steel 2011*. The Government of SAR. Hong Kong (2011).
24. Buildings Department. *Explanatory Report to the Code of Practice for the Structural Use of Steel 2005*. The Government of SAR. Hong Kong (2005).
25. Buildings Department. *Code of Practice for Structural Use of Steel 1987*. The Government of Hong Kong (1987).
26. Buildings Department. *Code of Practice for Site Supervision 2009*. The Government of SAR. Hong Kong (2009).
27. Building Department. *Practice Notes for Authorized Persons and Registered Structural Engineers*.

28. Burland J.B. and Wroth C.P. *Settlement of Buildings and Associated Damage*. Settlement of Structures, Pentech Press, London (1975).
29. Canadian Geotechnical Society (CGS). *Canadian Foundation Engineering Manual* (1978)
30. Canadian Geotechnical Society (CGS). *Canadian Foundation Engineering Manual 3rd Edition* (1992)
31. Canadian Geotechnical Society (CGS). *Canadian Foundation Engineering Manual 4th Edition* (2006)
32. Chan, Y.C. *Classification and Zoning of Marble Sites*, GEO Publication No. 29, GEO. (1994).
33. Cheng, Y.M. *PLATE User Manual*. (2013)
34. Chung, K.F. *Study of Load Transfer Mechanism of Rock-Socketed Steel Piles. Design or Rock-socketed Piles* (Editor, Victor Li), HKU SPACE and Centre for Research & Professional Development, pp. 19 – 25 (2005)
35. Civil Engineering and Development Department. *GEO Publication 1/2006 Foundation Design and Construction*. The Government of SAR. Hong Kong (2006)
36. Civil Engineering and Development Department. *GEOGUIDE 1 Guide to Retaining Wall Design*. The Government of SAR. Hong Kong (2000)
37. Civil Engineering and Development Department. *GEOGUIDE 2 Guide to Rock and Soil Descriptions*. The Government of SAR. Hong Kong (2000)
38. Civil Engineering and Development Department. *GEOGUIDE 3 Guide to Site Investigations*. The Government of SAR. Hong Kong (2000)
39. Civil Engineering and Development Department. *GEOSPEC 1 Model Specification for Prestressed Ground Anchors*. The Government of SAR. Hong Kong (1989)
40. Civil Engineering and Development Department. *Port Works Design Manual*. The Government of SAR. Hong Kong (2002)
41. Civil Engineering and Development Department – Standing Committee on Concrete Technology (SCCT). *Construction Standard CS1:2010 Volume 1 and 2*. The Government of SAR. Hong Kong (2010)
42. Civil Engineering and Development Department – Standing Committee on Concrete Technology (SCCT). *Construction Standard CS2:2012*. The Government of SAR. Hong Kong (2012)
43. Clark L.A., *The provision of Tension and Compression Reinforcement to resist In-Plane forces*, Magazine of Concrete Research, Vol. 28, No. 94, March 1976 (1976)
44. Coates, R.C., Coutie, M.G. and Kong, F.K. *Structural Analysis*, 2nd Edition, Van Nostrand Reinhold, pp 293 – 306 (1980)
45. Cornfield, G.M. *Discussion on ‘Pile driving analysis by the wave equation’ by Smith*. *Journal of the Soil Mechanics and Foundations Division*, American Society of Civil Engineers, vol. 87, no. SM1, pp 63-75. (1961)
46. Craig, R.F. *Soil Mechanics*, 7th Edition Spon Press, London & New York. (2004)
47. Davisson M.T. *High Capacities Piles*. Proceedings, Lecture Series, Innovation in Foundation Construction, SM&FD, ASCE, Illinois Section, Chicago (1972)
48. Department of the Navy Naval Facilities Engineering command Washington. *Design Manual NAVFAC DM-7*. March 1971. (1971)
49. Domone P. and Illston J. *Construction Materials – their nature and behavior 4th Edition* Spon Press (2010)
50. Douglas D.J. and Davis E.H. *The Movement of Buried Footings due to Moment and Horizontal Load and the Movement of Anchor Plates*. Géotechnique Vol. 14, pp115 – 132
51. Fellenius, B.H. *Unified design of piles and pile groups*. Transportation Research Board, no. 1169, pp 75-82. (1989).

52. Fleming K. Weltman A. Randolph M.F. Elson K. *Piling Engineering 3rd Edition* Taylor & Francis London and New York. (2008)
53. Foster S.J., Marti, P., and Mojsilović N. (2003) *Design of Reinforced Concrete Solids Using Stress Analysis* ACI Structural Journal November – December 2003.
54. Fox, E.N. *The Mean Elastic Settlement of a Uniformly Loaded Area at a Depth below the Ground Surface*, Proceedings of the Second International Conference on Soil Mechanics and Foundation Engineering, Rotterdam, Netherlands, Vol. 1, pp 129 – 132 (1948).
55. Fung, W.K., Wong, C.T. and Wong, M.K. (2004). *A study on capacity for driven piles*. The HKIE Transactions Vol. 11, No. 3, pp 10-16.
56. Goran Camitz (2009). *Corrosion and protection of steel piles and sheet piles in soil and water* Excerpt and translation of Report 93, Swedish Commission on Pile Research.
57. Hajnal, I., Morton, J., and Regele, Z., (1984) *Construction of Diaphragm Walls* – John Wiley & Sons Inc.
58. Highways Department, *Structural Design Manual for Highways and Railways Third Edition*. The Government of SAR. Hong Kong (2005)
59. Hiley, A. (1925), *Rational Pile Driving Formula and its Application in Piling Practice Explained*, Engineering, 657 and 7
60. Hiller D.M., and Crabb G.I. Groundborne vibration caused by mechanised construction works. TRL Report 429. Wokingham: TRL, (2000).
61. Hirsch T.J. *Modulus of Elasticity of Concrete Affected by Moduli of Cement Paste Matrix and Aggregate* Journal of the American Concrete Institute March 1962 (1962)
62. Housing Department, *Standard Specific Specifications*. The Government of SAR. Hong Kong (2010).
63. Institution of Civil Engineers (ICE) (1954), *Civil Engineering Codes of Practice No. 4 – Foundations*.
64. Johansen, K.W. *Yield Line Theory*, Cement and Concrete Association, London, (1962)
65. Lam, J. (2007). *Termination criteria for high-capacity jacked and driven steel H-piles in Hong Kong*, PhD Thesis, University of Hong Kong.
66. Lam S.C., Law C.W., Cheng Y.M *Elasto-plastic Analysis of Footing Structures by the Stiffness Method with Subgrade Structure Interaction*. The HKIE Transactions Vol. 16, No. 3, September 2009 (2009)
67. Lam S.C., Law C.W., *Discussion on the Design of RC Plate Bending Structures by the 'Stress' and 'Node Force' Methods*. The HKIE Transactions Vol. 16, No. 2, June 2009 (2009)
68. Law C.W., Cheng Y.M., Su R.K.L., *Approach for Reinforcement Design in Reinforced Concrete Structures Based on 3-Dimensional Stress Field*. The HKIE Transactions Vol. 14 No. 2, June 2007 (2007)
69. Law C.W., *Parametric Studies on Buckling of Piles in Cohesionless Soils by Numerical Methods* The HKIE Transactions Vol. 21 No. 1, March 2013 (2013)
70. Law C.W., Cheng Y.M., *Study on the P- δ Effects of Piles in Cohesionless Soil*. The HKIE Transactions Vol. 22 No. 3, September 2015 (2015)
71. Law C.W., Cheng Y.M., *Analysis of piled foundations with piles rigidly jointed to the pile caps under coupled support stiffness*. The HKIE Transactions Vol. 23 No. 2, July 2016 (2016) pp106-117.
72. Law C.W., Li, Victor *Bearing Capacity Factor N_q for Piles in Cohesionless Soil by Berezantsev*. Bridging Research and Practice – the VLA experience Edited by Victor Li Vol. 3 (2017)
73. Leung, K.W. *Settlement of buildings founded on caissons bearing on soil*. Proceedings of the Fourth International Conference on Tall Buildings, Hong Kong & Shanghai, vol. 1, pp 377-383 (1988)

-
74. Li, Victor. and Lam, J. *New criteria for formulating final set table for high-capacity steel H-piles*, Bridging Research and Practice – the VLA Experience, Victor Li (ed.), Centre for Research & Professional Development, pp 213-237. (2007)
 75. Li, K.S. (2007) *Use of plate load test for design of shallow foundations – A suggested alternative practice*. Bridging Research and Practice – the VLA Experience, pp191-199.
 76. MathSoft Engineering & Education, Inc. *Mathcad 2001i User's Guide with Reference Manual*.
 77. Meyerhof, G.G. *Discussion on Paper by Skempton, A.W. and Macdonald, D.H., 'The Allowable Settlement of Buildings,'* Proc. Instn. Civ. Engrs., Pt. II, vol 5, 774 (1956)
 78. Miguel A. Bermúdez and Pilar Alaejos *Models for Chloride Diffusion Coefficients of Concrete in Tidal Zone*, ACI Materials Journal Vol 107. No. 1 January – February 2010. (2010)
 79. MTRC *MTR New Works Design Standards Manual* (2008).
 80. Muki, R., *Asymmetric problems of the theory of elasticity for a semi-infinite solid and a thick plate*. Progress in Solid Mechanics, Vol. 1, North Holland Publishing Co., Amsterdam. (1961)
 81. Mylonakis, G. and Gazetas G. *Settlement and Additional Internal Forces of Group Piles in Layered Soil* Géotechnique, 48(1): 55 – 72 (1998)
 82. Neville A.M. *Properties of Concrete Fourth Edition*, Longman Group Limited. (1995)
 83. Neville A.M. *Neville on Concrete – An examination of Issues in Concrete Practice* ACI International (2003)
 84. Ng W.W., Yau L.Y., Li H.M. and Tang W. *New Failure Load Criterion for Large Diameter Bored Piles in Weathered Geomaterials*. Journal of Geotechnical and Geoenvironmental Engineering. June 2001.
 85. Poulos H.G. and Davis E.H. *Elastic Solutions for soil and Rock Mechanics*. John Wiley & Sons (1974)
 86. Poulos H.G. and Davis E.H. *Pile Foundation Analysis and Design*. John Wiley & Sons (1980)
 87. Randolph M.F., *A Theoretical Study of the Performance of Piles*. A dissertation submitted for the degree of Doctor of Philosophy at the University of Cambridge. December 1977. (1977)
 88. Randolph M.F., *PIGLET A Computer Program for the Analysis and Design of Pile Groups under General Loading Conditions*. (1980)
 89. Randolph, M.F. *The response of flexible piles to lateral loading*. Géotechnique, vol. 31, pp 247-259. (1981).
 90. Randolph, M.F. *Science and empiricism in pile foundation design: 43rd Rankine Lecture*, Géotechnique, vol. 53 No. 10, pp 847 – 875 (2003)
 91. Randolph M.F. *PIGLET Analysis and Design of Pile Groups Version 5.1* (Released May 2004, last edited July 2006)
 92. Sewell R.J. & Kirk P.A. (2002) *Geology of Tung Chung and Northshore Lantau Island*. Hong Kong Geological Survey Sheet Report No. 6, Geotechnical Engineering Office, Civil Engineering Department, 91 p.
 93. Siu, K.L. *Review of design approaches for laterally-loaded caissons for building structures on soil slopes*. Proceedings of the Twelfth Annual Seminar, Geotechnical Division, Hong Kong Institution of Engineers, Hong Kong, pp 67-89. (1992).
 94. Skempton, A.W., MacDonald, D.H. *Allowable Settlement of Structures*, Proc. Instn. Civ. Engrs., Pt. III, vol. 5, 727 – 768 (1956)
 95. Smith E.A.L. *Pile-driving Analysis by the Wave Equation – ASCE Transaction Vol. 127* 1962 pp.1145 – 1193 (1962).
 96. Standards New Zealand Concrete Standard Design Committee P3101 NZS 3101 : Part 1 and 2 *Concrete Structures Standard and Commentary* (2006)

-
97. Steinbrenner, W., *Tafeln zur Setzungsberechnung, Die Strasse*, Vol. 1, Oct, pp. 121-124. (1934).
 98. Terzaghi K. *Evaluation of coefficients of subgrade reactions*. Géotechnique, Vol. 5, pp297 – 326 (1955)
 99. Terzaghi, K. & Peck, R.B. (1967). *Soil Mechanics in Engineering Practice. (Second edition)* Wiley, New York.
 100. Tijou, J.C. (1984). *Integrity and dynamic testing of deep foundations – recent experiences in Hong Kong (1981-83)*. Hong Kong Engineer, Vol. 12, no. 9, pp 15-22.
 101. Timoshenko, S., and J. N. Goodier, *Theory of Elasticity*, 2nd ed., McGraw-Hill, New York (1951).
 102. Tomlinson M.J. *Piled Design and Construction Practice 5th Edition*. Taylor & Francis (2008).
 103. Triantafyllidis T. *On the Application of the Hiley Formula in driving long piles*. Géotechnique 51, No. 10 pp. 891 – 895 (2001)
 104. Wang, Y.H., Tham, L.G., Lee, P.K.K. and Yang J. *A study on Rock-socketed Piles. Design of Rock-socketed Piles* (Editor, Victor Li), HKU SPACE and Centre for Research & Professional Development, pp. 1 – 18 (2005)
 105. Vaziri H., Simpson B. Pappin J. W. and Simpson L. *Integrated forms of Mindlin's equations*. Géotechnique Vol. 32, Issue 3 pp. 275 – 278 (1982)
 106. Vesic, A.S. *A study of Bearing Capacity of Deep Foundations* Final Rep., Proj, B-189, School of Civil Eng., Georgia, Inst. Tech., Atlanta, Ga (1967)
 107. Vesic A.S. (1973) *Analysis of ultimate loads for shallow foundations*, Journal of the Soil Mechanics and Foundations Division, ACSE, Vol.99, No. SM1, 45-73
 108. Vesic A.S. (1975) Chapter 3 : Foundation Engineering Handbook, 1st Ed., ed. Winterkorn and Fang, Van Nostrand Reinhold, 751 pp.
 109. Wood R.H. *The reinforcement of slabs in accordance with a pre-determined field of moments*, Concrete, 2, pp 69–76, U.K. (1968)
 110. Zienkiewicz O.C., Taylor R.L. Zhu J.Z. Nithiarasu P. *The Finite Element Method 6th Edition*, Oxford, New York, Elsevier/Butterworth-Heinemann (2005)
 111. 王杰賢 · *動力地基與基礎*，科學出版社（北京）(2001)
 112. 鄭大同，*地基極限承載力的計算*，中國工業出版社 (1979)

